The effects of chronic hypoxia *in utero* on cardiovascular regulation in the offspring

By

William Rook

A thesis presented to the College of Medical and Dental Sciences
of the University of Birmingham for the degree of Doctor of Philosophy

School of Clinical and Experimental Medicine
College of Medical and Dental Sciences
University of Birmingham
Birmingham
B15 2TT

August 2011

Abstract

A common consequence of the complications of pregnancy, such as preeclampsia, is reduced supply of nutrients, including oxygen, to the developing fetus. The consequences for the offspring are wide ranging, but include increased risk of cardiovascular disease. However, the mechanisms by which this occurs are poorly understood. Using a rodent model, this study has examined the regulation of blood vessels, particularly those supplying skeletal muscle, by local, endothelially-derived factors, and by the sympathetic nervous system, in adult rat offspring following chronic hypoxia *in utero*.

The key findings include evidence that there are chronically high levels of oxidative stress in the skeletal muscle vasculature of the offspring. Further, the density of, and the activity in the sympathetic neurones supplying skeletal muscle blood vessels is markedly increased following chronic hypoxia *in utero*, but the vascular sensitivity to stimulation of these neurones is reduced. Following chronic hypoxia *in utero*, as the rats approached middle age, they became hypertensive relative to normal rats. Thus, the present study has offered some mechanistic insight, which adds to a growing body of literature, and which may help to explain why babies born of sub-optimal pregnancies are at higher risk of developing cardiovascular disease later in life.

Synopsis

1- It is well known that a suboptimal in utero environment, such as that experienced by a fetus during preeclampsia, increases cardiovascular disease in humans. Experimental animal models using chronic hypoxia *in utero* have shown endothelial dysfunction in isolated blood vessels, in part at least, caused by oxidative stress. Recent evidence has shown that there is a reduced role for adenosine in hypoxia-induced vasodilatation *in vivo*. Further, there is limited evidence, in isolated blood vessels, that responses to sympathetic neurotransmitters may be enhanced. Studies in the near-term hypoxic chick embryo have shown that sympathetic innervation density is increased in the femoral artery. Thus this study sought to comprehensively examine whether there are alterations in the control of the skeletal muscle vasculature, in terms of locally mediated control by the endothelium, and autonomic control by the sympathetic nervous system

2- Experiments were performed on 10-12 week old normal (N) Wistar rats, and on the 10-12 week offspring of pregnant Wistar dams who breathed 12%O_2 from day 10-20 of pregnancy, representing the second half of gestation (CHU rats). A further set of experiments was performed on N and CHU rats at 36-weeks of age. Experiments were performed under anaesthesia with the steroid anaesthetic Alfaxan.

3 – The cardiovascular and respiratory response to breathing 8%O_2 was similar in N and CHU rats, in that there was a marked increase in ventilation, and vasodilatation in skeletal muscle and cerebral vasculature. The magnitude of vasodilatation in

cerebral or skeletal muscle vasculature was similar between N and CHU rats. Further, there was similar waning of the hyperventilatory response to acute systemic hypoxia in N and CHU rats, indicating that the response to systemic hypoxia is as robust in CHU rats as in N rats. The superoxide dismutase (SOD) inhibitor DETC significantly reduced hindlimb vascular tone, indicating tonic production of superoxide anions.

4 – The hindlimb vasodilator response evoked by breathing 8%O_2 for 5 minutes was examined under control conditions, following L-NAME, during infusion of the NO donor SNAP, and then following blockade of either the adenosine A_1 or A_{2A} receptor subtypes. Following NOS blockade with L-NAME, the hindlimb vasodilator response to acute systemic hypoxia in CHU rats was significantly enhanced, suggesting that by blocking NOS restoring background NO levels, oxidative stress is reduced, and vasodilator responsiveness is enhanced. This is further evidence of oxidative stress in skeletal muscle vasculature of the CHU rat. Following NOS blockade, blocking the A_1 or A_{2A} adenosine receptor subtypes had no significant effect on the hypoxia-induced hindlimb vasodilatation, but blockade of both significantly reduced it. Blockade of the adenosine A_1 receptor under control conditions reduced hypoxia-induced hindlimb vasodilatation in both N and CHU rats, in contrast to that previously reported.

5 – Muscle sympathetic nerve activity (MSNA) was measured in the sympathetic neurones on the surface of the arteries supplying the spinotrapezius skeletal muscle in N and CHU rats. Discriminated single unit recordings contained cardiac and

respiratory rhythmicity. Ongoing firing rate was significantly higher in CHU rats than in N rats (0.56±0.075 vs 0.33±0.036Hz, $p<0.001$), but the increases in MSNA evoked by baroreceptor unloading, or by graded systemic hypoxia, were similar between groups. The degree of respiratory and cardiac modulation of ongoing MSNA was similar between groups. Sympathetic innervation density was assessed in the tibial artery, which supplies skeletal muscle, using the glyoxylic acid staining technique, and was also found to be significantly higher.

6 – In light of high ongoing MSNA and increased innervation density in CHU rats, the hindlimb vasoconstrictor response to lumbar sympathetic chain stimulation with a train of pulses at 2Hz, and bursts at 20 and 40Hz were tested. CHU rats showed smaller maximal vasoconstrictor responses to stimulation at all frequencies. In N rats, the neuropeptide Y Y_1 receptor antagonist BIBP-3226 significantly reduced vasoconstrictor responses to sympathetic chain stimulation in N rats at all frequencies, but had no significant blunting effect on the response in CHU rats, indicating that the role of NPY in sympathetically evoked vasoconstriction is reduced in CHU rats.

7 – Similar vasoconstrictor responses were tested in 36-week old N-A and CHU-A rats, to examine the effects of aging in CHU rats on sympathetic vasoconstriction. CHU-A rats were found to be hypertensive relative to N-A rats (139±3 vs 126±3mmHg, $p<0.01$). Vasoconstrictor responses evoked by stimulation of the lumbar sympathetic chain were similar in N-A and CHU-A rats. Further, there was no significant blunting of the vasoconstrictor response to sympathetic chain stimulation

by the NPY Y_1 receptor antagonist BIBP-3226. Thus, the reduced sensitivity to sympathetic chain stimulation seen in younger CHU rats is no longer evident by 36-weeks of age, and may explain why CHU-A rats are hypertensive relative to their control counterparts.

8 – In summary, this study presents evidence that there are high levels of oxidative stress in the skeletal muscle vasculature of the CHU rat. Further, ongoing sympathetic nerve activity in skeletal muscle vasculature is increased in CHU rats, as is the density of sympathetic neurones present on the surface of the tibial artery. Sensitivity to sympathetic nerve stimulation in the same vascular bed is reduced in CHU rats, and thus, ongoing vascular tone is similar to that of N rats. Arterial blood pressure is increased in middle aged CHU rats relative to middle aged N rats, indicating that along with the vascular dysfunction observed in the hindlimb vasculature, there may be dysfunction in other vascular beds, which may contribute to increased total peripheral resistance.

List of abbreviations

3-NT	3-nitrotyrosine
8-PT	8-phenyltheophylline
8-SPT	8-sulfophenyltheophylline
αSMA	α Smooth muscle actin
A_1	Adenosine A_1 receptor subtype
A_{2A}	Adenosine A_{2A} receptor subtype
ABP	Arterial blood pressure
ACh	Acetyl choline
AMP	Adenosine monophosphate
ANOVA	Analysis of variance
ANS	Autonomic nervous system
ATP	Adenosine triphosphate
BIBP-3226	Neuropeptide Y Y_1 receptor antagonist
BPM	Beats/breaths per minute
BSA	Bovine serum albumin
BH_4	Tetrahydrobiopterin
°C	Degrees centigrade
$[Ca^{2+}]_i$	Intracellular Ca^{2+} concentration
CHB	Chronic hypoxia from birth
CHU	Chronic hypoxia *in utero*
COX	Cyclooxygenase
CVC	Cerebral vascular conductance
CVLM	Caudal ventral lateral medulla
CU	Conductance units
DAPI	4',6-diamidino-2-phenylindole
DETC	Diethyldithiocarbamate
DPCPX	1,3-dipropyl-8-cyclopentylxanthine

DRG Dorsal respiratory group

eNOS Endothelial nitric oxide synthase

Exp Expiration

FBF Femoral blood flow

FITC Fluorescein isothiocyanate

FVC Femoral vascular conductance

FVR Femoral vascular resistance

HR Heart rate

I.A. Intraarterial

Insp Inspiration

intFVC Integrated femoral vascular conductance

intFVC Integrated femoral vascular resistance

I.V. Intravenous

L-NAME L-NG-Nitroarginine methyl ester

LSC Lumbar sympathetic chain

MAPB Mean arterial blood pressure

MFBF Mean femoral blood flow

NA Nucleus ambiguus

NOS Nitric oxide synathse

NTS Nucleus of the solitary tract

NPY Neuropeptide Y

NPY Y_1 Neuropeptide Y Y_1 receptor subtype

NR Nutrient restricted

P_aCO_2 Arterial CO_2 partial pressure

P_aO_2	Arterial O_2 partial pressure
PBS	Phosphate buffered saline
PBST	Phosphate buffered saline with 1% Tween20
PE	Preeclampsia
PGI2	Prostacyclin
PGN	Post-ganglionic sympathetic neurone
R_F	Respiratory frequency
RVLM	Rostral ventral lateral medulla
RU	Resistance units
SEM	Standard error of the means
SGA	Small for gestational age
SNAP	S-Nitroso-N-Acetyl-D,L-Penicillamine
SNP	Sodium nitroprusside
SOD	Superoxide dismutase
V_E	Ventilatory minute volume
VRG	Ventral respiratory group
V_T	Ventilatory tidal volume
ZM241385	ZM-241,385 (Adenosine A_{2A} receptor antagonist)

The effect of chronic hypoxia in utero on cardiovascular regulation in the offspring

William H R Rook

Oral communications

Rook WHR, Coney A, Brain K & Marshall JM. (2011). Chronic hypoxia in utero (CHU) induces increases in sympathetic innervation and activity that exist into early adulthood. In *Journal of Develpmental Origins of Health and Disease*, pp. S21. Portland, Oregon, USA.

Rook WHR, Marshall JM & Coney A. (2010). A sympathetic view of fetal programming of cardiovascular disease. In *Proc Physiol Soc*, pp. C17.

Rook WHR, Marshall JM & Coney A. (2009). Chronic Hypoxia in utero (CHU) increases superoxide production in the adult rat offspring. *Proc Physiol Soc* **14,** C1.

Rook WHR, Glen KE, Marshall JM & Coney AM. (2008). Changes in the regulation of vascular tone in adult male rats exposed to chronic hypoxia in utero. In *Proc Physiol Soc*, pp. C85.

Poster communications

Rook WHR, Coney A & Marshall JM. (2011a). Femoral vascular responses evoked by different patterns of sympathetic nerve stimulation in developmentally programmed rats. In *Journal of Developmental Origins of Health and Disease*, pp. S39.

Rook WHR, Johnson CD, Coney A, Brain K & Marshall JM. (2011b). Hypoxic fetal programming of the sympathetic nervous system. *FASEB J* **25,** 1029.1021

Rook WHR, Coney A, Brain K & Marshall JM. (2011c). Sympathetic hyperinnervation induced by chronic hypoxia in utero (CHU) persists into early adulthood. *Proc Physiol Soc* **23,** PC123.

Young T, **Rook WHR**, Ray C, Marshall J & Coney A. (2010). Prenatal hypoxia alters NO function in skeletal muscle of anaesthetised adult female rats. In *Proc Physiol Soc*, pp. PC26.

Rook WHR, Coney A & Marshall JM. (2009). Chronic hypoxia in-utero alters the role of superoxide anions in peripheral chemoreceptors in the anaesthetised adult rat. *Journal of Developmental Origins of Health and Disease* **1,** P-7C-331.

Rook WHR, Marshall JM, Coney AM & Glen KE. (2008). Chronic hypoxia in utero (CHU) in the rat changes capillarity and oxidative function in skeletal muscle of the offspring. In *Proc Physiol Soc*, pp. PC28.

Acknowledgement

There are a huge number of people who have surrounded me with encouragement for the last 3 years, all of whom I will forever be grateful to. I have an enormous amount of gratitude to Professor Janice Marshall (J-dizzle, The J Dog, The Janicisor) for her belief, guidance, support, and patience with my terrible grammar. I owe so much of what I've done since joining the lab to Dr Andy Coney, who has taught me a vast amount, not least how to combat a sarcastic boss, but also taught me a way of thinking which will never be unlearned. Thank you.

I am very grateful to the people with whom I have collaborated, particularly Dr Chris Johnson and Dr Steven Hudson. Both have been on the end of a phone more times than their duty required, and Steve offered up some little gems whilst writing, #JMMcorrectionsneverend being a particular favourite! I'm very thankful to Dr Keith Brain and Dr Wendy Leadbeater for their expert guidance with imaging techniques.

I'd like to thank everybody who was around the lab every day, and made my time so enjoyable. I'm grateful to Dr Clare Ray, who spent the first 6 months of my time rectifying my mistakes or consoling my manic depression after bad experiments. I'm grateful to Dr Katie Glen for not killing me whilst doing western blots, and John Hall-Jones for making a very dull activity exciting! I'm also hugely thankful for all the lovely people around the lab day to day that put up with my incessant crap-chat; Annie, Clara, Andy, Chris, Prem, Stuart, Dave, Dave W to name a few.

I've been lucky enough to have some amazing friends around me. Ben Nimmo has been a rock forever, taking me to the pub like a child during the dark 90 days of writing, and reminding me a world exists outside! (I must also thank him for not killing me for whistling in the office). Jamesy, Clare, Ali, George, Rob and Rumel have been fantastic friends throughout my studies, and have offered encouragement and support on countless occasions, as well as assisting in gin-based cell death on a regular basis. I must also thank Lara Murray, who was there when all this started, for putting up with my persistent excitement about rats in the early days; my apologies for that!

My family, Jane, George, Harri and Henry have put up with my scientific escapades and helped me through along the way, as well as surrounded me with love, and understood when I've needed them to. For that I'm always thankful.

Dedicated to the support of the people around me, and to 6 billion friends.

Table of Contents

Chapter 1 - General Introduction

1.1 Setting the scene

The paradigm that the environment to which a fetus is exposed during development affects its health later in life is well established Barker (1995). Factors such as macro- and micro-nutrient status (Barker, 1997), delivery of oxygen, maternal hormone levels (Owen *et al.*, 2005), maternal autoimmune disease (Roche *et al.*, 1992), and even maternal psychiatric disorders (Chung *et al.*, 2001) have all been found to affect the health outcomes of the progeny.

Reduced supply of nutrients to the fetus leads to an increase in risk of developing hypertension or coronary heart disease (Barker, 1995; Ojeda *et al.*, 2008). Of particular interest in the present study are the consequences of reduced fetal oxygen supply, which can occur as a result of preeclampsia, maternal anaemia, placenta previa, and the mechanisms by which this leads to cardiovascular disease. There is experimental evidence that chronic hypoxia *in utero* leads to endothelial dysfunction (Williams *et al.*, 2005b; Morton *et al.*, 2011), alterations in sympathetic innervation density (Ruijtenbeek *et al.*, 2000) and alterations in sensitivity to sympathetic neurotransmitters (Herrera *et al.*, 2007). Thus, the broad aims of the present study were to explore the roles of the endothelium and the sympathetic nervous system in the generation of cardiovascular pathology following fetal hypoxia.

In order to consider the mechanisms by which cardiovascular disease might manifest following adverse *in utero* conditions, first, the normal mechanisms of cardiovascular regulation must be considered.

Thus, this Introduction provides an overview of the general anatomy and functioning of the cardiovascular system, a number of control systems that regulate cardiovascular homeostasis, including the sympathetic nervous system, local, endothelial control, and particularly the role of oxidative radicals. The cardiovascular baro- and chemo-reflexes are also considered. Finally, a review of current evidence of the consequences of an adverse *in utero* environment for the cardiovascular system is given, including evidence gleaned from animal models of fetal programming.

1.2.1 The cardiovascular system

Control of vascular tone is a balance between locally released endothelium and tissue-derived vasoactive substances, such as NO or adenosine, and substances released from the varicosities of the sympathetic nerves which innervate most blood vessels.

1.2.2 Sympathetic nervous system

At its most basic level the sympathetic nervous system (SNS) can be considered to comprised 5 different classes of neurons. There are primary afferents, which convey information from sensory bodies, which are discussed later. These primary afferents are not always strictly considered part of the sympathetic nervous system, but vital in the functioning of the SNS. These primary afferents make direct connections with sympathetic premotor neurons (also known as presympathetic neurones) or with interneurons within the brainstem that convey sensory information to higher brain

centers, other areas within the brainstem, and then back to the sympathetic premotor neurons. Sympathetic premotor neurones project within the intermediolateral cell column (IML) onto the cell bodies of the sympathetic preganglionic neurones (SPNs), which are usually within the sympathetic ganglia and give rise to the sympathetic postganglionic neurone (PGNs) which innervate the end organ (Dampney, 1994). The exception to the rule is the adrenal gland, which receives direct efferent innervation from sympathetic preganglionic neurones.

1.2.3 Ongoing, rhythmic sympathetic nerve activity

It is well known from nerve recordings that there is ongoing activity in PGNs, particularly those which supply the vasculature. Much work has been performed on how sympathetic tone is generated to different organs, but for the purpose of this thesis, the focus is on the cardiovascular system. The exact source of what is a rhythmic ongoing activity, is a matter of much discussion. However, substantial work by Gebber and colleagues demonstrated the intrinsic, rhythm-generating nature of the medulla, even in the absence of afferent input (see Gebber 1980 for review). Notably, section of the brain above this region produces no significant fall in arterial pressure, whereas section below the medulla produces a profound fall. Various techniques have been employed to demonstrate involvement of several key areas of the medulla in the generation of ongoing sympathetic tone. Although the details are beyond the scope of discussion in this thesis, the regions are the rostral ventrolateral medulla (RVLM), the rostral ventromedial medulla (RVMM), the caudal raphe nuclei, the A5 cell group, and the paraventricular nucleus (PVN). See Dampney (1994) for

review of the anatomical and functional arrangement of these medullary neurones, and Malpas (1998) for review of the rhythms they generate.

The RVLM is clearly implicated in determining sympathetic outflow, as microinjection of the excitatory amino acid glutamate results in profound sympathoactivation (Willette *et al.*, 1983, 1984), whilst bilateral lesion of this region markedly depresses sympathetic outflow. Antidromic stimulation and neuroanatomical tracking have shown that the RVLM has direct synaptic projections to SPNs of the IML (Dampney *et al.*, 1982; Morrison *et al.*, 1988).

1.3 Autonomic afferent pathways

1.3.1 Baroreceptors

Arterial baroreceptors are located bilaterally in the carotid sinus, immediately distal to the carotid bifurcation, and in the aortic arch (Moore *et al.*, 2009). Information from these pressure-sensitive organs is conveyed centrally via the 9th and 10th cranial nerves, the glossopharyngeal and vagus nerves respectively. Rises in blood pressure stimulate baroreceptor afferents which elicit a reflex increase in parasympathetic nerve activity, as well an inhibition of sympathetic outflow.

These lead to bradycardia and a reduction in total peripheral resistance, and therefore lower blood pressure. The reverse is true when blood pressure falls from its normal values, leading to parasympathetic inhibition and sympathoexcitation which increases blood pressure (Berne *et al.*, 2003).

1.3.2 Chemoreceptors

The carotid chemoreceptors are also located at the bifurcations of the carotid arteries. They contain type I and II glomerular cells, the former of which detect changes in arterial O_2 tension, amongst other variables (for review of oxygen sensing mechanisms see Prabhakar (2006), and for review of the polymodal nature of the carotid body see (2007)). The carotid bodies are innervated by the 9th cranial nerve. There is also similar chemosensitive tissue located in the aortic bodies which are found in the wall of the arch of the aorta; these are innervated by the 10th cranial nerve. The integrated response to chemostimulation is covered elsewhere in this introduction, but the primary cardiovascular reflex is bradycardia and vasoconstriction, which may be heavily modulated by alterations in ventilation.

1.3.3 Central integration of afferent pathways

Both baro- and chemo-receptor afferents in the 9th and 10th cranial nerves have been show to terminate in the nucleus of the solitary tract (NTS) in the medulla. In fact, many other primary afferents, spinal and cranial, as well as afferents from higher centers also terminate in the NTS. Indeed, the NTS plays an essential role in reflex control of the cardiovascular system (Loewy, 1990; Dampney, 1994). Antidromic mapping shows that chemoreceptor afferents terminate mainly in the caudal regions of the NTS, whilst baroreceptor afferents terminate more rostrally (Donoghue *et al.*, 1984). Many other afferents terminate at discrete locations in the NTS, and although each type of afferent appears to have its own primary site for termination, there is a large degree of overlap (Taylor *et al.*, 1999). Efferent neurons of the NTS project

directly to the SPNs of the IML, but importantly, also project to other brainstem nuclei involved in generating and modulating the cardiovascular reflexes, particularly the RVLM and CVLM (See Loewy (1990) and Dampney (1994)).

CVLM neurones have been demonstrated to be broadly sympathoinhibitory, but appear to lack direct projections onto the IML. The CVLM receives inputs from several other brainstem nuclei, as well as from the NTS, and has direct GABAergic projections onto the RVLM. Indeed, the sympatho-inhibitory action of baroreceptor stimulation appears to be mediated by the inhibitory action of CVLM neurones on RVLM neurones. Thus, blockade of the CVLM with kynurenic acid abolishes the baroreflex (Koshiya *et al.*, 1993). It is also known that sympathetic outflow is reduced during inspiration, and enhanced during expiration (Seals *et al.*, 1990; Seals *et al.*, 1993). This is thought to be due to modulation of the baroreceptor input by central respiratory neurones projecting onto to the NTS, and the output from the NTS to the sympathoinhibitory CVLM (see Guyenet, 2000).

1.3.4 Autonomic efferent outflow

The generation of vasomotor tone by the ongoing activity observed in postganglionic sympathetic neurones innervating blood vessels, is a complex process. The RVLM plays a critical role, as inhibition of this area essentially abolishes such tone, and further, activity recorded in RVLM presympathetic neurones has been shown to largely mirror that seen in PGNs. However, the output of RVLM neurones is thought to be a complex interplay between the intrinsic activity of RVLM neurones and inputs from many subnuclei of the medulla, such as the CVLM, raphe nuclei, parabrachial

region and the lateral tegmental field, which interact to generate sympathetic tone (Guyenet, 2000)

As indicated above, the RVLM neurones are particularly modulated by the respiratory networks, the activity of which is a result of interactions between the pre-Boetzinger nucleus, the so called 'respiratory rhythm generator, and pools of interneurons. This explains why activity recorded from PGNs contains strong respiratory rhythm (Guyenet, 2000). The characteristics of activity recorded in PGNs, particularly in those supplying the vasculature of skeletal muscle, is discussed below.

1.3.5 Reflex control of the cardiovascular system – baroreflex

The primary afferents from the baroreceptors, the glossopharyngeal and vagal afferents, terminate in specific regions of the NTS (Taylor *et al.*, 1999). A rise in ABP, which loads the arterial baroreceptors, causes an increase in afferent firing rate, which evokes a rise in parasympathetic outflow to the heart, via the cardiac vagal nerves, and a reduction in sympathetic nerve outflow to blood vessels, reducing total peripheral resistance, and lowering arterial blood pressure. Conversely, a fall in ABP unloads the baroreceptors, reducing afferent activity, removing the sympathoinhibition and reducing vagal outflow to the heart. It is known that the NTS is the major relay site for baroreceptor afferents in the medulla.

It is also known that there is overlap between the central projections of baroreceptor afferents and the central respiratory neurones in the DRG and VRG. Thus, there is interaction between these groups, such that activity in baroreceptor afferents during

the expiratory phase of respiration evokes a vagally mediated fall in HR, but activity during the inspiratory phase does not (Spyer, 1996). Some of the mechanisms of this interaction are discussed by Dampney (1994), but are beyond the scope of this introduction.

The manner in which the baroreflex modulates sympathetic outflow has been extensively studied by many authors in humans and rodent models (Yamada *et al.*, 1989; Schreihofer & Sved, 1992; Thrasher, 2002, 2005). It is known that it generates cardiac rhythmicity in muscle vasoconstrictor nerves (Habler *et al.*, 1993, 1994). The effect of baroreceptor unloading on the activity in *individual* sympathetic nerves on the surface of arteries supplying skeletal muscle in the rat has recently been described by Hudson et al., (2011); unloading of the baroreceptors by an IV bolus of the nitric oxide donor SNP which reduced ABP resulted in a marked increase in muscle sympathetic nerve activity (MSNA) as was expected from previous observations of skeletal muscle arterial diameter responses to baroreceptor unloading (Hébert & Marshall, 1988).

1.3.6 Reflex control of the cardiovascular system – the peripheral chemoreflex

As indicated above, stimulation of the carotid body elicits the chemoreflex via the carotid sinus nerve (CSN) and the glossopharyngeal afferents, which terminate in the NTS. Excitatory NTS neurones then project onto the RVLM (Paton *et al.*, 2001), and cause sympathoexcitation. Inhibition of the RVLM with a glutamate receptor antagonist blocks the chemoreflex (Koshiya *et al.*, 1993), as does chemical inhibition

of the neurones in the caudal aspects of the NTS (Vardhan *et al.*, 1993). The neurones relaying chemosensitive information from the NTS to the RVLM do not display respiratory rhythm. However, they can directly control sympathetic outflow. However, whilst inhibition of respiratory rhythm generators such as the pre-Boetzinger nuclei does not abolish the sympatho-excitation induced by the chemoreflex, it does abolish its respiratory entrainment (see Guyenet, 2000).

Another group of neurones shown to be important in chemoreflex activation is the A5 cell group, a group of catecholaminergic neurones in the pons. These neurones are activated by peripheral chemoreceptor stimulation, and show strong respiratory rhythm (Guyenet *et al.*, 1993), and inhibition of their activity reduces the sympathoexcitation of the chemoreflex by around 50% (Koshiya & Guyenet, 1994). Recent studies have shown that they are only weakly activated by central chemoreceptors, indicating that they are mainly involved in the peripheral, and not the central chemoreflex (Kanbar *et al.*, 2011). Again, recent work by Hudson et al., (2011) has demonstrated that graded systemic hypoxia evokes a graded increase in MSNA recorded in individual sympathetic neurones on the surface of arteries supplying skeletal muscle.

1.4.1 Characteristics of MSNA

The characteristics of postganglionic sympathetic nerve activity were initially characterised in the cat, by extensive work by Janig and colleagues, who examined recordings from vasoconstrictor neurones identified as supplying skeletal muscle (MVCs), cutaneous vessels (CVCs), and sweat glands (sudomotor neurones) by the

characteristics of their firing activity. On this basis, activity in both MVCs and CVCs has been found to posses both cardiac and respiratory rhythms, although respiratory rhythm was less strong in the CVCs than MVCs. As indicated above, stimulation of the arterial baroreceptors lead to depression of activity in both types of neurone, while stimulation of the arterial chemoreflex, by giving the animal a hypoxic hypercapnic mixture to breathe, lead to a profound increase in MVC activity but a fall in CVC activity (See Janig, 1985 for review). Ongoing activity in MVCs of the cat was found to be 0.5-1.5Hz, although some MVCs are in fact silent unless otherwise stimulated (Horeyseck & Jänig, 1974). Ongoing activity in CVCs of the cat was 0.1-1.5Hz.

Some of the earliest work characterizing the activity of PGNs in the rat was carried out by Coote and colleagues. A study by Yusof & Coote (1988) showed that nerve activity from sympathetic neurones identified as supplying either skin or skeletal muscle of the rat hindlimb displayed cardiac rhythmicity, and was inhibited when arterial baroreceptors were stimulated by a rise in ABP induced by systemic infusion of phenylephrine. They also found that in the rat, the degree to which activity varied between nerves supplying different vascular beds is smaller than that found in the cat, with a more uniform pattern of response to stimulation of the medial regions of the lower brainstem (Yusof & Coote, 1988).

Later work carried out by Habler and colleages further characterised responses of PGNs to physiological stimuli in the rat (Habler *et al.*, 1993, 1994). They discriminated single unit activity in multiunit recordings taken from the saphenous

nerve, which contains fibres supplying cutaneous and skeletal muscle circulations. Single units that contained cardiac rhythmicity and were inhibited by the arterial baroreflex were identified as being sympathetic in nature, and then were classified as supplying muscle or skin based on the anatomical location of their projections.

They found that whilst most MVC neurones contained cardiac rhythmicity (82% of neurones recorded from), the CVC neurones contained either weak or no cardiac rhythmicity at all (Habler *et al.*, 1993). That said, the activity in both CVC and MVC neurones was inhibited by baroreceptor stimulation, although inhibition of CVC neurones by this reflex was slower than that of the MVC neurones. Around 90% of MVC and CVC neurones were found to contain respiratory rhythmicity, with facilitation being strongest during the post-inspiratory phase, but often extending through active expiration, and inhibition occurring during inspiration (Habler *et al.*, 1993).

In a further study, the same authors sought to determine how the degree of cardiac rhythmicity in ongoing and stimulated sympathetic nerve activity might change (Habler *et al.*, 1994). They used an arbitrary classification of strong, weak or absent to classify the degree of cardiac rhythm present, based on stimulus histograms, triggered by using peaks in the arterial pressure wave. They also quantified cardiac rhythm by examining the ratio between the peaks and nadirs of the stimulus histogram traces. The magnitude of cardiac rhythm was then used as an estimate of the degree to which sympathetic nerve activity is under the control of the arterial baroreflex. These authors also studied the effects of central chemoreceptor activation

on SNA using inspiratory hypercapnia. They found a strong activation of MVCs, but only around 50% of CVCs were activated by central chemoreceptor stimulation, whilst 35% of CVCs showed a reduction in activity (Habler *et al.*, 1993).

In a separate, interesting part of the study, the Habler et al., (1994) also found little evidence that different anaesthetics, in this case pentobarbital, chlorolose and urethane, have different effects on ongoing SNA, although Pentobarbital did appear to slightly augment ongoing activity. This effect of barbiturate anaesthesia has been reported elsewhere (Tucker *et al.*, 1982) but is far from unequivocally observed.

1.4.2 Sympathetic nerve activity in pathology and in programming

Despite the many studies that have implicated dysfunctional regulation of the sympathetic nervous system in states of cardiovascular pathology (Notarius *et al.*, 1999; Goso *et al.*, 2001; Simms *et al.*, 2009), to the authors knowledge, there have been no attempts to directly measure the effects of fetal programming on sympathetic nerve activity induced by any of the widely recognised stimuli.

1.5 Sympathetic cotransmission

The translation of sympathetic nerve activity to a functional response in the end organ is a complex process that is modulated by the patterning and intensity of nerve activity, the compliment of co-transmitters present in the post-ganglionic neurone, and by feedback mechanisms located around the neuroeffector junction. The synthesis, release mechanisms and actions of co-transmitters are discussed below.

Burnstock and Holman (1960) published the first study demonstrating in isolated guinea pig vas deferens, that repetitive stimulation of the hypogastric nerve led to excitatory junctional potentials which resulted in small, summated depolarisations of the post junctional smooth muscle cells, and eventually to a full 'junctional potential, depolarisation and contraction of the smooth muscle. This was the first demonstration of the coupling between sympathetic nerves and contraction of smooth muscle cells, forming what one can term 'the sympathetic unit'. This concept was later demonstrated in blood vessels (Sneddon & Burnstock, 1985).

That sympathetic nerves contained catecholamines was demonstrated much earlier, by Cajal (1905), and subsequently by many authors including Kuntz (1953), but it was Ulf von Euler's Nobel prize-winning work, which demonstrated that the major catecholamine was in fact noradrenaline (Euler, 1946). These sympathetic nerves are varicose in nature, with most of the neurotransmitter in the varicosities (Norberg & Hamberger, 1964; Chamley *et al.*, 1972). Later, by electronmicroscopy, vesicular storage of the main catecholamine present in sympathetic nerve terminals, noradrenaline (NA) was demonstrated, in dense-cored vesicles (Burnstock & Robinson, 1967). Further, the necessary synthetic and reuptake pathways have been shown to be present. The vesicles containing catecholamine have been morphologically and histochemically divided into large dense-cored vesicles (LDVs) and small dense-cored vesicles (SDVs), with more LDVs being present in the periarterial sympathetic nerves (Dermietzel, 1971) as opposed to the sympathetic nerve trunks.

Subsequently, it was demonstrated that ATP, which is now recognised as a major co-transmitter in sympathetic nerves (Kennedy *et al.*, 1986b; Burnstock, 1990b; Burnstock, 2009b; Burnstock, 2009a), is stored in both LDVs and SDVs (Lagercrantz & Stjarne, 1974; Fried, 1980), though predominantly in LDVs (Lagercrantz & Stjarne, 1974). Further, following the discovery of Neuropeptide Y (NPY) by Tatemoto (1982), co-localisation of NA, ATP and NPY was demonstrated within the LDVs present in sympathetic nerves (Lundberg *et al.*, 1982). For review see Lundberg (1996).

It is now well known that within the sympathetic neuroeffector junction of blood vessels, there are receptors for NA and ATP and NPY on the vascular smooth muscle and in the pre-junctional membrane innervated by sympathetic nerves (Burnstock, 1976; Drew & Whiting, 1979; Docherty & McGrath, 1980; Timmermans & Van Zwieten, 1980; Wahlestedt *et al.*, 1986).

The transmitters stored within the SDVs and LDVs are released into the neuroeffector junction by a process of exocytosis (Smith & Wrinkler, 1972) which is triggered by an increase in $[Ca^{2+}]_i$, secondary to depolarisation of the sympathetic neuron. It is important to note that the release of these so called 'quanta' into the neuroeffector junction is intermittent in nature, and it has been shown that at low frequency stimulation (1Hz), release of quanta from a particular varicosity can occur as rarely as once in 150 depolarisations (Cunnane & Stjärne, 1984), although the probability of transmitter release is increased with higher frequency stimulation.

The exact composition of the vesicles released into the neuroeffector junction, and the receptors they go on to interact with varies with end-organ or tissue. Of interest here is the manner in which sympathetic nerve control vascular smooth muscle. In fact there are variations in the magnitude of response evoked by sympathetic stimulation and the neurotransmitter and receptor profiles at different levels of the vasculature (Marshall, 1982; Morris, 1994, 1999)

1.5.1 Adrenergic transmission

The effects of sympathetic nerve stimulation on the blood vessels supplying skeletal muscle were demonstrated at several levels of the vascular tree by Marshall (Marshall, 1982). Marshall demonstrated that the primary and secondary arterioles (the higher and middle order arterioles) showed the most profound vasoconstriction to topical noradrenaline and to stimulation of the sympathetic paravascular nerve fibres at 10Hz, while terminal arterioles constricted initially but then relaxed during continued stimulation. Kobinger & Pichler (1981) showed, by infusing phenylephrine and noradrenaline into the hindquarter of the rat, and by using α_1- and α_2-selective adrenoreceptor antagonists, that both α_1 and α_2 subtypes are present in the hindlimb vasculature of the rat. Much work has since focused on the roles are for the two receptor subtypes. It was shown many years ago that both α1 and α2 receptor subtypes are present post-junctionally (Drew & Whiting, 1979; Timmermans & Van Zwieten, 1981), although there has been wide acceptance that the α_1 receptors are the most important post-junctional receptor, whereas the α_2 receptors are more important prejunctionally (See Rang et al., (2003)). Yamamoto et al., (1984) showed

that both receptor subtypes are involved in the pressor response to noradrenaline but found that in intestinal mesentry, only the α_1 receptor was involved in the vasoconstrictor response to nerve stimulation. Nevertheless, Coney & Marshall (2007) recently demonstrated, in the rat hindlimb, that α_2 receptors do play a significant role in the vasoconstriction evoked by stimulation of the sympathetic chain with low frequencies or with bursts of high frequency pulses. This finding is important in view of mounting evidence that post junctional α_2 receptors are important in regulation of skeletal muscle vasculature.

1.5.2 Local modulation of sympathetic noradrenergic transmission

Studies carried out by intra vital microscopy on the arterioles supplying the rat cremaster muscle and on arterioles from the isolated cremaster muscle showed that α_1 receptors are located predominantly in the proximal portions of the vasculature, along with α_2 receptors, but in the more distal arterioles, only α_2 receptors are present. Further, they found that the α_2 mediated component of vasoconstriction evoked by locally applied noradrenaline is reduced or abolished by reduced blood flow, designed to mimic hypoxia, or by acidosis, while the α_1 component is relatively resistant. (McGillivray-Anderson & Faber, 1991; Muldowney & Faber, 1991).

Other work has examined the blunting effect that local mechanisms have on sympathetically-evoked vasoconstriction in skeletal muscle during exercise, termed functional sympatholysis. This effect, was noted many years ago (Remensnyder *et al.*, 1962), and much work in rat and in human studies (Hansen *et al.*, 1994), has focused on elucidating the mechanisms. In rat cremaster muscle, Anderson and

Faber (1991) showed that when locally applying noradrenaline, it was α_2 mediated vasoconstriction that was most vulnerable to blunting during skeletal muscle contraction, likely due to the locally produced metabolic products. The α_1 component of vasoconstriction also became blunted at more intense exercise stimuli. Similar results were found by Thomas et al. (1994a). Further, VanTeeffelen and Jurgen, (2003) demonstrated by using intravital miscroscopy that in skeletal muscle vasculature, it was the smaller, 2A and 3A arterioles which were most vulnerable to sympathetic 'escape' while main arteries and 1A arterioles were relatively resistant during muscle contraction. Taken together with the work of McGilliray-Anderson and Faber, suggesting that constriction of more distal vessels, such as the 2A and 3A arterioles, is mediated primarily by α_2 receptors, and is vulnerable to local mediators such as acidity or hypoxia, this can be seen as a mechanism by which oxygen extraction can be increased without compromising systemic perfusion pressure. 3A arterioles control the number of perfused capillaries, and hence dilation of these arterioles, without upstream vasodilatation both increases effective capillary density, and slows flow in each capillary.

The mechanisms by which sympathetic vasoconstriction is blunted during muscle contraction in rodents and in humans, is heavily reliant upon NO (Thomas & Victor, 1998), and probably involves the activation of K_{ATP} channels by acidosis or hypoxia, which blunts the α_2-mediated component (Tateishi & Faber, 1995). It is thought that these mechanisms may well in fact interact to produce sympatholysis (see. Hansen et al., 2000 for review).

1.5.3 Purinotransmission

Some of the earliest evidence that ATP is released during sympathetic nerve transmission came from Su et al., (1971), who showed that enteric nerve sympathetic varicosities take up radiolabelled adenosine, synthesize ATP from it, and release it from the nerve terminals upon stimulation. In fact, it has been shown that usually it is ATP released from sympathetic nerves that are responsible for the EJPs recorded at the neuroeffector junction, and that if ATP receptors are desensitized with α,ß-methylene ATP, the EJP component of sympathetic cotransmission is abolished in the vas deferens (Sneddon & Burnstock, 1984). The contribution of ATP to cotransmission varies from one tissue and vascular bed to another, and also from species to species (see Burnstock (2008) for review). Early studies on isolated rat tail artery and mesenteric artery suggested that the role of ATP was predominately in initiating smooth muscle contraction to single impulses or couplets, and is not an important neurotransmitter during more sustained trains of sympathetic stimulation (Kennedy *et al.*, 1986a; Sjoiblom-Widfeldt *et al.*, 1990). However, more recent *in vivo* work in the rat hindlimb vasculature demonstrated that ATP plays a major role in cotransmission in response to lumbar sympathetic chain stimulation with both couplets in response to naturally-occuring patterns of sympathetic nerve activity (Johnson *et al.*, 2001). In fact, as much as 50% of the response to couplets of activity was still attributable to the action of NA, while ≈40% of the response to longer trains of nerve activity was attributable to ATP.

Both subclasses of P_2 purinergic receptor are present at the sympathetic neuroeffector junction; the ATP-gated cation channel (P2X) and the G-protein

coupled nucleotide (P2Y) receptor (see Boehm 2003 for review). The main post-synaptic ATP receptor is the P2X receptor, which mediates the EJP in smooth muscle.

P2Y receptors are present presynaptically, and inhibit the release of sympathetic neurotransmitter. P2X receptors are also present presynaptically, but they facilitate the neurotransmitter release (Miyahara & Suzuki, 1987; Boehm, 1999; Queiroz *et al.*, 2003)

1.5.4 Neuropeptide Y

NPY, predominantly found in LDVs and not SDVs in the sympathetic varicosity (Fried *et al.*, 1985; Lundberg *et al.*, 1989), acts on the post junctionally located NPY Y_1 receptor and the prejunctionally located NPY Y_2 receptor (Wahlestedt *et al.*, 1986).

Post junctionally, in skeletal muscle and vascular beds, stimulation of Y1 receptors leads to vasoconstriction (Donoso *et al.*, 1997; Ekelund & Erlinge, 1997), through increases in intracellular Ca^{2+} ($[Ca_2^+]_i$) and through potentiation of NA-mediated vasoconstriction (Linder *et al.*, 1996; Zhao *et al.*, 1997). Prejunctionally, the Y_2 receptor, at least in the rat vas deferens, has an autoinhibitory role, with stimulation of Y_2 receptors reducing release of NA from the sympathetic varicosity (Porter *et al.*, 1994).

There is conflicting evidence on the role of NPY in regulation of normal muscle blood flow under resting conditions. Pernow et al., (1989) in pigs, and Coney and Marshall

(2007) in rats, demonstrated *in vivo*, that the NPY Y_1 receptor antagonist BIBP-3226 has no effect on skeletal muscle vascular resistance under basal conditions. By contrast, Shoemakers group published evidence suggesting that NPY does play a role in regulating basal blood flow in the rat hindlimb muscle and human forarm(Jackson *et al.*, 2004; Hodges *et al.*, 2009; Jackson *et al.*, 2010); in the rat at least, this disparity may be explained by different anaesthetics. This is discussed in more detail in Chapter 6.

It has been shown that systemic plasma NPY concentration is not a viable option for measuring the contribution of NPY spillover from sympathetic nerves to basal skeletal muscle blood flow, as the gut and liver are major contributors to this level (Morris *et al.*, 1997). However, even if this is considered, it is known that circulating plasma [NPY] under resting conditions is around 20pM at most. Moreover, in humans, it has been shown that infusions for NPY which raise plasma concentrations to 356pM have no cardiovascular effects (Pernow *et al.*, 1987). NPY is considered to be most important during high frequency sympathetic nerve activity, such as that found following shock or myocardial infarction (Zukowska-Grojec & Vaz, 1988; Qureshi *et al.*, 1998; Kuo & Zukowska, 2007), according with the results of Coney & Marshall (2007).

Thus far, there has been no attempt to examine how the role of NPY is sympathetic vasoconstriction may be programmed by the *in utero* environment. This may be important, given evidence that responses to adrenergic agonists are altered following chronic hypoxia *in utero* (Rouwet *et al.*, 2002; Herrera *et al.*, 2007).

1.6.1 Fetal development of the sympathetic nervous system

The sympathetic nervous system originates from the migration and neurochemical differentiation of a longitudinal part of the neuroblast from the embryological neural crest (See Burnstock et al., (1981) for review), and is regulated largely by Nerve Growth Factor (NGF, (Storkebaum & Carmeliet, 2011)). Cochard et al., (1978; 1979) demonstrated that initial phenotypic characteristics, such as expression of tyrosine hydroxylase and catecholamine-related fluorescence, are evident in the developing rat embryo by day 11.5 of the 22 day gestation period, although these characteristics appear to be transient, and perhaps, are markers of developing sympathetic nerves, rather than of functioning enzymes. However, noradrenaline uptake mechanisms on nerve terminals are evident at day 12.5 and persist until at least day 17.5. (Jonakait *et al.*, 1979). Further, by day 13, adrenal medullary cells were clearly identifiable, and in most major nerve bundles, axons which appeared to be of sympathetic nature, were visible. In the rabbit Cowen et al., (1982) demonstrated a perivascular sympathetic nerve plexus around the carotid and renal arteries at days 25 and 30 respectively of gestation, which is around 30 days. It appears that in humans, more advanced sympathetic innervation may be present earlier in gestation than in other mammals. Thus, Pearson et al., (1980) and Edvinsson et al,. (1976) showed that there is a well developed sympathetic innervation of the carotid arteries, including terminal neurons, by 9-10 weeks of gestation in the developing human fetus, although they suggested that the cerebral circulation may become innervated earlier

than other systems due to its proximity to the neural crest during embryonic development.

An important point when considering the development of the sympathetic nervous system is the time at which the coordinated action of nerve, neurotransmitter, enzymes, pre- and post-junctional receptors, and reuptake mechanisms are able to work in a coordinated fashion, to form a 'sympathetic unit'. In the vasculature, an important part of the sympathetic unit is the ability of the vascular smooth muscle to react to noradrenaline. Su et al., (1977b) demonstrated that at day 53 of the lamb's 147 day gestation period, ie. about a third of the way through gestation, the carotid artery can respond to exogenous NA. They went on to propose a time course of events at the 'sympathetic unit' in the vasculature, after studying the maturation of blood vessels in various vascular beds (Su *et al.*, 1977a); see figure below.

The time at which the whole sympathetic unit becomes functional is not entirely clear. Nuwayhit et al. (1975) demonstrated that α-adrenerenoreceptor blockade in lamb fetuses of less than 1600g in weight (birthweight is ≈5000g) led to fall in arterial pressure of ≈28%, indicating that even at this early age, there is a contribution of sympathetic tone to the maintenance of arterial pressure. Ganglionic blockade had similar, but less marked effects. Moreover, ganglionic stimulation of fetuses of 1100-3700g increased heart rate and arterial pressure, indicating the capability of the

sympathetic nerves to control fetal heart rate. Nuwayhit et al., (1975) concluded that the magnitude of sympathetic tone in the lamb fetus increases with the maturity of the fetus, but that full maturity is not achieved until sometime after birth. Thus, it is clear sub-optimal conditions during the period when sympathetic innervation of blood vessels is developing has the potential for profound consequences for the fetus as it matures post-partum. Such consequences are discussed and examined in chapter 5.

1.6.2 Postnatal development of sympathetic control

It is generally agreed that development of the full compliment of autonomic reflexes and control of the vasculature largely takes place postnatally. Studies carried out in the piglet, which the authors argue shares the characteristics of the developing human baby, demonstrated that constrictor responses can be evoked in the mesenteric vasculature by reflex activation of sympathetic nerves or direct stimulation in the neonate (Gootman *et al.*, 1972; Gootman *et al.*, 1978), but these responses were not completely mature until 2 months of age. Consistent with these findings, Buckley et al., (1976) demonstrated that there is ongoing activity in the splanchnic sympathetic nerves which is modulated by the respiratory cycle in 1 week old neonatal swine.

The post-natal development and maintenance of the sympathetic innervation is less well understood. It is known that a variety of molecules produced by vascular smooth muscle cells, and sympathetic neurones maintain the integrity of the sympathetic innervation. Survival of perivascular sympathetic nerves is dependent on NGF (Chun

& Patterson, 1977; Ruit *et al.*, 1990; Orike *et al.*, 2001). Thus, Stewart et al., (2008) found that in pelvic ganglia from newborn mice, neutotrophin-3 increased outbranching of sympathetic neurones, whilst Francis et al., (1999) found that targeted disruption of the NT-3 gene halved the number of superior cervical ganglion neurones that survived to birth. A number of molecules derived from the extracellular matrix of vascular smooth muscle cells have also been implicated in the post natal regulation of sympathetic innervation, in terms of regulating nerve density and neurotransmitter profile (See Storkebaum & Carmeliet (2011) for recent review). Recent evidence shows that vascular endothelial growth factor (VEGF) also plays an important role in maintaining the neuroeffector junction, as its neutralization *in vivo* leads to and failure of re-innervation following femoral artery denervation (Marko & Damon, 2008). Further, mice that genetically express low levels of VEGF are found to have structurally and functional defects in the sympathetic neurovascular junction (Storkebaum *et al.*, 2010).

Aside from regulating the structure and function of the sympathetic neurovascular junction, neurotrophin signaling can modulate the firing properties of sympathetic neurones. Treatment with NGF increases firing probability in superior cervical ganglion sympathetic neurones (Luther & Birren, 2009).Furthermore, various factors, including NGF and BDNF (brain derived neurotropic factor) are important in regulating ion channel expression, and thus firing probability, in sympathetic neurones during development (Raucher & Dryer, 1995) and in adulthood (Lei *et al.*, 2001; Ford *et al.*, 2008).

In the rat, postnatal development involves the initiation of vital autonomic cardiovascular reflexes, which take place in the first stages of postnatal growth. For example, the carotid chemoreflex, which is immature at birth, matures during the first 14 days of life in the rat (Eden & Hanson, 1987b). These reflexes are present in the late gestation fetal lamb (Blanco *et al.*, 1984), but occur post-natally in the rat.

As indicated above, the development and post-natal maintenance of sympathetic control of the vasculature is a complex process. No attempt has yet been made to establish how the effects of an adverse pre-natal environment (Ruijtenbeek *et al.*, 2000; Rouwet *et al.*, 2002; Anderson *et al.*, 2006) are carried through adult life. The correct maturation of cardiovascular and respiratory reflexes involving the sympathetic nervous system are vital for cardiorespiratory homeostasis. Thus, it is apparent that adverse developmental environment has the potential to perturb normal development, and disturb normal cardiovascular regulation. These possibilities are discussed in more detail in chapter 3.

1.6.3 Sympathetic Innervation: Aged related changes

It is now well established that sympathetic control of blood vessels changes with age, both in terms of innervation density and functioning (Burnstock, 1990a). Cowen et al., (1982) demonstrated that within a single species arteries from different vascular beds change differently with age. Thus, innervation density in the femoral artery, as assessed by fluorescent area and number of varicosities per unit area peaked at 6 weeks of age, and then progressively fell through to 3 years of age. The same indices in the basilar artery increased progressively over the same period, while in

the renal artery peaked at around 6 months of age, before falling sharply. In rats, the density of the perivascular nerve plexus in the arteries of the circle of Willis peaks around 1 month postnatally, and then falls. However, further to this, the NA content of the remaining nerves appears to fall with age in these arteries, although NPY expression remains constant (Mione *et al.*, 1988). However, it appears that this pattern of change may be limited to the cerebral circulation. Recent studies by Omar and Marshall (2010) using 4-5, 10-11, and 42-44 week old young, mature and middle aged rats have shown that in the arteries supplying the brain, sympathetic innervation density declines as rats move into middle age (42-44 weeks). Conversely, in the caudal ventral tail artery and the femoral artery, innervation increases from 12 weeks of age and they progress towards middle age.

There is evidence that chronic hypoxia *in ovo* increases the sympathetic innervation density of the femoral artery of the hypoxic chick embryo (Ruijtenbeek *et al.*, 2000). However, no study has been performed of the equivalent effect of chronic hypoxia *in utero* and the subsequent effects in mammals in post-natal life. Thus, experiments examining this are presented in Chapter 5.

1.7.1 The integrated autonomic and local response to acute systemic hypoxia

Hypoxia occurs when tissue O_2 delivery is inadequate for normal functioning. When this occurs in tissues across the body, it is termed systemic hypoxia. The respiratory and cardiovascular response to acute systemic hypoxia is a multifaceted response,

involving local and neurohumoral factors. Generally, the outcome tends to maintain blood perfusion and O_2 delivery to tissues, and to alleviate tissue hypoxia, although in certain conditions the local and neurohumoral responses are inadequate and thus, tissue hypoxia persists and ultimately, death may occur by circulatory and respiratory collapse (Thomas & Marshall, 1995).

The mechanisms that contribute to the vascular elements of the response to acute systemic hypoxia include factors that are locally produced by the vascular endothelium, vascular smooth muscle, and the tissues surrounding these, that are superimposed on reflex, neural influences that are integrated in the central nervous system and which control the network of sympathetic nerves that innervate the vascular tree.

1.7.2 Characterisation of the cardiovascular response to acute systemic hypoxia

Comprehensive studies have been carried out to elucidate the cardiovascular response to acute systemic hypoxia. Marshall and Metcalfe (1988a) were the first to examine the cardiovascular responses of Saffan anaesthetised rats to graded levels of acute systemic hypoxia, breathing 15, 12, 8 or 6% O_2 in N_2 for 3 minute periods. They showed, in rats anaesthetised with the steroid anaesthetic Saffan, that graded hypoxia induced graded respiratory and cardiovascular changes, such that by the end of the 2nd minute of acutely breathing 8% O_2 or 6% O_2, P_aO_2 was reduced to ~33mmHg. These changes comprised graded hyperventilation, a fall in systemic

arterial blood pressure (ABP) and tachycardia, as well as graded vasodilatation in hind limb, mesenteric and renal vasculature.

1.7.3 Longer periods of acute hypoxia

Work carried out by Thomas & Marshall (1994) showed how these responses changed during longer 10 minute periods of acute systemic hypoxia (8% O_2); they and also recorded internal carotid blood flow (CBF), as an index of brain blood flow. They demonstrated that the initial hyperventilation began to wane by the third-fifth minute of hypoxia, due mainly to a fall in tidal volume (V_T) and the initial tachycardia waned towards or below the original control level. Concomitantly there was vasodilatation in the cerebral circulation, similar to that shown in the hindlimb, mesenteric and renal vascular beds. However, from the 5th min of hypoxia, CBF fell towards or below control level even though it was well maintained initially. It was also evident that ABP tended to fall further in the latter part of hypoxia over the time when ventilation, HR and CBF were falling. Thomas & Marshall proposed that this pattern of response would lead to a positive feedback loop and to death caused by respiratory failure, and cardiovascular collapse (see below for further discussion).

1.7.4 Reflex changes induced by acute systemic by hypoxia

Consiering the mechanisms underlying the pattern of respiratory and cardiovascular response described above, the hyperventilatory response to acute systemic hypoxia is attributable to stimulation of the peripheral chemoreceptors (Marshall, 1994). Moreover, a series of studies performed by Marshall and colleagues demonstrated some of the mechanisms underlying the other components of the biphasic response

in the rat. It should be noted that at the time these studies were performed it was well established from experiments on dogs and cats, that hyperventilation evoked by peripheral chemoreceptor stimulation can lead to tachycardia evoked by lung stretch receptor stimulation, hypocapnia and increased central respiratory drive, and that this tachycardia can override the reflex bradycardia that is the primary reflex response to stimulation of the peripheral chemoreceptors, (Sapru & Krieger, 1977; Marshall, 1987; Daly, 1997). It was also known that in the dog, stimulation of lung stretch receptors and hypocapnia evoked reflex vasodilatation predominantly in skeletal muscle.

1.7.5 Interactions between respiratory and cardiovascular responses to acute hypoxia

On testing the hypothesis that lung stretch receptor afferent stimulation underlies the initial tachycardia observed in acute hypoxia, Marshall & Metcalfe (1988a) demonstrated that in the rat, after vagotomy, when both lung stretch afferents and cardiac vagal efferents are sectioned, the tachycardia response remained intact. Further, hyperinflation induced by exerting positive pressure, to experimentally stimulate the lung stretch receptors, failed to induce significant tachycardia(Marshall & Metcalfe, 1988b). Moreover, addition of 300-400 p.p.m SO_2 to the inspirate of spontaneously breathing, anaesthetised rats, which selectively inhibits pulmonary stretch receptors, had no effect on the hypoxia-induced tachycardia (Marshall & Metcalfe, 1988a). Finally, administration of guanethidine, which depletes sympathetic nerve terminal variscosities considerably blunted the tachycardia, suggesting the simple conclusion that it was mainly sympathetically-mediated, rather than due to

inhibition of cardiac vagal activity. Taken together these findings indicated that lung stretch receptor stimulation makes little or no contribution to the tachycardia induced by acute systemic hypoxia in the rat.

Further, Marshall & Metcalfe (1988a), showed that when eucapnia was maintained during systemic hypoxia in the rat by adding CO_2 to the inspirate, tachycardia still occurred during hypoxia but it was attenuated, whereas bradycardia occurred in severe hypoxia. Further, during bilateral pneumothorax and constant ventilation, hypoxia evoked an attenuated initial tachycardia, followed by secondary bradycardia (Thomas & Marshall, 1994). Taken together, these results indicated that hypocapnia secondary to the chemoreceptor-induced hyperventilation contributes to the initial tachycardia of acute systemic hypoxia, but that the tachycardic effect of central inspiratory drive on cardiac vagal and cardiac sympathetic activities is also important. Although it could be surmised that bradycardia as a primary response to peripheral chemoreceptor stimulation contributes to the secondary bradycardia, the local effect of hypoxia on the heart could not be excluded. See below for further discussion.

Importantly, it should be noted that none of the experimental interventions used to interfere with lung stretch receptors or P_aCO_2 had significant effects on the hypoxia-induced fall in ABP or vasodilatation in the hindlimb muscle in the rat. Thus, there was no reason to suppose that lung inflation or hypocapnia secondary to hyperventilation induced reflex vasodilatation in skeletal muscle in the rat, as was shown in the dog (Daly, 1997). Further, it should be noted that peripheral chemoreceptor stimulation is generally considered to evoke a reflex increase in

sympathetic nerve activity to all major vascular beds, including skeletal muscle, intestine and kidney which leads to vasoconstriction (see Marshall, 1994). Thus, the vasodilatation seen in these vascular beds during hypoxia can not be explained as a primary response to hypoxic stimulation of peripheral chemoreceptors. This raised the possibility that local factors contributed to the peripheral vasodilator response, and indeed to the fall in ABP and to the secondary bradycardia.

Considering the cerebral vascular responses, it may also be noted that in the cerebral circulation the hypocapnia secondary to hyperventilation may limit the cerebral vasodilatation of systemic hypoxia (Thomas & Marshall, 1994). There is however, much evidence that local hypoxia *per se* is responsible for cerebral vasodilatation in systemic hypoxia (Kontos *et al.*, 1978; Berne *et al.*, 1981). The secondary fall in CBF that occurs during more prolonged systemic hypoxia (see above) was attributed to arterial pressure falling below the cerebral autoregulatory range (Thomas *et al.*, 1994b)

1.8.1 The role of local factors in hypoxia

Berne and colleagues (Berne *et al.*, 1983) published a review of early evidence indicating that adenosine is released in heart, skeletal muscle and brain when O_2 demand outstrips O_2 supply, and that adenosine is an important mediator of vasodilatation in coronary, skeletal muscle and brain vasculature during increased cardiac work, or during local hypoxia (Berne *et al.*, 1983). There is also evidence that adenosine can act on the sino-atrial node to produce bradycardia (Belardinelli *et al.*,

1988), and within the brain to produce hypoventilation (Eldridge *et al.*, 1984). These pieces of information led Marshall and colleagues to carry out extensive work to investigate the role of adenosine in systemic hypoxia.

In light of evidence available at the time, Neylon & Marshall, (1991) hypothesised that adenosine contributes to the secondary hypoventilation, bradycardia, and vasodilatation in cerebral and peripheral vascular beds induced by acute systemic hypoxia. Thus, they used theophylline, an adenosine receptor and phosphodiesterase (PDE) inhibitor which is used clinically, and 8-phenylthelophyline (8-PT), a selective adenosine receptor antagonist, which has negligible PDE activity. Both antagonists, in anaesthetized rats, abolished the secondary hypoventilation, secondary bradycardia, the muscle vasodilatation and the cerebral vasodilatation indicating that adenosine plays an important role in all of these components of the response. The results also suggested that theophylline acts predominantly by blocking adenosine receptors, rather than by inhibiting PDE.

These experiments were extended by Thomas and Marshall (1994b). They tested the effect of 8-PT on artificially ventilated rats during 10 min periods of acute hypoxia. Under these conditions, 8-PT did not prevent the secondary bradycardia. Thus, it seems from these results that a major role of adenosine is in inhibiting ventilation, and that when secondary hypoventilation occurs in the spontaneously breathing animal, bradycardia occurs as a consequence of this. This conclusion was compatible with other findings by the same authors, in that 8-SPT (8-sulfophenyltheophylline), a selective adenosine receptor antagonist that cannot cross

the blood brain barrier, had no effect on the pattern of ventilatory response to hypoxia, nor the secondary bradycardia, (Thomas & Marshall, 1994).

On the other hand, evidence that adenosine is released locally within the brain and acts directly on cerebral vessels to cause vasodilatation in hypoxia, has been provided by several studies which have shown that local application of adenosine receptor antagonists attenuate hypoxia-induced cerebral vasodilatation (Berne *et al.*, 1981; Morii *et al.*, 1987; Coney & Marshall, 1998). Further, there is much evidence that in skeletal muscle, locally-released adenosine makes a major contribution to the muscle vasodilatation of acute systemic hypoxia, including evidence gained from local application (Mian & Marshall, 1991).

Considering skeletal muscle in more detail, Skinner & Marshall (1996), showed in anaesthetized rats, that the NO-synthesis inhibitor NG- Nitro-L-arginine methyl ester (L-NAME) decreased baseline femoral vascular conductance (FVC; the femoral vascular bed mainly comprises that of skeletal muscle) in anaesthetised rats, attributable to blockade of the tonic dilator influence of NO. L-NAME also reduced the increase in FVC induced by systemic hypoxia by ~80%, and that induced by adenosine infusion by ~50%. This suggested that the adenosine component of hypoxia-induced muscle vasodilatation is NO-dependent and that there is an additional component that is NO-dependent but adenosine-independent (Skinner & Marshall, 1996).

Subsequently, Bryan & Marshall (1999a), showed that although simulation of adenosine A_1 and A_{2A} receptors contributes equally to muscle vasodilatation induced by infusion of exogenous adenosine, only blockade of A_1 adenosine receptors attenuated the increase in FVC induced by hypoxia, by ≈50%. They concluded that in the setting of acute systemic hypoxia, the A_{2A} adenosine receptors are not stimulated, and it is the A_1 receptor which is important (Bryan & Marshall, 1999a, b). They hypothesised that the disparity between the effects of exogenous adenosine and systemic hypoxia is attributable to the different location of A_1 and A_{2A} receptors, and/or the fact that A_1 receptors have greater sensitivity to adenosine; the EC_{50} for adenosine at the A_1 receptor is 0.31μM, and 0.73μM at the A_{2A} receptor (Fredholm *et al.*, 2001).

In a second study, Bryan & Marshall (1999b) showed that the increase in FVC induced by infusion of both selective A_1 and A_{2A} receptor agonists are almost entirely NO-dependent, and were attenuated by glibenclamide, a K_{ATP} channel blocker. This extended the earlier finding that glibenclamide reduced the initial part of the increase in FVC induced by systemic hypoxia, and strengthened the hypothesis that the adenosine-mediated component of muscle vasodilatation in hypoxia is initiated by opening of K_{ATP} channels triggered by adenosine A_1 receptor stimulation (Marshall *et al.*, 1993).

Building on all of the above, Ray *et al.*, (2002) showed *in vitro* that adenosine can release NO from endothelium of rat aorta and iliac artery by stimulating either A_1 or A_{2A} receptor subtypes, as measured by an NO sensitive electrode. Further, Ray &

Marshall, (2005) showed that both adenosine infusion and systemic hypoxia cause significant release of NO in the venous efflux of skeletal muscle, and this was blocked by L-NAME or blockade of adenosine A_1 receptors. Together these findings led to the conclusion that the role of the adenosine in skeletal muscle during hypoxia is via the A_1 receptor and is NO-mediated.

1.8.2 Other vasodilator factors in skeletal muscle during systemic hypoxia

In light of the fact that prostaglandin (PG) synthesis inhibition can reduce hypoxia-induced vasodilatation of isolated skeletal muscle arterioles *in vitro (*Messina *et al.,* 1992*)*, the role of prostaglandins in the response to systemic hypoxia was also investigated. Ray *et al.*, (2002) showed that cyclooxygenase (COX) blockade with indomethacin reduced systemic hypoxia-induced muscle vasodilatation, as well as that of exogenous adenosine infusion. Further, diclofenac, another COX inhibitor, attenuated muscle vasodilatation induced by infusion of an adenosine A_1 receptor. This *in vivo* evidence was consistent with *in vitro* findings made on excised aorta which showed that the A_1, but not the A_{2A} component of adenosine-mediated NO release was sensitive to diclofenac, and that A_1 receptor stimulation caused PGI_2 synthesis release from the excised rat aorta.

Further studies by Ray & Marshall, (2006) on the aorta showed that by acting on A_1 receptors, adenosine evokes K_{ATP}-channel-induced Ca^{2+} influx which stimulates PLA_2 to liberate arachadonic acid (AA) from the plasma membrane, and so increases COX production of diffusible PGI_2. Their evidence suggested that PGI_2 acts back on IP receptors in the endothelial cell membrane, and hence produces an increase in

$[cAMP]_i$ which stimulates phosphorylation of eNOS by PKA, so releasing NO. There may also be a component of A_1 receptor-induced NO synthesis which is directly dependent on an increase in $[Ca2+]_i$, increasing eNOS-derived NO production, although the fact that A_1-mediated NO release is virtually abolished by COX inhibition suggests this is unlikely (Ray & Marshall, 2006).

1.8.3 NO-mediated adenosine release

Importantly, there is also evidence that NO plays a crucial role in adenosine release from endothelial cells during systemic hypoxia. At the mitochondrial cytochrome oxidase of endothelial and other cells, NO competes with molecular O_2 for the same binding site (Clementi *et al.*, 1999), and causes inhibition of ATP regeneration (Brown & Cooper, 1994; Cleeter *et al.*, 1994; Schweizer & Richter, 1994). Following this up, Edmunds *et al.*, (2003) provided evidence that during systemic hypoxia, the decrease in the O_2 available to compete for the binding site on mitochondrial cytochrome oxidase during systemic hypoxia allows a relative increase in binding of the NO that is tonically generated by shear stress, increasing adenosine release, presumeably as a result of mitochondrial inhibition. Thus, they showed that hypoxia-induced, or adenosine-induced vasodilatation in the hindlimb could both be significantly attenuated by blockade of NOS with L-NAME, and adenosine- and hypoxia-induced vasodilatation were both restored when an NO donor was infused at a rate sufficient level to restore baseline FVC, and thus tonic levels of NO. However, hypoxia-induced vasodilatation was not restored by infusion of cGMP, the second messenger for NO signalling. This indicated that NO is required for adenosine to be released by hypoxia, whereas adenosine can act to produce vasodilatation providing the cGMP

level is sufficiently high. Accordingly, in a perfused system of cultured aortic endothelial cells grown on microbeads, DETA-NO, an NO donor was able to cause adenosine release, in an L-NAME resistant manner, whereas bradykinin (BK) and agonist that is known to increase NO synthesis caused release of NO that was blocked by L-NAME. This suggested that the NO mimics hypoxia sensing in these cells (Edmunds *et al.*, 2003). A detailed overview of them mechanisms by which adenosine, NO and prostaglandins interact in endothelial and vascular smooth muscle signaling is provided in Figure 1.

1.8.4 Summary of the effects of acute systemic hypoxia

Acute systemic hypoxia in the anaesthetised rat causes hyperventilation and an associated fall in P_aCO_2. It also causes transient tachycardia and vasodilatation in several major vascular beds, including skeletal muscle and brain, and is associated with a fall in ABP. As acute systemic hypoxia progresses, there is waning of the hyperventilation and the initial tachycardia. ABP tends to fall further and CBF falls. The secondary hypoventilation, bradycardia, muscle and cerebral vasodilatation have been attributed to local effects of adenosine released by brain and skeletal muscle.

The majority of the studies described above were carried out in rats. However, studies in humans have demonstrated that similar mechanisms are evoked by acute systemic hypoxia in terms of interactions between NO and adenosine and prostaglandins (MacLean *et al.*, 1998), and the role of NO (Mortensen *et al.*, 2007; Mortensen *et al.*, 2009a; Mortensen *et al.*, 2009b; Nyberg *et al.*, 2010). No studies have examined the effects of chronic hypoxia *in utero* on the pattern of respiratory

and cardiovascular response to acute systemic hypoxia, or whether the mechanisms of vasodilatation induced by hypoxia are altered following this adverse *in utero* environment. This issue is of particular interest because chronic hypoxia from birth *does* change the responses evoked by acute hypoxia.

1.8.5 Chronic Hypoxia from Birth

After birth, there is normally a change from the fetal response to acute systemic hypoxia which includes inhibition of breathing movements *in utero* (Rudolph, 1984; Giussani *et al.*, 1994), to the adult response which allows hyperventilation (Hanson *et al.*, 1989). But, work in cats and rats showed that chronic hypoxia from birth (CHB, induced by rearing the newborn in 12%O_2) delays the onset of the reflex hyperventilatory responses to acute hypoxia, in part by impeding the normal increase in peripheral chemoreceptor sensitivity to hypoxia, but also by impairing disappearance of the central inhibitory effects of hypoxia (Eden & Hanson, 1987a; Landauer *et al.*, 1995). Further, by experiments on rat pups that were similarly made chronically hypoxic from birth (CHB rats), Thomas and Marshall (1995) showed that at 8 weeks of age CHB rats not only showed an accentuated secondary hypoventilation, but also accentuated secondary bradycardia relative to the N rat, when breathing 8%O_2 for 10 minutes. Concomitantly, they showed muscle vasodilatation and cerebral vasodilatation, but in contrast to N rats, CHB rats showed a progressive fall in CBF (see chapter 3 for further detail). In other words, CHB rats showed accentuation of the components of the response to acute hypoxia that lead to a positive feedback loop which may eventually lead to respiratory and circulatory collapse. Indeed, Thomas & Marshall, (1995) proposed that this may be the

mechanism behind cot death in human infants. Interestingly, the adenosine receptor antagonist 8-PT attenuated the secondary hypoventilation and secondary bradycardia in CHB rats as in N rats, but had no effect on hypoxia-induced muscle or cerebral vasodilatation in hypoxia. Therefore, it seems that adenosine does not explain vasodilatation of acute hypoxia in CHB rats. This raises the question as to whether similar changes occur as a consequence of chronic hypoxia in utero. This is further examined in Chapter 3.

1.8.6 Reactive O_2 species and cardiovascular disease

Reactive O_2 species have recently become an important focus of research into the origins of cardiovascular disease. O_2 free radicals, such as superoxide anions ($O_2^{-\cdot}$) and $NO^{\cdot}$, as well as other reactive O_2 species such as peroxynitrite ($ONOO^-$) and hydrogen peroxide (H_2O_2) are now recognised to be important in modulating cell signaling pathways (Cai & Harrison, 2000). However, accentuated production of reactive O_2 species (ROS) is implicated in atherosclerotic plaque generation, insulin resistance, and in impaired endothelium-dependent vasodilatation with hypertension, aging and the menopause (Mugge *et al.*, 1991; Taddei *et al.*, 2001).

At a molecular level, O_2^- has high affinity for bioactive NO. Indeed, O_2^- has at least 3 times higher affinity for NO than for the enzyme superoxide dismutase (SOD), which dismutes this potent oxidative molecule into the less potent H_2O_2. Thus, excessive levels of O_2^- not only result in increased interaction of O_2^- and NO, to produce the potentially damaging molecule, peroxynitrite ($ONOO^-$), but also reduce the

bioavailability of NO, and thus its dilator influence. Since SOD is very important in regulating the final concentration of O_2^- generated by all sources, some attention is given below to the functioning of SOD, before considering the sources of O_2^-.

1.8.7 Superoxide Dismutase (SOD)

The SODs are a family of three metalloenzymes, which dismute the O_2^- into O_2 and H_2O_2. The SOD1 isoform, Cu-Zn-SOD, exists predominantly in the cytosolic compartment, while SOD2, or Mn-SOD, is mitochondrial. SOD3, another Cu-Zn-SOD, is found in the extracellular space as well as plasma and hence, is often known as ecSOD; it is also found in the space between the endothelium and vascular smooth muscle. The ecSOD in the endothelium-vascular smooth muscle space is very important as it is this space that NO must traverse to reach vascular smooth muscle cells (VSMCs). Thus, ecSOD can essentially regulate NO bioavailability for the vascular smooth muscle through modulation of O_2^- levels (Jung *et al.*, 2003; Nozik-Grayck *et al.*, 2005).

It has been shown that NO also regulates ecSOD expression in cell lines of VSMCs, in that increased NO levels upregulated ecSOD expression (Fukai *et al.*, 2000). This relationship has been confirmed *in vivo* in that eNOS-/- mice have low levels of ecSOD. Thus, it was concluded that the relationship between NO and SOD acts as a feed-forward mechanism that protects against increased NO production while the NO crosses the extracellular space *en route* to adjacent VSMCs. In further support of this relationship, the same group demonstrated that exercise training in mice not only increased eNOS protein expression, but was associated with increased ecSOD

protein expression. In contrast, in $eNOS^{-/-}$ mice, and hence in the absence of endothelial derived NO, exercise had no effect on ecSOD expression, showing the importance of normal interaction of NO with ecSOD (Fukai *et al.*, 2000).This interaction is important when considering potential sources of increased generation of ROS and the effect this may have on cardiovascular function.

1.8.8 Sources of ROS

There are several sources of ROS, particularly of the superoxide anion ($O_2^{\cdot-}$), that have been implicated in cardiovascular pathology. These are reviewed below.

Xanthine Oxidase

Xanthine Oxidase (XO) is an enzyme that is highly localized to the vascular endothelium, and can exist in its XO form as well as Xanthine Dehydrogenase (XD). The XO form metabolises hypoxanthine, which is a product of adenosine metabolism, into xanthine and uric acid, and this step is coupled to the generation of a superoxide anion (O_2^-). It has been demonstrated that there is increased O_2^- production in aortae of the spontaneously hypertensive rat, which is attributable to XO metabolism of hypoxanthine, for the O_2^- production was reversed by the XO inhibitor oxypurinol (Nakazono *et al.*, 1991). Adenosine is of course implicated in the muscle and cerebral vasodilator response to acute hypoxia, and thus, this is a potential source of O_2^- in systemic hypoxia.

NAD(P)H Oxidase

The non-phagocytic form of the multi-subunit, membrane-bound enzyme NAD(P)H Oxidase (Nox) has also been recognized as a source of vascular ROS and increased levels of Nox-derived ROS have been implicated in vascular aging (RodrÌguez-MaÒas *et al.*, 2009). However, Nox-derived ROS have also been shown to be integral to healthy physiological vascular regulation (For review see Paravicini & Touyz (2006, 2008). For example, vasodilatation induced by bradykinin in coronary arterioles has been attributed to H_2O_2 derived from O_2^- (Larsen *et al.*, 2009). Increased Nox derived ROS has been demonstrated with angiotensin II or thrombin stimulation in rat vasculature (Rajagopalan *et al.*, 1996). The role of Nox-derived ROS in normal vascular regulation, and in vascular pathology have been discussed by many authors (Paravicini & Touyz, 2006, 2008). The role of Nox-derived ROS in systemic hypoxia have received little attention in young or older individuals.

Mitochondrial respiratory chain

It has long been accepted that the mitochondrial respiratory chain generates reactive oxygen species. The role of these free radicals is still not completely clear, and it appears that they have both intra- and extra-mitochondrial activities. In cardiac myocytes, significant numbers of mitochondria-derived superoxide anions can escape the mitochondrial membrane into the cytoplasm, indicating that their role could be either within or outside the mitochondria (Nohl & Hegner, 1978). There is also significant evidence that they are involved in O_2 sensing in pulmonary artery vascular smooth muscle cells (PAVSMCs) and therefore in hypoxia-induced pulmonary vasoconstriction: H_2O_2 derived from mitochondrial SOD stimulates membrane bound K_{ATP} channel opening (Moudgil *et al.*, 2005).

As described above, Clementi *et al.*, (1999) demonstrated that NO can inhibit mitochondrial complex IV (cytochrome c oxidase). Further, there is evidence in isolated mitochondria that inhibition of mitochondrial complex IV facilitates O_2^- generation at complex I and III (Dawson *et al.*, 1993). Thus, there is a clear possibility that hypoxia-induced NO production not only inhibits mitochondrial complex IV so leading to decreased ATP synthesis and adenosine release (Edmunds *et al.*, 2003), but also increases complex I- and III-derived O_2^-.

Cyclooxygenase

Kukreja *et al.*, (1986) demonstrated the capacity for prostaglandin H synthase to produce the superoxide anion, and Holland *et al.*, (1990) showed that BK stimulation of human endothelial cells resulted in superoxide production that was partly sensitive to cyclooxygenase inhibition. As indicated above, stimulation of endothelial COX by adenosine A_1 receptors is an integral part of the mechanism by which acute hypoxia causes muscle vasodilatation. Thus, COX is another potential source of O_2^- in acute hypoxia.

Endothelial nitric oxide synthase - eNOS

The endothelial isoform of the NOS family, eNOS, is a dimer, the first subunit of which catalyses the hydroxylation of L-Arginine to form NG-hydroxy-L- arginine. The second subunit transfers an electron from NADPH onto the hydroxylated L-arginine to form L-citrulline and NO (Andrew & Mayer, 1999). It is this electron transfer step that gives eNOS the capability to generate O_2^-, for when the two subunits become

unlinked, or uncoupled, the electron that is normally transferred from NADPH to form the NO free radical is instead transferred to molecular O_2 to form the O_2^-. Uncoupling usually occurs in states in which availability of the cofactor tetrahydrobiopterin (BH_4) or the substrate L-arginine are decreased (Andrew & Mayer, 1999).

For example, Landmesser *et al.*, (2003) used lucigenin-fluorescence to monitor O_2^- production and demonstrated an increase in ROS production in arterial vessels taken from rats with deoxycorticosterone acetate (DOCA) salt-induced hypertension, compared to normal rats, and the ROS production was sensitive to NOS inhibition. However, while the $nNOS^{-/-}$ mouse shows a similar increase in ROS production during DOCA salt-induced hypertension, the $eNOS^{-/-}$ mouse does not, indicating that the increased ROS production is probably due to uncoupled eNOS. Accordingly, measurements of BH_4 content, and its oxidized counterpart BH_2 in homogenized aorta, demonstrated increased BH_2 and decreased BH_4 content in those isolated from the DOCA salt-treated mice, relative to the sham operated mice, whereas dietary supplementation with BH_4 substantially reduced O_2^- production. These findings led to the cascade hypothesis of hypertension, which proposes that increased ROS production by Nox and NO production by eNOS, leads to increased levels of $ONOO^-$. Both $ONOO^-$, and the O_2^-, oxidize BH_4, reducing the bioavailability of this cofactor for eNOS, so leading to its uncoupling, and perpetuating O_2^- production, and hence endothelial dysfunction (Landmesser *et al.*, 2003)

Landmesser *et al.*, (2003) also demonstrated that arteries from DOCA salt-treated hypertensive rats, which already showed impaired endothelium-dependent

vasodilatation, were more dependent on H_2O_2 for this vasodilatation than control rats. Thus, there was a further reduction in endothelium-dependent vasodilatation on catalase treatment in DOCA salt-treated rats, which was not observed in controls. This suggests that the increased production of O_2^- is to some extent compensated by the action of SOD-mediated production of H_2O_2, effectively masking the underlying vascular dysfunction, which may well be more severe than many measurements of endothelial dysfunction currently suggest (Landmesser *et al.*, 2003).

There is also evidence that whereas phosphorylation of eNOS in its coupled state by various agonists results in increased NO production, phosphorylation of the uncoupled eNOS results in an increase in O_2^- production (Chen *et al.*, 2008).

Given that activation of eNOS is an integral part of the muscle vasodilator response to systemic hypoxia, questions arise as to whether eNOS activation also generates O_2^- and/or whether the ability of eNOS to generate O_2^- in hypoxia may be facilitated by O_2^- generated from other sources by uncoupling of eNOS, and/or whether the effects of O_2^- in hypoxia are regulated by SOD.

1.8.9 The role of reactive oxygen species in the response to acute systemic hypoxia

With the knowledge that reactive oxygen species can be produced by several systems involved with vacular regulation (see above), Pyner *et al.*, (2003) sought to assess the role of free radicals in muscle vasodilatation of systemic hypoxia. Focusing initially on the role of XO, as hypoxia can increase conversion of XD to XO, which acts to metabolise adenosine (Kayyali *et al.*, 2001), they showed that inhibition

of XO with oxypurinol decreased the magnitude of hypoxia-induced muscle vasodilatation induced by a 5 minute period of systemic hypoxia, whilst infusion of exogenous SOD increased the magnitude of the muscle vasodilatation. These results suggested that O_2^- derived from XO during hypoxia is dismuted by endogenous SOD to H_2O_2, which then contributes to the muscle vasodilatation. The fact that exogenous SOD enhanced hypoxia-induced muscle vasodilatation suggested that excess O_2^- were generated during hypoxia which decreased the bioavailability of dilator NO by forming $ONOO^-$, or that O_2^- were generated by uncoupled eNOS. That acute systemic hypoxia can generate ROS was supported by the observation that the application of dihydroethidium (DHE) to the spinotrapezius muscle *in vivo* allowed ethidium fluorescence to be seen in and around endothelial cells of vasculature at the end of a 5 minute period of hypoxia (Pyner *et al.*, 2003). DHE is converted to ethidium bromide in the presence of ROS and is particularly sensitive to O_2^-.

1.9 Developmental Programming

There is extensive evidence that a sub-optimal environment *in utero* leads to vascular dysfunction in adult offspring, both at the endothelial and smooth muscle level, which may, or may not lead to hypertension (Byrne & Phillips, 2000; Franco *et al.*, 2003b). In the western human population, preeclampsia (PE) is a leading cause of intra uterine growth restriction (IUGR) and it is well known that PE is either caused by, or causes, reduced uterine perfusion (Page (1939), see Roberts and Gammill (2005) or Alexander (2007) for recent review). IUGR is a major risk factor for later

disease in the child. The potential mechanisms, and methods of modeling this complex syndrome and its consequences are discussed below.

1.9.1 The role of nutrition in programming

In 1944-45, for 15 months, in a localized region of Holland, the Dutch population ate rations that accounted for less than a quarter of their recommended daily intake, because they were sieged by the Nazis. The offspring born of pregnancies during this period, known as “the Dutch famine,” have been extensively studied to investigate the role of maternal nutrition on health outcomes (Barker, 1991; Barker, 1995; Barker, 1998). Amongst many other observations, it has been found that coronary artery disease was diagnosed, on average, 3 years earlier in this group, compared to age-matched controls, clearly demonstrating a link between the prenatal environment and cardiovascular pathology in adult life (Painter, 2006; Painter *et al.*, 2006). In fact, so extensive are studies of this cohort, and the many other cohorts that have been studied as a result of this seminal work that the term ‘The Barker Hypothesis’ is now widely used. The volume of work in this area has increased so much that recently the Journal of the Developmental Origins of Health and Disease (J DOHAD) began print. It publishes epidemiological work and papers resulting from the vast amount of basic scientific studies designed to elucidate the mechanisms underlying these epidemiological observations in models of such diseases. Further, such is the importance of this work that recently ‘Horizon: The nine months that made you’ was aired on BBC2, bringing about much increased public awareness of the consequences of a poor fetal environment.

In order to investigate the underlying mechanisms of this epidemiological link, various animal models of nutritional programming have been developed using *in utero* protein restriction in pregnant rats. In such studies, Torrens et al., (2003) showed impaired endothelium-dependent vasodilator function in mesenteric resistance vessels in adult rats that had been exposed to protein restriction *in utero* throughout pregnancy. They observed reduced sensitivity to ACh and to isoprenaline from a preconstricted state in an isolated vessel myography set up of resistance vessels, but also that conduit vessel (aorta) function was not affected by maternal protein restriction (Torrens *et al.*, 2003).

In a study using the same model of nutritional programming, Rodford *et al*., (2008), sought to elucidate the role of O_2^- in attenuating endothelium-dependent vasodilatation, by assessing the responses of isolated mesenteric resistance vessels to ACh in the presence of the free radical scavenger tempol (Rodford *et al.*, 2008). They concluded that endothelial dysfunction could not be simply explained by increased O_2^- generation, as Tempol had no effect on responses evoked by ACh in mesenteric vessels from programmed rats. However, they did demonstrate reduced antioxidant enzyme expression in the liver of the rats suggesting that they may have reduced antioxidant protection at a systemic level. They therefore proposed that they may be more susceptible to damage from physiological levels of ROS (Rodford *et al.*, 2008).

On the other hand, Franco and colleagues have demonstrated increased Nox-derived O_2^- generation in mesenteric arterioles in adult female Wistar rat offspring

from pregnant rats who were fed 50% of the dietary intake of matched controls. These animals also became hypertensive by 14 weeks of age. Further, by using intravital microscopy to measure the diameter of second order mesenteric arterioles, they found that either the cell permeant SOD mimetic MnTMPyP or apocynin, which inhibits Nox, significantly improved endothelium-dependent vasodilatation. They also showed increased presence of O_2^- in these vessels in the absence of increased SOD activity, and which is reversed by blocking Nox (Franco *et al.*, 2003a; Franco *et al.*, 2007).

At 1 year of age, Sathishkumar et al., (2009) found that the female rat offspring from protein restricted pregnancy were hypertensive relative to the control rat. At this stage the programmed rat showed impaired endothelium-dependent responses to ACh, and reduced basal and agonist stimulated nitrate/nitrite production, concurring with other studies indicating endothelial dysfunction, and supporting the idea that hypertension also develops with age following *in utero* insult.

In another study Brawley et al., (2003), examined male rat offspring from the same model of protein-restricted pregnancy used by Torrens et al., (2003), at 87 and 164 days of age. More generalised vascular dysfunction was found, both at the endothelial and vascular smooth muscle level, and in terms of responses to vasoconstrictors and vasodilators. These programmed male rats developed hypertension when compared to normal controls, as measured in the conscious animal at 130 days of age.

Thus, studies such as those described above consistently demonstrate endothelial dysfunction in offspring of general- and protein-nutrient restricted pregnancy. Although the exact underlying mechanisms differ slightly between studies, there is a strong running theme of oxidative stress.

1.9.2 Models of developmental programming

Many animal models of developmental programming centre around the production of the IUGR phenotype that is known to lead to increased rates of cardiovascular disease. In pregnant sheep, there are at least five models which are well characterised and which lead to IUGR; placental carunclectomy, partial placental embolization, maternal hyperthermia, umbilical artery ligation and maternal overfeeding following embryonic transplant into and adolescent ewe (See Morrison et al., 2008 for review). Each model has its limitations, and produces the IUGR phenotype in different ways. Placental embolization is known to induce fetal hypoxaemia (Murotsuki *et al.*, 1996), as does single umbilical artery ligation (Supramaniam *et al.*, 2006) and uterine carunclectomy (Edwards *et al.*, 1999), although in all cases this is concomitant with nutrient restriction and activation of the hypothalamic-pituatary-adrenal (HPA) axis. A sixth, different model in sheep involves the pregnant ewe undergoing gestation at high altitude, as used by Hererra and colleagues (Herrera *et al.*, 2007), although this has involved sheep which have spent at least 50 generations at altitude. There is a similar Llama model used by Llanos and colleagues, for the Llama is a species genetically adapted over many generations to living at high altitude (Llanos *et al.*, 2003).

The hypoxic chick egg model has also been used to eliminate the secondary effects of reduced dietary intake on the pregnant mother, and has been studied by groups led by Le Noble, De Mey and Giussani (Ruijtenbeek *et al.*, 2000; Rouwet *et al.*, 2002; Giussani *et al.*, 2007). However, no studies to date have examined the long term effects of hypoxia *in ovo* in chickens, they have tested only the consequences at the pre-hatching stage.

More useful for mechanistic studies, particularly for studies of the offspring, are rodent models, because rodents have a short life span relative to longer-living species such as sheep. Maternal protein or nutrient intake restriction are used by many laboratories to induce IUGR in rodents as indicated above (Langley & Jackson, 1994; Torrens *et al.*, 2003; Franco *et al.*, 2007). Surgically-induced reductions in uterine perfusion have also been employed, by occlusion of the uterine arteries (Alexander, 2003). The chronic hypoxia *in utero* model of IUGR are used by several research groups to investigate the mechanisms by which hypoxia may lead to IUGR and increase the risk of cardiovascular disease. The main variant in these hypoxic models is the severity and duration of hypoxia within the 21 day gestation period of the rat. Studies by Davidge and colleagues have used 12% inspired O_2 from days 15-21 of pregnancy (Morton *et al.*, 2010), while work by Marshall and colleagues used 12% inspired O_2 from day 11-21 (Coney & Marshall, 2010). Giussani and colleagues used 14% inspired O_2 from days 6-21 of pregnancy (Camm & Giussani, 2010), whilst the earlier work of Rosenfeld used 13-14% inspired O_2 from days 14-21 (Tapanainen *et al.*, 1994).

1.9.3 Chronic hypoxia in utero and fetal programming

It is widely accepted that fetal hypoxaemia induced by chronic hypoxia of the pregnant female is another example of fetal programming of adult cardiovascular function (Louey & Thornburg, 2005). Fetal hypoxia is commonly incurred as a result of placental insufficiency, but also occurs in fetal anaemia and in pregnancy at altitude. Indeed, it is known that in women who are not acclimatized to it, pregnancy at altitude is linked with reduced birth weight of the offspring (Postigo *et al.*, 2009). Moreover, mothers with a lower haemoglobin concentration during pregnancy give birth to children who have higher blood pressure by 4.5 years of age than their counterparts from pregnancies with normal levels of haemoglobin (Law *et al.*, 1991), although recent evidence suggests this may not always be the case (Brion *et al.*, 2008). It is clear that reduced birth weight is associated with increased risk of cardiovascular disease (Painter, 2006), and it is well proven that restriction of substrates during gestation almost always lead to IUGR (Thompson & Weiner, 1999; Bae *et al.*, 2003; Williams *et al.*, 2005b; Morrison, 2008). What is not clear, however, is whether the observed programming effects of hypoxia are caused by hypoxia *per se* or by the possible secondary effects on dietary intake of the pregnant female who is made hypoxic, the endocrine adaptations to such physiological insults, and on placental nutrient transport. It seems clear that both elements of substrate restriction contribute in the hypoxia model, as studies have shown differences in vascular function with and without changes in birth weight even after matching of food intake during pregnancy (Thompson & Weiner, 1999; Williams *et al.*, 2005b). These studies

do not rule out changes that are secondary to changes in makeup of total body weight as the offspring grow.

Williams and colleagues sought to differentiate the effects of chronic hypoxia *in utero* (CHU) and the secondary effects on of reduced maternal dietary intake. They compared rats born of normal pregnancies (N rats) to rats exposed to chronic hypoxia *in utero* (d15-21, CHU rats), and rats exposed to normoxia *in utero*, but the same level of maternal dietary intake seen in the pregnant dams of the CHU group (NR rats). They found that at 4 months of age, mesenteric resistance vessels taken from CHU rats showed attenuated endothelium-dependent vasodilatation compared to control or nutrient restricted (NR) offspring, although by 7 months of age this difference was no longer apparent. However, at 7 months of age, the NOS inhibitor L-NAME caused a significantly smaller reduction in endothelium-dependent vasodilatation in the CHU arteries than the NR or control arteries, indicating that the role of NO was reduced. By using exogenous SOD, to reduce O_2^- levels, they showed that SOD had no effect on endothelium-dependent relaxations in mesenteric arteries of N rats. By contrast, in CHU arteries SOD significantly enhanced relaxations induced by low concentrations of methacholine, such that it reduced the EC_{20}, but had no effect on relaxations induced by higher concentrations. Therefore they suggested that there may be a small, but significant increase in basal O_2^- generation in the mesenteric arteries of CHU rats, which decreases the role of NO in endothelium-dependent relaxations in the mesenteric circulation. This idea is consistent with the findings made in the protein restriction *in utero* models discussed above, which indicated that *in utero* stressors lead to changes in the oxidative stress

in arterial vessels, so altering NO-related mechanisms. How these described effects translate into changes in functional responses *in vivo* has not been investigated.

Ruijtenbeek et al., (2003) carried out a similar study to Williams et al., (2005b) by using a chick embryo model, in which fertilized hens' eggs were either incubated in 15% O_2 for 14 days of their 21 day gestation, or had 10% of their albumin removed to model protein restriction. The vascular function of the femoral arteries taken from chicks at day 19 of gestation was then assessed. Whilst both conditions led to significant growth retardation, only the chronic hypoxic condition led to vascular dysfunction: reduced arterial sensitivity to ACh in the femoral artery. The mechanisms underlying this dysfunction were not investigated.

Whilst these studies represent further evidence that CHU has programming effects that are distinct from nutritional aspects, it is not clear in this model whether the vascular dysfunction evident at day 19 of gestation persists into adulthood and leads to cardiovascular pathophysiology. Further, it is not clear whether the changes observed in the femoral artery are evident in mammals.

1.9.4 The effect of chronic hypoxia in utero on the sympathetic nervous system

To the authors knowledge, there are no studies examining the effect of chronic hypoxia *in utero* on sympathetic nervous control of the peripheral vasculature in the offspring. Work on the hypoxic chick embryo has found that in the late gestation fetus the femoral artery is hyperinnervated with catacholaminergic neurones relative to control chicks, shown directly (Ruijtenbeek *et al.*, 2000) and functionally (Rouwet *et*

al., 2002). Similarly, Herrera et al (2007) found that isolated femoral arteries taken from newborn sheep from high altitude pregnancies showed increased maximum responses to an α_1-adrenoreceptor agonist and increased maximal response *and* sensitivity to noradrenaline. It was also shown that following placental caruclectomy in sheep, levels of circulating catecholamines in the fetal circulation are higher than in a normal pregnancy throughout late gestation. This has been attributed to increased catecholamine synthesis in developing sympathetic nerves, although no direct evidence for this was produced (Simonetta *et al.*, 1997). However, this finding concurred with similar results in the placental embolization model in the same species (Gagnon *et al.*, 1994). It is of course possible, given the results of Ruijtenbeek et al., (2000) that the increased plasma catecholamine is a consequence of an increased density of sympathetic nerves. What is not clear from current evidence is whether such alterations that are manifest *during* pregnancy persist, or have an effect on the offspring of these adverse pregnancies. To date, nobody has investigated the effect of hypoxia *in utero* on the *in vivo* function of the sympathetic nervous system in adults.

1.10 General aims

The aims of the present study were to examine the effects of CHU on:

1. The pattern of cardiovascular and respiratory response to acute systemic hypoxia.
2. The role of endothelially-derived relaxing factors on baseline cardiovascular regulation, and in the cerebral and skeletal muscle vasculature in response to

acute hypoxia *in vivo,* with particular with respect to NO, adenosine, and reactive oxygen species

3. Sympathetic nerve activity in those fibres that supply skeletal muscle vasculature.
4. Sympathetic innervation density and vascular responsiveness to sympathetic nerve stimulation *in vivo*.
5. Aging of the cardiovascular system in Wistar rats, with particular focus on the mechanisms of sympathetic vasoconstriction.

The particular hypotheses that were tested are explained in the relevant chapters.

Figure 1.1

Schematic representation of the production of vasoactive substances from endothelial cells of the skeletal muscle vasculature, and their interaction with the vascular smooth muscle.

5'AMP – adenosine-5-monophosphate
BK_{Ca} – Calcium-sensitive potassium channel
A1 – adenosine A1 receptor
A2A – adenosine A2A receptor
ATP – adenosine-triphosphate
P2Y – purinergic P_{2Y} receptor subtype
AC – adenylate cyclase
COX – cyclooxygenase
cAMP – cyclic adenosine-monophosphate
eNOS – endothelial nitric oxide synthase
GS – stimulatory G-protein subunit
IP – AC-linked prostacyclin receptor
IP3R – inositol triphosphate receptor
KATP – ATP-sensitive potassium channel
MSB – Myosin-binding subunit
MLCK – myosin light-chain kinase
NO – nitric oxide
PDE3 – phosphodiesterase 3
RBCs – red blood cells
sGC – soluable guanylate cyclase

Adapted from Olsson & Pearson (1990), Merkel et al., (1992), Carvajal et al., (2000) Hofmann et al., (2000) Lynge & Hellsten (2000), Sausbier et al., (2000), Klinger et al., (2002), Edmunds et al., (2003), Rybalkin et al., (2003), Ray & Marshall, (2006), Kass et al., (2007), Sprague et al., (2010).

Figure 1.1

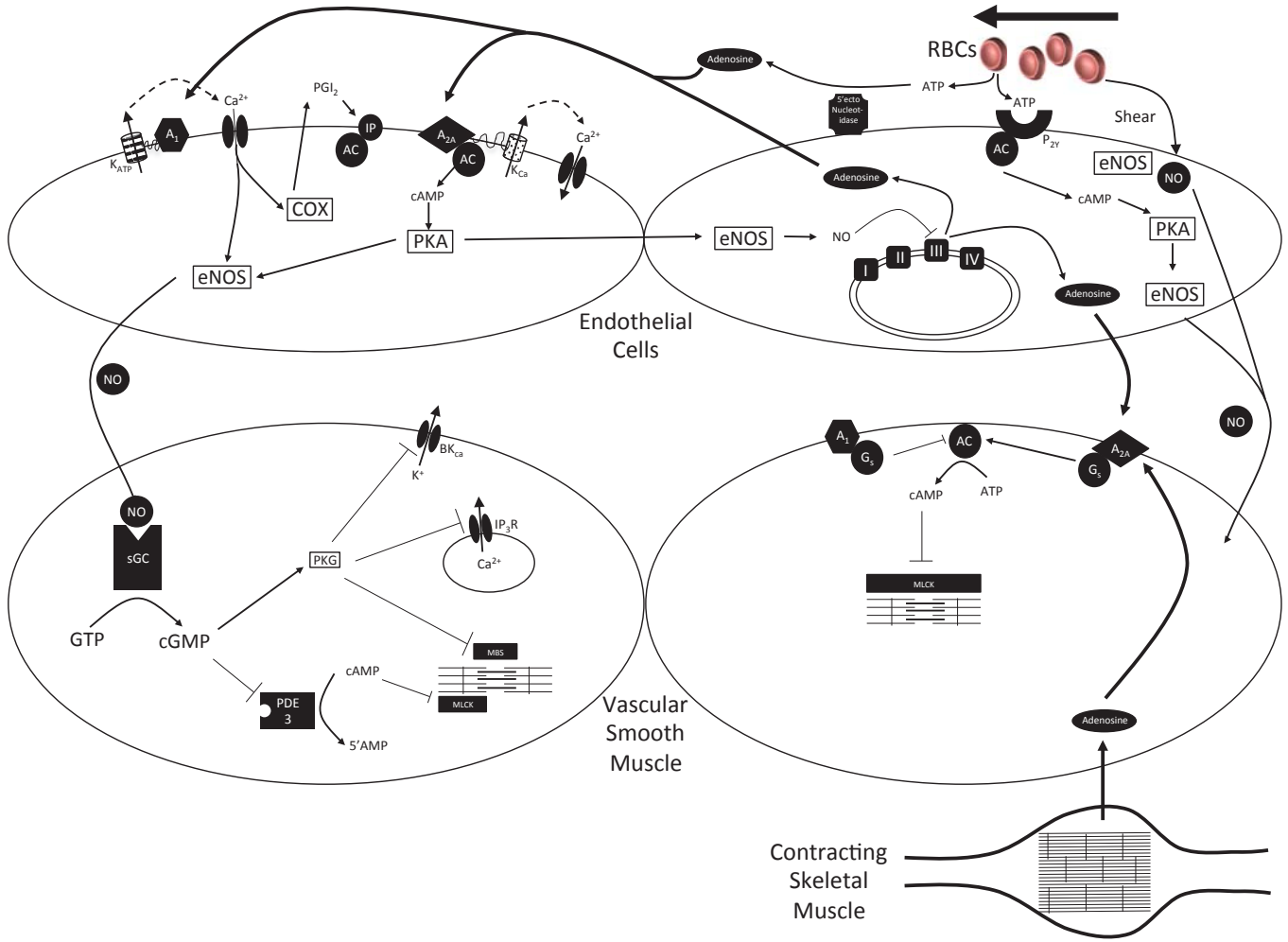
RBCs
ATP
ATP
Shear
Adenosine
5'ecto Nucleot-idase
AC
P2Y
eNOS
NO
cAMP
PKA
eNOS
Adenosine
eNOS
NO
I
II
III
IV
Adenosine
eNOS
Endothelial Cells
NO
A1
Ca2+
PGI2
IP
AC
A2A
AC
Ca2+
KATP
KCa
COX
cAMP
PKA
eNOS
NO
BKca
K+
sGC
PKG
IP3R
Ca2+
GTP
cGMP
MBS
cAMP
PDE 3
MLCK
5'AMP
Vascular Smooth Muscle
A1
Gs
AC
A2A
Gs
cAMP
ATP
MLCK
NO
Adenosine
Contracting Skeletal Muscle

Figure 1.1

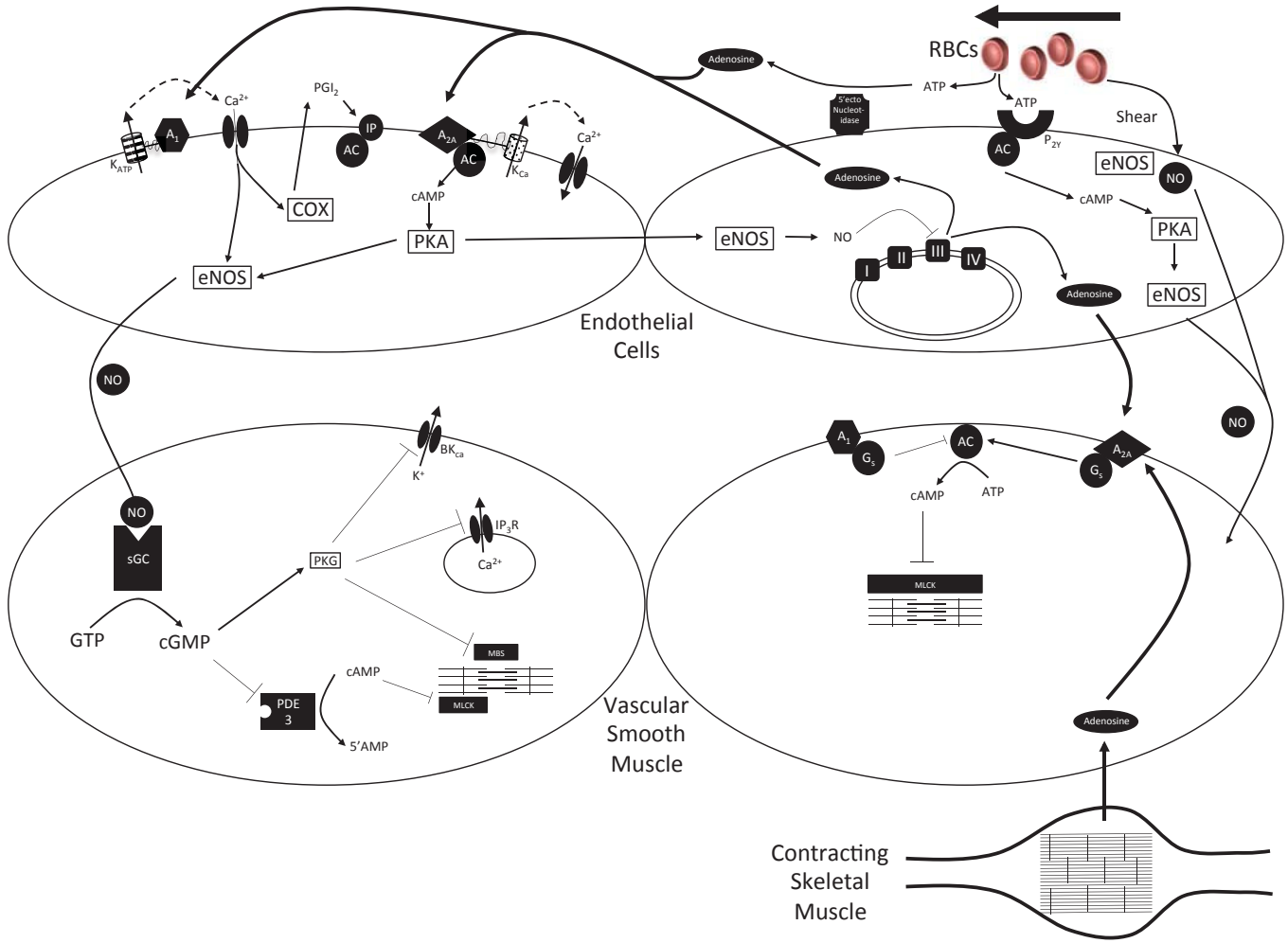
RBCs
ATP
ATP
Shear
Adenosine
5'ecto Nucleot-idase
AC
P_{2Y}
eNOS
NO
cAMP
PKA
eNOS
Adenosine
A_1
K_{ATP}
Ca^{2+}
PGI_2
IP
AC
A_{2A}
AC
Ca^{2+}
K_{Ca}
COX
cAMP
PKA
eNOS
eNOS
NO
I
II
III
IV
Adenosine
eNOS
Endothelial Cells
NO
NO
sGC
GTP
cGMP
BK_{Ca}
K^+
PKG
IP_3R
Ca^{2+}
MBS
cAMP
MLCK
PDE 3
5'AMP
Vascular Smooth Muscle
A_1
G_s
AC
cAMP
ATP
A_{2A}
G_s
MLCK
NO
Adenosine
Contracting Skeletal Muscle

Chapter 2 - General Methods

All experiments were carried out in accordance with the UK Home Office Animals (Scientific Procedures) Act of 1986, under an approved project, site, and personal licence.

2.1.1 Experimental Animals

All animals used in this study are Wistar rats, originally supplied by Charles River Laboratories (Kent, UK). Control normoxic (N) rats used in the studies were predominantly those purchased from Charles River Laboratories as 8-week old male Wistar rats. Three litters of N rats were bred on-site at the Biomedical Services Unit, University of Birmingham from male and female Wistar rats purchased from Charles River Laboratories.

For generation of CHU rats, 'timed-mated' female Wistar rats were purchased from Charles River Laboratories, and delivered to the Biomedical Services Unit, University of Birmingham, 6 days after confirmation of pregnancy by the presence of a vaginal plug. At day 10 of pregnancy the pregnancy rat was placed, within her cage, in a hypoxic chamber, containing 11.5-12.5% O_2 (See below for details). At gestational day 20, the pregnant dam was removed from the hypoxic chamber, and housed in standard laboratory conditions. Pregnant dams gave birth 1 or 2 days following removal from the hypoxic chamber. Chronic hypoxia from days 10-20 of gestation was chosen as it represents a period of gestation as close to that during which, in a human fetus, the adverse effects of preeclampsia are experienced. Previous unpublished work by this laboratory found that chronic hypoxia from days 0-20 was

rarely lead to a completed pregnancy. Chronic hypoxia during the first half of pregnancy produced an improved, but still significant rate of failed pregnancies, but importantly, is less likely to model the adverse consequences of conditions such as preeclampsia. As part of the hypoxic ventilatory response to breathing 12%O_2 it is likely that the fetuses were exposed to a degree of hypocapnia during the period of chronic hypoxia *in utero*. It was chosen not to try to monitor or modulate this, firstly because in the conscious, pregnant mother, it would have been impractical to monitor end-tidal CO_2 without significantly affecting the pregnancy, and introducing effects on the period of gestation that were a result of the invasive monitoring rather than the hypoxic insult itself. Secondly, making such a change to the previously used model would have made the results substantially less comparable with those of other research groups using similar models. Finally, making such a methodological change to previously used methods would have required significant validation, which was not practical.

Following birth, the offspring of the pregnant dams that had been in the hypoxic chamber (CHU rats) were raised under standard laboratory conditions, with food and water available *ad libatum*. Acute experiments were performed on N and CHU rats at 10-12 weeks of age, with a final group of experiments being performed on a group of N and CHU rats at 36-weeks of age.

2.1.2 Hypoxic chamber

Figure 2.1 is a schematic diagram showing the construction of the custom-built hypoxic chamber into which the pregnant dams were placed. An O_2 sensor

(Biospherix, Lacona, NY, USA) was placed in a large Perspex chamber (approximately 1x1x2m, WxDxH) and connected to an O_2 controller unit (ProOx P110, Biospherix, Lacona, NY, USA). A large cylinder of N_2 (BOC Gasses, West Bromwich, Birmingham, UK) was also connected to the Oxygen controller unit, which controlled the flow of N_2 into the chamber, to maintain the within-chamber O_2 level at ~12% O_2 (11.5-12.5%). The chamber was deliberately 'leaky' such that if the N_2 supply failed, O_2 concentration within the chamber would rise. Excess pressure development was further prevented with a pressure trap. In order to control humidity levels, air from within the chamber was drawn through a refrigerator followed by Silica Gel (SG). Humidity remained between 45 and 60%. Further, to remove ammonia, gas was passed through a molecular sieve (MS), and to remove excess CO_2, gas was passed through soda lime (SL). Air was circulated within the chamber with a small electric fan. O_2 level was recorded via a MacLab data acquisistion system (ADInstruments Ltd., Oxford, UK), on an Apple Mac computer (Apple Inc, CA, USA).

2.2.1 Surgical preparation

The basic anaesthetic regimen for the *in vivo* experiments described in this thesis is described here, as is the generic procedure for cannulation of arterial or venous vessels.

Anaesthesia was initially induced by placing the rat in an enclosed flow-through box, as part of a custom-made anaesthetic rig. The box was filled with ~3.5% Isofuorane (Isoflurane – VET, Merial Animal Health Ltd., Harlow, Essex, UK) in O_2, via an

anaesthetic vapouriser unit (General Anaesthetic Services, Keighly, West Yorkshire, UK). Once anaesthetised, the rat was placed supine on a homeothermic blanket (Harvard Apparatus, Kent, UK) and a mixture of 3.5% Isoflurane in 2L/min O_2 (BOC gasses, West Bromwich, Birmingham, UK) was provided via a facemask, connected to an anaesthetic scavenger unit (Harvard, Kent, UK). Surgical anaesthesia was assessed by absence of the paw pinch reflex.

Once surgical anaesthesia was achieved, a rectal thermometer, connected to the homeothermic blanket, was inserted using petroleum jelly, and used to maintain body temperature at 37.5°C. Next, the right jugular vein was isolated superior to the thoracic cage, and lateral to the midline, via a small transverse incision made with surgical dissecting scissors, followed by blunt dissection. Once isolated, the jugular vein was permanently occluded by a surgical knot at the distal end of the isolated portion of the vessel, with 6-0 gauge silk surgical suture (Surgical Specialties Corporation, Reading, PA, USA, via Harvard Apparatus, Kent, UK). The proximal end was occluded, but not tied, using a loop of 6-0 suture under gentle tension, and a small cut was made in the jugular vein.

A length of silicon tube (0.5mm Bore x0.5mm wall, Sterilin Ltd, Caerphilly, UK), filled with a solution of Alfaxan (3.5mg.ml^{-1}, Vetoquinol, Buckingham, UK) in saline (0.9% NaCl in distilled water) was inserted, which was in turn connected to a 50ml syringe with a 21G needle (BD Biosciences, Oxford, UK), ensuring no air was present in the cannula. The 50ml syringe, filled with Alfaxan solution was connected to an anaesthetic infusion pump (Perfusor compact S, B. Braun Melsungen AG, Germany).

The cannula was secured in place within the vessel distally and proximal with the 6-0 sutures previously mentioned. The Isoflurane gas was then withdrawn, and small boluses (0.05ml) of Alfaxan were given so as to maintain anaesthesia. Once respiratory rate was suitably recovered from the depression induced by boluses of Alfaxan on top of residual effects of Isoflurane, indicating that the continuing effects of Isoflurane had worn off, continuous infusion of Alfaxan solution was commenced, at approximately 1.0-1.5ml.hr^{-1}, to maintain surgical anaesthesia.

For maintenance of a patent airway, and for control of inspiratory gasses (see below), a tracheal cannula (T-shaped metal cannula, custom built, Biosciences workshop, University of Birmingham, UK) was passed into the trachea. The trachea was isolated from the surrounding muscle using blunt dissection, via the same skin incision made for isolating the jugular vein. A length of 4-0 suture (Surgical Specialties Corporation, Reading, PA, USA, via Harvard Apparatus, Kent, UK) was passed around the trachea, a small cut was made in the trachea, the cannula introduced, advanced approximately 5mm proximally, and then tied in place with the suture. The tracheal cannula was of approximately 15mm in length, and 3mm in internal diameter.

The other blood vessel cannulations carried out in each animal were dependent on the specific requirements of each experiment. However, the procedure for cannulation of each vessel was the same, in that the blood vessel was isolated by blunt dissection, the proximal and distal ends were occluded, a small cut was made with fine scissors and a heparinised saline (10IU/ml in 0.9% NaCl in dH_2O) filled

cannula was introduced and advanced, and then the cannula secured with surgical suture. The tubing used is detailed below.

Table 2.1 – Tubing used to cannula arteries and veins

Vessel	Tubing	External Diameter	Internal Diameter	Needle attachment
Brachial Artery	Portex Polythene	0.8mm	0.4mm	25G
Femoral Artery	Portex Polythene	0.96mm	0.58mm	23G
Caudal Ventral Tail Artery	Portex Polythene	0.8mm	0.4mm	25G
Femoral Vein	Sterilin Silicon tube	1.5mm	0.5mm	21G

For cannulation of the brachial artery, an incision was made in the axilla, and the vessel isolated with blunt dissection. For cannulation of the femoral artery or vein, an incision was made half way between the knee joint and the penis, followed by blunt dissection in a superiomedial manner. For cannulation of the caudal ventral tail artery a midline incision was made in the proximal third of the tail, followed by blunt dissection. The connective tissue covering the vessel was cut using fine surgical scissors, and the vessel exposed.

2.2.2 Manipulation of inspiratory gasses

During the experiments described in the following chapters, in which manipulation of inspiratory gasses was required, this was achieved by using a system of Rotameters

(Cole Parmer, Niles, IL, USA) connected via tubing to gas cylinders containing N_2 and O_2 (BOC Gasses, West Bromwich, Birmingham, UK). The mixture of gasses inspired by the animals was controlled by adjusting the ratio of O_2 and N_2 by using the rotameter. This was connected to the side arm of the tracheal cannula via flexible silicon tubing, such that the mixture of gasses was blown cross the opening of the sidearm, at a flow rate that excessed the animals inspiratory intake, such that it inspired the mixture of gasses blown over the side arm.

2.2.3 Measurement of respiratory parameters

For measurement of ventilatory tidal volume and respiratory frequency, a small animal spirometer head (FE141, AD Instruments, Oxford, UK) was fitted in series between the tracheal cannula, and the tube delivering inspiratory gasses. This was calibrated online (see 'data acquisition').

Arterial blood gas measurements

Where appropriate, blood gasses were measured using a Gem4000 blood gas analyser (Instrumentation Laboratory, Warrington, UK). Arterial blood was sampled via an arterial cannulation. The solution of saline and blood within the cannula was run out, and then 'fresh' arterial blood was run into a glass capillary tube (Instrumentation Laboratory, Warrington, UK), and was then immediately inserted into the blood gas analyser. P_aO_2, P_aCO_2 and $_PH$ were measured.

2.2.4 Blood Flow measurement

For measurement of blood flow in the femoral artery the femoral artery was exposed and freed from surrounding tissue as described above for cannulation of the femoral

artery. A small flow probe head (Model 0.7B, Transonic Systems via Linton Instrumentation, Norfolk, UK) was mounted on a manipulator (Narishige, Japan), and arranged such that the femoral artery, distal to the inguinal fat pad, lay in the 'hook' of the flow probe, covered in acoustic medium (H-R Lubricating Jelly, Mohawk Medical Supply, Utica, NY, USA). The probe was connected to a small animal blood flow meter (T206, Transonic Systems via Linton Instrumentation, Norfolk, UK).

For measurement of blood flow in the carotid artery, the carotid artery was exposed via an extension of the incision made for the cannulation of the jugular vein in the distal direction, lateral to the midline of the neck. Blunt dissection was used to isolate the artery, care being taken around the area of the carotid body and sinus, to ensure no damage occurred. The external carotid branch of the common carotid artery was ligated with 6-0 suture distal to the carotid bifurcation, as far distal as was practically possible. Thus, flow measured in the common carotid artery is largely representative of internal carotid artery blood flow, as has been previously described (Thomas & Marshall, 1995). The flow probe (Model 0.7B, Transonic Systems via Linton Instrumentation, Norfolk, UK) was placed on the common carotid artery with acoustic medium, and connected to the second channel of the T206 small animal blood flow meter mentioned above.

2.3 Data acquisition

For experiments in chapter 3, 4, 6 and 7, recordings of cardiovascular and respiratory variables were acquired using the AD Instruments PowerLab hardware, and LabChart software. For recording arterial blood pressure (ABP), a pressure

transducer (DTX Plus disposable pressure transducer, BD Biosciences, Oxford, UK) was connected to an either a brachial or femoral artery. The pressure transducter was connected to a MacLab bridge amplifier (ADInstruments Ltd, Oxford, UK), which was connected to a Powerlab 4/20 data acquisition system (ADInstruments, Oxford, UK). For recording of femoral or carotid blood flow (FBF and CBF respectively), the output of the T206 flowmeter was connected to two channels of the Powerlab 4/20. For recording of respiratory variables, the spirometer was connected to another channel of the PowerLab 4/20.

The PowerLab 4/20 was connected to an Apple Computer (Apple Inc., Cupertino, CA, USA) via USB cable. LabChart (v6.1, ADInstruments, Oxford, UK). Arterial blood pressure (ABP), femoral blood flow (FBF), carotid blood flow (CBF), and air flux (raw data from spirometer) were all recorded online at a 1kHz sampling rate. Femoral vascular conductance (FVC), femoral vascular resistance (FVR), carotid vascular conductance (CVC), heart rate (HR), mean FBF (MFBF), mean CBF (MCBF), mean ABP (MABP), ventilatory tidal volume (V_T) and respiratory frequency (R_F) were all derived online. FVC and CVC is computed online by dividing MFBF or MCBF by MABP. V_T was computed by the cyclical integration of calibrated air flux measured in the spirometer R_F and HR are calculated online from the peaks in the respiratory and ABP traces.

Figure 2.1

Schematic representation of the hypoxic chamber used to induce CHU

SG; silica gel, MS; molecular sieve, SL; soda lime, N_2; nitrogen gas.

Figure 2.1

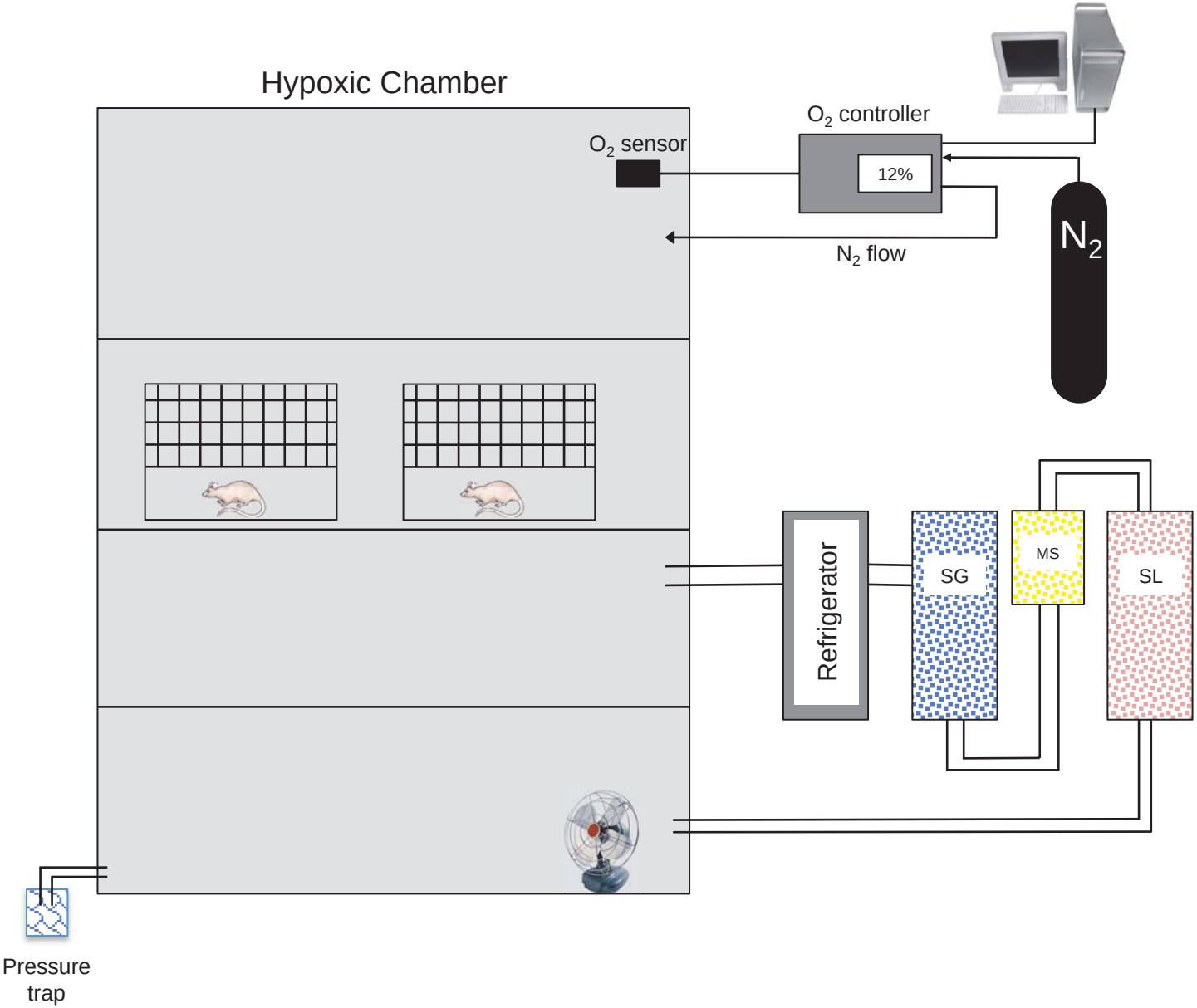
Hypoxic Chamber
O_2 sensor
O_2 controller
12%
N_2 flow
N_2
Refrigerator
SG
MS
SL
Pressure trap

Chapter 3 – Cardiovascular responses to acute systemic hypoxia, and the role of oxidative stress

3.1 Introduction

Reduced fetal oxygenation can result from pregnancy at altitude, but also from the placental insufficiency incurred in pre eclampsia (Gagnon, 2003). Although placental insufficiency results in both reduced oxygen and nutrient supply to the fetus, the fetal hypoxaemia itself has been shown to have cardiovascular consequences for the adult offspring distinct from under nutrition alone (Williams *et al.*, 2005b).

Notably, femoral arteries taken from chick embryos that were incubated at high altitude, and therefore exposed to reduced oxygenation, showed reduced sensitivity to the endothelium-dependent vasodilator acetylcholine (Ruijtenbeek *et al.*, 2003). Futher, Williams et al (2005a) showed that arteries from different tissues taken from neonatal rats were not all affected in the same way by chronic hypoxia *in utero*. Thus, in neonatal CHU rats, exposed to 12%O_2 during day 15-21 of pregnancy, carotid arteries showed blunted responses to both phenylephrine and endothelin, whereas the femoral arteries showed enhanced vasoconstriction to phenylephrine relative to femoral arteries of control (N) rats. Such *in vitro* studies of conduit vessels give an indication that there may be differences in the manner in which different vascular beds are affected by chronic hypoxia during fetal development, but they cannot of course predict how more distal sections of the vascular tree may behave.

Further studies by Williams et al. (2005b) demonstrated that isolated mesenteric resistance arteries taken from 4-month old CHU offspring show reduced endothelium-dependent vasodilatation to methacholine relative to those of control rats, that was reversed by the presence of exogenous superoxide dismutase (SOD).

This suggested that oxidative stress contributed to the reduced vasodilatation, i.e. O_2^- may have reduced the bioavailability of NO and SOD may have prevented this by dismuting the O_2^- into H_2O_2. In accord with this interpretation, in mesenteric arteries taken from CHU rats at 7 months of age, the NOS inhibitor L-NAME had no blunting effect on endothelium-dependent dilatation, whereas it attenuated the dilatation in N rats, indicating a reduced role for NO in arteries from CHU. Thus, it seems that in the mesenteric arteries of CHU rats, by 7 months of age, the functional role of NO was taken over by other endothelially-derived vasodilators.

Much work by Marshall and collaborators has demonstrated that the adenosine A_1 receptor is important in mediating a large proportion of the vasodilatation induced in skeletal muscle by acute systemic hypoxia, and that it is mediated by NO release (Skinner & Marshall, 1996; Bryan & Marshall, 1999a, b; Ray *et al.*, 2002). By contrast, recent *in vivo* studies on CHU rats have shown that there is no role for the adenosine A_1 receptor in mediating the hypoxia-induced muscle vasodilatation (Coney & Marshall, 2010), even though the vasodilatation was comparable in magnitude to that of N rats, and adenosine still evoked muscle vasodilatation via A_1 receptor in CHU rats. This suggested that other mechanisms of vasodilatation compensate in the hypoxia-induced vasodilatation, and raised the possibility that the mechanism of release and action of adenosine are disrupted in CHU rats; in N rats both are NO dependent (see General Introduction).

In view of these findings, and taking into consideration the results of Williams et al., (2005a; 2005b), we hypothesised that in CHU rats, the vasodilator H_2O_2 (Rubanyi &

Vanhoutte, 1986; Matoba *et al.*, 2000) produced by SOD (Matoba & Hiroaki, 2003) from O_2^- generated during systemic hypoxia contribute to vasodilatation induced by systemic hypoxia, as has been shown by Pyner et al., (2003), and that this contribution is much greater in CHU rats than in N rats. Therefore, this hypothesis was investigated in the present study in anaesthetised CHU and N rats by using DETC to inhibit SOD. Further experiments exploring the mechanisms underlying hypoxia-induced vasodilatation in CHU rats are described in Chapter 4.

In designing a study to elucidate the potential role of H_2O_2, it was decided to take the opportunity of investigating the effect of chronic hypoxia *in utero* on the respiratory and cardiovascular response evoked by longer lasting periods of acute systemic hypoxia, and to consider the cerebral circulation as well as the skeletal muscle circulation, for the reasons discussed below.

Eden and Hanson (1987b) showed that in conscious 5- and 14-day old rat pups that breathed 12% O_2 from birth (CHB rats), there was no significant respiratory response to acute systemic hypoxia hypoxia (12 or 8%O_2), while in the N rat pup at the same ages, a biphasic respiratory response occurred; initial hyperventilation which waned with time. By 5-10 weeks of age, it was found that breathing 8%O_2 only, and not 12%O_2, evoked a biphasic response in CHB rats, whereas in the N rats, the biphasic hypoxic response was evident at both 12 and 8%O_2. At this age also, recordings from the afferent carotid sinus nerve of CHB and N rats showed that both had a similar excitatory response to acute isocapnic hypoxia, indicating that the impairment of hypoxic respiratory response was likely of central origin.

Building on this work, Thomas & Marshall (1995) studied the respiratory and cardiovascular responses evoked by 10 minutes of acute hypoxia, comparing responses between 7-8 week old N rats, and CHB rats that breathed 12%O_2 from birth. When anaesthetised CHB rats were switched from continuously breathing 12%O_2 to 8%O_2 for 10 minutes, they showed a more marked secondary fall in ventilation and in heart rate than occurred in N rats when they were exposed to the greater change of switching from breathing 21% to 8%O_2. CHB rats also showed an exaggerated fall in brain blood flow (CBF). Thomas & Marshall (1995) therefore proposed that chronic hypoxia from birth may enhance vulnerability to the positive feedback loop described in the General Introduction, which leads to cardiovascular collapse as a result of falls in ventilation, HR and CBF.

Turning to the effects of CHU on the respiratory response to acute systemic hypoxia, Peyronnet et al (2000) showed that at 3 weeks of age, CHU rats exposed to 10%O_2 *in utero* showed an enhanced increase in ventilation during acute hypoxic episodes, but by 9 weeks of age, this had reversed such that the respiratory response was diminished relative to the same response in N rats of the same age.

Thus, there is already evidence that chronic hypoxia during development, before or after birth, can have serious consequences for the developing offspring's ability to hyperventilate in response to acute systemic hypoxia. There is strong evidence that chronic hypoxia from birth affects the cardiovascular, particularly the cerebrovascular, response to acute systemic hypoxia, in a detrimental way. Thus, it

was reasonable to hypothesise that chronic hypoxia *in utero* would similarly affect the cardiovascular and respiratory response to acute systemic hypoxia in the offspring.

Therefore, the present study tested cardiovascular and respiratory responses to 10 minutes of acute systemic hypoxia (8%O_2) in N and CHU rats before and during SOD inhibition, testing the hypotheses that:

1. CHU rats will show a reduced ventilatory response, and reduced ability to maintain HR and CBF during acute systemic hypoxia
2. Oxidative stress is present in CHU rats, and that it limits endothelial function, and hence the vasodilatation evoked by acute systemic hypoxia in the hindlimb and cerebral vascular beds.

3.2 Methods

In vivo and *in vitro* experiments were carried out in this study. The *in vivo* experiments were performed on 12 N rats (298±15g, 70±2 days old) and 11 CHU rats (348±14g, 5 litters, 71±1 days old). The *in vitro* experiment, an analysis of frozen sections of skeletal muscle, were performed on samples of skeletal muscle obtained from 6 N rats (431±9g) and 6 CHU rats (411±14g, 6 litters).

3.2.1 In vivo experiments

The basic surgical preparation and data acquisition protocols, including anaesthetic regimen for induction and maintenance, and recording of cardiovascular and respiratory variables are described in Chapter 2. ABP was measured from the right brachial artery and arterial blood for blood gas analysis was sampled from the left brachial artery. Drug infusion was given via the left femoral vein.

FBF was recorded from the right femoral artery, and CBF from the right common carotid artery, following ligation of the external carotid artery. Femoral and carotid vascular conductance (FVC and CVC) were calculated online by dividing MFBF or MCBF by MAPB.

Tracheal air flux was measured using a MacLab spirometer, and R_F, V_T and V_E were calculated in the manner described in Chapter 2.

3.2.2 Protocol

After a stabilisation period of 40 minutes following surgery, when animals breathed 21%O_2, inspiratory O_2 was switched from 21% O_2 to 8% O_2 in N_2 for 10 minutes and then switched back. Arterial blood samples were taken for blood gas analysis during the final minute before hypoxia, and during the final minute of the 10-minute hypoxic period. Once a steady baseline was re-established during normoxia, infusion of the cell permeable SOD inhibitor diethyl-dithiocarbamate (DETC, Sigma Aldrich, UK) was commenced (5mg.kg^{-1}.min^{-1} i.v.). At least 10 minutes after steady baselines had been re-established, the inspirate was once again switched to 8% O_2 for 10 minutes, and arterial blood samples for blood gas analysis were taken as described above, whilst the infusion of DETC continued.

3.2.3 Data Analysis and statistics

All data are presented as mean±SEM of N or CHU rats. MABP, HR, FBF, CBF, FVC, CVC, R_F, V_T and V_E are presented as mean values across the 10 minute period of hypoxia, and as means of the 10 second period at each minute during the 10 minutes. The magnitude of the vasodilatation was computed offline as the integral of FVC or CVC during the 10 minute period immediately before the hypoxic period minus the integral of FVC or CVC during the 10 minute period of hypoxia (∆intFVC and ∆intCVC). This calculation indicates how much vascular conductance changed during the hypoxic period, and has been described previously (Coney & Marshall, 2010). The intFVC presented in the minute by minute analysis represents integrated FVC in the final 10 seconds of each minute, compared to the 10 seconds immediately preceding the bout of hypoxia.

Statistical analysis was carried out using Statview 5 (SAS Institude Inc., NC, USA) on an Apple Mac computer (Apple Inc, CA, USA). Comparisons of baseline variables between groups, and before and during infusion of DETC within groups, were made with a mixed design two way ANOVA with Scheffé *post hoc* test. Comparisons of how the respiratory and cardiovascular variables changed over the 10-minute period of hypoxia were made using a repeated measures ANOVA with Scheffé *post hoc* test. Particular attention was paid to the differences observed between the normoxic baseline, and values recorded at the end of the 1st minute, and end of the 10th minute of breathing 8%O_2, as these allowed comparison of the initial changes caused by acute systemic hypoxia, and the secondary changes induced by more prolonged hypoxia, allowing this study to address the first hypothesis put forward in the introduction. This time-based comparisons were made using a repeated measured ANOVA and Scheffé *post hoc* test. Comparisons of blood gasses between groups, and within groups before and during DETC infusion, were made using a 2-way mixed design ANOVA with Scheffé *post hoc* test. Comparison of body mass between groups was made using Students unpaired samples t-test.

3.2.4 Ex vivo analysis of oxidative stress

To examine the levels of oxidative stress in the small arteries and arterioles supplying hindlimb skeletal muscle, a variation upon the method published by Yang et al (2009) was used. Immunohistochemistry was used to colocalise 3-nitrotyrosine, a marker of oxidative stress, and α-smooth muscle actin, a marker of the smooth muscle in arterial vessels, in transverse sections of the tibialis anterior (TA) muscle from N and CHU rats. NB. These were not the same rats used for the *in vivo* study.

3.2.5 Tissue isolation

Following cervical dislocation under isofluorane anaesthesia the proximal portion of the left TA was carefully freed by blunt dissection from surrounding tissue, and removed with the aid of a scalpel. The proximal third was mounted on cork with OCT (Optimal cutting temperature compound, Thermo Scientific, Northumberland, UK), and frozen in liquid N_2 cooled isopentane (2-methylbutane, Sigma Aldrich, MO, USA). When frozen, samples were stored at -86°C. Sections were cut (10μm at -23°C) from TA blocks using a cryostat (Clinicut 60, Bright Instruments Co ltd., Huntingdon, UK), and mounted onto Polysine-coated glass slides (VWR International, PA, USA) for staining. After 30 minutes at room temperature, when sections were dried, they were stored in a sealed box at -86°C.

3.2.6 Staining protocol

Slides were allowed to warm to room temperature for 30 minutes before slide boxes were opened. Slides were fixed in ice-cooled acetone for 5 minutes, then washed in 0.1M phosphate buffered saline (PBS Sigma Aldrich, MO, USA) for 5 minutes, followed by two 5 minute washes in PBST (PBS with 1% Tween-20, Sigma Aldrich, MO, USA) to wash and permeabilise the tissue sections. Slides were then placed into a slide incubation rack, and sections were circled with a wax pen, and a blocking solution (1% Bovine Serum Albumin (IHC grade), Sigma Aldrich, MO, USA, in PBST,) was applied for 1 hour at room temperature in a humidified chamber (Thermo Fisher Scientific, Northumberland, UK) to prevent drying.

After 1 hour, the blocking solution was allowed to run off, and a solution containing primary antibodies was applied, which contained the following 0.1M PBS, 1% Tween20, 0.1% bovine serum albumin, Mouse monoclonal IgG against 3-nitrotyrosine at a 1/1000 dilution (ab61392, Abcam, Cambridge, UK) and Rabbit polyclonal IgG against α-smooth muscle actin – 1/500 dilution (ab5694, Abcam, Cambridge, UK)

This staining solution was applied overnight at 4°C in a humidified chamber. Following this primary staining, slides were washed three times for 5 minutes in PBST, and then, in a darkened room, a solution containing secondary antibodies was applied. This solution contained: 0.1M PBS, 1% Tween20, 0.1% bovine serum albumin, tetramethylrhodamine-conjugated Goat polyclonal IgG against mouse IgG in a 1/500 dilution (T-2762, Invitrogen, Paisley, UK) and fluorescein isothiocyanate-conjugated sheep polyclonal IgG against rabbit IgG in a 1/1000 dilution (ab6791, Abcam, Cambridge, UK).

Slides were incubated with the solution of secondary antibodies for 1 hour at room temperature in a humidified chamber in the dark. Following incubation slides were washed once in PBST for 5 minutes, followed by two, 5-minute washes in PBS. After washing, excess fluid was tapped off, and glass coverslips were mounted with Vectashield mounting medium containing DAPI (Vector laboratories Ltd, Peterborough, UK). Coverslips were secured with clear nail varnish, and stored in the dark at 4°C until visualization.

Unless otherwise stated all materials were obtained from Sigma Aldrich (MO, USA)

3.2.7 Visualization of fluoresense

Slides were visualized using a Carl Zeiss Axioskop2 fluorescence microscope (Carl Zeiss, Oberkochen, Germany) with an Osram HB100W fluorescent bulb (Osram AG, Munich, Germany) using a 20X objective (Carl Zeiss, Oberkochen, Germany). Exposure was optimized such that all exposure under each filterset was the same for all slides, and the optical intensity of all images was within the dynamic range, and not saturated. For visualisation of DAPI staining, filterset 1, 400ms exposure was used. For visualization of α-SMA staining, filterset 9, 400ms exposure, and for visualization of 3-NT staining, Filterset 14, 800ms exposure (Filtersets from Carl Zeiss, Oberkochen, Germany).

Photomicrographs were acquired using the Axio-vision software (v4.1, Image Associates Ltd) on a computer attached to a 1.3 megapixel AxioCam MRc (Carl Zeiss, Oberkochen, Germany) which was connected to the microscope.

All isolation and sectioning procedures described above were identical, the antibody staining was done in parallel in one batch for all the samples, and exposure settings identical. Thus, any differences in the integrated optical density of the images acquired can be considered to represent different quantities of protein present. This means that direct comparisons can be made between images of sections from N and CHU rats.

3.2.8 Image analysis

Images were processed using ImageJ software (v1.44, NIH, USA). The “region of interest” function was used to select areas representing the vascular wall of skeletal muscle arterioles; i.e. areas which showed positive αSMA staining, which matched the vessel morphology expected of a small artery or arteriole, and contained spots of DAPI staining indicating a mass of cells. This region of interest was then overlayed onto the equivalent image displaying 3-NT staining, and this area was measured for integrated optical density. The integrated optical density was divided by the size of the area of interest, giving a measure of the optical intensity of 3-NT staining. In each image there were many small traces of αSMA staining, which probably reflected small arteriole staining, but these were too small to be reliably differentiated from background staining.

There were usually 3-5 regions in each section that were suitably clear, and discernable from background staining in the surrounding tissue. In each case, photomicrographs of the three clearest regions were obtained from each section. Three sections from each rat were stained and analysed, meaning that overall 9 regions of arteriolar staining were analysed in each rat. For analysis, the relative intensity of staining was averaged within each section analysed, and then the 3 mean values were averaged to give an average value for each rat. This value from each rat was grouped, to form group mean±SEM for either N or CHU rats. The same analysis was performed on tissue from 36-week old N and CHU rats (described in Chapter 7) and hence, statistical comparisons between mean staining in N and CHU rats, at this

age and at 36-weeks of age, were made by factorial ANOVA and Scheffé *post hoc* test.

3.3 Results

3.3.1 In vivo studies

3.3.2 Comparison of baselines

The cardiovascular and respiratory baseline values for N and CHU rats breathing 21%O_2 are shown in Tables 3.1 and 3.2, and arterial blood gasses and pH in Table 3.3. There were no significant differences between baselines, although P_aO_2 showed a strong tendency to be lower in CHU than N (p=0.06).

3.3.3 Responses to breathing 8% oxygen for 10 minutes

As expected, by the 10th minute of breathing 8% O_2, P_aO_2 had fallen substantially in both N and CHU, and the concomitant hyperventilation resulted in hypocapnia as well as alkalosis in both groups, (see Table 3.3). The effects on respiratory and cardiovascular variables can be seen in Figures 3.1-3.3. Figure 3.1 shows an original recording from an N rat during 10 minutes of acute Hypoxia. Figure 3.2 shows the mean absolute values in normoxia and systemic hypoxia in N and CHU rats, and figure 3.3 shows the changes evoked from normoxic baselines by breathing 8%O_2. In Figure 3.2 symbols are used to show differences between the responses evoked in N and CHU rats. In Figure 3.3 symbols are used to show differences between the changes recorded between baselines and the 1st minute of hypoxia, and baselines and the 10th minute of hypoxia, and changes between the 1st and 10th minutes of hypoxia.

In both N and CHU, hypoxia resulted in an initial increase in R_F at 1 min, which waned to baseline levels by the 10th minute of hypoxia (Figures 3.1 & 3.3). By contrast, the concomitant initial increase in V_T was sustained in hypoxia in both N and CHU, although ΔV_T was of a larger magnitude in CHU than N (Figure 3.2). As a result, V_E was significantly raised in both N and CHU throughout the 10-minute period of hypoxia, although ΔV_E was significantly less at the 10th minute than at the 1st minute in both N and CHU (Figure 3.3).

Concomitantly, hypoxia induced a profound fall in ABP in both N and CHU. In N, there was a sustained increase in intFVC, indicating hindlimb vasodilatation, and such that FBF was maintained. In CHU, the increase in intFVC during hypoxia was not significantly different from that of the N rats. However, the fall in ABP tended to be greater in CHU than N rats (p=0.06, Figure 3.2), and when FBF was expressed as change from baseline, there was a significant difference between N and CHU in the FBF response to acute hypoxia (Fig. 3.2). IntCVC was modestly increased in both groups, but only reached statistical significance in CHU (Figure 3.3). This was not sufficient to counteract the fall in ABP, and therefore, although CBF was initially maintained, by the 10th minute of hypoxia it had fallen significantly from baseline in both groups (N: -0.66±0.19, p<0.01, CHU: -0.83±0.23, p<0.01, ml.min^{-1}, figure 3.3).

3.3.4 The effect of DETC on cardiovascular and respiratory baselines

The cardiovascular and respiratory baseline values recorded during infusion of DETC are shown in Tables 3.1 and 3.2, whilst arterial blood gasses sampled during DETC infusion are shown in Table 3.3. Of note, DETC significantly reduced PaO_2 in

normoxia in both N and CHU such that PaO_2 values became comparable in N and CHU (Table 3.3). DETC infusion significantly reduced $PaCO_2$ in CHU, but this effect did not reach significance in N (p=0.06). DETC had no significant effect on baseline V_E (see table 3.1) in either group, although it tended to reduce baseline R_F (N: p=0.15, CHU: p=0.11) and increased V_T (N: p<0.05 CHU: p=0.07).

DETC infusion had no significant effect on baseline ABP. Of particular importance, DETC had no effect on baseline FVC in N rats, but caused a significant decrease in baseline intFVC in CHU rats (p<0.001, Table 3.1), indicating an increase in baseline vasoconstrictor tone in CHU rats. This was accompanied by a significant reduction in FBF in CHU, but not in N rats (p<0.001, Table 3.1). DETC had no significant effect on CVC or CBF in the N or CHU rats.

3.3.5 Effects of DETC on the cardiorespiratory response evoked by acute hypoxia

During DETC infusion, PaO_2 fell to a significantly lower level in hypoxia in both N and CHU during acute hypoxia than under control conditions. P_aCO_2 fell to similar level to those seen during the control response (Table 3.3).

In N rats, DETC infusion had no significant effect on the respiratory response to hypoxia. There was still a significant increase in R_F and V_T, and the increase in R_F waned by the 10^{th} minute of hypoxia (Figure 3.4), as it did before DETC (Figure 3.3). However, in CHU rats, DETC significantly blunted the increase in R_F evoked by acute

hypoxia, and as a consequence the hypoxia-induced increase in V_E over the full 10 minutes was also significantly blunted compared to control conditions (Figure 3.4).

During DETC infusion, ABP was better maintained during hypoxia in N than under control conditions. In contrast, any effect of DETC on the fall in ABP evoked by systemic hypoxia in CHU rats did not reach statistical significance (Figure 3.4). DETC had no significant effect increase in intFVC during hypoxia in either N or CHU rats. However, as a result of a tendency for ABP to be slightly better maintained during hypoxia with DETC infusion in CHU rats, and the increase in intFVC to be slightly greater than control conditions. In CHU rats, FBF was significantly higher during hypoxia with DETC infusion compared to the control condition (Figure 3.4). DETC infusion did not have any significant effect on the increase in intCVC during hypoxia in either N or CHU rats. However, in both N and CHU, the significant fall in CBF by the 10^{th} minute of hypoxia that occurred under the control conditions (Figure 3.3), did not occur during hypoxia with DETC infusion in either group. This was largely attributable to better maintenance of ABP (Figure 3.4).

3.3.6 In vitro experiments

This study used histochemical colocalisation of staining for the marker of oxidative stress, 3-nitrotyrosine, an α smooth muscle actin as a marker of vascular smooth muscle, to examine the level of vascular oxidative stress in CHU rats relative to N rats. DAPI was used to visualise cell nuclei.

When analysing photomicrographs of the staining, it was clear that there was significantly more staining of all kinds in the wall of the arterial vessels than there is in the skeletal muscle cells surrounding them (See figure 3.6). In the examples shown, the blood vessels are surrounded by skeletal muscle fibres, as indicated by the blue DAPI stained nuclei, and the level of background 3-NT staining, which is likely to be specific staining of 3-NT in skeletal muscle cells, rather than non-specific staining. However, αSMA staining was isolated only to areas that resembled arterial or arteriolar morphology.

Where arterial vessels were particularly small (<50μm in external) diameter, it was difficult to resolve the 3NT staining associated with the vessel from that of the surrounding skeletal muscle cells and therefore they were not included in the quantative analysis. The lumen of all vessels (a clear example of which is shown in Figure 3.6A-C), no matter what angle they were sectioned at, was excluded.

There was marked variation in the angles at which the arteries and arterioles were sectioned, due to the branching nature of the vascular supply to the TA muscle, with some sectioned obliquely to give an elliptical view (Figure 3.7 C&G), and some being sectioned more or less transversely to give a circular cross-section. It is also possible that some the elliptically shaped vessels were thinner walled venous vessels that were sectioned transversely, although in most cases, arterial and venous vessels ran close together, and so differentiation by eye, based on the vessel wall morphology, was obvious. It is also possible that some vessels were sections in an almost-parallel fashion, giving rise to long sections of what may be an arterial vessel curving (see

figure 3.7 B&F). Examples of the images obtained by transecting vessels at different angles are shown in figure 3.7. Because the angle at which vessels were sectioned was often not clear, making an accurate assessment of the lumen diameter was not possible, except in those vessels that were obviously sectioned exactly transversely, such as those shown in figure 3.6. The majority of these transversely sectioned vessels had a lumen of approximately 20-30μm, although on occasion they were smaller, at around 10μm (~10 times in total). Given the thickness of the vascular wall it seems like these vessels were all arterial vessels rather than venous vessels.

This study used negative controls of primary-only and secondary-only staining protocols to determine whether the primary or secondary antibodies led to non-specific fluorescence in muscle sections (as shown in figure 3.5). What appeared to be a low level of non-specific fluorescent staining was found on the innermost layer of the larger arteries studied, as shown in Figure 3.5 D, F and H. This layer was excluded from the region of interest analysis. Thus, 3-NT staining analysis represents a measurement of oxidative stress in the vascular smooth muscle wall, not the endothelium. Further, cross reactivity of each secondary antibody with the opposite primary antibody was checked, and found to give very low levels of non-specific fluorescence, and none in the vascular wall, the region of interest.

Figure 3.6 shows examples of the levels of staining achieved with the 3-NT antibody. When merged with the image of the staining of α-smooth muscle actin, it is clear that the staining was localized to the vascular smooth muscle of the small artery shown. Yellow staining in the merged images (figure 3.6 D & H) indicates co-staining of

vascular smooth muscle and the marker of oxidative stress, 3-NT. Figure 3.8 A shows the quantification of fluorescent intensity achieved with 3-NT staining and shows that there is no significant difference in the level of staining achieved in N and CHU rats. It was not possible to resolve the endothelium of these vessels. Thus, no comment can be made on the level of oxidative stress in the endothelium of either N or CHU rats.

The level of 3-NT staining in areas representing the smooth muscle of the vascular wall within sections of proximal TA was not different between N and CHU rats (figure 3.6).

Table 3.1 – Mean cardiovascular baselines in N and CHU rats before and during infusion of a SOD inhibitor

Condition	ABP (mmHg)	HR (beats.min^{-1})	intFVC (CU)	FBF (ml.min^{-1})	intCVC (CU)	CBF (ml.min^{-1})
N	136.0 ±3.4	467 ±14	7.54 ±1.10	1.58 ±0.18	13.2 ±1.5	2.9 ±0.28
CHU	144.6 ±3.8	458 ±6	6.38 ±0.85	1.52 ±0.17	13.5 ±1.6	2.86 ±0.40
N+DETC	137.2 ±3.0	484 ±10	7.27 ±0.75	1.50 ±0.12	19.2 ±2.9	3.23 ±0.28
CHU+DETC	148.2 ±2.2††	478 ±10	4.48 ±0.49**	1.13 ±0.13***	17.4 ±3.0	2.93 ±0.47

Mean cardiovascular baselines in N and CHU rats before (N, CHU) and during DETC infusion (N+DECT, CHU+DETC) whilst breathing 21% O_2.

ABP; arterial blood pressure, HR; heart rate, intFVC; integrated femoral vascular conductance, FBF; femoral blood flow, intCVC; integrated carotid vascular conductance, CBF; carotid blood flow. Values shown are mean±SEM (N: n=12, CHU: n=11)

*, **, *** - P<0.05, P<0.01 and P<0.001 vs control conditions respectively

†† - p<0.01 N vs CHU under same condition

Table 3.2 – Mean respiratory baselines in N and CHU rats before and during infusion of a SOD inhibitor

Condition	R_F (breaths.min^{-1})	V_T (ml.kg^{-1})	V_E (ml.min.kg^{-1})
N	97.6±3.3	2.46±0.15	241±20
CHU	93.3±3.1	2.23±0.12	207±12
N+DETC	93.2±3.6	2.66±0.18	250±22
CHU+DETC	86.9±4.3	2.39±0.15	207±16

Mean respiratory baselines in N and CHU rats before (N, CHU) and during DETC infusion (N+DETC, CHU+DETC) whilst breathing 21% O_2.

R_F; respiratory frequency, V_T; ventilatory tidal volume, V_E; respiratory minute ventilation. Values shown are mean±SEM (N: n=12, CHU: n=11).

Table 3.3 – Arterial blood gasses in N and CHU rats during normoxia and hypoxia before and during infusion of a SOD inhibitor.

Condition	P_aO_2 (mmHg)	P_aO_2 (mmHg)	P_aCO_2 (mmHg)	P_aCO_2 (mmHg)	pH_a	pH_a
	Normoxia	Hypoxia	Normoxia	Hypoxia	Normoxia	Hypoxia
N	85.0 ±2.2	29.4 ±1.5	38.8 ±1.2	24.6 ±0.8	7.427 ±0.004	7.503 ±0.024
CHU	80.1 ±1.6 (p=0.06)	30.4 ±1.6	41.5 ±1.1	25.5 ±0.9	7.438 ±0.010	7.482 ±0.023
N+DETC	71.8 ±2.3***	23.0 ±1.2**	36.5 ±1.4 p=0.062	24.3 ±1.2	7.465 ±0.010**	7.544 ±0.017
CHU+DETC	72.4 ±1.9***	24.5 ±1.4**	38.6 ±1.0*	26.1 ±0.8	7.456 ±0.010*	7.511 ±0.014

Mean arterial blood gasses (P_aO_2, P_aCO_2, pH_a) in N and CHU rats breathing 21% O_2 and 8% O_2 (Hypoxia) before and during DETC infusion. Values shown are mean±SEM (N: n=12, CHU: n=11)

*, **, *** - $p<0.05$, $p<0.01$, $p<0.001$ respectively, vs control condition

p=0.062 – CHU vs N

Figure 3.1 – Original recording of cardiovascular and respiratory variables during a 10 minute period of acute systemic hypoxia (breathing 8%O_2) in an N rat.

The bar beneath the trace indicates the period during which the rat was breathing 8%O_2.

Abbreviations as per Tables 3.1 and 3.2.

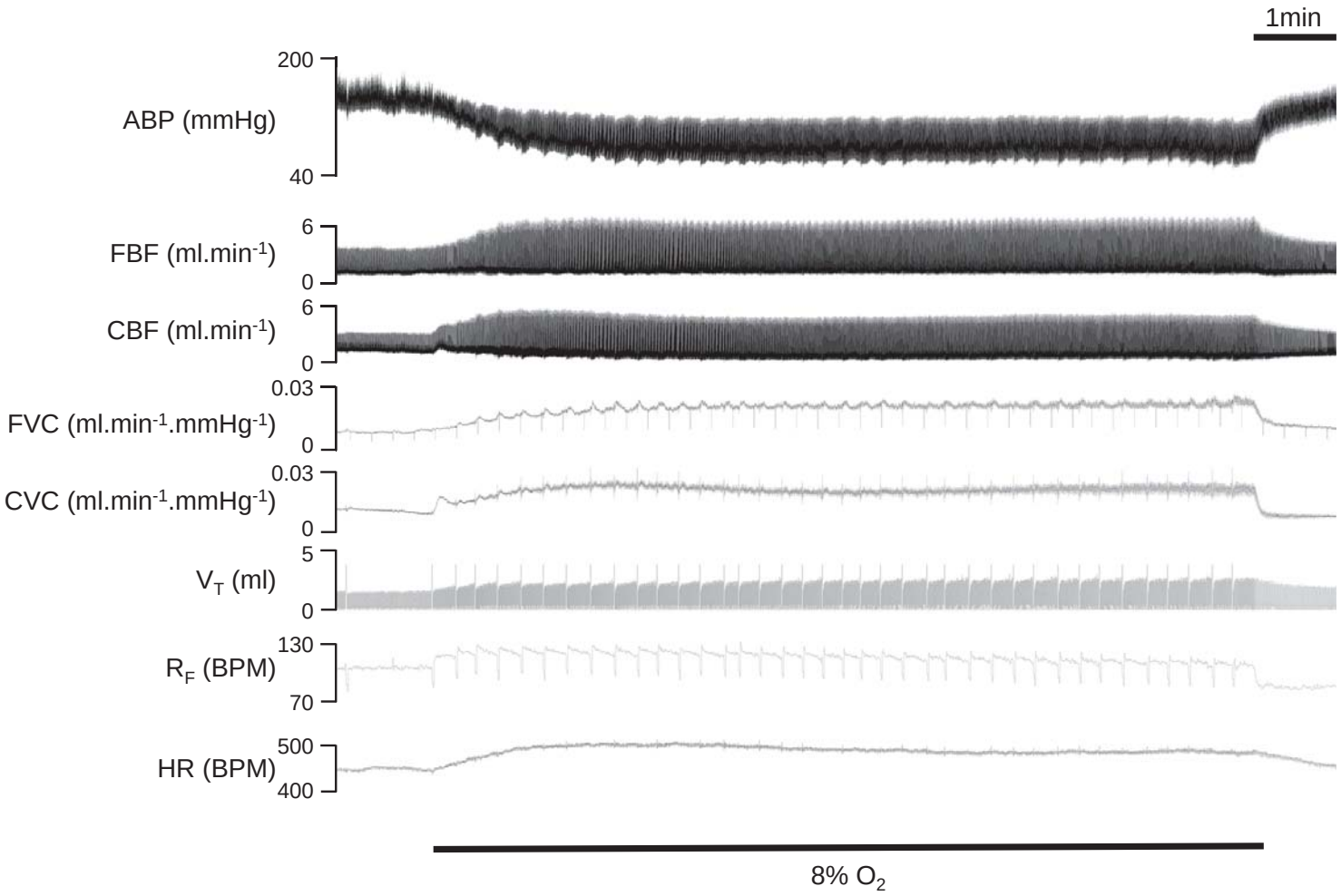
1min
200
ABP (mmHg)
40
6
FBF (ml.min-1)
0
6
CBF (ml.min-1)
0
0.03
FVC (ml.min-1.mmHg-1)
0
0.03
CVC (ml.min-1.mmHg-1)
0
5
VT (ml)
0
130
RF (BPM)
70
500
HR (BPM)
400
8% O2

Figure 3.1

Figure 3.2 – Mean cardiovascular and respiratory variables recorded at 1 minute intervals during acute systemic hypoxia in N and CHU rats.

Data presented as mean±SEM N (n=12, filled squares) and CHU (n=11, filled circles).

Abbreviations as per Tables 3.1 and 3.2.

** - P<0.01, N vs CHU hypoxia response.

P=0.06 – N vs CHU hypoxia response.

Figure 3.2

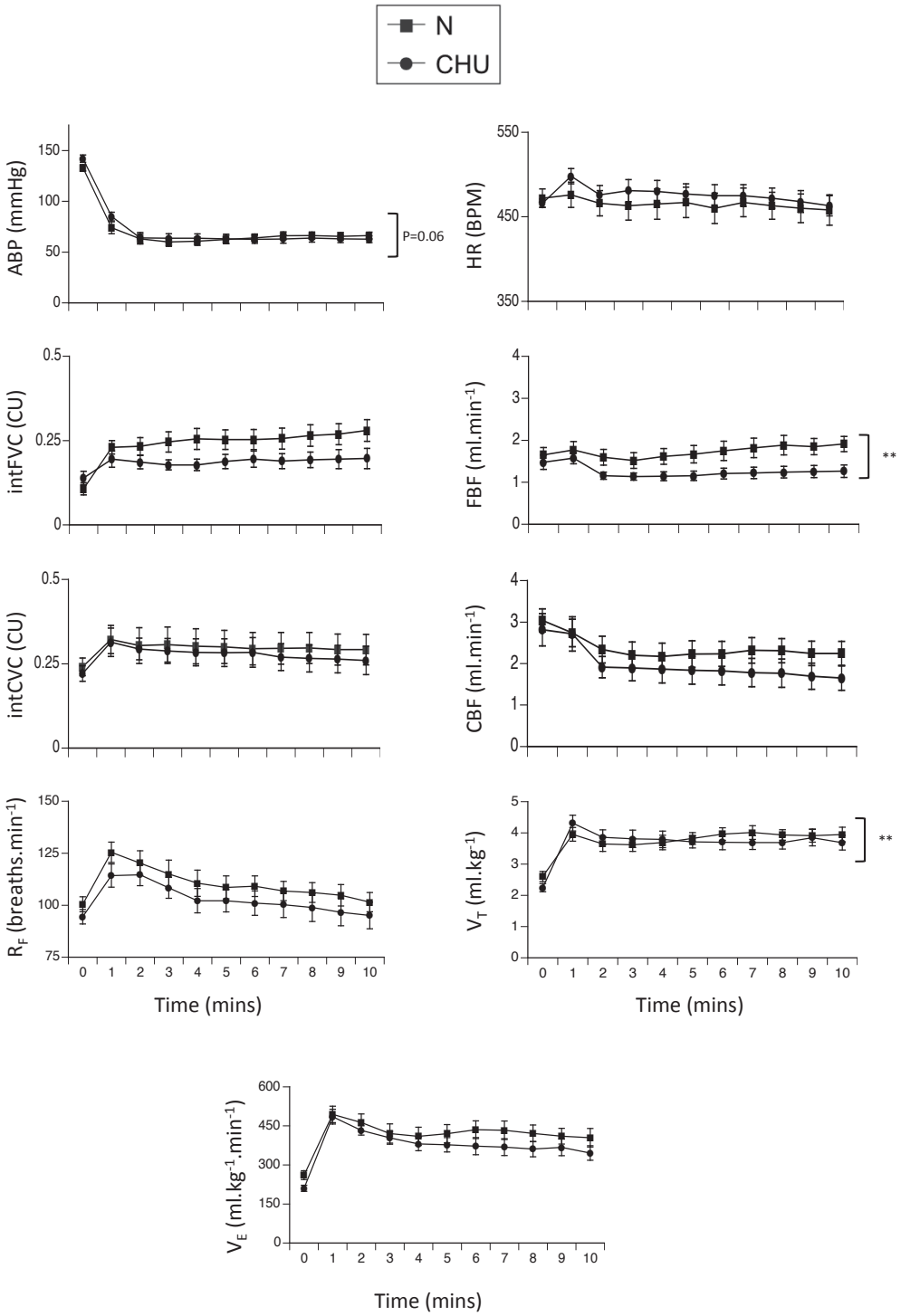
N
CHU
ABP (mmHg)
150
100
50
0
P=0.06
HR (BPM)
550
450
350
intFVC (CU)
0.5
0.25
0
FBF (ml.min-1)
4
3
2
1
0
**
intCVC (CU)
0.5
0.25
0
CBF (ml.min-1)
4
3
2
1
0
RF (breaths.min-1)
150
125
100
75
0 1 2 3 4 5 6 7 8 9 10
Time (mins)
VT (ml.kg-1)
5
4
3
2
1
0
**
0 1 2 3 4 5 6 7 8 9 10
Time (mins)
VE (ml.kg-1.min-1)
600
450
300
150
0
0 1 2 3 4 5 6 7 8 9 10
Time (mins)

Figure 3.3 - Mean changes from baseline in cardiovascular and respiratory variables recorded at 1-minute intervals during acute systemic hypoxia.

All values are presented as the mean±SEM change (Δ) from the mean baseline of the minute preceding acute systemic hypoxia, in N (n=12, filled squares) and CHU (n=11, filled circles).

Abbreviations as per Tables 3.1 and 3.2

*, *** - $p<0.05$ and $p<0.001$ respectively, between time points in N rats.

§, §§, §§§ - $p<0.05$, $p<0.01$ and $p<0.001$ respectively, between time points in CHU rats.

NB. Statistical differences between variables recorded at minutes 0 and 10 are described in the results section of this chapter.

Figure 3.3

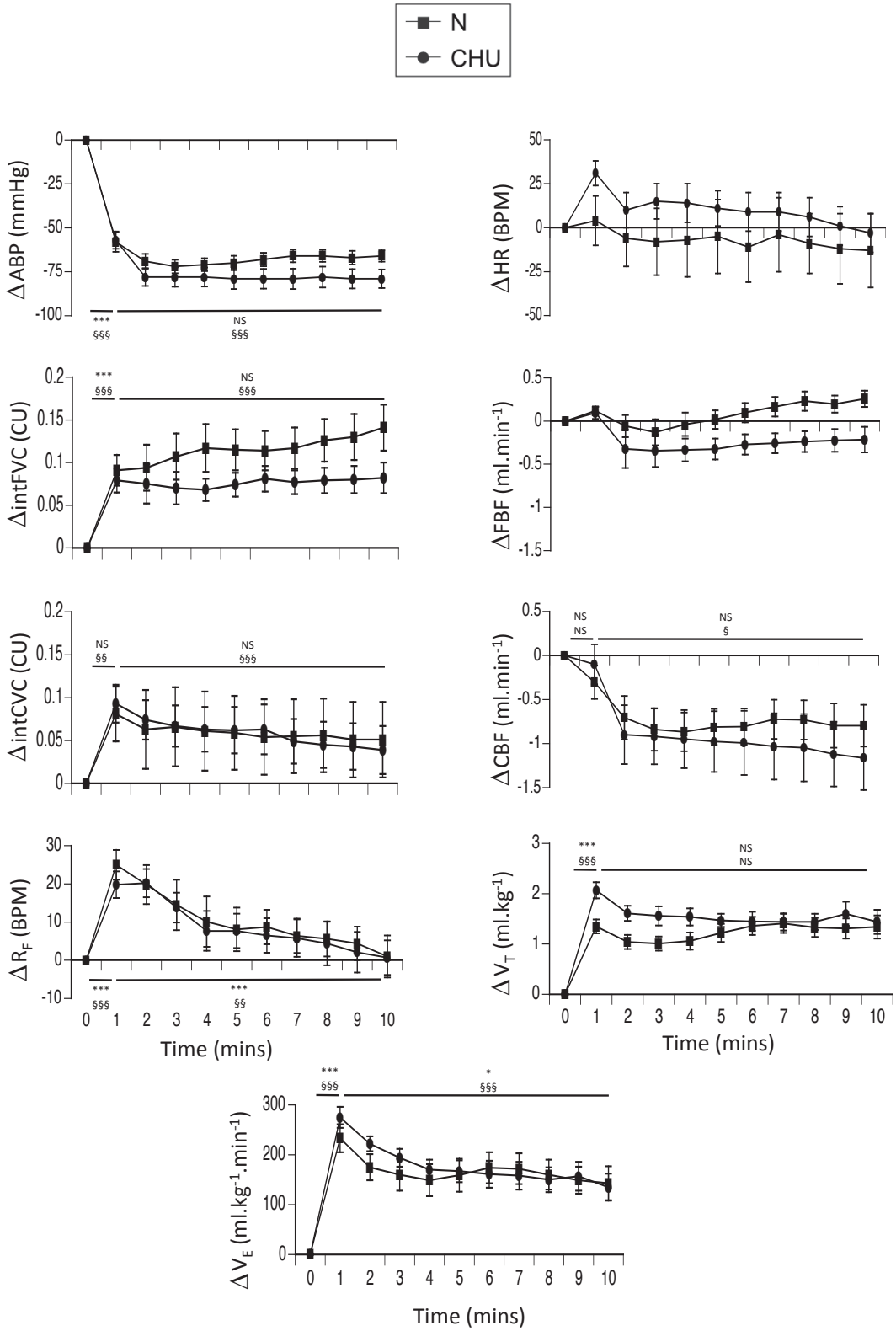
N
CHU
ΔABP (mmHg)
ΔHR (BPM)
ΔintFVC (CU)
ΔFBF (ml.min-1)
ΔintCVC (CU)
ΔCBF (ml.min-1)
ΔRF (BPM)
ΔVT (ml.kg-1)
ΔVE (ml.kg-1.min-1)
Time (mins)
Time (mins)
Time (mins)

Figure 3.4 - Mean changes from baseline in cardiovascular and respiratory variables recorded at one minute intervals during acute systemic hypoxia before and during infusion of a SOD inhibitor.

All values are presented as the mean±SEM change (∆) from the mean baseline of the minute preceding acute systemic hypoxia, in N (n=12, filled squares) and CHU (n=11, filled circles), before (closed symbols) and during (open symbols) infusion of the SOD inhibitor DETC.

Abbreviations as per Table 3.1 and 3.2.

*, **, *** - $p<0.05$, $p<0.01$ and $p<0.001$ between time points in N rats during DETC infusion

§, §§, §§§ - $p<0.05$, $p<0.01$ and $p<0.001$ between time points in CHU rats during DETC infusion

NB. Statistical differences between time points under control conditions can be found in Figure 3.3.

Figure 3.4

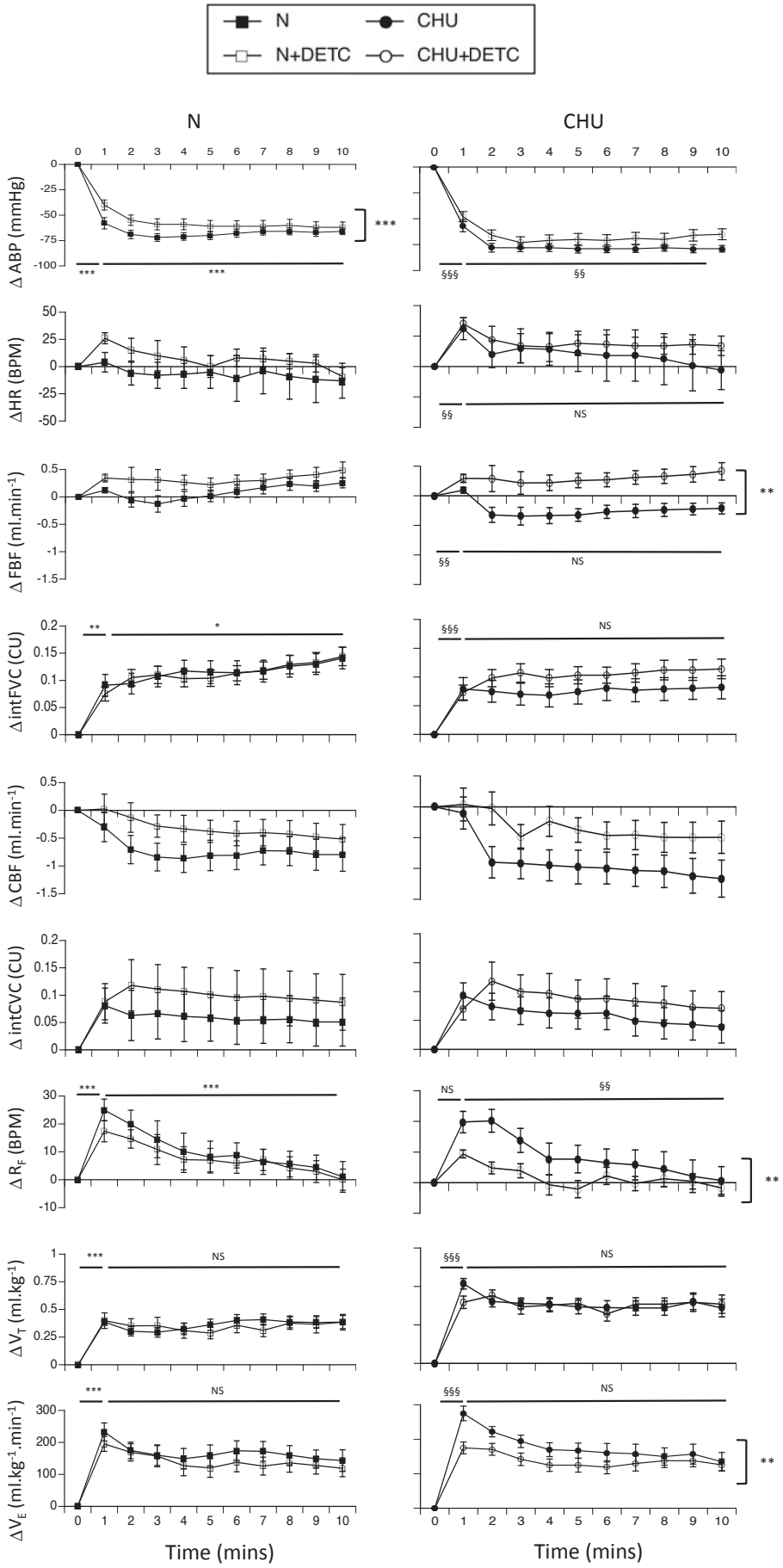
N
CHU
N+DETC
CHU+DETC
N
CHU
Δ ABP (mmHg)
ΔHR (BPM)
Δ FBF (ml.min-1)
Δ intFVC (CU)
Δ CBF (ml.min-1)
Δ intCVC (CU)
Δ RF (BPM)
Δ VT (ml.kg-1)
Δ VE (ml.kg-1.min-1)
Time (mins)
Time (mins)

Figure 3.5 - Example photomicrographs of negative controls for immunohistochemical colocalisation of αSMA and 3-NT in transverse sections of small arterial vessels within the tibialis anterior muscle.

A, C, E, G – DAPI staining, showing cell nuclei.

B: Same field as in A. Visualization following incubation with rabbit polyclonal anti-αSMA1°Ab only, demonstrating no visible fluorescence.

D: Same field as in C. Visualization following incubation with sheep-anti-rabbit IgG-FITC conjugate 2° antibody, with no primary antibody, demonstrating only low levels of non-specific staining of the endothelium, and very little staining of the arterial smooth muscle, or surrounding tissue.

F: Same field as in E. Visualization following incubation mouse monoclonal anti-3NT. 1°AB only, demonstrating low levels of background fluorescence, particularly in the region of the endothelium.

H: Same field as in G. Visualization following incubation with goat-anti-mouse IgG-rhodamine conjugate 2° antibody, with no primary antibody, demonstrating only low levels of non-specific staining of the endothelium, and very little staining of the arterial smooth muscle, or surrounding tissue.

Figure 3.5

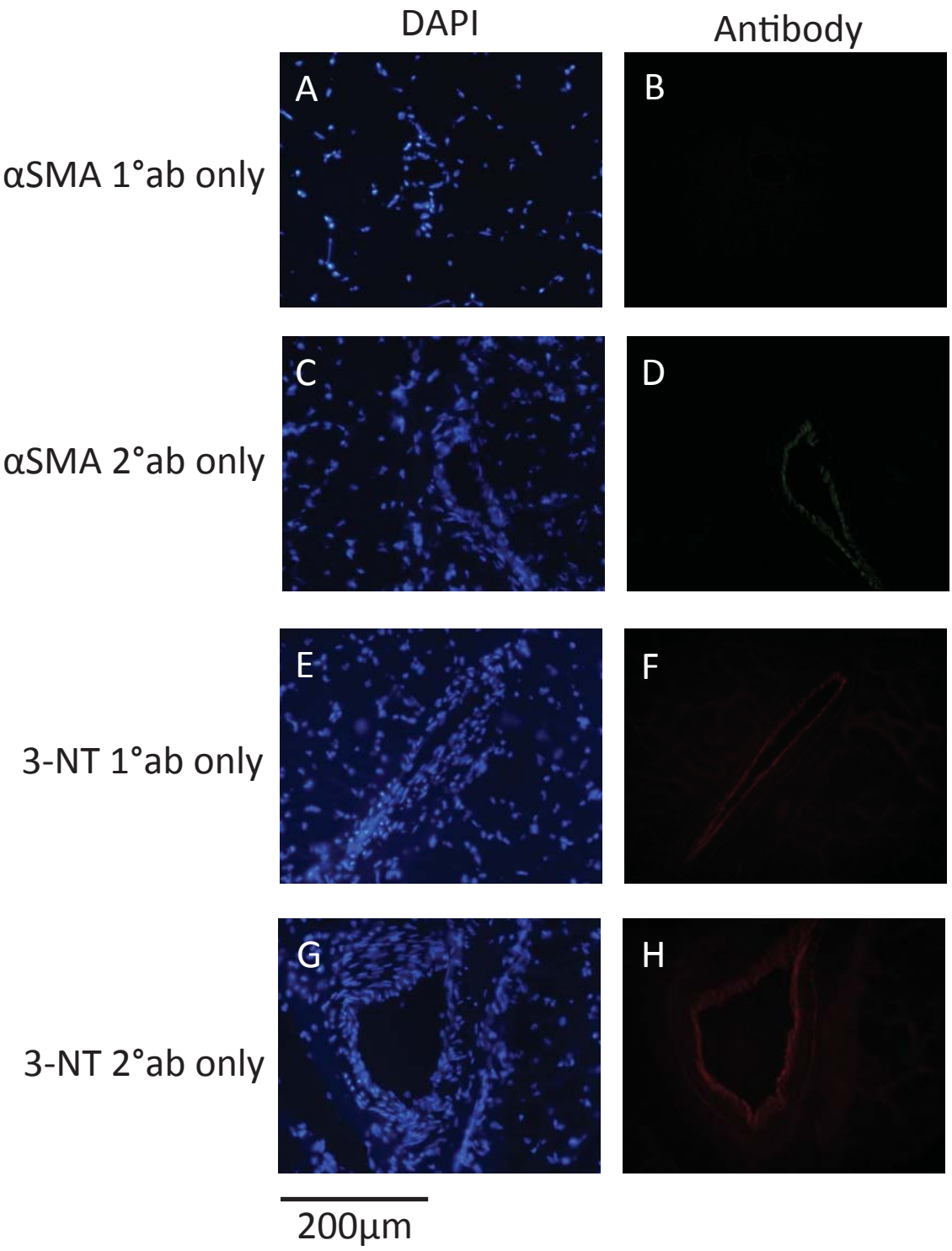
DAPI
Antibody
A
B
αSMA 1°ab only
C
D
αSMA 2°ab only
E
F
3-NT 1°ab only
G
H
3-NT 2°ab only
200µm

Figure 3.6 - Representative dual αSMA and 3NT staining of arterial vessels within transverse sections of TA muscle from 10-12 week old N and CHU rats

A & E: DAPI staining in N and CHU rats respectively

B & F: α-SMA staining in N and CHU rats respectively

C & G: 3-NT staining in N and CHU rats respectively

D & H: Merge of all three staining images. Yellow denotes combined α-SMA and 3-NT staining, indicating vascular interaction with peroxynitrite.

Figure 3.6

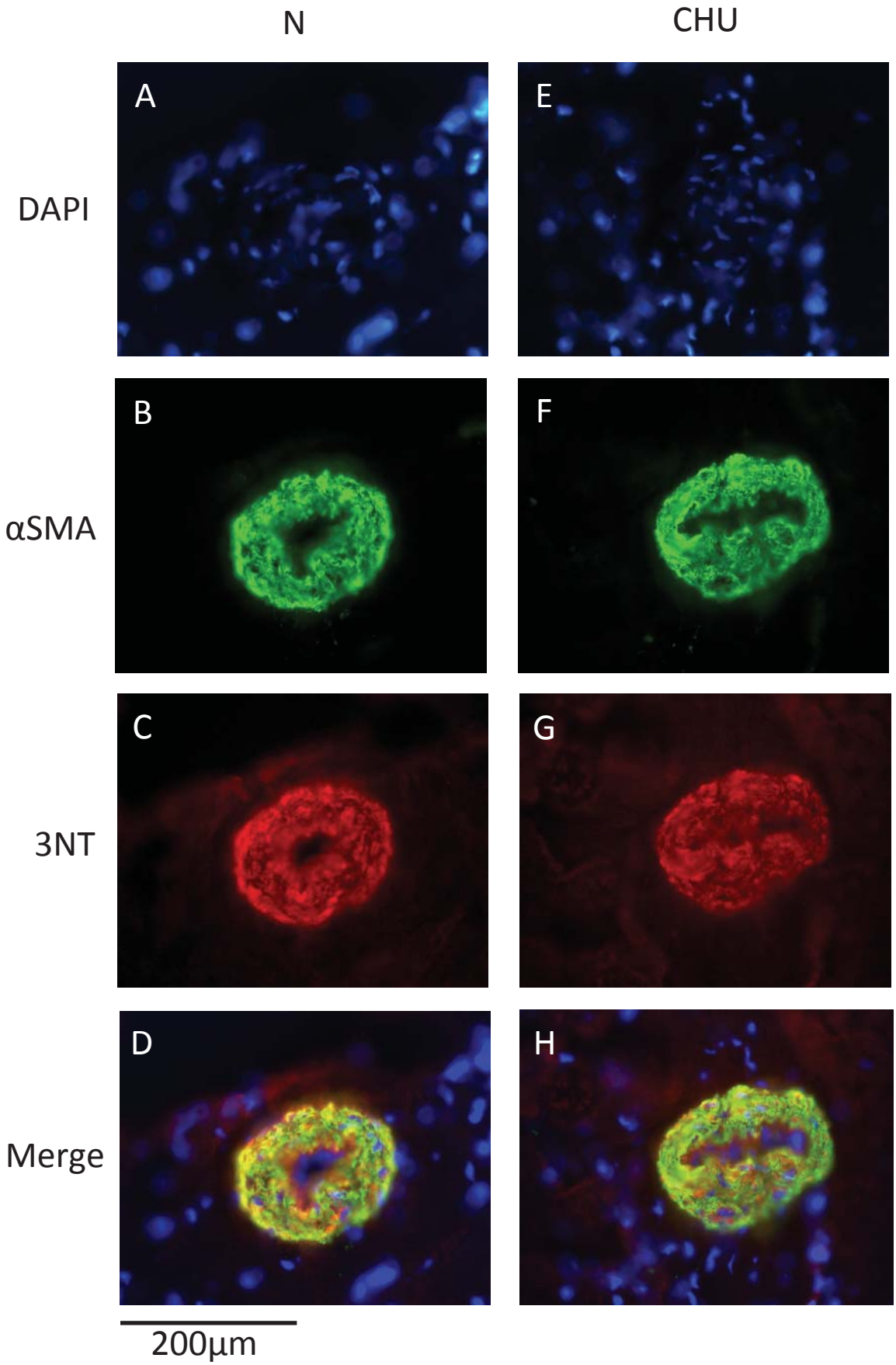

Figure 3.7 - Examples of stained vessels with different morphology, and the associated 3-NT staining. Images A, D, E and H are taken from N rats, whereas images B, C, F and G are taken from CHU rats. Left panels indicate αSMA staining, right hand panels indicate 3-NT staining.

Figure 3.7

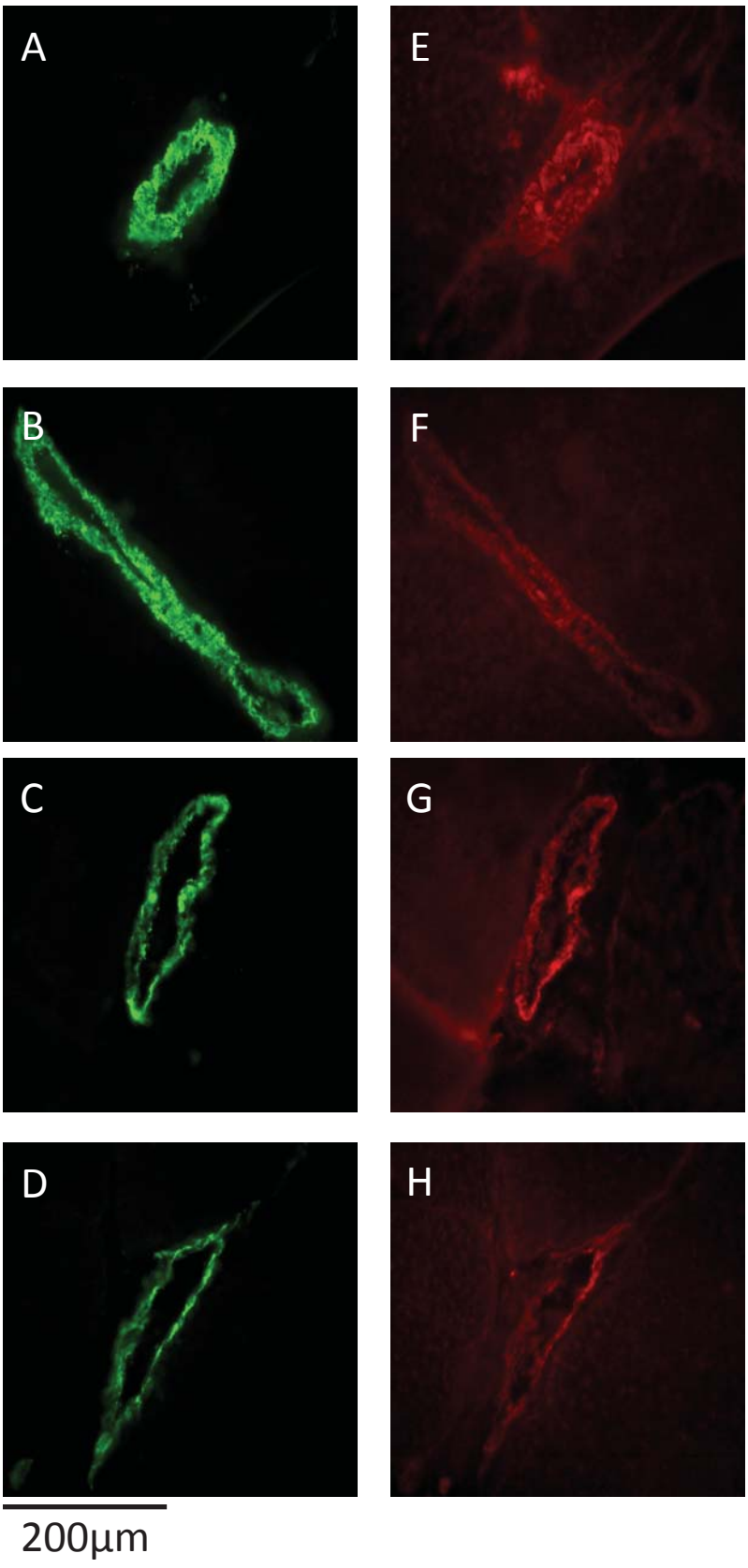

Figure 3.8 – Comparison of oxidative stress levels in arterial vessels in N and CHU rats.

Fluorescent intensity in selected ‘regions of interest’ (See section 3.3, arbitrary units, mean±SEM) of 3-NT staining in 10-12 week old N (n=6) and CHU (n=6, 6 litters) rats, indicating the level of peroxynitrite present in the vessels wall of arterial vessels of TA muscle. Fluorescent intensity is similar in N and CHU rats. There was no significant difference in fluorescent intensity measured in N and CHU rats.

Figure 3.8

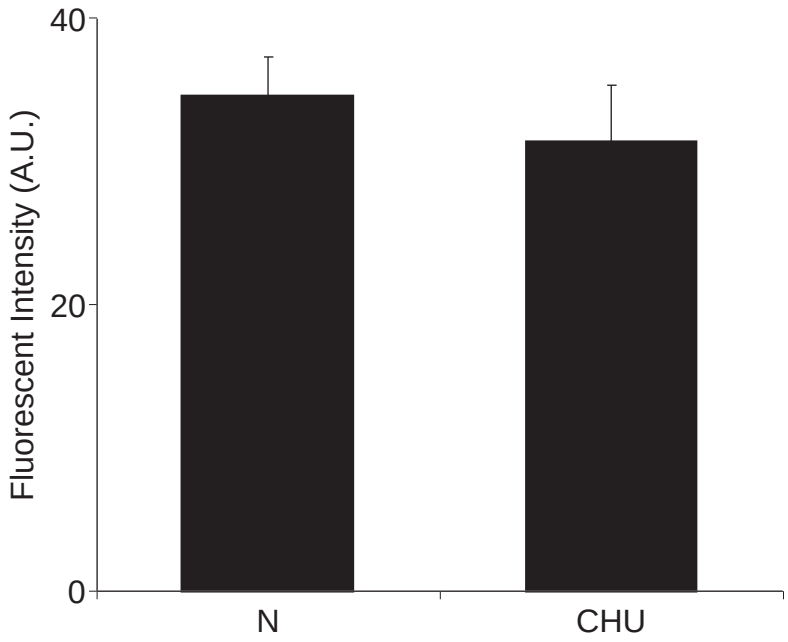

3.4 Discussion

3.4.1 Main Findings

These main findings of the present experiments were that at 10-12 weeks of age, the baseline cardiorespiratory variables measured under Alfaxan anaesthesia were similar in N and CHU rats. Further, the CHU rats show an equally robust response to a 10 minute period of relatively severe hypoxaemia (breathing 8%O_2) to that seen in the normal N rat, in that R_F and CBF showed a similar waning during systemic hypoxia in N and CHU rats. However, when DETC was used to inhibit SOD, there was a reduction in baseline intFVC and FBF in CHU rats only, indicating an increase in baseline vasoconstrictor tone. DETC did not significantly affect the cardiovascular responses evokd by acute systemic hypoxia, but in CHU rats, DETC reduced the increase in R_F evoked by breathing 8%O_2, and hence reduced the hyperventilation evoked by systemic hypoxia. In contrast, DETC did not significantly affect the respiratory response to systemic hypoxia in N rats. *Ex vivo* analysis of vascular oxidative stress in the vascular smooth muscle of small arteries and arterioles of the TA muscle showed similar levels of 3-nitrotyrosine staining in the N and CHU rats.

3.4.2 Cardiorespiratory baselines relative to other studies

Several points must be considered before interpreting these results. The surgical preparation used in the present study is based on that described by Thomas and Marshall (1994). However, their study on N rats was conducted using Saffan anaesthesia, a mixture of alfaxolone and alphadolone, which is no longer

commercially available, rather than Alfaxan, which contains only alfaxalone. Nevertheless, all the baseline cardiovascular and respiratory characteristics measured in the N rats used in the two studies were similar. The pattern of response evoked by acute systemic hypoxia in this study was also similar to that of the previous study, but there were some key differences.

Firstly, Thomas and Marshall (1994) found that during acute systemic hypoxia V_E substantially increased, and then waned towards the latter stages of the hypoxic period, due to a waning of V_T but not R_F. By contrast, in the present study, although V_E waned in a similar fashion in N rats, it was because R_F fell; V_T was well maintained throughout the hypoxic period (see figure 3.2 & 3.3). This might be due to the different anaesthetics. However, it seems more likely to reflect natural changes in the neural processing in the Wistar strain of rat, as these studies were conducted 15 years apart. Thus, in a recent study conducted by Hudson et al., (2011) examining cardiorespiratory and autonomic variables in N rats which were under Saffan anaesthesia, the baseline variables were similar to those reported in the present study, and as in the present study, when 8%O2 was breathed for 10 minutes, it was R_F that began to wane whereas V_T was well maintained. It may be noted that there is considerable variation between published studies as to whether RF, VT or both wane during hypoxia when the hypoxic period is maintained (See Teppema & Dahan, 2010).

Secondly, HR was relatively well maintained throughout the 10 minute period of hypoxia in N rats of the present study, whereas results of previous studies have

shown a secondary fall after initial tachycardia (Neylon & Marshall, 1991; Thomas & Marshall, 1994). This may be attributed to the different anaesthetic regimens; the recent study by Hudson et al., (2011), also conducted under Saffan anaesthesia, as the previous studies were, also showed a secondary fall in HR. The disparity cannot be attributed to the differences in the ventilatory response to hypoxia, for it was V_T that fell in the studies by Thomas & Marshall, and Neylon & Marshall, but R_F that fell in the study of Hudson et al.

Thirdly, CBF showed a more profound fall throughout hypoxia in the present study than in previous studies (Neylon & Marshall, 1991; Thomas & Marshall, 1994), where CBF was maintained until at least the second minute of hypoxia. This may be related to the fact that ABP fell further, to less than 50mmHg, by the first minute of hypoxia in the present study, and thus may be below the autoregulatory range for the maintenance of brain blood flow.

Although the differences between the present study on N rats, and previous similar studies that some of the hypotheses are based on are unfortunate, they do not affect the outcome of the present study, as the aim was to compare the mechanisms of the cardiovascular and respiratory response evoked by acute systemic hypoxia between N and CHU rats, and to establish how the contribution of oxidative stress may be altered in CHU rats.

3.4.3 Comparison of responses evoked by a 10-minute period of hypoxia in N and CHU rats

Overall patterns of response to acute systemic hypoxia were very similar between N and CHU rats; hyperventilation which waned with time, little change in HR, a fall in ABP, and vasodilatation in skeletal muscle and brain which allowed FBF to be maintained, but CBF fell. Addressing the first hypothesis, that CHU rats are more prone to cardiovascular collapse during severe acute hypoxia (see General Introduction) in the present study, the N rats showed similar patterns of response to those observed by Thomas and Marshall (Thomas & Marshall, 1994, 1995). There was still a substantial hyperventilatory response, associated with vasodilatation in both cerebral and femoral vascular beds. However, in contrast to the results of Thomas & Marshall, CBF fell significantly by the 10th minute of breathing 8%O_2, despite substantial vasodilatation. Thomas & Marshall (1994) found that CBF was still maintained at the 10th minute of hypoxia in Wistar rats of a similar size (~350g). However, in the 7-8 week old N rats used by Thomas & Marshall (1995) by the 5th minute of breathing 8%O_2, CBF already showed a strong tendency to be reduced, relative the baseline recorded during normoxia.

The changes measured in blood gasses whilst breathing 8%O_2 were comparable between N and CHU rats, and the hyperventilation seen in CHU was no more prone to waning over the 10 minutes examined than it is in N. CBF fell over 10 minutes in both N and CHU rats, despite the substantial increase in CVC (figure 3.3), but HR was maintained throughout.

Thus, this study found no evidence that CHU rats are more prone to respiratory and cardiovascular collapse than N rats. It is possible that the positive feedback loop, described by Thomas & Marshall (1995), of falling ventilation, heart rate and brainblood flow would have been observed in both the N and CHU rats in this study if the period of hypoxia had been longer or more severe. There is certainly no reason to argue that chronic hypoxia in utero leads to an accentuation of the local, deleterious effects of hypoxia on ventilation, HR and thereby on ABP and CBF, as chronic hypoxia from birth does. Thus, the first hypothesis of this study is largely disproved.

3.4.4 Use of DETC as an inhibitor of SOD

DETC inhibits SOD by acting as a copper chelator, hence removing the copper cofactor required for activity of the cytosolic and extracellular SOD (see General Introduction). The dose of DETC used in this study, $5mg.kg^{-1}.min^{-1}$, was the same as that used *in vivo* by Zou et al., (2001) in rats to inhibit SOD activity in the renal medulla, which was based on *in vitro* studies where similar plasma concentrations have been shown to produce 80-100% inhibition of SOD in cultured spinal neurones (Rothstein *et al.*, 1994). Given that DETC is cell permeant, intracellular concentrations are likely to have been similar to those found in the plasma, and as such the concentrations needed in cell culture are likely similar to those required *in vivo*. A continuous infusion of DETC was used in the present study to ensure maximal inhibition continued, as DETC has been reported to have a short half-life (Voll *et al.*, 1999). However, it was not possible to prove the inhibition of SOD without an *in vitro* assay of SOD activity, which was not easily available. It should be noted

that DETC likely had non-selective effects, beyond inhibition of SOD. Copper is a cofactor for cytochrome C oxidase (complex IV), and for dopamine ß-hydroxlase (Hamza & Gitlin, 2002). However, as the choice of compounds available for *in vivo* manipulation of oxidant systems is limited, such non-selective effects are difficult to avoid, if they occurred under the conditions of the present study.

A further difficulty with the use of DETC is that at low doses it can act as an antioxidant and as a reductant (Liu *et al.*, 1996) and has therefore been used in the treatment of oxygen toxicity (Frank *et al.*, 1978). If the hypothesis, that CHU rats experience chronically high levels of oxidants in the vasculature is true, then administration of DETC to inhibit SOD would be expected to decrease the dismutation of O_2^- to H_2O_2 by SOD, i.e. to have a pro-oxidant effect and acutely accentuate the effect of excess levels of superoxide anions. However, if it is also acting *directly* as an anti-oxidant, then this pro-oxidant effect may be masked.

3.4.5 Effects of DETC during normoxia

With these provisos, it is clear that in the present study DETC reduced baseline FVC indicating an increase in basal vasoconstrictor tone in the femoral vasculature in CHU rats, but not N rats. This finding is consistent with the proposed hypothesis, that CHU rats experience chronically high levels of oxidative stress, for, by inhibiting SOD, DETC would be expected to lead to high levels of O_2^-, which would reduce NO bioavailability, and reduce the ongoing vasodilator effect of shear stress-induced NO release, which is uncovered in N rats when NOS is inhibited with L-NAME (Skinner & Marshall, 1996). In addition, by inhibiting SOD, DETC may also have attenuated an

ongoing vasodilator effect of H_2O_2 produced from O_2^-. This mechanism is well characterised in the coronary circulation of pigs, humans and dogs (Matoba & Hiroaki, 2003; Miura *et al.*, 2003; Yada *et al.*, 2003); SOD dismutes endothelially derived O_2^- into H_2O_2, which move into the subendothelial space, increase the open probability of vascular smooth muscle K_{Ca2+} channels, so decreasing vascular tone (Matoba *et al.*, 2000; Shimokawa & Matoba, 2004).

In further support of the interpretation of the effects of DETC, each of the non-selective effects of DETC mentioned above would likely have vasodilator effects. Inhibition of cytochrome C oxidase would lead to increased release of adenosine (Edmunds *et al.*, 2003), whilst inhibition of dopamine ß-hydroxylase would lead to failure of synthesis of adrenaline and noradrenaline. Moreover, such effects would have been expected in N rats, as well as CHU rats. Thus, the vasoconstrictor effect of DETC in CHU rats is likely to be a result of DETC inhibiting SOD and not a non-selective affect. Whether it achieved its main effect in CHU rats by decreasing the bioavailability of tonically released NO, or by decreasing the production of H_2O_2 cannot be deduced from the present findings. However, the present finding does allow the conclusion that there is a chronically higher level of oxidative stress in the femoral vascular bed in CHU rats than in N rats, which is consistent with the work of Williams et al., (2005b).

Interestingly, in the present study, DETC had no significant effect on baseline CVC, but did significantly increase ABP in CHU rats. Thus, there is no reason to suppose that tonic oxidative stress was present in the cerebral vasculature of CHU rats.

Therefore, the increase in ABP may be a sign that DETC is having a similar vasoconstrictor effect in other tissues, such as the mesenteric vascular bed that Williams et al., (2005b) examined, and therefore having an affect on total peripheral resistance.

DETC significantly reduced P_aO_2 in both N and CHU rats. Given that baseline R_F and V_T did not change, this raises the possibility that DETC attenuated the respiratory response to hypoxic stimulation of the peripheral chemoreceptors, even though the fall in P_aO_2 was too small to have a significant effect on ventilation. This is likely a non-specific effect of DETC, as it occurred equally in N and CHU rats. It is known that SOD-derived H_2O_2 is a possible mechanism involved in hypoxic pulmonary vasoconstriction (Waypa *et al.*, 2001; Waypa *et al.*, 2006), and thus, it is possible that by inhibiting SOD with DETC, inappropriate blood flow distribution within the lung may have resulted in this reduction in P_aO_2. Further, the possibility that DETC caused pulmonary oedema, or another such oxygen-transport limiting effect in the lungs, cannot be ruled out. However, the limited *in vivo* use of DETC makes it difficult to comment further on this finding in the context of any literature.

3.4.6 The effect of DETC on cardiovascular and respiratory response evoked by acute systemic hypoxia

In N rats, DETC had relatively small effects on the response to acute systemic hypoxia in N rats. The fall in ABP during acute system hypoxia was slightly attenuated, although during DETC infusion, the increase in femoral or cerebral

vascular conductance was unaltered. This suggests that there may have been a smaller hypoxia-induced vasodilatation in vasculature other than skeletal muscle and brain, which leads to total peripheral resistance not falling as much as under control conditions, or a reduction in cardiac output. In N rats, there was no effect of DETC on the magnitude of increase in ventilation evoked by breathing 8%O_2, even though PaO_2 fell to a lower value than under control conditions. This is surprising, given that the ventilatory response is initiated by the fall in P_aO_2 acting on peripheral chemoreceptors (Marshall, 1994). It raises the possibility that DETC may have inhibited the ventilatory response to hypoxia by acting peripherally or centrally, in N rats, as previously suggested by the fall in baseline P_aO_2 induced by DETC.

By contrast, during DETC infusion in CHU rats, there is a tendency for ABP to fall less than under control conditions, and for FVC to rise further; consequently, FBF is better maintained during DETC infusion than control conditions. The reasons for this are not easily explained. If we propose that there was an increased rate of O_2^- accumulation under control conditions in CHU rats, then whilst breathing 8%O_2, the hypoxia-induced increase in intFVC would be smaller, because DETC inhibited the dismuting of O_2^- to H_2O_2. Indeed, Pyner et al., (2003) presented evidence demonstrating that in skeletal muscle vasculature of the N rat, systemic hypoxia-induced an increase in O_2^- formation, and showed that the xanthine oxidase inhibitior oxypurinol inhibited O_2^- formation from adenosine. Exogenous SOD accentuated the hypoxia-induced muscle vasodilatation, indicating a role for H_2O_2 in hypoxia-induced vasodilatation in the rat hindlimb, and proposed that it is likely that these superoxide anions are tonically dismuted to form vasodilator H_2O_2.

An alternative possibility is that during DETC infusion in CHU rats not only was SOD inhibited, but the non-selective inhibitory effects of DETC on mitochondrial cytochrome C oxidase (see above) led to an increase in adenosine release during systemic hypoxia, in the same fashion as that proposed for NO by Edmunds et al., (2003). Thus the vasoconstrictor effects of O_2^- were attenuated, and the hypoxia-induced muscle vasodilatation accentuated, and this lead to a non-significant trend for FVC to increase further than under control conditions. The possible roles of adenosine and NO in the hypoxia-induced increases in FVC are explored in Chapter 4.

The striking effect of DETC in CHU rats, was that it greatly reduced the hypoxia-induced increase in R_F, but had no affect on V_T; as a result, the increase in V_E evoked by breathing 8%O_2 was significantly blunted. The mechanism by which this occurs is not clear. The most obvious possibilities are that DETC inhibited the stimulatory effect of hypoxia on the carotid body, or in some way altered the central response to carotid body activity, such that the rise in R_F during stimulation was blunted. The role of reactive oxygen species in oxygen sensing, particularly in the carotid body, are poorly understood. The generation of O_2^- and H_2O_2 by SOD in pulmonary artery smooth muscle cells has been shown to play a role in oxygen sensing (Waypa *et al.*, 2001; Waypa *et al.*, 2006), and some argue that the presence of mitochondrial ROS are required for oxygen sensing (Brunelle *et al.*, 2005). In the carotid bodies of rabbits with pacing-induced heart failure, albeit a model of disease, O_2^- has been shown to enhance the sensitivity of the carotid bodies (Ding *et al.*,

2009a; Ding *et al.*, 2009b). In the present study, if DETC is increasing the accumulation of O_2^- in the carotid bodies of CHU rats, the opposite effect is observed. However, if it were argued that the high levels of O_2^- were reducing the bioavailability of NO, then the mechanism of O_2 sensing described by Edmunds et al., (2003) may be impaired following SOD inhibition, and this may explain the blunting of the hypoxia-induced increase in ventilation. It is not possible to make firm conclusions from the findings of this study, but investigation into the role of ROS in O_2 sensing, and the hypoxia-induced increase in ventilation require further exploration.

3.4.7 Ex vivo analysis of oxidative stress

The immunohistochemical analysis of 3-nitrotyrosine levels in the skeletal muscle vasculature was intended to independently examine whether there is chronically increased oxidative stress in CHU rats, as 3-nitrosylated tyrosine residues are formed when peroxynitrite reacts with tyrosine. The limitations of the methods used must be considered before any attempt is made to interpret the results. First, it should be noted that the initial aim was to examine oxidative stress in medium and small arterioles, but it became clear that because of the ongoing role of free radicals as signaling molecules in skeletal muscle (Jackson *et al.*, 2007), it was difficult to differentiate 3NT staining in small vessels lying between skeletal muscle fibers from staining within the skeletal muscle fibres. Thus, analysis had to be focussed on larger vessels where the smooth muscle vascular wall was more obviously distinguishable.

This study did not have a positive control to confirm the specificity of the 3-NT antibody. To the author's knowledge, there is no published study on sections of any tissue that has employed a positive control for nitrotyrosine expression. The study by Yang et al., (2009) on mesenteric arterial vessels, on which this analysis was based, did not show positive or negative controls for 3NT staining. Other studies have been published with the same methodology used here but in other tissues (Khan *et al.*, 2008; Rump *et al.*, 2010).

The outcome of the image analysis was that there was no significant difference in the level of 3-NT staining observed in the vascular smooth muscle layer of arterial vessels within the TA muscle in N and CHU rats. As argued above, the simplest conclusion to draw from the *in vivo* experiment involving DETC, is that there was increased tonic production of O_2^- from the skeletal muscle vasculature of CHU rats relative to N rats. If it is the correct conclusion, then the results of the immunohistochemical analysis indicate that it is likely that the oxidative stress present is confined to the endothelium, where it can influence endothelial mechanisms that regulate vascular tone, and does not cause marked effects in the vascular wall of larger arterioles and small arteries. This does not rule out the possibility of effects on the vascular smooth muscle of smaller arterioles, where the proportion of vascular smooth muscle cells to endothelial cells is smaller.

Confirming increased rates of superoxide formation in skeletal muscle vasculature, at the level of the small arterioles will remain technically challenging for the reasons indicated above. However, open vessel preparations of larger arterial vessels could

be employed to test this hypothesis, that the endothelium is the site of generation of O_2^-, by using 3NT staining, or other techniques for monitoring O_2^- production. Further, analysis of markers of oxidative stress, such as 3NT in venous efflux from skeletal muscle vasculature during normoxic and hypoxic conditions, may also provide further insight.

In conclusion, the results presented from the experiments in this Chapter suggest that may be a tonically increased level of oxidative stress in the skeletal muscle vasculature of CHU rats, which has the net effect of inducing tonic vasodilatation via the action of H_2O_2 from SOD. The source of the O_2^- is likely to lie within the vascular endothelium. The studies indicate that CHU rats are not more prone to cardiovascular or respiratory failure during severe acute hypoxia than N rats. However, DETC inhibits the SOD isoforms in the extracellular space and in the cytoplasm, and has effects the ventilatory response evoked by hypoxia in CHU rats, which are as yet unexplained.

Chapter 4 – Chronic hypoxia *in utero* and the role of adenosine

4.1 Introduction

As discussed in the General Introduction, there is much evidence that a suboptimal environment *in utero* can result in endothelial dysfunction in several different vascular beds in the offspring.

Thus, Williams et al (2005b) found that in small mesenteric arteries isolated from 7 month old rats subjected to CHU from days 15-21 of pregnancy, exogenous SOD increased endothelium-derived relaxations to methacholine, but had no effect on the equivalent arteries taken from control (N) rats. This suggested that there is either tonic or increased agonist induced-production of O_2^- in this vascular bed after exposure to the *in utero* stressor. The results of chapter 3 are consistent with these findings, as they suggest that *in vivo*, H_2O_2 generated from O_2^- exerts a tonic dilator influence on skeletal muscle vasculature of 1-12 week old CHU rats. A pilot study in this laboratory showed that whilst in anaesthetised N rats, L-NAME significantly reduced hypoxia induced vasodilatation in the rat hindlimb, it did not significantly reduce it in CHU rats, suggesting that there may be a reduction in the contribution of NO to the hindlimb vasodilatation induced by systemic hypoxia in CHU rats (Rook *et al.*, 2008a). Further, a very recent study by Morton et al., (2011) showed that the role of NO in flow-mediated dilatation of the small mesenteric arteries was abolished in rats that had been exposed to hypoxia in the latter third of pregnancy, again suggesting impaired NO bioavailability.

As described in the General Introduction, in N rats, during systemic hypoxia, adenosine acts on A_1 receptors to induce dilatation in the arteries supplying skeletal

muscle. Stimulation of the adenosine A_1 receptor on the endothelium releases NO, in part by generating PGI_2 as an intermediate. This has been demonstrated during acute systemic hypoxia in rats and in humans *in vivo* (Ralevic, 2002; Ray & Marshall, 2006; Markwald *et al.*, 2011). Further, Edmunds et al., (2003) provided evidence that the mechanism by which endothelial cells release adenosine in systemic hypoxia is dependent on the interaction between O_2 and NO at complex IV of the electron transport chain, which leads to reduced ATP resynthesis and release of adenosine when O_2 levels fall, providing that a tonic level of NO is present, such as that generated by ongoing shear stress.

In contrast to these findings, Coney & Marshall (2010) recently found that in CHU rats, acute systemic hypoxia-induced hindlimb vasodilation that was as large as that in N rats, but found that blockade of the A_1 receptor did not result in any impairment of the hypoxia-induced dilatation. However, infusion of adenosine in CHU rats resulted in a similar magnitude of vasodilatation to that seen in N rats, and this dilatation was partly attenuated by A_1 receptor blockade as it is in N rats. In view of these findings, Coney & Marshall (2010) suggested that decreased bioavailability of NO in CHU rats may impair the release mechanism of adenosine from the endothelium during systemic hypoxia. Thus, the aims of the experiments described in this chapter were to explore the roles of NO and adenosine in the vasodilatation induced in the muscle vasculature by acute systemic hypoxia in CHU rats, comparing the findings with those observed in N rats.

Hypotheses

1. The role of NO in hypoxia-induced vasodilatation is smaller in CHU rats than N rats because the bioavailability of NO is lower in CHU rats.

2. Because the bioavailability of NO is lower in CHU rats, the sensitivity of the endothelium to a fall in PO_2 is decreased, and less adenosine is released during systemic hypoxia. This decreases the role for the adenosine A_1 receptor in hypoxia-induced vasodilatation, as seen by Coney & Marshall (2010). Therefore, if background levels of NO are restored with the NO donor SNAP, after NO synthesis inhibition, adenosine release and the role of the adenosine A_1 receptor in hypoxia-induced vasodilatation will be restored. These hypotheses were tested by recording vascular responses evoked by acute systemic hypoxia before and after L-NAME, then after the influence of NO was restored by infusion of the NO donor SNAP, and then in the presence of the adenosine A1 receptor antagonist DPCPX.

   Unexpectedly, during SNAP infusion, the vasodilatation was restored in CHU, as well as N rats, but DPCPX did not reduce the vasodilatation during systemic hypoxia in either N or CHU rats, in contrast to previous findings on N rats (Edmunds *et al.*, 2003). Therefore, the effectiveness of DPCPX as an adenosine A_1 receptor antagonist was checked in both N and CHU rats. Having established that the DPCPX being used in the present study was an effective A_1 receptor antagonist in both N and CHU rats, it was hypothesized that:

3. There is large redundancy in the mechanisms of hypoxia-induced muscle vasodilatation, and that under the condition of SNAP infusion after NOS inhibition hypoxia-induced vasodilatation may be mediated by adenosine acting on A_{2A} receptors in N and/or CHU rats. To test this hypothesis the effect of the adenosine A_{2A} receptor antagonist ZM-241,385 on hypoxia-induced muscle vasodilatation was investigated during SNAP infusion following NOS inhibition. As a final step, the effect of DPCPX was tested after ZM-241,385.

4.2 Methods

4.2.1 General characteristics of the animals used

A total of 63 rats were used in this experiment. They consisted of 3 study groups; Study one was performed on 12 N rats (weight 385±11g, age 66±1 days) and 14 CHU rats (weight 388±12g, age 65±1day, 5 litters). Study 2 was performed on 5 N rats (weight 384±11g) and 6 CHU rats (weight 394±13g, age 71±2 days, 3 litters). Study 3 was performed on 12 N rats (weight 356±14g, age 78±1day) and 14 CHU rats (weight 389±7g, age 84±3 days, 4 litters).

4.2.2 Animal preparation

The surgical preparation used for each rat in these studies is described in Chapter 2. In study groups 1 and 3, ABP was measured via the right brachial artery, whilst blood for arterial blood gas measurements was sampled via the left brachial artery. Drug infusions were given via the caudal ventral tail artery, or via the left femoral vein. FBF was recorded from the right femoral artery. FVC and HR was calculated as described in Chapter 2. Airflux was recorded from the side arm of the tracheal cannula, R_F, V_T and V_E derived as described in chapter 2.

A similar preparation was used in the rats that are part of study 2. ABP was measured from the right brachial artery. Drug infusions were given via the left femoral vein, whilst FBF was recorded from the right femoral artery.

In all rats where arterial blood gasses were sampled, normoxic values were obtained from blood samples taken in the final minute before hypoxia, and hypoxic values were obtained from blood taken in the final minute of breathing 8%O_2.

4.2.3 Protocols

4.2.4 Study 1 – The role of NO and the adenosine A_1 receptors

At least 30 minutes after the completion of the surgical preparation rats, were exposed to 5 minutes of breathing 8% O_2 in N_2. This was repeated two to three times, with at least 15 minutes between stimuli, to ensure the response to acute systemic hypoxia was consistent. The NO synthase (NOS) inhibitor L-NG-Nitroarginine methyl ester (L-NAME 10mg.kg^{-1} i.a.) was then given via the tail artery. At least 20 minutes later, and when cardiovascular baselines had become stable at their new levels, the response to 8%O_2 was recorded again. After cardiovascular variables had returned to their resting values again, an infusion of S-nitroso-N-acetylpenicillamine (SNAP, ~10µg.min^{-1}.kg^{-1} i.a.) was commenced, infused a rate sufficient to restore baseline FVC to a level similar to that seen in control conditions; this was adjusted as appropriate in each animal. Once this was achieved and stable for at least 10 minutes, the response to 8%O_2 was re-tested. Following this the adenosine A_1 receptor antagonist 8-cyclopentyl-1,3-dipropylxanthine (DPCPX, 0.1mg.kg^{-1} i.v.) was given. This dose was sufficient to reverse responses to the selective A_1 receptor agonist CCPA (Bryan & Marshall, 1999a). At least 20 minutes later, after cardiovascular variables had stabilised once more, the response to acute systemic hypoxia was re-tested.

4.2.5 Study 2 – The functional roles of adenosine A_1 receptors in N and CHU

To ensure that the effect of DPCPX in N and CHU rats was consistent with the findings of previous studies (Bryan & Marshall, 1999a; Coney & Marshall, 2010) the cardiovascular responses to acute systemic hypoxia and infusion of adenosine were tested in N and CHU rats before and after the adenosine A_1 receptor antagonist DPCPX. Following a 30-minute equilibration period, the responses evoked by breathing 8% O_2 in N_2 for 5 minutes, and by infusion of adenosine (0.5mg.kg^{-1}.min^{-1} i.a.) given via the caudal ventral tail artery were tested, in a randomised order. After consistent responses to the stimuli were achieved, the DPCPX was given, at the same dose as used in study 1. After 30 minutes, the response evoked by infusion of adenosine and by 8%O_2 were re-tested.

4.2.6 Study 3 – the role of the Adenosine A_{2A} receptors

After a 30 minute period of equilibration control responses evoked by acute systemic hypoxia and by infusion of adenosine (0.5mg.kg^{-1}.min^{-1} i.a.) were recorded in a randomised order, as in study 2. Then, as in study 1, L-NAME (10mg.kg^{-1} i.a.) was given via the caudal ventral tail artery. At least 20 minutes later, responses to infusion of adenosine or acute systemic hypoxia were retested. Following this, as in study 1, SNAP was infused at a rate sufficient to restore baseline FVC to that of control conditions. Once this was achieved, responses to infusion of adenosine and to acute systemic hypoxia were re-tested before and after the selective adenosine A_{2A} receptor antagonist ZM241385 (0.05 mg kg^{-1}, I.V. as described by Bryan & Marshall(1999a)) was given. Finally, both responses were re-tested at least 20 minutes after DPCPX was given.

4.2.7 Data analysis and statistics

All data are presented as mean±SEM of N or CHU rats. MABP, HR, FBF and FVC are presented as mean values across the 5-minute periods of hypoxia or adenosine infusion. The magnitude of vasodilatation was computed offline as the integral of FVC during the 5 minute period immediately before the hypoxia or adenosine response subtracted from the integral of the FVC recorded during hypoxia or adenosine infusion, and is presented as ∆intFVC. Only mean baseline R_F, V_T and V_E are presented, as the focus of the studies was on vascular responses evoked in the hindlimb. Mean R_F, V_T and V_E presented was that recorded in the 5-minute period preceding the first stimuli.

Statistics analysis was carried out using Aable 20/20 data vision v3.0.5 software (Gigawiz, Tulka, OK, USA). Comparison of blood gasses and cardiovascular baselines between N and CHU rats was made with Students unpaired t-test. Within group comparisons of blood gasses and responses evoked under different conditions was made using repeated measures ANOVA with Scheffés *post hoc* test.

4.3 Results

4.3.1 Study 1 - The role of NO and the adenosine A_1 receptors

Baseline ABP, FBF and FVC were similar in the N and CHU rats of group 1 (see Table 4.1). However, HR was significantly lower in CHU than in N, as was V_T and V_E. Arterial blood gasses (P_aO_2, P_aCO_2 and $_PH_a$) were similar between groups. (Table 4.2).

4.3.2 Responses evoked by acute systemic hypoxia

In N rats, acute systemic hypoxia caused the expected substantial fall in PaO_2, and a fall in $PaCO_2$, while pH_a rose as a result of the hyperventilation induced (Table 4.2). There was an increase in HR and an increase in intFVC indicating muscle vasodilatation, whilst ABP fell; FBF was maintained over the 5 minute period (Figure 4.1, left hand panels). The pattern of response evoked by hypoxia in CHU rats was very similar (cf. Tables 4.1, 4.2 and Figure 4.1). The magnitude of response in all variables recorded was similar between N and CHU rats, as previously reported (Coney & Marshall, 2010).

4.3.3 Effect of L-NAME

Administration of L-NAME caused an increase in baseline ABP and a fall in HR and in baseline intFVC, in N and CHU rats. (cf. Figure 4.1). Under this condition, the increase in intFVC evoked by breathing 8%O_2 was substantially decreased in both N and CHU rats (cf. Figure 4.1 I & J). The values of P_aO_2, P_aCO_2 and pH_a were not

significantly affected by administration of L-NAME in either N or CHU rats (Table 4.2).

4.3.4 Effect of SNAP infusion

As intended, the NO donor SNAP was infused at a rate sufficient to restore FVC to a similar level to that recorded before L-NAME (Figure 4.1 cf. E&F). However, ABP was significantly lower than before L-NAME in N and CHU rats (Figure 4.1 cf. A&B), and HR was significantly increased (Figure 4.1 cf. C&D).

During infusion of SNAP in N rats, the increase in intFVC evoked by breathing 8%O_2 was restored to a magnitude similar to that seen before L-NAME. By contrast, under the same conditions in CHU rats, the magnitude increased in intFVC was significantly increased relative to that seen before L-NAME ($p<0.01$, cf. figure 4.1 I & J). ABP fell and HR was increased during hypoxia in both N and CHU rats as under the control condition.

4.3.5 Effect of adenosine A_1 receptor inhibition

During infusion of SNAP in N rats, DPCPX significantly reduced baseline intFVC (Figure 4.1 cf. E&F), and significantly increased baseline ABP (Figure 4.1 cf. A) and HR (Figure 4.1 cf. C) relative to baselines during SNAP infusion. The magnitude of the increase in intFVC evoked by breathing 8%O_2 was not affected by DPCPX (Figure 4.1 cf. I), nor was the magnitude of the fall in ABP (Figure 4.1 cf. A).

By contrast, in CHU rats during SNAP infusion, there was no effect of DPCPX on baseline intFVC (Figure 4.1 cf. F). DPCPX significantly increased baseline ABP, HR, and FBF (Figure 4.1 cf. B, D and H). As in N rats, DPCPX had no significant effect on the magnitude of hypoxia-induced increase in intFVC (Figure 4.1 cf. J).

4.3.6 Study 2 – The effect of DPCPX

In this study, baseline ABP, FBF and FVC were similar between groups of N and CHU (Table 4.1). In contrast to study 1, HR was significantly higher in CHU than N rats (Table 4.1).

In N rats, infusion of adenosine caused a significant fall in ABP ($p<0.001$, Figure 4.2A) and HR ($p<0.05$, Figure 4.2C). Adenosine induced a significant increase in intFVC ($p<0.05$), and FBF was maintained. Acute systemic hypoxia, induced by breathing 8%O_2, evoked a significant fall in ABP ($p<0.001$, Figure 4.2A), and a rise in HR (n.s. Figure 4.2C). There was a significant rise in intFVC ($p<0.05$); FBF was maintained.

In CHU rats, infusion of adenosine caused a comparable fall in ABP and HR, and increase in intFVC as in N rats (Figure 4.2H). By contrast, FBF fell significantly during adenosine infusion ($p<0.01$). Further, the increase in intFVC evoked by breathing 8%O_2 was comparable to that recorded in N rats, as was the fall in ABP and rise in HR (Figure 4.2 B,D & H). FBF was maintained during acute hypoxia (Figure 4.2F).

DPCPX had no significant effect of baseline ABP, HR, FBF or intFVC in N rats (data not shown), although it did tend to result in higher HR (p=0.052). Similarly, in CHU rats, there was no significant effect of DPCPX on baselines, and HR was unchanged (p>0.5).

Following DPCPX, in N rats the adenosine induced-increase in intFVC was significantly reduced (Figure 4.2G) and the fall in ABP was blunted (Figure 4.2A) and the bradycardia was reversed to a tachycardia (Figure 4.2C). The increase in intFVC evoked by breathing 8%O_2 tended to be attenuated following DPCPX in N rats (Figure 4.2E, p=0.08). The fall in ABP was attenuated (Figure 4.2A), but the hypoxia-induced tachycardia was unchanged (Figure 4.2C).

In CHU rats the adenosine-induced increase in intFVC was significantly reduced (Figure 4.2F) and the fall in was ABP attenuated (Figure 4.2B) and HR was significantly increased rather than decreased (Figure 4.2D). The increased in intFVC evoked by breathing 8%O_2 was significantly attenuated (Figure 4.2F), and the fall in ABP was blunted (Figure 4.2A).

4.3.7 Study 3 – The effect of an adenosine A_{2A} receptor antagonist

Baseline ABP, HR, FBF, FVC, R_F V_T and V_E were again similar between the N and CHU rats used in group 3 of this study (Table 4.1) and P_aO_2, P_aCO_2 and $_PH$ were also similar between groups (Table 4.2).

In N rats, the pattern of response evoked by breathing 8%O_2 was similar in nature and in magnitude to that described for study 1; ABP fell but there was an increase in intFVC, and increased HR (figure 4.3, left hand panels). The pattern of response evoked by breathing 8%O2 was comparable in the CHU rats. The increase in FVC evoked by hypoxia in N and CHU rats were not significantly different (Figure 4.3 cf. I&J)

Similarly, in both N and CHU rats, under control conditions, infusion of adenosine evoked a fall in ABP and a small fall in HR (Figure 4.4 A-D), and an increase in intFVC (Figure 4.4 cf. E&F). The increases in intFVC evoked by infusion of adenosine were not significantly different in N and CHU rats (Figure 4.4 cf. I&J).

4.3.8 The effect of L-NAME

The effects of L-NAME were comparable to those described in study 1: In N and CHU groups baseline intFVC, FBF and HR were reduced, whilst ABP was increased (Figure 4.3 A-H). Arterial blood gasses were not significantly affected by L-NAME (Table 4.2).

Following L-NAME, breathing 8%O_2 evoked a fall in ABP (Figure 4.3A&B), and rise in HR (Figure 4.3C&D), but the increase in intFVC was significantly attenuated in both N and CHU rats (Figure 4.3 cf. I&J).

Similarly, following L-NAME there was still a fall in ABP during adenosine infusion in N and CHU rats (Figure 4.4A&B). In contrast, adenosine infusion evoked an increase

in HR (Figure 4.4C&D). The increase in intFVC evoked by adenosine infusion was abolished by L-NAME in N rats (Figure 4.4 I), and significantly attenuated in CHU rats ($p<0.001$, Figure 4.4J).

4.3.9 Effect of SNAP infusion

The effect of SNAP infusion on baselines was similar to that described in study 1. Baseline FVC was restored to similar level to control conditions both N and CHU rats. However, as is shown in Figure 4.3 E and F, the restoration of FVC to control values was not as satisfactory as that achieved in study 1. PaO_2 tended to be increased compared to before L-NAME in N rats, and was significantly increased compared to before L-NAME in CHU rats (Table 4.3). $PaCO_2$ was significantly lower than before L-NAME in N and CHU (Table 4.3).

As in study 1, in N rats of study 3, during SNAP infusion, breathing 8%O_2 evoked a fall in ABP, and rise in HR, and the magnitude of increase in intFVC was similar to that seen before L-NAME ($p>0.5$, Figure 4.3 cf. A, C & I).

Further, during SNAP infusion, the responses evoked by adenosine infusion in N rats was similar in nature to that of control conditions; a fall in ABP (Figure 4.4 cf. A), a fall in HR (figure 4.4 cf. C) and an increase in intFVC (Figure 4.4 cf. E). However, the adenosine-induced increase in intFVC was significantly larger than before L-NAME (Figure 4.4 cf. I).

In CHU rats, during SNAP infusion, breathing 8%O_2 again evoked a fall in ABP, rise in HR, whilst intFVC increased. In contrast to the results of study 1, the magnitude of the increase in intFVC evoked by breathing 8%O_2 was similar to before L-NAME.

In CHU rats, during SNAP infusion, similar results were obtained during infusion of adenosine to those observed in N rats; a fall in ABP, fall in HR, and a rise in intFVC (Figure 4.4 B, D & F). Similarly to N rats, the increase in intFVC substantially larger than recorded before L-NAME ($p<0.01$, Figure 4.4 J).

4.3.10 The effect of ZM241385

The adenosine A_{2A} receptor antagonist ZM241385 increased baseline ABP in bothN and CHU rats (Figure 4.3 cf. A&B) and HR (Figure 4.3 cf. C&D). There was no significant effect on baseline intFVC in N or CHU rats (Figure 4.3 I&J) or on PaO_2, $PaCO_2$, or pH relative those seen during SNAP infusion (Table 4.3). ZM241385 had no effect on the hypoxia-induced increase in intFVC in either N or CHU rats (Figure 4.3 cf. I&J). However, ZM241385 caused a significant reduction in the magnitude of the adenosine-induced increase in intFVC in both N and CHU rats (Figure 4.4 cf. I&J).

4.3.11 Effect of DPCPX

DPCPX, given after ZM241385, had no effect on baseline ABP in N or CHU rats (figure 4.3 A&B), caused a small increase in HR in N rats (Figure 4.3C). IntFVC was reduced in CHU rats only (Figure 4.3 cf. F).

After DPCPX, the increase in intFVC evoked by breathing 8%O_2 showed a strong tendency to be reduced relative to that following ZM241385 in N rats ($p=0.052$, Figure 4.3 I), and was significantly reduced in CHU rats ($p<0.001$, figure 4.3J). The hypoxia-induced fall in ABP was not significantly affected.

After DPCPX, infusion of adenosine did not induce a significant increase in intFVC in either N or CHU rats ($p>0.05$, Figure 4.4 E&F), and as such the change in intFVC induced by adenosine was significantly reduced from that evoked after ZM241385 in both N and CHU rats (Figure 4.4 cf. I&J).

Table 4.1 – Baseline cardiovascular variables in N and CHU rats used in study 1, 2 and 3.

Group	Drug regimen	Group	ABP (mmHg)	HR (bpm)	FBF ($ml.min^{-1}$)	FVC ($ml.min^{-1}.mmHg^{-1}$)	R_F (bpm)	V_T ($ml.kg^{-1}$)	V_E ($ml.min^{-1}.kg^{-1}$)
1	L-NAME SNAP DPCPX	N (n=12)	139 ±3.8	433 ±9	1.67 ±0.1	0.0122 ±0.0012	102 ±2	2.1 ±0.06	217± 6
		CHU (n=13)	135 ±2.9	391 ±10**	1.60 ±0.1	0.0119 ±0.00062	101 ±2	1.85 ±0.05**	186 ±4.2**
2	DPCPX	N (n=4)	135 ±10	407 ±11	1.58 ±0.16	0.0122 ±0.0022	n/a	n/a	n/a
		CHU (n=6)	136 ±4.1	456 ±7*	1.95 ±0.24	0.0146 ±0.0022	n/a	n/a	n/a
3	L-NAME SNAP DPCPX ZM241385	N (n=12)	134 ±3.3	427 ±8	1.64 ±0.09	0.0122 ±0.00063	103 ±3	1.91 ±0.1	197 ±14
		CHU (n=14)	134 ±3.8	414 ±7	1.53 ±0.13	0.01145 ±0.00096	104 ±2	1.83 ±0.04	191 ±6

Baseline cardiovascular and respiratory variables recorded in N and CHU rats in groups one, two and three.

ABP; arterial blood pressure, HR; heart rate, FBF; femoral blood flow, FVC; femoral vascular conductance, R_F; respiratory frequency, V_T; ventilatory tidal volume, V_E; ventilatory minute ventilation.

*, ** - $p<0.05$, $p<0.01$ respectively CHU vs N

Table 4.2 – Arterial blood gasses during normoxia and hypoxia in N and CHU rats in study 1

Condition	Group	P_aO_2	P_aO_2	P_aCO_2	P_aCO_2	$_PH_a$	$_PH_a$
		Normoxia	Hypoxia	Normoxia	Hypoxia	Normoxia	Hypoxia
Control	N (n=12)	82.8 ±1.2	33.4 ±4.5	44.1 ±0.8	29.6 ±1.7	7.427 ±0.008	7.515 ±0.016
	CHU (n=13)	80.7 ±1.3	28.4 ±1.2	44.6 ±0.5	28.3 ±0.7	7.410 ±0.006	7.524 ±0.017
+L-NAME	N (n=12)	81.0 ±2.1	31.7 ±0.8	40.3 ±1.3	28.0 ±0.6	7.433 ±0.011	7.434 ±0.015
	CHU (n=13)	78.8 ±2.8	27.4 ±1.0	41.4 ±0.9	28.5 ±1.0	7.398 ±0.011	7.420 ±0.013
+SNAP	N (n=12)	96.4 ±2.6	34.9 ±0.8	34.1 ±1.2	25.6 ±0.7	7.472 ±0.008	7.501 ±0.016
	CHU (n=13)	90.1 ±5.0	32.6 ±1.6	34.0 ±0.8	26.1 ±0.7	7.446 ±0.007	7.481 ±0.011
+DPCPX	N (n=12)	95.6 ±1.7	32.0 ±0.7	33.1 ±0.9	24.3 ±0.5	7.50 ±0.009	7.555 ±0.018
	CHU (n=13)	96.6 ±1.6	30.5 ±1.0	32.1 ±0.5	23.0 ±1.4	7.474 ±0.005	7.515 ±0.010

Arterial blood gasses during normoxia (21% O_2) and during the 5th minute of hypoxia (8%O_2) in study 1, under control conditions, following L-NAME, during SNAP infusion, and following DPCPX.

P_aO_2; arterial oxygen partial pressure, P_aCO_2; arterial carbon dioxide partial pressure, $_PH_a$; arterial $_PH$.

Table 4.3 - Arterial blood gasses during normoxia and hypoxia in N and CHU rats in study 3

Condition	Group	P_aO_2 mmHg	P_aO_2 mmHg	P_aCO_2 mmHg	P_aCO_2 mmHg	$_PH_a$	$_PH_a$
		Normoxia	Hypoxia	Normoxia	Hypoxia	Normoxia	Hypoxia
Control	N (n=5)	75.3 ±2.5	24.8 ±1.5	43.0 ±1.4	25.1 ±0.79	7.41 ±0.009	7.561 ±0.016
	CHU (n=10)	75.6 ±1.15	25.7 ±0.9	41.3 ±1.5	27.6 ±1.0	7.42 ±0.010	7.523 ±0.013
+L-NAME	N (n=5)	83.8 ±3.6	25.2 ±1.8	36.8 ±0.8	24.6 ±1.1	7.44 ±0.007	7.51 ±0.012
	CHU (n=10)	75.9 ±1.7	25.6 ±0.8	38.2 ±0.8	24.4 ±0.9	7.41 ±0.006	7.47 ±0.017
+SNAP	N (n=5)	95.2 ±3.4	33.8 ±2.7	30.5 ±1.2	22.5 ±0.9	7.48 ±0.009	7.53 ±0.012
	CHU (n=10	91.2 ±1.9	30.3 ±1.1	30.4 ±0.8	21.3 ±0.6	7.47 ±0.008	7.49 ±0.011
+ZM241385	N (n=5)	82.5 ±2.3	28.8 ±2.2	32.6 ±1.1	22.0 ±0.6	7.46 ±0.009	7.55 ±0.020
	CHU (n=9)	86.2 ±1.7	30.8 ±1.3	31.3 ±0.6	21.4 ±0.6	7.45 ±0.007	7.50 ±0.011
+DPCPX	N (n=5)	89.7 ±1.6	26.2 ±1.3	29.0 ±0.7	21.0 ±0.9	7.50 ±0.008	7.60 ±0.017
	CHU (n=9)	89.1 ±2.3	26.1 ±1.0	28.5 ±0.8	22.2 ±0.7	7.48 ±0.009	7.53 ±0.013

Arterial blood gasses during normoxia (21% O_2) and in the 5th minute of hypoxia (8%O_2) in N and CHU rats in study 3, under control conditions, following L-NAME, during SNAP infusion, following ZM241385, and following DPCPX.

Abbreviations as per table 4.2

Figure 4.1 – Cardiovascular responses to acute systemic hypoxia in N and CHU rats in study group 1.

Mean cardiovascular variables recorded during normoxia (21% O_2, black bars) and acute systemic hypoxia (8% O_2, open bars) in N (left hand side) and CHU (right hand side) rats. Values shown are mean±SEM for N (n=12) and CHU (n=14), represent mean values recorded over the 5-minute periods of hypoxia. ∆intFVC represents the increase in intFVC recorded during hypoxia from the preceding normoxic baseline.

ABP; mean arterial blood pressure, HR; heart rate, intFVC; integrated femoral vascular conductance, FBF; femoral blood flow, ∆intFVC; change in integrated femoral conductance during acute systemic hypoxia.

*** - $p<0.001$ – Between L-NAME and Control condition

§, §§, §§§ - $p<0.05$, $p<0.01$, $p<0.001$ respectively between L-NAME+SNAP and control conditions

††, ††† - $p<0.01$, $p<0.001$ respectively between L-NAME+SNAP+DPCPX and L-NAME+SNAP conditions.

Figure 4.1

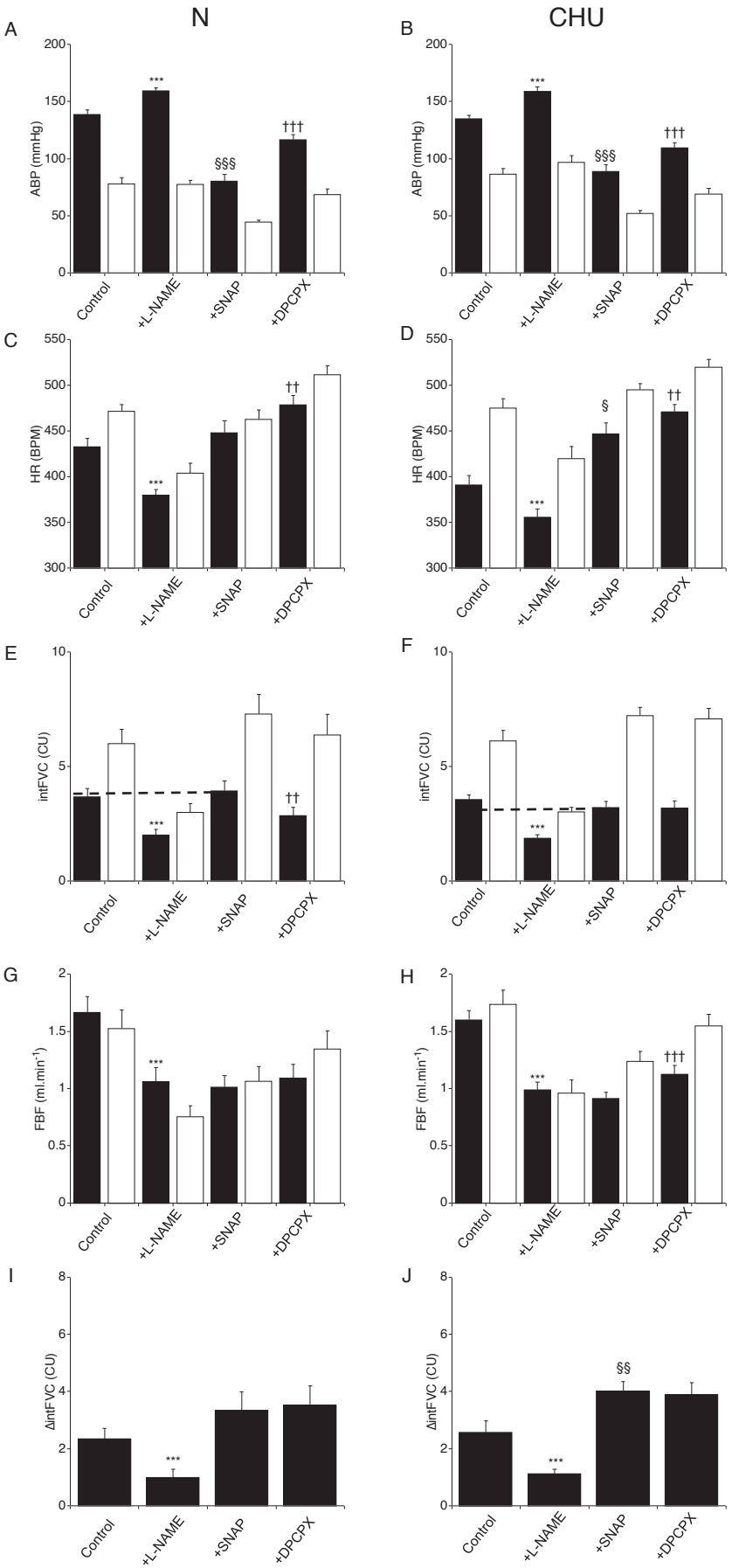
N
CHU
A
B
C
D
E
F
G
H
I
J
ABP (mmHg)
HR (BPM)
intFVC (CU)
FBF (ml.min-1)
ΔintFVC (CU)
Control
+L-NAME
+SNAP
+DPCPX
***
§§§
†††
§
§§
††

Figure 4.2 – The effect of an adenosine A1 receptor antagonist on cardiovascular responses evoked by adenosine or acute systemic hypoxia.

Data presented as mean±SEM changes from baseline during adenosine infusion (left hand side of panels) and acute systemic hypoxia (Right hand side of panels) in N (left column of graphs) and CHU rats (right column of graphs), under control conditions (solid bars) and following administration of the adenosine A_1 receptor antagonist DPCPX (patterned bars)

Abbreviations as per figure 4.1

*, ** - $p<0.05$, $p<0.01$ respectively between control and +DPCPX conditions

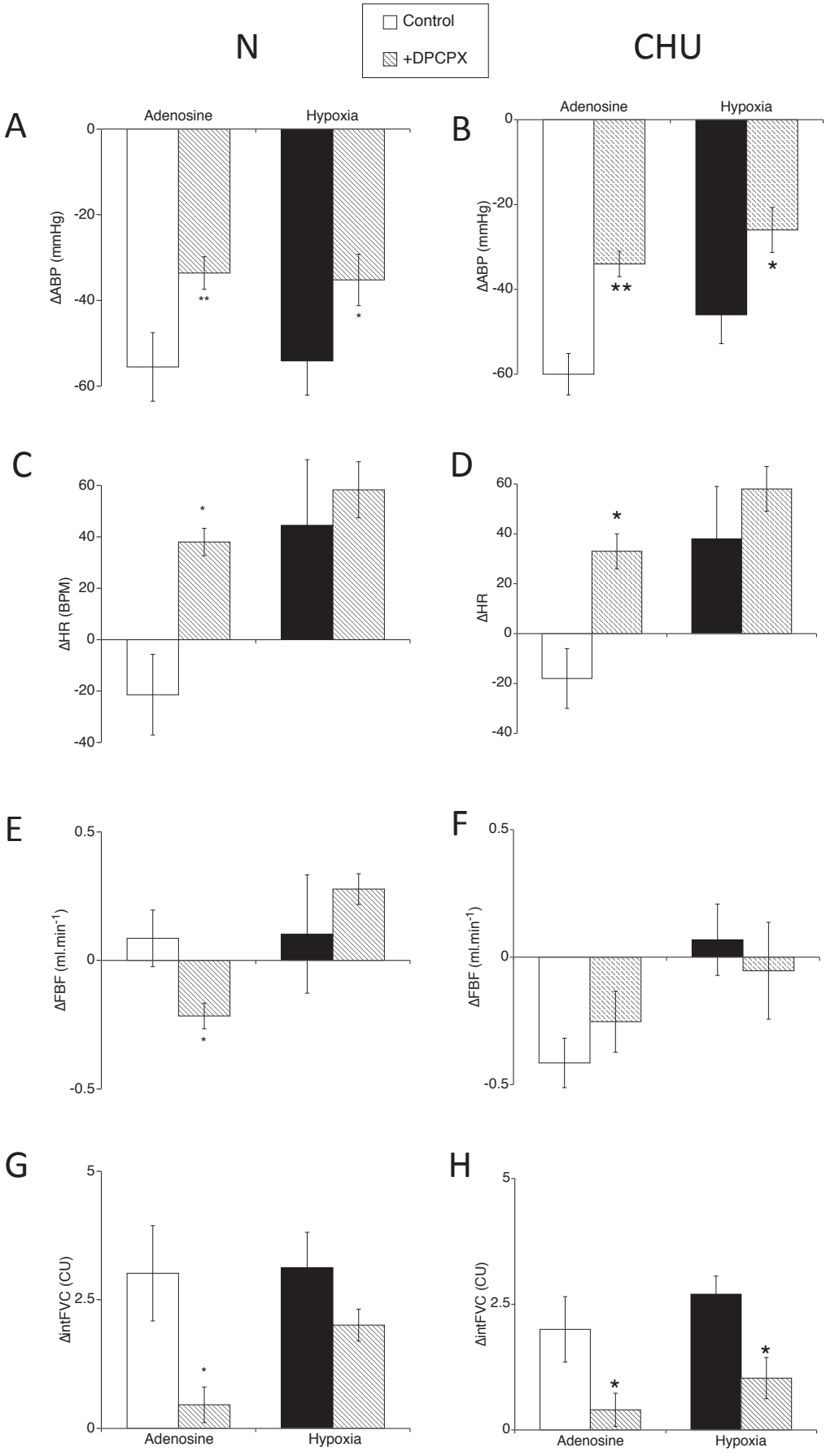
N
CHU
Control
+DPCPX
A
B
C
D
E
F
G
H
Adenosine
Hypoxia
ΔABP (mmHg)
ΔHR (BPM)
ΔHR
ΔFBF (ml.min-1)
ΔintFVC (CU)
0
-20
-40
-60
60
40
20
-40
0.5
-0.5
5
2.5
*
**

Figure 4.3 - Cardiovascular responses to acute systemic hypoxia in N and CHU rats in study group 3.

Mean cardiovascular variables recorded during normoxia (21% O_2, black bars) and acute systemic hypoxia (8% O_2, open bars) in N (left hand side) and CHU (right hand side) rats. Values shown are mean±SEM for N (n=12) and CHU (n=14), represent mean values recorded over the 5-minute periods of hypoxia. ΔintFVC represents the increase in intFVC recorded during hypoxia from the preceding normoxic baseline.

Abbreviations as per figure 4.1

*** - p<0.001 between control and +L-NAME conditions

§§§ - p<0.001 between control and +L-NAME+SNAP conditions

††,††† - p<0.01, p<0.001 respectively between +L-NAME+SNAP and L-NAME+SNAP+DPCPX conditions

#, ##, ### - p<0.05, p<0.01, p<0.001 respectively between +L-NAME+SNAP and +L-NAME+SNAP+DPCPX+ZM241385.

Figure 4.3

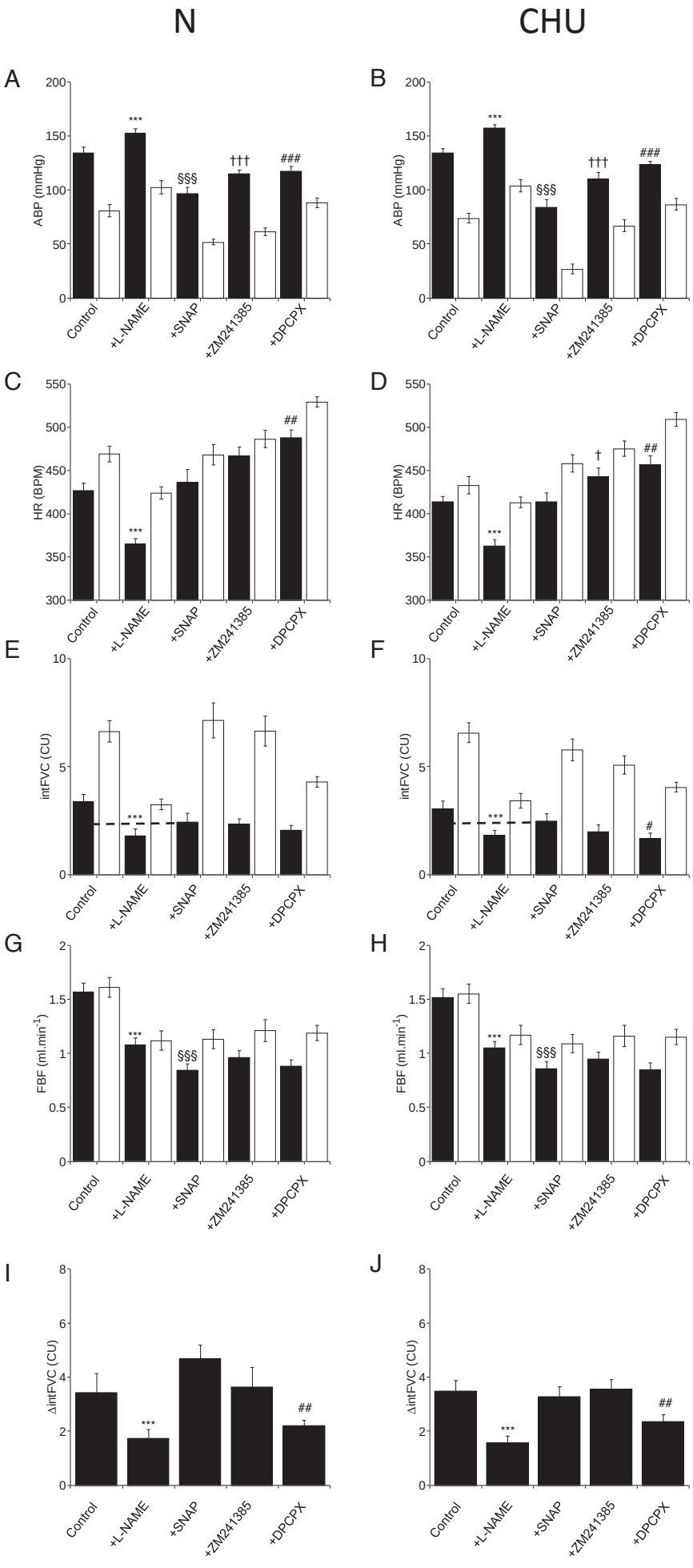
N
CHU
A
B
C
D
E
F
G
H
I
J
ABP (mmHg)
HR (BPM)
intFVC (CU)
FBF (ml.min-1)
ΔintFVC (CU)
Control
+L-NAME
+SNAP
+ZM241385
+DPCPX
***
§§§
†††
###
##
†
#

Figure 4.4 - Cardiovascular responses to adenosine infusion in N and CHU rats in study group 3.

Mean cardiovascular variables recorded under baseline conditions (black bars) and during infusion of adenosine (open bars) in N (left hand side) and CHU (right hand side) rats. Values shown are mean±SEM for N (n=12) and CHU (n=14), and represent mean values recorded over the 5-minute periods of hypoxia. ∆intFVC represents the increase in intFVC recorded during hypoxia from the preceding normoxic baseline. Statistical tests on baseline values are not shown in this figure, as similar comparisons were displayed in Figure 4.3.

Abbreviations as per Figure 4.1

*** - p<0.001 between control and +L-NAME conditions

§§, §§§ - p<0.01, p<0.001 respectively between control and +L-NAME+SNAP conditions

††† - p<0.001 between +L-NAME+SNAP and L-NAME+SNAP+DPCPX conditions

- p<0.001 respectively between +L-NAME+SNAP and +L-NAME+SNAP+DPCPX+ZM241385.

Figure 4.4

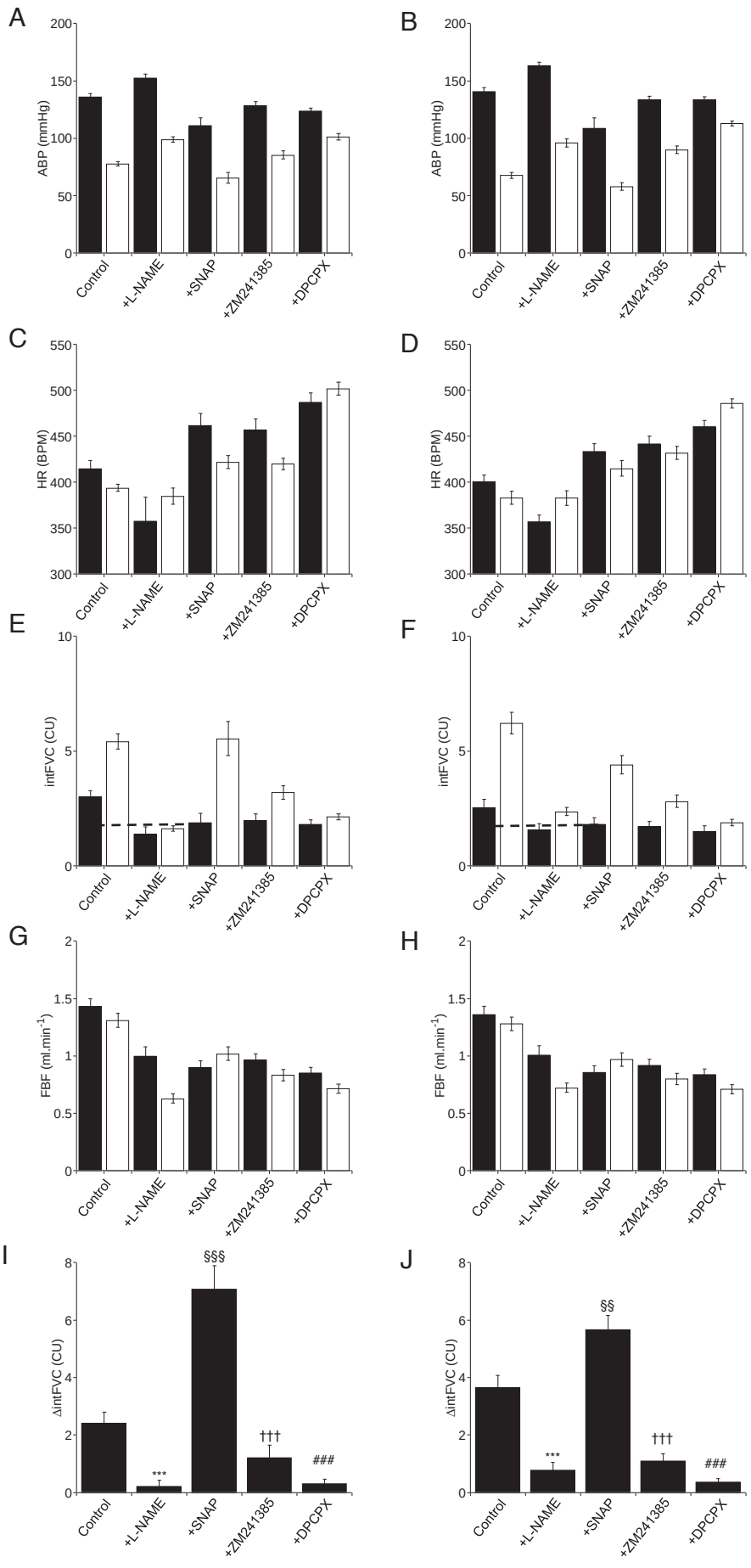
N
CHU
A
B
C
D
E
F
G
H
I
J
ABP (mmHg)
HR (BPM)
intFVC (CU)
FBF (ml.min-1)
ΔintFVC (CU)
Control
+L-NAME
+SNAP
+ZM241385
+DPCPX
§§§
§§
***
†††
###

Figure 4.5 – Schematic representation of the possible mechanisms of hypoxia-induced vasodilatation in the hindlimb following L-NAME and during SNAP infusion.

It is proposed that in the presence of DPCPX, the mechanisms in the green shaded area have the potential to be responsible for hypoxia-induced vasodilatation, and that in the presence of ZM241385, the mechanisms in the area shaded red that have the potential to be responsible for hypoxia-induced vasodilatation. When DPCPX is given in the presence of ZM241385, the hypoxia-induced vasodilatation is significantly reduced in N and CHU rats. The pathways outlined are based on those described by Ray & Marshall (2006) and Edmunds et al., (2003)

A_1 – adenosine A_1 receptor subtype, A_{2A}; adenosine A_{2A} receptor subtype, COX; cyclooxygenase, PGI_2; prostacyclin, PKA; protein kinase A, K_{Ca}; Calcium-sensitive potassium channel, K_{ATP}; ATP-sensitive potassium channel, Ca^{2+}; calcium ion, G_s; stimulatory G-protein subunit, G_i; inhibitory G-protein subunit.

Figure 4.5

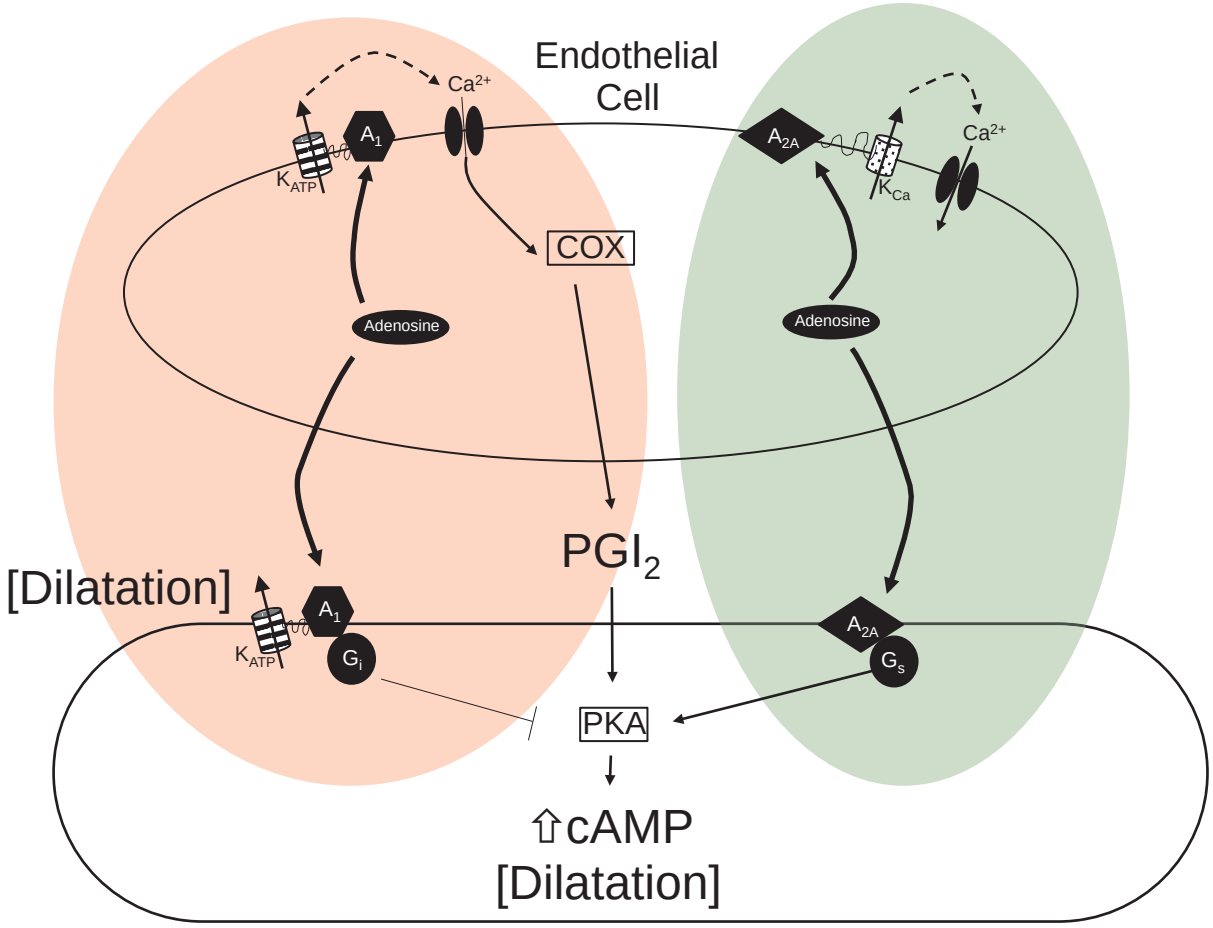
Endothelial
Cell
Ca2+
A1
K ATP
A2A
Ca2+
K Ca
COX
Adenosine
Adenosine
PGI2
[Dilatation]
A1
K ATP
Gi
A2A
Gs
PKA
⇧cAMP
[Dilatation]
Vascular Smooth Muscle

4.4 Discussion

4.4.1 Main findings

In the present study, it was shown that restoring baseline FVC by infusion of the NO donor SNAP following NOS inhibition, resulted in a larger hypoxia-induced increase in intFVC in CHU rats, but not in N rats. Following NOS inhibition and during SNAP infusion, inhibition of the adenosine A_1 receptor with DPCPX had no effect on the hypoxia-induced increase in intFVC in N or CHU rats, contrary to previous findings in N rats. Nevertheless, DPCPX, given alone, was shown to be an effective adenosine A_1 receptor antagonist in N and CHU rats, and significantly reduced the adenosine- and hypoxia-induced increases in intFVC in both N *and* CHU rats. In a further study, following NOS inhibition and SNAP infusion, the adenosine A_{2A} receptor antagonist ZM241385 had no significant effect on the hypoxia-induced increase in intFVC in N or CHU rats, but when DPCPX was subsequently given, the hypoxia-induced increase in intFVC was reduced in both groups.

The discussion that follows considers the disparities with the findings of previous studies, and considers the present results in relation to the hypotheses proposed in the introduction. The baseline levels of respiratory and cardiovascular variables were comparable in CHU and N rats, except that in particular groups presented in this chapter, HR was in some cases different between CHU and N rats, as was V_T. However, baseline blood gas values were comparable in N and CHU, as were the cardiovascular responses, and changes in blood gasses, induced by acute systemic hypoxia. Thus, the emphasis in the discussion that follows is on changes in femoral

vascular conductance (ΔintFVC), as this was the emphasis of the hypotheses proposed.

4.4.2 The role of NO in Hypoxia induced hind limb vasodilatation during acute systemic hypoxia

In the N rats in the present study, the effect of the NOS inhibitor L-NAME was consistent with previously published data (Skinner & Marshall, 1996) in that it reduced both baseline hind limb vascular (FVC) tone as well as reducing the increase in FVC evoked by acute systemic hypoxia (groups 1 and 3) and during adenosine infusion (group 3). Whilst preliminary evidence from a pilot study on a small number of rats had suggested that L-NAME had less of a blunting influence on the hypoxia-induced increase in FVC in CHU rats than in N rats (Rook *et al.*, 2008a), the results of the present study indicate this is not the case, as L-NAME had similar effects on baseline FVC and hypoxia-induced increases in FVC in N and CHU rats (Figure 4.1).

In N rats, when baseline FVC was restored with SNAP infusion after L-NAME the magnitude of increase in intFVC evoked by breathing 8%O_2 was restored to a level similar to that recorded before NOS inhibition, as has previously been observed in N rats (Edmunds *et al.*, 2003). In N rats it was deduced that providing the tonically-generated level of NO was restored, this restored both the ability of hypoxia to release adenosine from the endothelium, and also the dilator action of adenosine (See General Introduction).

In contrast, in CHU rats, restoration of baseline intFVC with the NO donor resulted in the increase in intFVC evoked by breathing 8%O_2 being significantly greater than the response before NOS inhibition (Figure 4.1J). The results of Chapter 3 suggested that there is a tonic level of oxidative stress in CHU rats, but that the H_2O_2 tonically generated from this O_2^- causes an ongoing vasodilatation, and hence baseline FVC is similar to that of N rats. It is known that uncoupled NOS is a source of reactive oxygen species (Andrew & Mayer, 1999; Landmesser *et al.*, 2003; Chen *et al.*, 2008). Thus, it is possible that one of the sources of oxidative stress in CHU rats is uncoupled eNOS, such that it generates not only NO, but also O_2^-. Given that O_2^- decreases the bioavailability of NO by producing $ONOO^-$ it might be expected that in CHU the competition between O_2 and NO for the complex IV binding site in the mitochondria, described by Edmunds et al., (Edmunds *et al.*, 2003), would be less pronounced and less sensitive to the fall in O_2 induced by hypoxia, and would lead to less adenosine release. With NOS inhibition followed by infusion of SNAP, the eNOS source of O_2^- would be abolished, but a tonic level NO would be provided, and as such the competition between NO and O_2 would be increased relative to that before L-NAME and SNAP infusion in CHU rats. Therefore, it could be deduced that the release of adenosine from endothelial cells during hypoxia would be increased. The fact that NOS inhibition had a similar effect on baseline FVC in CHU as in N rats is consistent with this interpretation, for NOS inhibition would have decreased tonic generation of NO, and also decreased the level of the dilator H_2O_2 generated from the O_2^- produced by eNOS. Thus, the finding that NOS inhibition with SNAP infusion accentuated the hypoxia-induced increase in FVC is consistent with the results presented in Chapter 3, suggesting that there is ongoing oxidative stress in the

muscle vasculature of CHU rats. The results of the present study suggest that one of the sources of this oxidative stress is uncoupled eNOS.

4.4.3 The role of the adenosine A_1 receptor subtype

In the present study it was hypothesised that in CHU rats, when background levels of NO were restored after NOS blockade, the bioavailability of NO in CHU rats would be increased sufficiently that the release mechanism for adenosine described by Edmunds et al., (2003), and thought to be absent in CHU rats by Coney & Marshal (2010), would be restored. In this setting the role of the adenosine A_1 receptor in mediating hypoxia-induced vasodilatation would be restored.

However, in the present study, when background levels of NO were restored in the presence of NOS inhibition, there was no significant effect of DPCPX on the hypoxia-induced increase in FVC in either CHU *or* N rats (Figure 4.1 I&J). Considering N rats: what might explain this disparity with previously published findings? Firstly it was important to confirm that the DPCPX used in the present studies effectively inhibited the action of the adenosine A_1 receptor. The experiments performed in study 2 were designed to address this. The results obtained in the N rats showed that DPCPX markedly reduced the increase in intFVC evoked by infusion of adenosine and during systemic hypoxia in N rats, and indicate that DPCPX, at the dose chosen in this study was effective in inhibiting the adenosine A_1 receptor. Notably, the same dose has previously been shown to abolish the response evoked by the selective adenosine A_1 receptor specific agonist CCPA (Bryan & Marshall, 1999a). On this basis the possibility that DPCPX did not provide effective A_1 receptor inhibition in this

study can be discounted. Interestingly, the experiments of study 2 were also carried out in CHU rats, and the results obtained were remarkably similar to those found in N rats, in contrast to the findings of Coney & Marshall (2010). The possible explanations for this are discussed below.

If it is true in N rats, that during NOS inhibition with SNAP infusion, the mechanism by which NO allows for release of adenosine from endothelial cells is restored (Edmunds *et al.*, 2003), then mechanism by which adenosine evoked vasodilatation in the present study must be different. Adenosine can act via different pathways; A_1 receptors (Dart & Standen, 1993) via the opening of K_{ATP} channels on vascular smooth muscle, and via direct action on vascular smooth muscle A_{2A} receptors, which evoked vasorelaxation via an increase in $[cAMP]_i$. Thus, the fact that following restoration of the adenosine release mechanisms, A_1 receptor blockade with DPCPX had no significant blunting effect on the hypoxia-induced vasodilatation suggests that even after the loss of A_1 mediated vasodilatation, there is a sufficient degree of redundancy that even though A_1 mediated vasodilatation is important under normal conditions, under these conditions the other mechanisms are capable of producing adequate hypoxia-induced vasodilatation. This possibility graphically represented in Figure 4.5, indicated by the mechanisms highlighted in green. In other words, the present results allow the new hypothesis, that the A_{2A} mechanism is stronger in the N rats of the present study than the N rats of previous studies (Edmunds *et al.*, 2003)

Moving on to consider the CHU rats, the results obtained in study 2 showed that in contrast to the findings of Coney & Marshall (2010), DPCPX *did* significantly blunt the

hypoxia- as well as the adenosine-induced increase in intFVC in CHU rats. The reasons for this disparity are unclear. Under the conditions used in this study, it is clear that during hypoxia, the adenosine A_1 receptor plays an important role in vasodilatation in the rat hindlimb in N and CHU rats, and it is clear from the results of the adenosine infusions, that DPCPX did block the A_1 receptor. The anaesthetic regimen was similar, although this study is carried out under Alfaxan (alfaxolone only) infusion, whilst Coney and Marshal (2010) used Saffan (a mixture of alfaxolone and alfadolone). These two anaesthetics have similar mechanisms of action. It is technically possible that this is the reason for the disparity, but it seems unlikely. The age of rats used in the two studies was similar, as were the baseline cardiovascular variables. Thus, the exact reasons for this disparity remain unclear. However, in the study of Coney & Marshall (2010) the adenosine receptor antagonist 8-SPT which is non-selective between A_1 and A_{2A} receptors tended to reduce the hypoxia-induced vasodilatation in CHU rats (see Figure 2 of their study), suggesting that there may have been an underlying role for adenosine receptors in hypoxia-induced hindlimb vasodilatation in CHU rats.

4.4.4 The role of the adenosine A_{2A} receptor

The present finding, in CHU rats, that during SNAP infusion following NOS inhibition the increase in FVC evoked by breathing 8%O_2 was significantly larger than in N rats has been discussed above. However, as in N rats, DPCPX had no blunting affect on the hypoxia-induced hindlimb vasodilatation. At this stage in the discussion, these findings cannot be interpreted any further.

In light of the results obtained in study groups 1 and 2 of this study, the aim of study 3 was to investigate whether there was a role for the adenosine A_{2A} receptor following NOS inhibition and during SNAP infusion in N or CHU rats. It should be noted that previously the A_{2A} receptor was shown not to have a role in hypoxia-induced vasodilatation evoked by breathing 8%O_2, although blockade of the adenosine A_{2A} receptor in this setting did significantly blunt the vasodilatation evoked by breathing 12%O_2 (Edmunds & Marshall, 2001). Adenosine can induce an A_{2A} receptor-mediated vasodilatation in the rat hindlimb (Bryan & Marshall, 1999a).

The protocol in used in study 3 was initially similar to that used in study 1; responses evoked by systemic hypoxia were recorded under control conditions, following NOS inhibition, and then during SNAP infusion, but in addition, responses evoked by 5 minute infusion of adenosine were also tested at each stage, to ensure that adenosine receptor blockade was achieved. Following responses under the first three conditions, responses during A_{2A} receptor blockade with ZM241385, and then finally responses following A_{2A} and A_1 receptor blockade with DPCPX were tested. The control responses evoked by acute systemic hypoxia and by adenosine infusion were similar to those described in studies 1 and 2, and similar to those previously described (See Coney & Marshall, 2010). However, following NOS inhibition, when SNAP was infused, the matching of baseline FVC to the control FVC before NOS inhibition was not as good as in study 1. This was because once the baselines had been matched, the SNAP infusion rate after NOS inhibition was not changed for the rest of the protocol, and FVC tended to gradually fall with time. This was probably because the protocol in study 3 was more than twice as long as that of study 1.

Consequently, the baseline FVC presented for N and CHU rats, following NOS inhibition and during SNAP infusion tended to be lower than before NOS inhibition. Thus, it is not surpising that although the intFVC evoked by breathing 8%O_2 was significantly enhanced in CHU rats following SNAP infusion in study 1, in study 3 this was not the case. Indeed, it may be that as a consequence of not as adequately restoring FVC to control levels with an NO donor, there was less bioavailable NO, and as such the same effect was not observed.

Although the FVC baselines were not as effectively matched, the results of study 3 do allow comments to be made on mechanisms underlying the hypoxia-induced muscle vasodilatation. Firstly, it should be noted that L-NAME greatly attenuated the vasodilatation induced by exogenous adenosine, just as it did the hypoxia-induced vasodilatation, i.e. both responses were, at least, NO-dependent in both N and CHU rats, and had potential to be NO-mediated. Then, addressing the potential role for the A_{2A} receptor, following NOS inhibition and SNAP infusion, the adenosine A_{2A} receptor antagonist ZM241385 was effective in reducing the restored increase in FVC evoked by exogenous adenosine in both N and CHU rats. It had no significant effect on the restored increase in FVC evoked by breathing 8%O_2 in N or CHU rats. However, when DPCPX was given following ZM241385, the increase in FVC evoked by exogenous adenosine was further reduced in both groups, and there was a significant reduction in the increase in FVC evoked by breathing hypoxia in both groups. These results are consistent with the idea that, following NOS inhibition and during SNAP infusion, both the adenosine A_1 and A_{2A} receptors are capable of producing vasodilatation in skeletal muscle vasculature. This is presumably by acting

directly on A_1 or A_{2A} receptors on vascular smooth muscle, providing that a tonic level of cGMP is present (the second messenger for NO, see de Wit et al., (1994)), or by releasing something other than NO from the endothelium.

Further, it seems that the A_{2A} receptors alone play no significant role in hypoxoa-induced muscle vasodilatation in either N or CHU rats, given ZM241385 had no effect on this vasodilatation. However, the fact that DPCPX in the presence of ZM241385 did attenuate the hypoxia-induced vasodilatation indicated, firstly that infusion of NO did restore adenosine release mechanisms that operate during hypoxia in both N and CHU rats, and secondly, that when A_{2A} receptors were blocked, the vasodilator action of adenosine on A_1 receptors during hypoxia was revealed in both N and CHU rats. [This is illustrated in figure 4.5; during SNAP infusion after NOS inhibition, blockade of either the A_1 or the A_{2A} receptor mediated pathways reveals the contribution of the opposite pathway.]

In conclusion, evidence presented in this chapter further adds to a mass of evidence that there is ongoing oxidative stress in the skeletal muscle vasculature of CHU rats. The results suggest that uncoupled eNOS may be a source of oxidative stress in CHU rats, as NOS inhibition with SNAP infusion appears to allow hypoxia-induced vasodilatation to be accentuated, and hence ameliorate the effects of oxidative stress.

Further, the evidence presented here indicates some differences between the CHU rats studied in this thesis, and the CHU rats studied previously (Coney & Marshall,

2007), particularly in relation to the role of adenosine. In the present study the role of adenosine in hypoxia-induced vasodilatation was similar in N and CHU rats. There are some disparities with previously published experimental data that have been discussed.

Chapter 5 – Sympathetic control of muscle vasculature following chronic hypoxia *in utero*

5.1 Introduction

In humans, the association between being small for gestational age and developing hypertension in adult life is well established (See Huxley et al., (2000) for systematic review of the literature). However, the mechanisms underlying this are not well understood. One of the few points that is well established is that prenatal insult during the crucial developmental window for nephrogenesis can lead to a reduction in nephron number, leading to renal-induced hypertension (Ojeda *et al.*, 2008).

Importantly, there is also evidence suggesting that sympathetic nerve activity may be increased. Thus, IJzerman et al., (2003) showed that there was an inverse association between tertile of birth weight and the degree of ongoing cardiac sympathetic control, as measured by analysis of cardiac pre-ejection period and respiratory sinus arrhythmia traces in young adult humans. Moreover, direct recordings of *en masse* muscle sympathetic nerve activity from the peroneal nerve in young adult humans (16-17 years of age) who were born small for gestational age (SGA) showed that there is an inverse correlation between birth weight and MSNA. The MSNA burst frequency and incidence was higher in the SGA group than in a control group of young adults from normal sized births, and even at this young age, ABP tended to be higher in the SGA group than their control equivalents.

Several states of cardiovascular disease are associated with alterations in the control of sympathetic nerve activity. For example, Goso et al., (2001) found that in patients with congestive heart failure there was a loss of lung inflation mediated reflex inhibition of sympathetic nerve activity. Further, by using the working heart-brainstem

preparation, Simms et al., (2009) recorded ongoing activity in the preganglionic sympathetic nerves of the lumbar sympathetic chain of the spontaneously hypertensive (SHR) rat, and found that the SHR rat had augmented coupling of sympathetic outflow to the respiratory cycle relative to control rats, and proposed that this may be a cause of the underlying the hypertension.

Not only sympathetic nerve activity, but also the density of sympathetic innervation are important in determining how blood vessels are controlled. Of note in the present context, a study by Rouwet et al., (2002) showed that in isolated mesenteric arteries taken from chick embryos made hypoxic during development (see General Introduction), basal vascular tone was increased, responses to α-adrenoreceptor antagonist phentolamine were enhanced, but sensitivity to topically applied noradrenaline was comparable to that of normoxic chick embryos. However, responses to tyramine, which releases sympathetic neurotransmitters from the nerve varicosities were enhanced relative to a normal embryo. They therefore concluded that there must be a higher density of sympathetic nerves on the surface of the mesenteric arteries of chronically hypoxic chick embryos, or that the nerves contain more noradrenaline than the normoxic embryos. This suggestion accords with another study carried out on the hypoxic chick embryo, which showed that just before hatching the femoral artery had a higher density of sympathetic innervation relative to that of a normoxic chick embryo (Ruijtenbeek *et al.*, 2000). It is well known that in mammals the development of fully functional sympathetic innervation continues well after birth in mammals (Gootman *et al.*, 1972; Gootman *et al.*, 1978). Thus, it cannot be deduced what the functional consequences of this increase in sympathetic

innervation density in a bird might be for mammals, particularly as the offspring develop post-natally.

It has been suggested that in the spontaneously hypertensive rat (SHR), the increased sympathetic hyperinnervation observed in the cerebral arteries during most of postnatal development may be causal in the hypertension they develop (DhÌtal *et al.*, 1988; Albert & Campbell, 1990; Kondo *et al.*, 1992). On the other hand Smeda et al., (1990) presented evidence that this cerebral hyperinnervation may actually represent a mechanism of protection from stroke.

Thus, even though there is indirect evidence that there is a role for the sympathetic nervous system in the generation of cardiovascular disease following a suboptimal *in utero* environment, there has not yet been a study to examine the effects of hypoxia *in utero* on ongoing, or reflex stimulated activity in individual postganglionic sympathetic neurones of any vascular bed. As indicated in the General Introduction, firing frequency, patterning and reflex modulation of individual sympathetic neurones is a major determinant of neurotransmitter release, and of the relative contribution of the different cotransmitters in the evoked vasoconstriction. Recent studies performed on the rat have shown the relative importance of ATP, NA and NPY in vasoconstriction evoked by different patterns of activity in hindlimb muscle vasculature (Johnson *et al.*, 2001; Coney & Marshall, 2007). Moreover, a recent study showed that it was possible to record sympathetic nerve activity from single sympathetic neurones on the surface of arterial vessels of the spinotrapezius muscle of the rat, and show how single unit nerve activity changes with stimulation of the

baroreceptors and peripheral chemoreceptors (Hudson *et al.*, 2011). No such studies have been yet been performed on CHU rats.

Further, there has been no study of the effect of hypoxia *in utero* on the density of vascular sympathetic innervation in the adult offspring, or in fact, in any mammalian model at any stage of development. It is known that some of the factors that regulate sympathetic nerve density and function, such as NGF and VEGF also play a role in regulating ongoing activity (Raucher & Dryer, 1995; Lei *et al.*, 2001; Ford *et al.*, 2008), and as such it was important to examine both innervation density, and nerve activity. In addition, the density of sympathetic innervation would be expected to influence the amount of the different neurotransmitters released per unit area, and to the vascular smooth muscle of blood vessels. Therefore, in light of this literature, the studies described in this chapter tested the hypothese that young adult CHU rats;

1. Have higher levels of ongoing MSNA than N rats
2. Have more high frequency couplets and triplets of activity in individual neurones innervating the blood vessels supplying skeletal muscle. These hypotheses were tested using the experimental preparation for recording MSNA in the vasculature of the spinotrapezius muscle, described by Hudson et al., (2011)
3. Have greater sympathetic innervation density on the surface of arteries supplying skeletal muscle relative to N rats.

In addition, the reflex increases in MSNA during baroreceptor and chemoreceptor stimulation were tested in N and CHU rats.

5.2 Methods

Baseline recordings of MSNA were attempted in 59 N and 40 CHU rats, and were successful in 27 N rats (343±22g) and 17 CHU rats (351±18g, 10 litters), giving success rates of 46% and 43% respectively.

5.2.1 Preparation for recording of MSNA

The regimen for induction and maintenance of anaesthesia, and the methods of preparation for measurement of cardiovascular variables, administration of drugs, and for sampling arterial blood are described in detail in chapter 2. In particular, ABP was recorded from the right femoral artery, whilst arterial blood was sampled from the left femoral artery. Drugs were administered via the left femoral artery.

The surgical preparation used for recording of MSNA from the surface of blood vessels supplying the spinotrapezius muscle was based on the preparation decribed by several authors for *in vivo* microscopy on individual vessels of the vascular bed supplying the muscle (Zweifach & Metz, 1955; Gray, 1973; Marshall, 1982), with the modifications recently described by Hudson et al., (2011). The spinotrapezius muscle is a thin superficial muscle attached along the thoracic and upper lumbar vertebral column and inserting onto the scapula. In brief, with the rat lying prone, the overlying skin was removed, and the connective tissue between spinotrapezius and the underlying muscle was carefully dissected away by gently lifting the lateral border of the spinotrapezius muscle with covered forceps, and removing the underlying connective tissue. Several 6/0 sutures were then looped around the thin strip of muscle that adjoins spinotrapezius on its lateral border. The rat was then placed on

its left side and the sutures were used to arrange the spinotrapezius muscle over a Perspex stage, ventral surface uppermost. Under a dissecting microscope, the muscle was further isolated from the underlying muscle as far medial as possible, without interfering with nerves, blood vessels or tendons, ensuring that the control of the blood vessels remains as physiologically intact as possible, but allowing the majority of the muscle to be arranged in the horizontal plane. Using Superglue (Loctite, Henkel Ltd., Hertfordshire, UK) a template of Saran Wrap (SC Johnson, WI, USA) was attached to the lateral border of the spinotrapezius muscle, and used to form the base of a three-sided watertight bath that was constructed using dental impression material (President light body surface activated dental impression material, Coltene/Whaledent AG, Alstatten, Switzerland). This material is a soft mixture that was moulded to the contours of the rat's dorsal surface to form a seal, such that the rat's dorsal surface formed the fourth side of the bath (See Hudson et al., 2011)

The layer of very fine connective fascia was then removed from the ventral surface of the muscle to more clearly expose the blood vessels. Throughout the preparation the tissue was kept moist with physiological saline (0.9% NaCl in dH_2O). Once the muscle was cleared of all connective tissue, the constructed bath was filled with physiological saline for the remainder of the experiment, during which nerve recordings were made.

5.2.2 Focal recording electrode

As described by Johnson et al (1996) and Hudson et al., (2011), borosilicate capillary tubes (GC150T-10, ID=1.17mm, OD=1.5mm, Harvard, Holliston, MA, USA) were pulled on a vertical electrode puller (Ealing, UK). Electrodes were made, such as to have a short, very fine tip, and then the tip was gently broken back with fine forceps under a microscope (Zeiss ACP microscope, 10x eye piece, 32x objective with graticule) to a tip diameter of 50-100μm. Tips were smoothed by advancing a headed platinum filament towards the tip to leave a tip of 20-40μm internal diameter.

It became clear that the shape of electrodes was critical to the success rate of recording MSNA from the preparation. Electrodes with a long tapered point produced a noisy recording, but often produced a high signal to noise ratio. Electrodes with a short 'blunt' tapered point, gave lower noise, lower signal to noise ratios, but higher success rates. The latter electrodes also gave more stable recordings. It was established that they had to have a sufficiently small aperture to allow spikes to be reliably discriminated from the background noise. Thus, the general aim was to produce an electrode with a small aperture and a short tapered point, to produce reliable, stable recordings with a sufficiently high signal to noise ratio.

5.2.3 Recording MSNA

The methodology used to record MSNA is base on that described by Hudson et al., (2011). In order to record MSNA, the focal recording electrode was mounted in a microelectrode holder (MEH2SW15, World Precision Instruments, USA). This

allowed a fine silver electrode to be placed within the shaft of the recording pipette, and a tight seal to be formed around the shaft. Suction was applied via a 10ml syringe connected with flexible tubing to the barrel of the microelectrode holder. The microelectrode holder was connected to a Neurolog head-stage pre-amplifier (NL100AK Neurolog, Digitimer Ltd. UK), which was mounted on a micromanipulator which allowed for very careful positioning of the recording electrode on the surface of individual blood vessels. A silver reference electrode was loosely coiled around the shaft of the recording electrode with its tip placed in close proximity to that of the focal recording electrode. It was found that by keeping the recording and reference electrodes close together ECG-related interference was minimised. Further, all recordings were attempted with the confines of a custom built faraday cage, to minimize external electrical interference.

For recording purposes, normal saline was drawn up ~two thirds of the way up the barrel of the recording pipette from the organ bath constructed around the spinotrapezius muscle. Under the dissecting microscope, the tip of the electrode was gently placed onto the surface of an arterial vessel supplying the muscle, gentle suction being applied to aid stability of the recordings. Recordings were most successful from sites that were around branch points of the main feed artery that supplies the spinotrapezius muscle at its rostral end, and on the 2^{nd} or 3^{rd} branches of this artery.

5.2.4 Data acquisition

For the experiments described in this Chapter, physiological variables including nerve activity were recorded using a NeuroLog system (Digitimer Ltd, Hertfordshire, UK). ABP and tracheal pressure (TP) were recorded via pressure amplifiers (NL108, NeuroLog, UK), using pressure transducers (DTX Plus disposable pressure transducer, BD Biosciences, Oxford, UK). The head-stage pre-amplifier used for recording was connected to the NeuroLog system via a HumBug (Quest scientific, Vancouver, BC, Canada) to reduce electrical interference caused by 50/60Hz oscillations in mains electricity. This was in turn connected to a second pre-amplifier (NL104, NeuroLog, Digitimer Ltd, Hertfordshire, UK). Signals were amplified (10k gain), and filtered (150Hz-1kHz band pass, NL125 filter, NeuroLog, Digitimer, Hertfordshire, UK). Raw data was digitalised and sampled via the micro1401 (Cambridge Electronic Design, Cambridge, UK) at 20,000Hz, connected to a computer running Windows XP (Apple Inc, California, USA). ABP and TP information was sampled at 100Hz.

5.2.5 Off-line analysis

HR was derived from the peaks in the ABP wave using the memory buffer function. Respiratory frequency (R_F) was similarly derived, using the nadir of the tracheal pressure trace. Both were written to new channels and manually checked for correct triggering.

5.2.6 Spike discrimination

Raw multiunit recordings of MSNA were analysed using the wavemark facility with Spike2 software (Version 7, Cambridge Electronic Design, Cambridge, UK). Single unit MSNA, representative of ongoing activity in a single sympathetic neurone, was discriminated based on the amplitude, duration and shape. Templates were constructed from spikes that were triggered by the raw data recording passing below a set voltage. Spikes were considered to match a template when 70% of points in a spike matched the template. New templates were created when a minimum of 8 spikes not already matched to a template were found to have 70% of points within similarity boundaries. During discrimination, the 'auto-fix' function was used, i.e. as the shape of a spike evolved with time due to slow movement of the blood vessel, or slow loss of suction, the shape of the template evolved to reflect this. Each 'auto-fixed' template was based on the previous 64 spikes matched to that template. Principal component analysis was used when spikes appeared to have different templates but be of similar shape to test whether they represented two different units, or were in fact the same unit.

When all templates were created and confirmed, each one was allocated a hexadecimal code and written to a new Wavemark channel. All single units were confirmed as representing MSNA by their tri- or bi-phasic shape, and by the fact they had cardiac- and respiratory-rhythmicity, confirmed using cross correlation histogram analysis from the derived HR and R_F channels (See figures 5.2 & 5.4). This methodology is similar to that described by Hudson et al., (2011). The nerve activity presented in this chapter all conformed to the principles just described.

5.2.7 Experimental protocol

Recordings of MSNA were not considered for experimentation unless they were stable for at least 5 minutes of baseline recording. After 5 minutes of stable baseline recording the animal was randomly selected to receive either graded levels of systemic hypoxia, or baroreceptor unloading. Graded systemic hypoxia was induced, following a 5 minute period breathing 21%O_2 in N_2, by switching the inspirate to 12%O_2 in N_2 for 2 minutes, then to 10%O_2 in N_2 for 2 minutes and finally to 8% O_2 in N_2 for 2 minutes sequentially. Baroreceptor unloading was achieved by giving a bolus injection of sodium nitroprusside (SNP, ≈60µg.kg^{-1} i.a.), to induce a fall in ABP similar to that seen during the final stages of graded hypoxia (8%F_iO_2). If the recording was stable after the first stimulus, at least another 10 minutes of baseline recording was made, whilst breathing 21%O_2 before the other stimulus was attempted. Where successful recordings of MSNA during graded systemic hypoxia were made, hypoxic arterial blood was sampled for blood gas analysis immediately following the final minute of breathing 8%O_2, before switching back to normoxic inspirate. Normoxic blood gas analysis was carried out on blood samples in the same rat, at least 5 minutes following the end of the graded systemic hypoxia, whilst breathing 21%O_2.

5.2.8 Cardiac and respiratory cycle modulation of MSNA

As indicated above, the presence of cardiac and respiratory rhythmicity was a requirement for inclusion in analysis of MSNA. Cardiac rhythmicity was assessed using stimulus-triggered histogram analysis. The HR trigger channel was used as a trigger for sweeps of 1s of discriminated, single unit MSNA. Spikes occurring in this 1s sweep were placed in one of 100 bins according to where they occur. When

compared to a waveform average of the ABP trace, of the same width, and triggered by the same trigger, an assessment of whether cardiac rhythmicity was present was made. Examples are presented in figure 5.2C&D and 5.4C&D. Similar analysis was carried out to assess the presence of respiratory rhythm, using the respiratory frequency channel as a trigger, and making sweeps of 3s, with 100 bins. The stimulus trigger histograms generated in this fashion were compared to the tracheal pressure waveform average. Examples of these can be found in Figure 5.2 A&B and 5.4 A&B.

In a further development of the method described by Hudson et al., (2011) it was considered important to assess *the strength* of the cardiac and respiratory rhythmicity; the degree of augmentation during the excitement phase, and the degree of silencing during the inhibition phases. The extent of cardiac and respiratory modulation of the ongoing sympathetic nerve activity was quantified in N and CHU rats by using phase histogram analysis. For analysis of the cardiac cycle phase relationship, the HR trigger derived from the ABP trace was used to trigger each cycle. Discriminated single unit activity was swept from the trigger point, and each spike was placed into one of 360 bins, with the end of the phase occurring at the next trigger. Examples of this analysis in N and CHU rats are shown in Figure 5.5 A-D. The equivalent analysis was carried out using the respiratory rate trigger from the tracheal pressure trace. Examples of this can be found in Figure 5.6 A-D. In order quantify, and compare cardiac and respiratory modulation of MSNA, the proportion of activity in each unit occurring within + or - 60° of the peak in activity, and the proportion falling outside these boundaries. The exact phase relationship of each unit

varied slightly, and hence for graphical representations of mean data, the mean values for the phase histograms were aligned so that their peaks were all aligned, and then the data was averaged (see Figures 5.5 and 5.6).

5.2.9 Estimation of sympathetic innervation density in skeletal muscle vasculature

The studies of sympathetic innervation density were carried out on tibial arteries isolated from 10 N rats (416±9g) and 13 CHU rats (5 litters, 359±13g). Following cervical dislocation under isofluorane anaesthesia (3.5% isofluorane in 5L O_2 BOC Gasses, Worsley, Manchester, UK), the deep tibial arteries, which supply the hindlimb skeletal muscles, were very carefully freed from the surrounding skeletal muscle, and excised using fine scissors, to ensure as little disruption of the artery structure as possible. Sympathetic noradrenergic fibres were then stained using the staining procedure that has previously been described by Furness & Costa (1975). In short, the excised vessels were immediately placed in the staining solution: 2% (w/v) glyoxylic acid (Sigma Aldrich, MO, USA) in 0.1M phosphate buffer, with pH adjusted to pH 7 with 10M NaOH. Vessels were incubated in this solution for 45 mins, before being placed onto glass slides and air-dried as a whole vessel preparation. The whole vessels were then dried onto the glass slide with the aid of a cool fan, giving a drying time of around 5 minutes. To develop the catecholamine fluorescence, slides were heated in an oven for 4 minutes at 100°C, after which they were removed, and covered with a small amount of mineral oil to exclude moisture from the air. A temporary coverslip was placed on to the slide to protect the stained vessels and they were kept in the dark at ≤4°C to maintain stability.

5.2.10 Visualisation

Stained vessels were viewed using an Olympus confocal microscope using a 40X oil immersion objective. The excitation wavelength was 395-440nm, and emission bandwidth 450-550nm. Owing to the three dimensional structure of blood vessels, the upper and lower bounds of the perivascular nerve plexus were found by manually adjusting the focal plain. Images were then acquired at 800x800 pixels at 1μm slice intervals. Typically ~80 slices were acquired. Images were acquired from at least 3 different areas of each vessel imaged.

5.2.11 Analysis

For analysis, all slices acquired of a single vessel were compiled into a z-stack using ImageSXM software and the resulting image was saved as a TIFF file (see figure 5.12 for examples).

For analysis of 'fluorescent intensity', many 'non-stained' areas on a given image were selected, and their mean image density and standard deviation noted. This represented a 'background' fluorescence level for each individual image. "Thresholding" was then used, to reveal all staining for which intensity was more than 3 standard deviations above the mean background fluorescence. Staining of this intensity and above was deemed representative of catecholamine-induced fluorescence. The proportion of the area above the threshold was then calculated as a percentage of the whole vessel area.

For analysis of ‘sympathetic nerve density’, a grid with horizontal and vertical lines spaced at 44 pixels intervals was overlayed on the image, such that each square represented 2000 pixels. The grid was arranged such that the vertical lines ran parallel to the border of the vessel. A count was then made of the number of times that sympathetic nerve intersected the grid lines. The outermost horizontal and vertical lines were not included, as they often represented many nerves overlaying each other, because of the wall of the vessel folding around, and as such would misrepresent the nerve density. This methodology for analysis was used by Omar & Marshall (2010).

5.2.12 Statistical analysis

All numerical data is given as mean±SEM. Students paired or unpaired t-test was used to make single comparisons of paired or unpaired data respectively, such as baseline comparisons or comparisons of variables before and during baroreceptor unloading. Where appropriate a repeated measures ANOVA was used to make multiple within group comparisons, such as comparing MSNA during the stages of graded systemic hypoxia to the baseline values. A Dunnets *post hoc* test was used to determine statistical significance. Results were considered statistically significant when $p<0.05$.

5.3 Results

5.3.1 In vivo experiments - General characteristics of the experimental group

Recordings were attempted in 59 N and 40 CHU rats. Recordings of muscle sympathetic nerve activity (MSNA) were successfully made in 27 N and 17 CHU rats (success rate 46% and 43% respectively). ABP, HR and R_F were similar between N and CHU rats (Table 5.1). However, in both N and CHU rats, ABP was tended to be lower than that reported in Chapters 3 and 4, although baseline HR and R_F were similar. Arterial blood gasses measured in a small number of N and CHU rats are reported in Table 5.2. PaO_2 was significantly lower in the 5 N rats from which it was sampled, compared to the 9 CHU rats ($p<0.05$), but $PaCO_2$ and pH were similar (Table 5.2).

Recordings were obtained in 27 N rats, 5 of which appeared to be single-unit, and 39 multi-unit. In total, 198 single units were discriminated from the raw single and multiunit MSNA recordings, and the mean ongoing firing frequency was 0.33±0.03Hz (range 0.02-1.41Hz, Table 5.1). Examples of single units recorded from a single recording of MSNA are shown in Figure 5.1. By stimulus triggered histogram analysis of single unit activity, each unit included in the analysis contained cardiac rhythmicity, comprising augmented activity during the diastolic phase, and lower activity during the systolic phase (Figure 5.2 cf. C & D). Similar analysis using the respiratory cycle demonstrated that each unit contained activity that was augmented during the post-expiratory and pre-inspiratory phase, and suppressed during the inspiratory and post-inspiratory phases, indicating respiratory rhythmicity (See figure 5.2 A & B).

In 17 CHU rats 5 single unit, and 30 multiunit recordings were made. In total, 157 single units were discriminated from raw MSNA, and the mean ongoing firing frequency was 0.56±0.07Hz (range 0.02-2.41). In all single units analysed there was cardiac and respiratory rhythmicity, which was of a similar nature to that described above for N rats (Figure 5.4 A-D).

The mean firing rates in N and CHU rats were not normally distributed (Shapiro-Wilks test) and hence non-parametric statistics were used for comparison of mean ongoing firing rate between N and CHU rats. The mean, ongoing firing rate in CHU rats, whilst breathing 21% O_2 under baseline conditions, was substantially higher than that recorded in N rats ($p=0.001$, Mann-Whitney U test, Table 5.1).

5.3.2 Cardiac and respiratory modulation

All units were recorded for at least 5 minutes in order to be included in these analyses, and all units analysed contained cardiac and respiratory rhythmicity (See Figure 5.2 and 5.4). To assess the *degree* to which activity was augmented during the post-expiratory phase, and reduced during the inhibitory phase of the respiratory cycle, mean phase histograms were computed (Figure 5.6 E and F, see methods). The proportion of the spikes falling within the augmented phase (considered to be ±60° of the respiratory cycle), and the proportion falling in the inhibited phase are presented in Figure 5.6 G. The strength of respiratory and of cardiac modulation in single unit MSNA was similar in CHU and N rats (see figure 5.6). Similar analysis of the strength of cardiac-related modulation of single unit MSNA was carried out (see

Figure 5.5), and no significant difference in the strength of cardiac rhythmicity was found between N and CHU rats.

5.3.3 Instantaneous frequencies recorded in baseline MSNA

The interspike intervals in ongoing, discriminated single unit MSNA was analysed, and is presented as the proportion of all interspike intervals recorded in a single unit falling into bins represented by the frequencies shown in Figure 5.7. It can be seen that the proportion of spikes recorded in MSNA with instantaneous frequencies in the 1-10Hz band was significantly greater in CHU rats than in N rats (Figure 5.7A). Further, of these spikes, there were significantly more spikes representing instantaneous frequencies of 1-5Hz (Figure 5.7B) in CHU rats than N rats.

5.3.4 MSNA during baroreceptor unloading

In 7 N rats, infusion of a bolus of SNP was used to cause a fall in ABP and hence to unload baroreceptors. The fall in ABP was accompanied by a reflex rise in HR, and an increase in R_F (see Figure 5.8 for example and Figure 5.9 for mean data). During infusion of SNP, MSNA firing rate, recorded in 37 discriminated single units was significantly elevated relative to baseline conditions (Figure 5.9).

In the 6 CHU rats in which recordings of MSNA during SNP infusion were made, baseline MSNA firing frequency tended to be higher than in the 7 N rats ($p=0.057$, 28 discriminated single units). Infusion of SNP also caused the expected significant fall in ABP reflex increase in HR, and increased R_F. In contrast to N rats, in rise in MSNA firing rate during SNP infusion did not reach statistical significance ($p=0.056$).

Considering these results in more detail, in 3 CHU rats, SNP bolus caused firing rate to more than double, and in 2 rats, firing rate was increased by ~50%. On the other hand, in N rats, in four of the seven successful recordings, firing rate was more than doubled, and in two cases tripled, whilst one rat showed less than a 50% increase in single unit MSNA.

5.3.5 MSNA during graded systemic hypoxia

Owing to the large number of augmented breaths that occurred during systemic hypoxia (see Figure 5.10), and the difficulty in completely isolating the spinotrapezius muscle from movement during such augmented breaths, recordings during graded hypoxia were difficult to achieve and were often lost soon after the onset of hypoxia. Isolating the muscle, and the vessels within it, from the movement associated with augmented breaths was particularly challenging, particularly as the frequency of these is markedly increased during acute hypoxia (Marshall & Metcalfe, 1988b). Significant pressure on the thorax was required, achieved with a rounded metal block, so as to stop the spinotrapezius muscle moving relative to the rest of the body. This was undesirable as it restricted respiratory effort, and so a balance between pressure and free respiratory movement was found.

Some discriminated units contained both cardiac and respiratory rhythmicity, but showed no change at all during graded systemic hypoxia. These neurones were not included in the analysis as they didn't fulfill the previously described characteristics of MSNA (Hudson *et al.*, 2011) or muscle vasoconstrictor neurones (Janig, 1985;

Habler *et al.*, 1993, 1994).Thus, it was only possible to record MSNA reliably for the 6 minutes of graded hypoxia in a small number of rats.

In N rats, graded hypoxia caused the expected reduction in P_aO_2 and P_aCO_2, and caused a small increase in pH_a (Table 5.2). During graded hypoxia there was a graded fall in ABP and rise in HR, although this did not reach statistical significance (see Figure 5.10 for example and Figure 5.11 for mean data). Further, R_F increased from the onset of graded hypoxia, and waned somewhat when breathing 8%O_2. Graded hypoxia induced a graded increase in MSNA firing rate, recorded in 27 individual units from 6 N rats, and the change achieved statistical significance when breathing 8%O_2.

In 5 CHU rats in which recordings were stable during hypoxia, graded hypoxia also caused a large fall in P_aO_2, a fall in P_aCO_2 and a small rise in pH_a (See Table 5.2). Graded hypoxia induced the expected graded fall in ABP (Figure 5.11), although ABP reached a significantly lower level than that recorded in the N rats during systemic hypoxia ($p<0.001$, Figure 5.11A). Graded hypoxia evoked a significant increase in R_F and HR (Figure 5.11). Graded hypoxia induced a graded rise in MSNA firing rate in the 24 units analysed, which achieved significance when breathing 8%O_2.

5.3.6 In vitro studies - The effect of CHU on sympathetic nervous innervation of the anterior tibial artery

The fluorescent intensity of isolated anterior tibial arteries was markedly higher in CHU rats than N rats (Figure 5.12 for example, 5.13 for mean data) indicating increased levels of catecholamine-related fluorescence. The innervation density, i.e. the number of intersects per unit area on the surface of the anterior tibial artery, was also markedly higher in CHU rats relative to N rats (Figure 5.13B).

Table 1 – Baseline characteristics of N and CHU rats used for recordings of MSNA

Group	MABP (mmHg)	HR (bpm)	R_F (bpm)	Single units analysed	Mean Firing Rate (Hz)	Range (Hz)
N (n=27)	122±2	430±6	104±2	198	0.33±0.036	0.02-1.41
CHU (n=17)	117±2	421±7	105±12	157	0.56±0.075 *** vs N	0.02-2.41

General characteristics of the N and CHU rats that MSNA was recorded from. Data is presented as mean±SEM. ABP, HR and R_F were similar between the two groups. Mean firing frequency was significantly higher in CHU relative to N. Range indicates the range of mean, ongoing frequencies recorded in discriminated single units.

*** - $p<0.001$, Students t-test between groups.

Figure 5.1 – Example baseline MSNA recording in an N rat

A: Example recording of baseline cardiorespiratory variables (ABP, Tracheal pressure, HR, RF) and ongoing multiunit MSNA in an N rat. Raw MSNA signal is displayed (labeled MSNA), along with discriminated spikes (all units) and rate histograms for individual units.

B: Spike templates and overdrawn spikes discriminated from the raw multiunit recording.

Figure 5.1

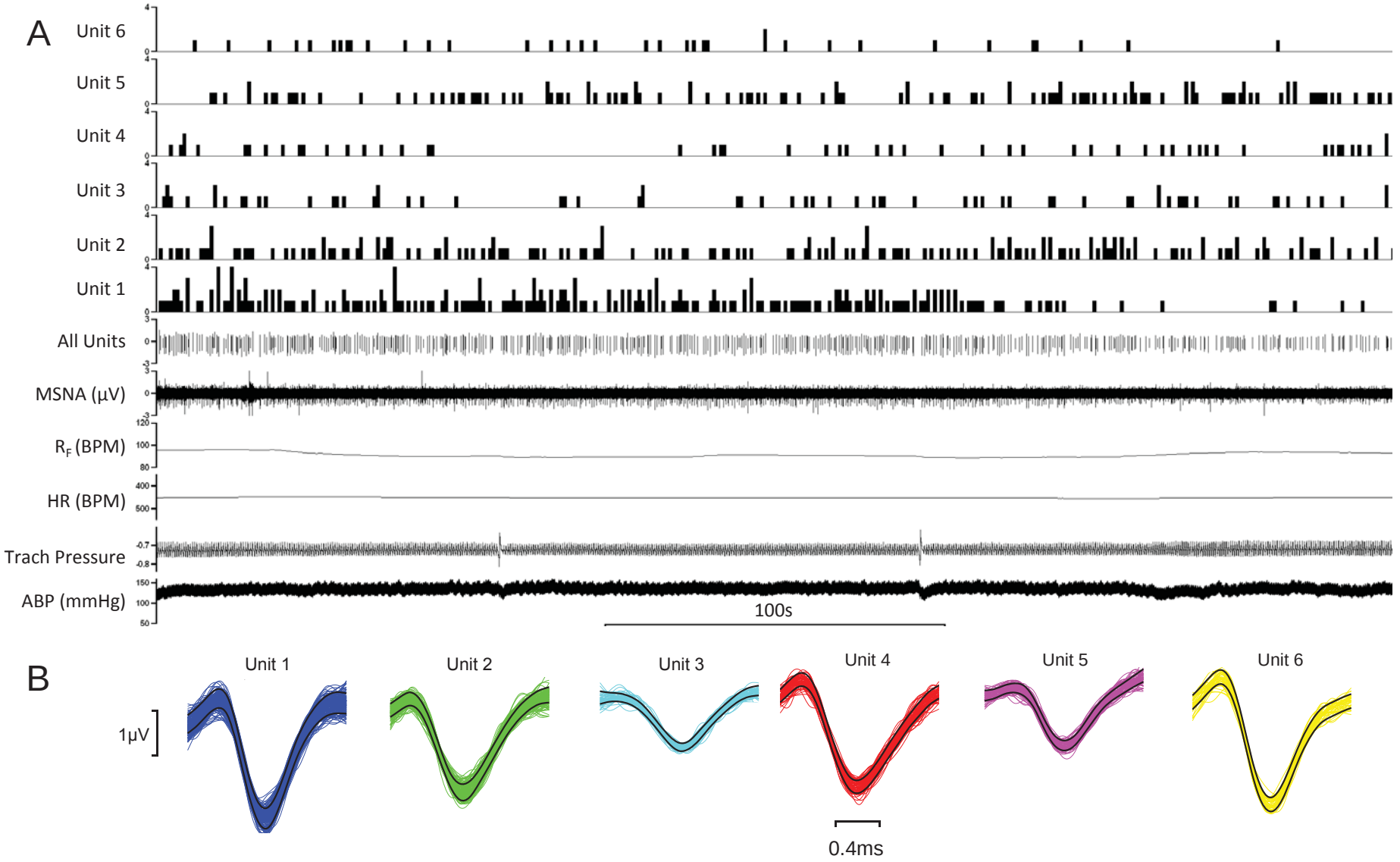
A
Unit 6
Unit 5
Unit 4
Unit 3
Unit 2
Unit 1
All Units
MSNA (μV)
R_F (BPM)
HR (BPM)
Trach Pressure
ABP (mmHg)
100s
B
Unit 1
Unit 2
Unit 3
Unit 4
Unit 5
Unit 6
1μV
0.4ms

Figure 5.2 – Analysis of cardiac and respiratory rhythm in an MSNA recording from an N rat

A: Stimulus triggered histogram of baseline MSNA shown in figure 5.1, triggered from the peaks in tracheal pressure (expiration), demonstrating respiratory rhythmicity in multiunit activity and each discriminated unit (60 bins, 0.05s bin width)

B: Wave form average of tracheal pressure triggered from peaks in tracheal pressure (1s width).

C: Stimulus triggered histogram of baseline MSNA shown in figure 5.1, triggered from the peak of the arterial pressure wave, demonstrating cardiac rhythmicity in multiunit MSNA and each discriminated unit (100 bins, 0.01s bin width)

D: Waveform average of ABP pressure wave triggered from the peak of the arterial pressure (1s width).

Figure 5.2

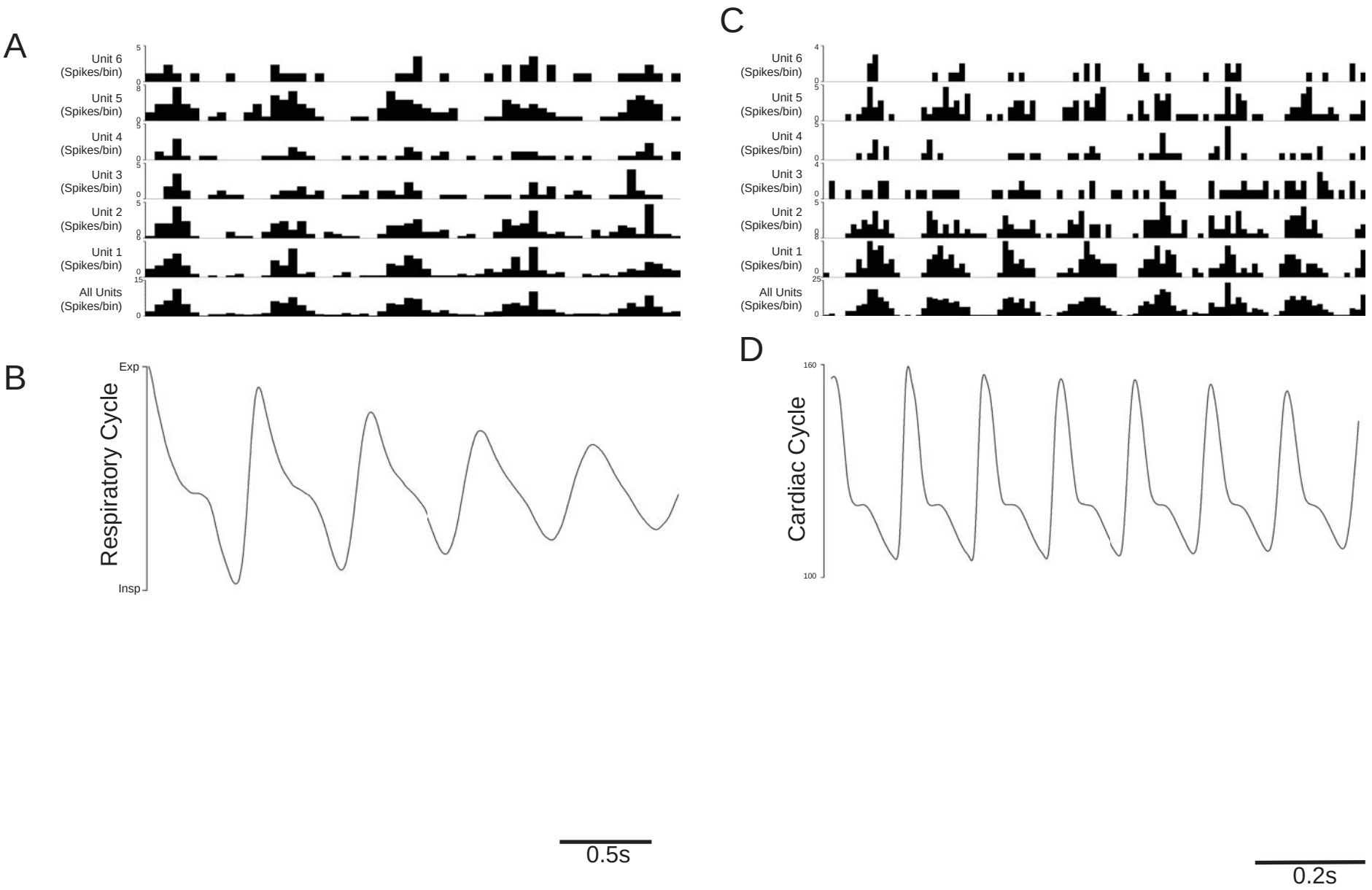
A
Unit 6 (Spikes/bin)
Unit 5 (Spikes/bin)
Unit 4 (Spikes/bin)
Unit 3 (Spikes/bin)
Unit 2 (Spikes/bin)
Unit 1 (Spikes/bin)
All Units (Spikes/bin)
B
Exp
Respiratory Cycle
Insp
0.5s
C
Unit 6 (Spikes/bin)
Unit 5 (Spikes/bin)
Unit 4 (Spikes/bin)
Unit 3 (Spikes/bin)
Unit 2 (Spikes/bin)
Unit 1 (Spikes/bin)
All Units (Spikes/bin)
D
Cardiac Cycle
0.2s

Figure 5.3 – Example baseline MSNA recording in a CHU rat.

A: Example recording of baseline cardiorespiratory variables (ABP, Tracheal pressure, HR, RF) and ongoing multiunit MSNA in a CHU rat. Raw MSNA signal is displayed (labeled MSNA), along with discriminated spikes (all units) and rate histograms for individual units.

B: Spike templates and overdrawn spikes discriminated from the raw multiunit recording.

Figure 5.3

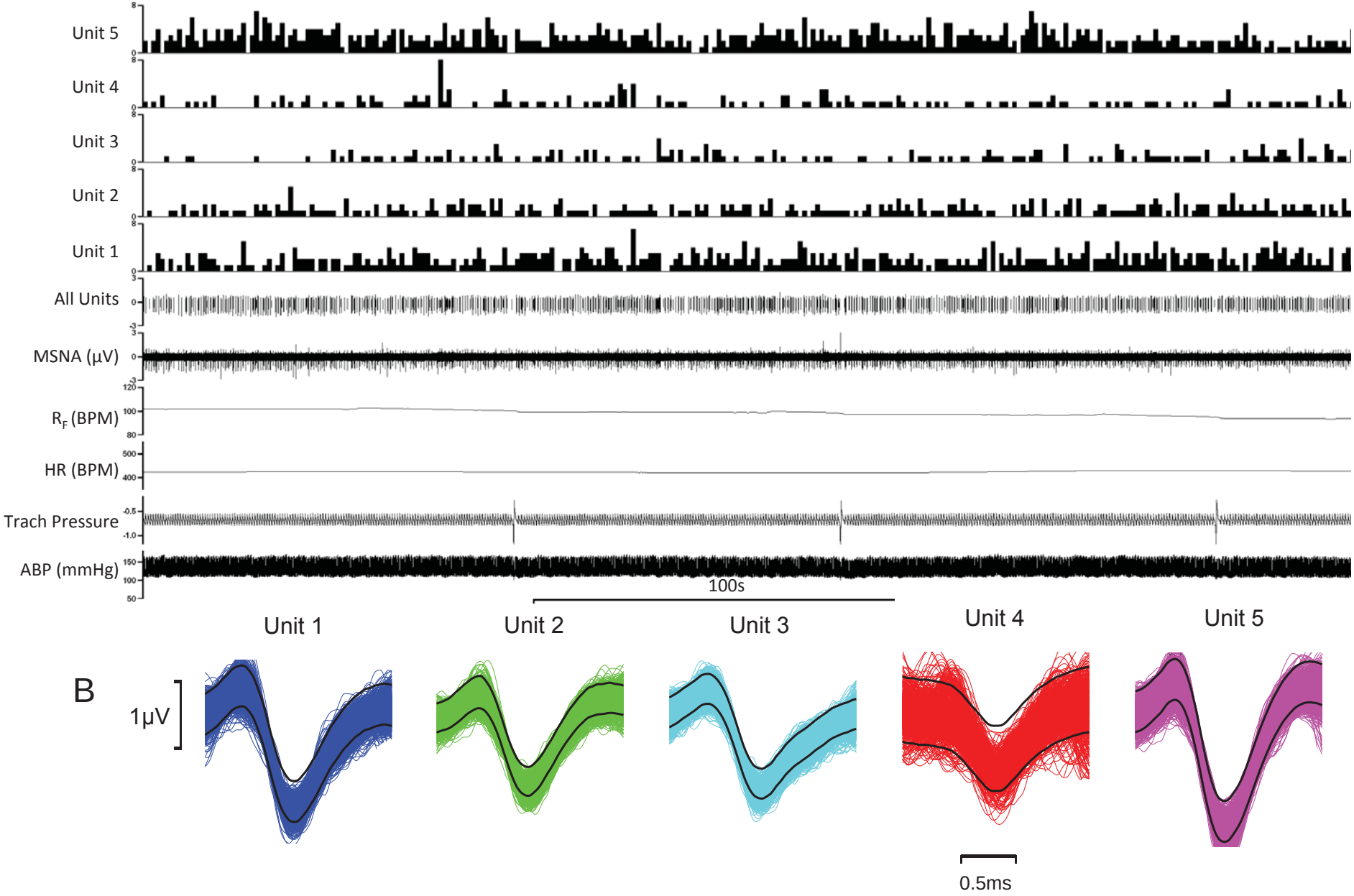
A
Unit 5
Unit 4
Unit 3
Unit 2
Unit 1
All Units
MSNA (µV)
R_F (BPM)
HR (BPM)
Trach Pressure
ABP (mmHg)
100s
Unit 1
Unit 2
Unit 3
Unit 4
Unit 5
B
1µV
0.5ms

Figure 5.4 - Analysis of cardiac and respiratory rhythm in an MSNA recording from a CHU rat

A: Stimulus triggered histogram of baseline MSNA triggered from the peaks in tracheal pressure, demonstrating respiratory rhythmicity in each discriminated unit (60 bins, 0.05s bin width)

B: Wave form average of tracheal pressure triggered from peaks in tracheal pressure (1s width).

C: Stimulus triggered histogram of baseline MSNA shown in figure 5.3, triggered from the pressure wave of ABP, demonstrating cardiac rhythmicity in each discriminated unit (100 bins, 0.01s bin width)

D: Waveform average of ABP pressure wave triggered from peaks in arterial pressure (1s width).

Figure 5.4

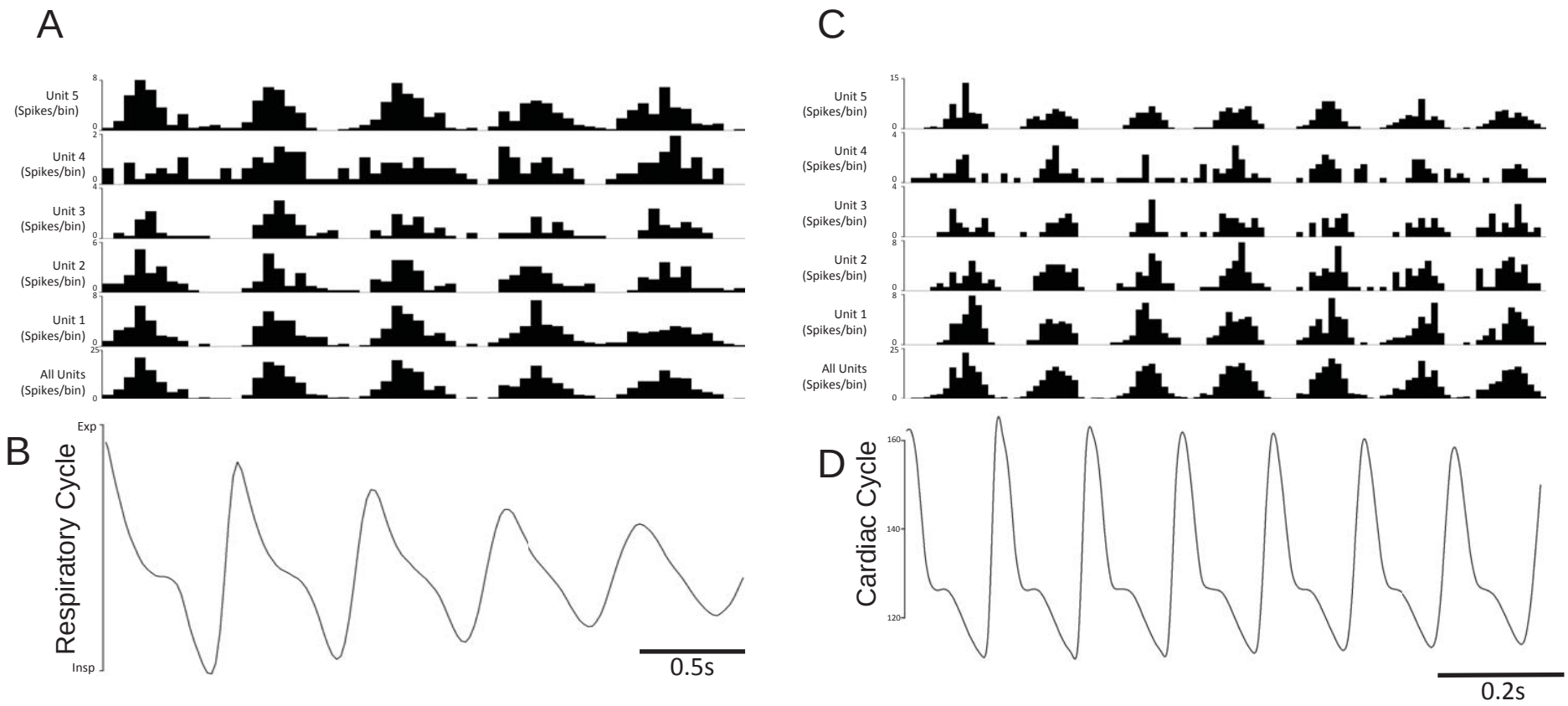
A
Unit 5 (Spikes/bin)
Unit 4 (Spikes/bin)
Unit 3 (Spikes/bin)
Unit 2 (Spikes/bin)
Unit 1 (Spikes/bin)
All Units (Spikes/bin)
B
Exp
Respiratory Cycle
Insp
0.5s
C
Unit 5 (Spikes/bin)
Unit 4 (Spikes/bin)
Unit 3 (Spikes/bin)
Unit 2 (Spikes/bin)
Unit 1 (Spikes/bin)
All Units (Spikes/bin)
D
Cardiac Cycle
0.2s

Figure 5.5 – Phase histogram analysis of cardiac rhythmicity in MSNA in N and CHU rats

A: Phase histogram of multiunit MSNA in an N rat triggered from peak of the arterial pressure wave (180bins, HR trigger begins and ends cycle, 0.3s max cycle).

B: Phase histogram of multiunit MSNA in a CHU rat triggered from peak of the arterial pressure wave (180bins, HR trigger begins and ends cycle, 0.3s max cycle).

C: Waveform average of ABP pressure wave in the same N rat, triggered from the peak in ABP (width 0.25s).

D: Waveform average of ABP pressure wave in the same CHU rat, triggered from the peak in ABP (width 0.25s).

E & F: Mean phase histograms of all single units analysed in N (panel E) and CHU (panel F) rats, triggered by peaks in the arterial pressure wave. All histograms are realigned to peak at 180°, and displayed as percentage of total spikes analysed in each bin (360 bins per cycle). Grey area represents ±60° of the cycle peak.

G: Proportion of MSNA falling within and outside ±60° of the peak of MSNA in the cardiac triggered phase histogram in N and CHU rats, demonstrating the strength of cardiac modulation in single unit MSNA from each group.

Figure 5.5

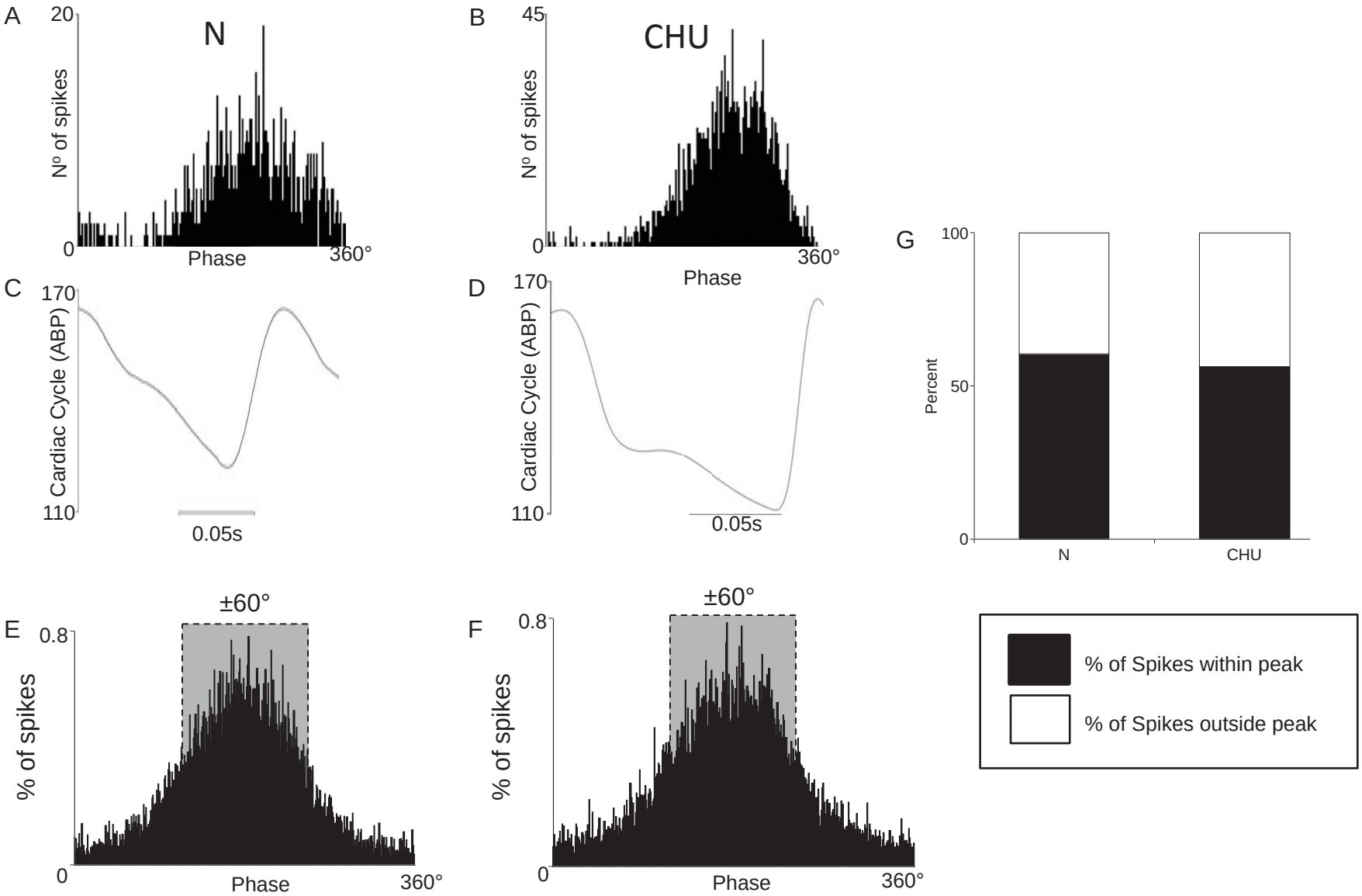
A
N
20
0
Nº of spikes
Phase
360°
B
CHU
45
0
Nº of spikes
Phase
360°
C
170
110
Cardiac Cycle (ABP)
0.05s
D
170
110
Cardiac Cycle (ABP)
0.05s
G
100
50
0
Percent
N
CHU
E
±60°
0.8
0
% of spikes
Phase
360°
F
±60°
0.8
0
% of spikes
Phase
360°
% of Spikes within peak
% of Spikes outside peak

Figure 5.6 - Phase histogram analysis of respiratory rhythmicity in MSNA in N and CHU rats

A: Phase histogram of multiunit MSNA in an N rat triggered from peak of the tracheal pressure wave (180bins, HR trigger begins and ends cycle, 0.3s max cycle).

B: Phase histogram of multiunit MSNA in a CHU rat triggered from peak of the tracheal pressure wave (180bins, HR trigger begins and ends cycle, 0.3s max cycle).

C: Waveform average of tracheal pressure wave in the same N rat, triggered from the peak in tracheal pressure (width 0.25s).

D: Waveform average of tracheal pressure wave in the same CHU rat, triggered from the peak in tracheal pressure (width 0.25s).

E & F: Mean phase histograms of all single units analysed in N (panel E) and CHU (panel F) rats, triggered by peaks in the tracheal pressure wave. All histograms are realigned to peak at 180°, and displayed as percentage of total spikes analysed in each bin (360 bins per cycle). Grey area represents ±60° of the cycle peak.

G: Proportion of MSNA falling within and outside ±60° of the peak of MSNA in the respiratory triggered phase histogram in N and CHU rats, demonstrating the strength of respiratory modulation in single unit MSNA from each group.

Figure 5.6

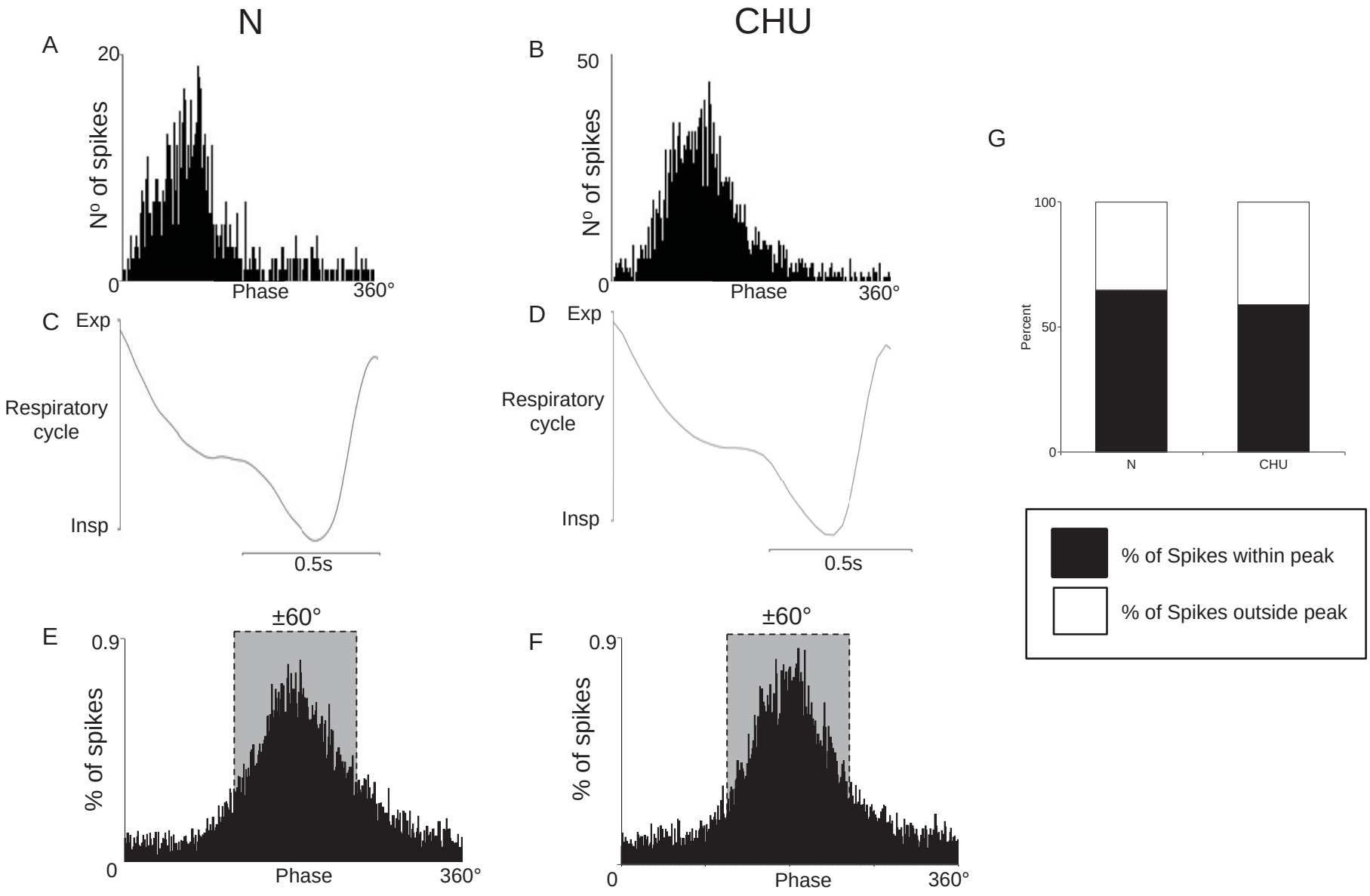
N
CHU
A
B
20
50
Nº of spikes
0
Phase
360°
C
D
Exp
Respiratory cycle
Insp
0.5s
E
F
±60°
0.9
% of spikes
G
100
50
Percent
N
CHU
% of Spikes within peak
% of Spikes outside peak

Table 5.2 – Arterial blood gasses in N and CHU rats before, and at the end of graded systemic hypoxia

	Normoxia (N; n=5, CHU; n=9)			End of graded hypoxia (N; n=3, CHU; n=7)		
	P_aO_2	P_aCO_2	pH_a	P_aO_2	P_aCO_2	pH_a
N	78±2	44±2	7.42±0.08	28.6±4	29±2	7.54±0.05
CHU	87±2*	40±2	7.42±0.01	24.4±3	23±1	7.57±0.008

Baseline arterial blood gasses (P_aO_2, P_aCO_2, pH) in N and CHU rats during normoxia (left) and at the end of a 6 minute period of graded hypoxia. Blood gasses were sampled in only a small number of experiments for technical reasons. Data presented are mean±SEM.

* - $p<0.05$ vs N.

Figure 5.7 – Analysis of the instantaneous frequencies generated by MSNA recorded in N and CHU rats

A: Histogram showing the proportion of all action potentials recorded in each single unit with interspike intervals producing instantaneous frequencies of 1-10Hz, 10-20Hz, 20-40Hz and 40-80Hz in N and CHU rats. * - $p<0.05$ vs N.

B: Histogram showing the proportion of all action potentials recorded in each single unit with interspike intervals producing instantaneous frequencies of 1-5Hz and 5-10Hz in N and CHU rats. *** - $p<0.001$ vs N.

Figure 5.7

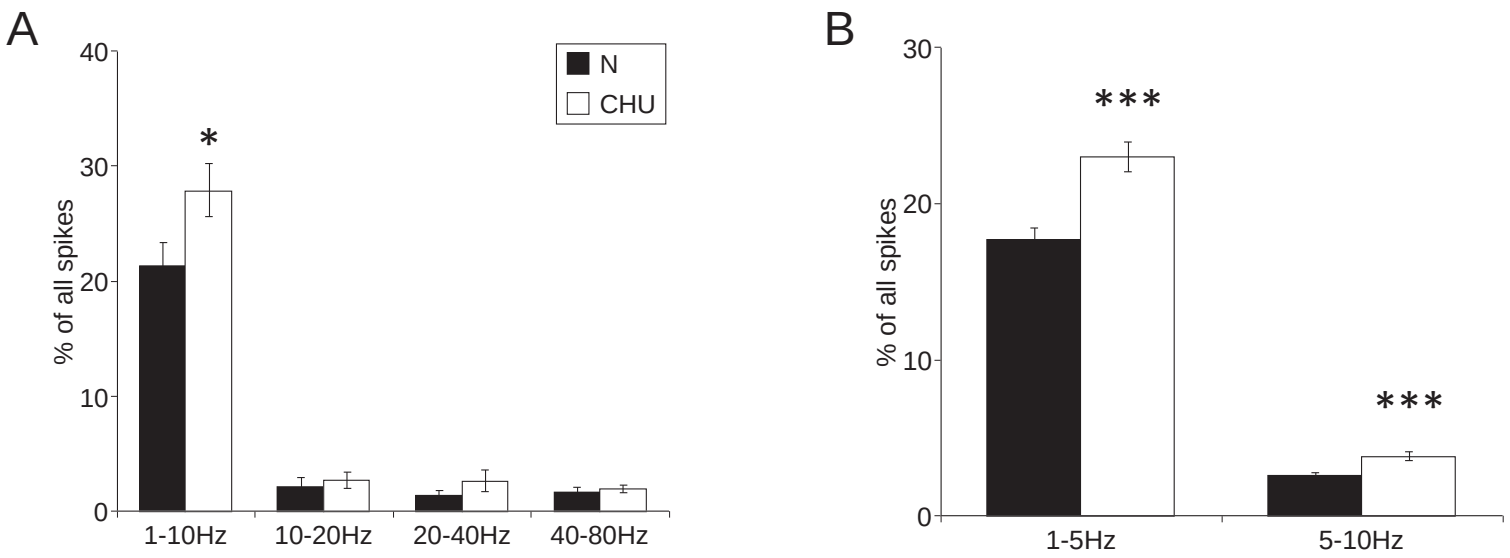
A
40
30
20
10
0
% of all spikes
N
CHU
*
1-10Hz
10-20Hz
20-40Hz
40-80Hz
B
30
20
10
0
% of all spikes
***
***
1-5Hz
5-10Hz

Figure 5.8 – Example recording of MSNA during bolus infusion of SNP to unload the arterial baroreceptors in an N rat

Example recording of cardiorespiratory variables (ABP, HR, tracheal pressure), raw MSNA, multiunit discriminated MSNA (all units), and rate histogram (spikes/5s) for the multi unit MSNA in an N rat during baroreceptor unloading with a bolus of SNP (time marked by solid arrow).

§ and arrow indicates movement artifact, causing electrical interference in the nerve activity recording.

Figure 5.8

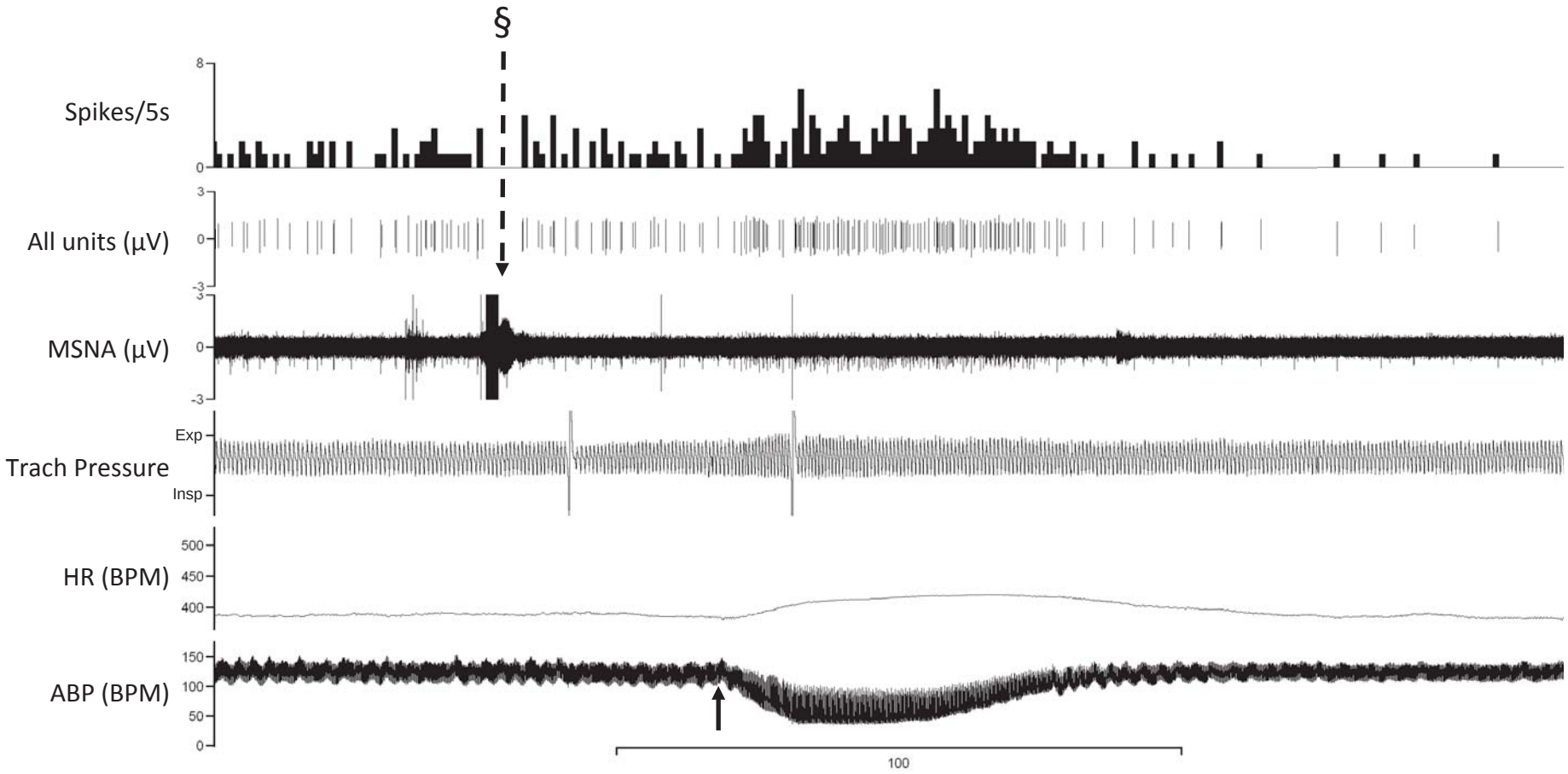
§
Spikes/5s
8
0
All units (µV)
3
0
-3
MSNA (µV)
3
0
-3
Trach Pressure
Exp
Insp
HR (BPM)
500
450
400
ABP (BPM)
150
100
50
0
100

Figure 5.9 – The effect of unloading the arterial baroreceptors on cardiovascular variables, including MSNA, in N and CHU rats.

Mean±SEM data in N and CHU rats during baseline and during baroreceptor unloading with SNP

A: Mean ABP during baseline and following administration of SNP in N (red lines, red squares) and CHU rats (blue lines, blue circles). SNP caused a significant fall in ABP in N and CHU rats. *** and ††† - $p<0.001$ from respective baselines.

B: Mean MSNA firing frequency during baseline and following administration of SNP in N (red lines, red squares) and CHU rats (blue lines, blue circles). SNP caused a significant rise in firing frequency in N rats (** - $p<0.01$), but no significant rise in CHU rats.

C: Mean HR during baseline and following administration of SNP in N (red lines, red squares) and CHU rats (blue lines, blue circles). Administration of SNP induced a significant rise in HR in N (* - $p<0.05$) and CHU rats (††† - $p<0.001$).

D: Mean R_F during baseline and following administration of SNP in N (red lines, red squares) and CHU rats (blue lines, blue circles). SNP induced a significant rist in RF in N and CHU rats (*, † - $p<0.05$ vs respective baselines).

Figure 5.9

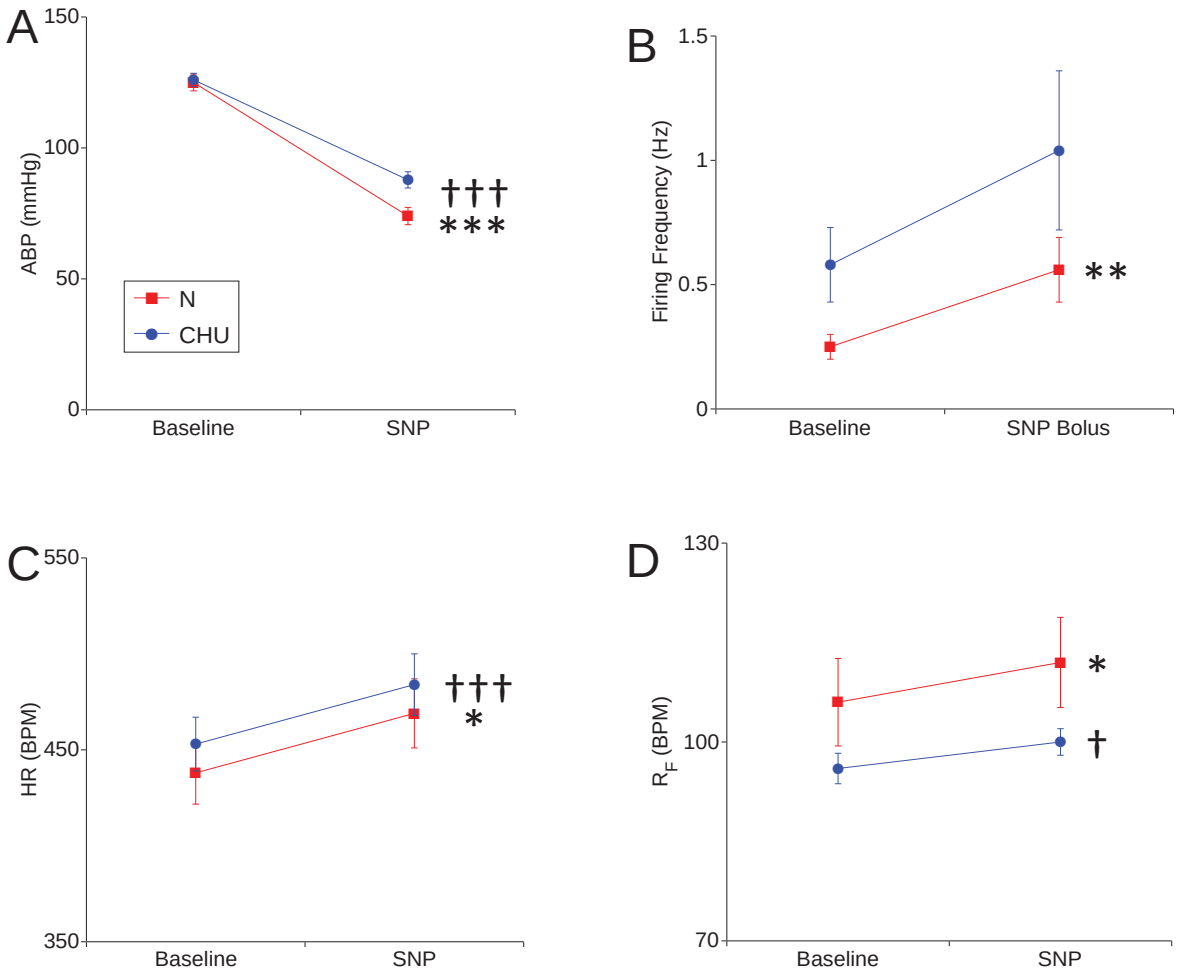
A
150
100
50
0
ABP (mmHg)
N
CHU
†††
***
Baseline
SNP
B
1.5
1
0.5
0
Firing Frequency (Hz)
**
Baseline
SNP Bolus
C
550
450
350
HR (BPM)
†††
*
Baseline
SNP
D
130
100
70
R_F (BPM)
*
†
Baseline
SNP

Figure 5.10 – Example recording of MSNA during graded systemic hypoxia in an N rat.

Example recording of cardiorespiratory variables (ABP, tracheal pressure, HR, R_F), raw multiunit MSNA, multiunit discriminated MSNA (all units) and rate histogram for discriminated multiunit MSNA (spikes/5s) during baseline and 6 minutes of graded hypoxia (12%, 10%, 8% FiO_2, 2 minutes each).

Figure 5.10

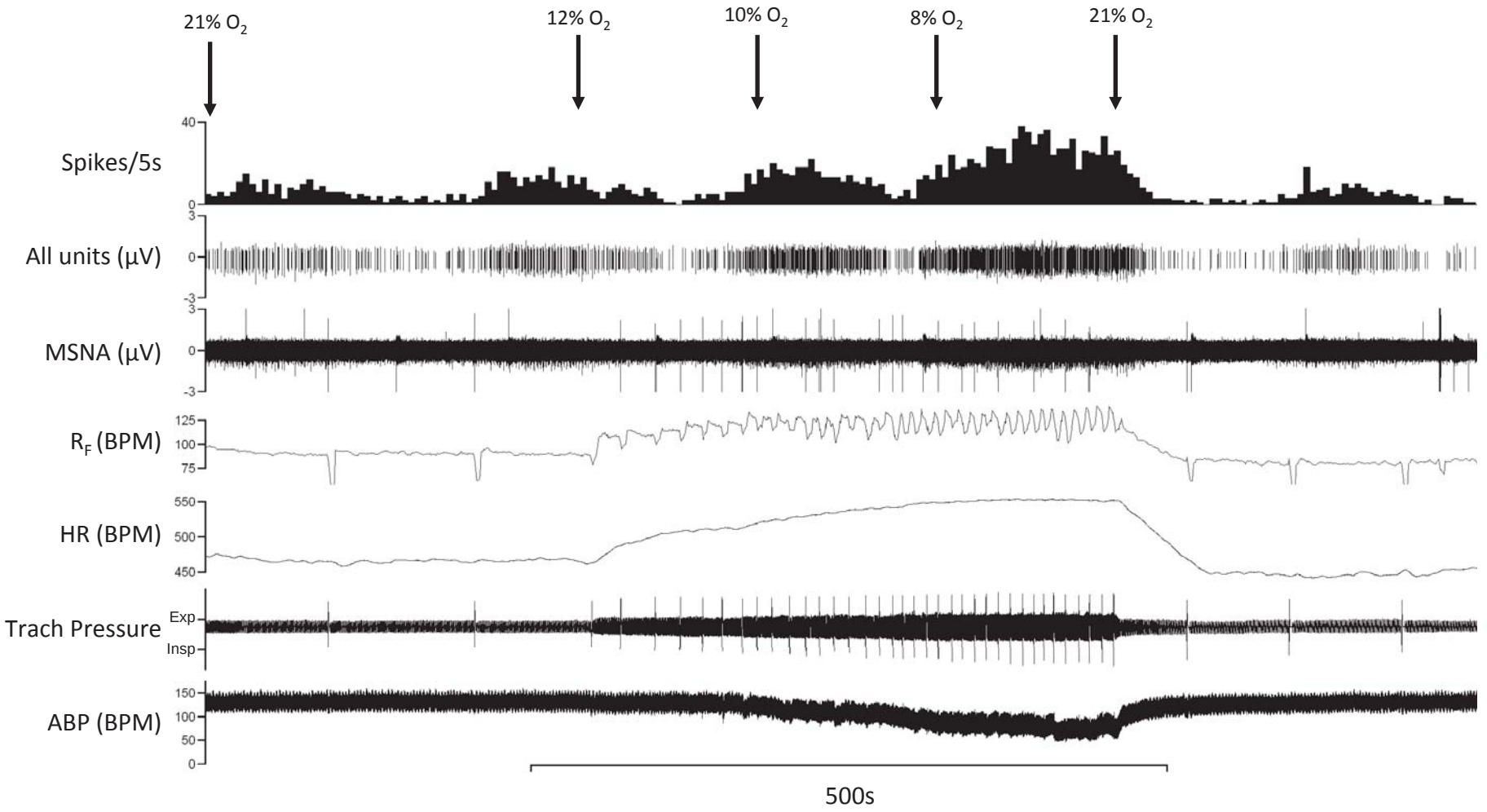
21% O2
12% O2
10% O2
8% O2
21% O2
Spikes/5s
40
0
All units (μV)
3
0
-3
MSNA (μV)
3
0
-3
RF (BPM)
125
100
75
HR (BPM)
550
500
450
Trach Pressure
Exp
Insp
ABP (BPM)
150
100
50
0
500s

Figure 5.11 - The effect of graded systemic hypoxia on cardiovascular variables, including MSNA, in N and CHU rats.

Mean±SEM data in N and CHU rats during baseline and 6 minutes of graded hypoxia A: Mean ABP during normoxia, and graded hypoxia in N (red lines, red squares) and CHU (blue lines, blue circles). * - $p<0.05$ vs normoxia, ***, ††† - $p<0.001$ vs normoxia.

B: Mean MSNA firing frequency during normoxia, and graded hypoxia in N (red lines, red squares) and CHU (blue lines, blue circles). *,† - $p<0.05$ vs normoxia.

C: Mean HR during normoxia, and graded hypoxia in N (red lines, red squares) and CHU (blue lines, blue circles). †, †† - $p<0.05$ and $p<0.01$ respectively vs normoxia in CHU.

D: Mean R_F during normoxia, and graded hypoxia in N (red lines, red squares) and CHU (blue lines, blue circles). ††† - $p<0.001$ vs normoxia in CHU.

Figure 5.11

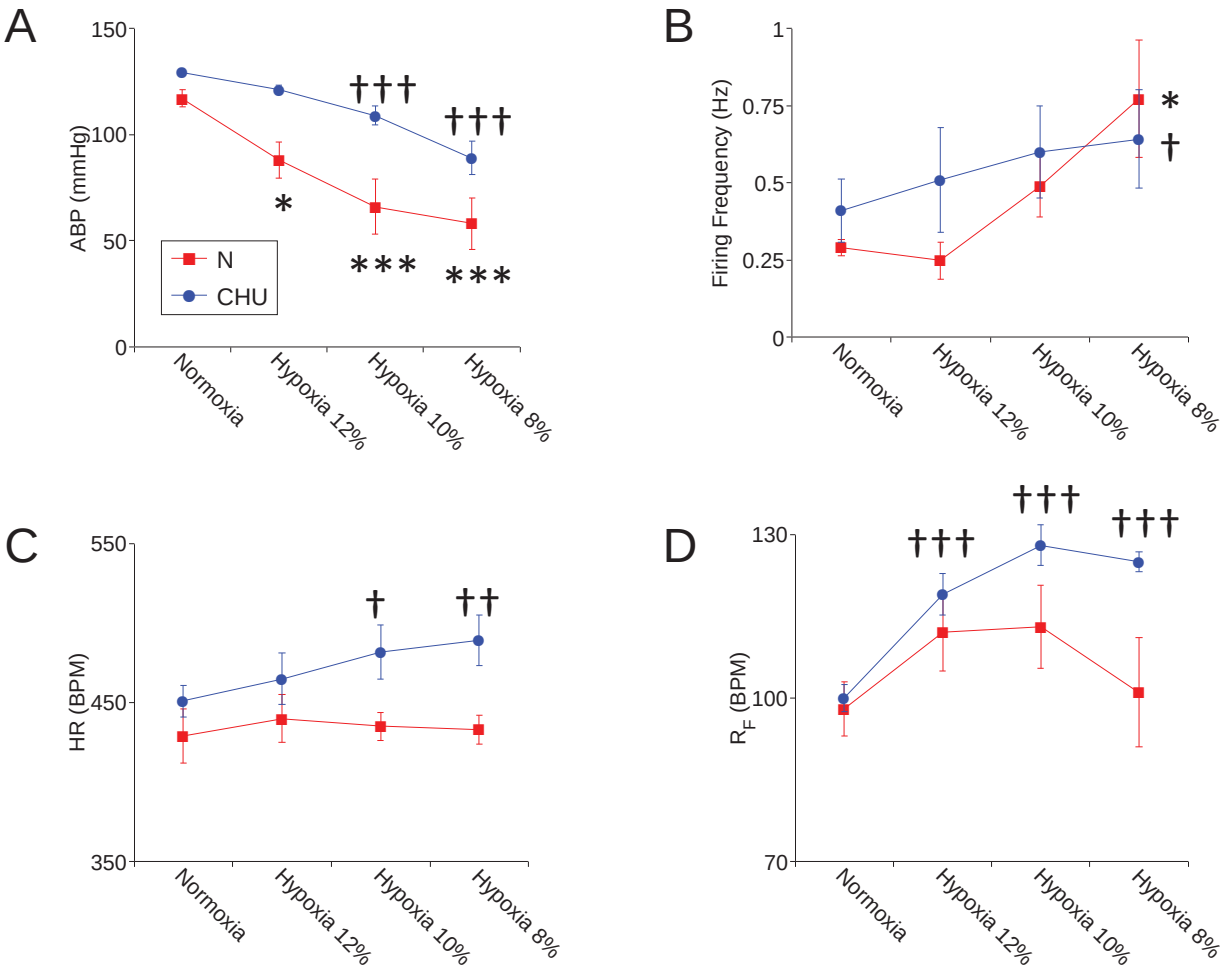
A
150
100
50
0
ABP (mmHg)
N
CHU
†††
†††
*
***
***
Normoxia
Hypoxia 12%
Hypoxia 10%
Hypoxia 8%
B
1
0.75
0.5
0.25
0
Firing Frequency (Hz)
*
†
Normoxia
Hypoxia 12%
Hypoxia 10%
Hypoxia 8%
C
550
450
350
HR (BPM)
†
††
Normoxia
Hypoxia 12%
Hypoxia 10%
Hypoxia 8%
D
130
100
70
R_F (BPM)
†††
†††
†††
Normoxia
Hypoxia 12%
Hypoxia 10%
Hypoxia 8%

Figure 5.12 – Example photomicrographs of glyoxylic acid staining of tibial arteries in an N and a CHU rat.

A: Photomicrograph of stained preparations of a section of tibial artery from an N rat showing the sympathetic noradrenergic innervation on the surface of the blood vessel, visualized under fluorescent confocal microscopy using the glyoxilic acid method.

B: Photomicrograph of stained preparations of a section of tibial artery from a CHU rat showing the sympathetic noradrenergic innervation on the surface of the blood vessel, visualized under fluorescent confocal microscopy using the glyoxilic acid method.

Figure 5.12

A

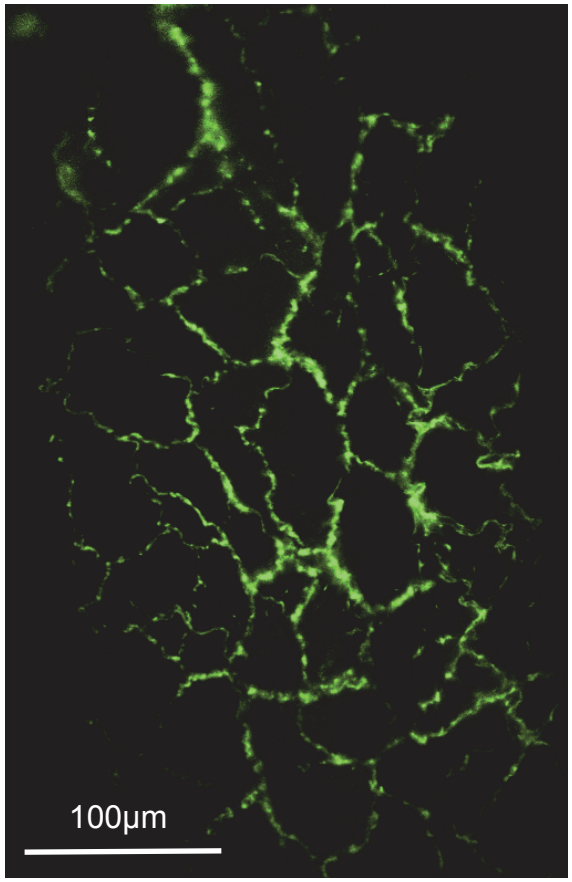

N

B

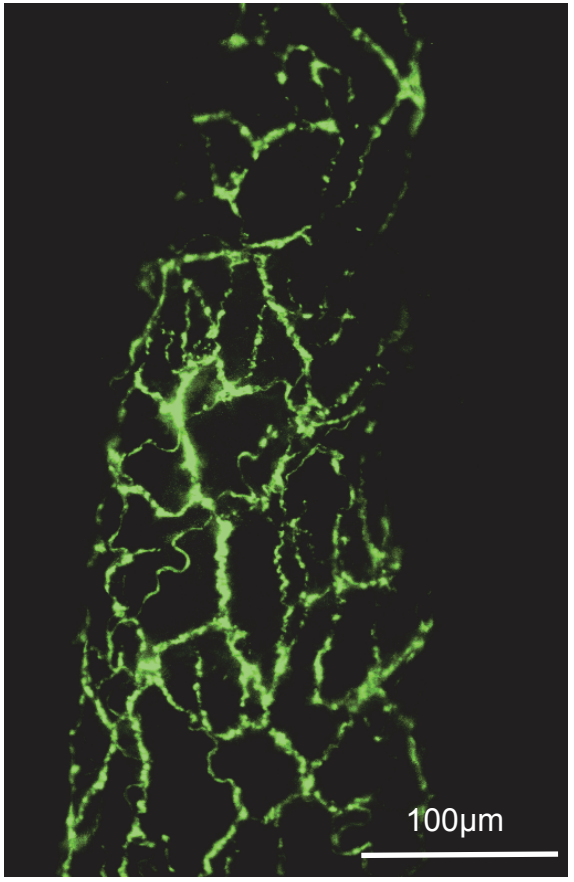

CHU

Figure 5.13 – The effect of CHU on sympathetic innervation density in the tibial artery

A: Mean fluorescent density of catacholamines stained on the surface of the tibial artery in N and CHU rats, indication the noradrenaline content on the surface of the blood vessel. * - $p<0.05$ vs N.

B: Mean innervation density of catacholaminergic neurones on the surface of the tibial artery in N and CHU rats, indicating the number of neurones present per unit area. *** - $p<0.001$ vs N.

Figure 5.13

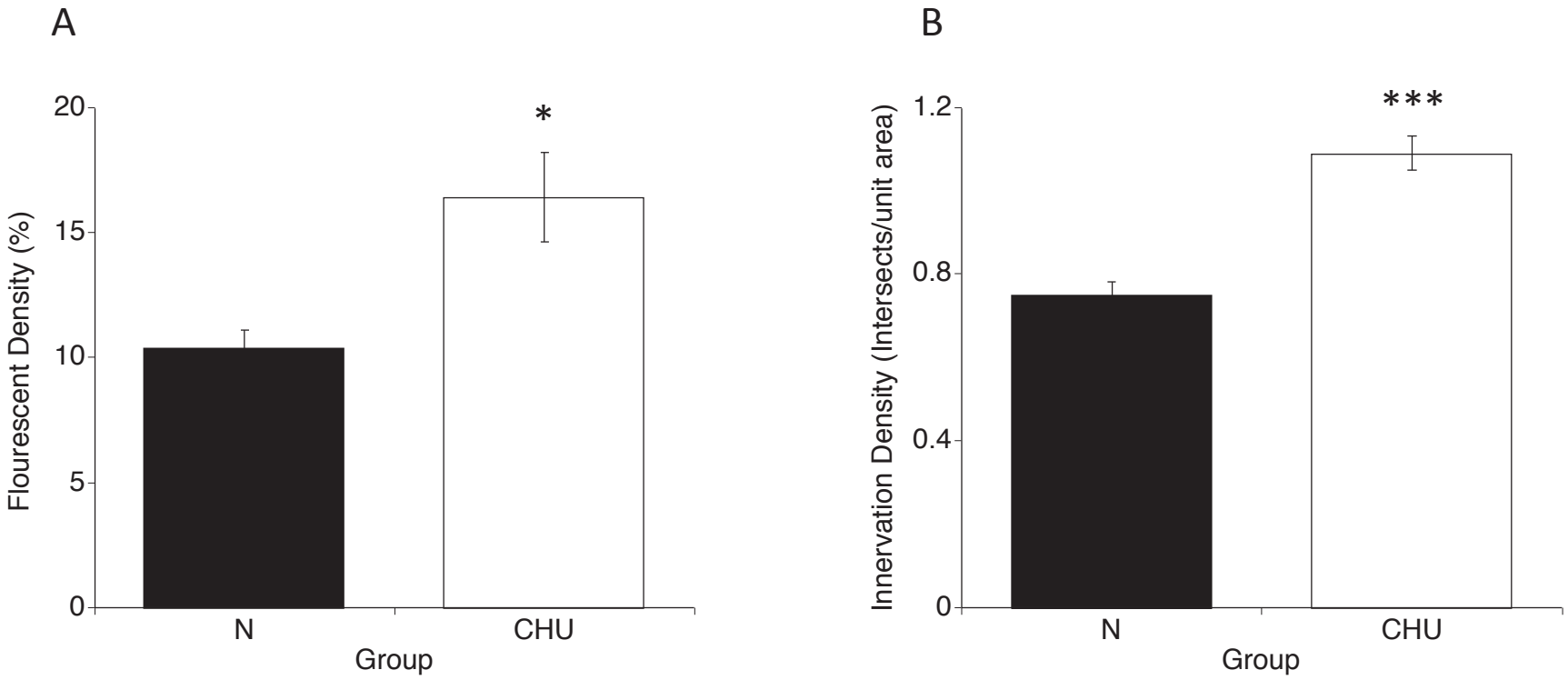
A
Flourescent Density (%)
20
15
10
5
0
*
N
CHU
Group
B
Innervation Density (Intersects/unit area)
1.2
0.8
0.4
0
***
N
CHU
Group

5.4 Discussion

5.4.1 Main findings

The results presented in the present study demonstrate that in CHU rats, ongoing MSNA in fibres supplying spinotrapezius muscle vasculature was substantially higher than N rats, reflecting an increase in the single units with instantaneous firing frequencies between 1 and 10Hz. However, the increase in activity in single post-ganglionic sympathetic neurones supplying skeletal muscle that was evoked by SNP infusion was similar in CHU and N rats, as were the increases in MSNA evoked by graded levels of systemic hypoxia. The density of sympathetic noradrenergic neurones on the surface of the tibial artery was significantly higher in CHU rats than N rats.

5.4.2 MSNA Recordings

Recording MSNA from the surface of the spinotrapezius arterial vessels by using the focal recording technique presented many technical challenges. In more than half of the preparations, no recordings of MSNA were achieved. It is possible that this was due to damage to the paravascular nerve fibres or the nerve plexus during surgical isolation of the muscle, or to damage more proximal at the neurovascular bundle supplying the muscle, even though great care was taken to avoid this. Alternatively, it may simply be that by chance, the recording electrode was not placed sufficiently close to fibres or fibre bundles with ongoing activity to detect nerve activity. The density of sympathetic nerves on the surface of skeletal muscle vasculature is low,

and much lower than that found in the caudal ventral tail artery, where this preparation has been successfully used with a success rate >60% (Johnson & Gilbey, 1994, 1996).

There were significant difficulties associated with electrical isolation of the recording setup from background noise, caused particularly by the anaesthetic infusion pump, the homeothermic blanket, ECG interference, and interference associated with the proximity of the operators' hands. As indicated in the methods, this was minimised with the aid of a Faraday cage, through which all cannulae, and electrical cables were passed.

5.4.3 Characterisation of the recorded nerve activity

Moving on to consider the successful recordings of MSNA made using the focal recording electrode from the surface of arterial vessels supplying the spinotrapezius muscle: These were expected to be of sympathetic origin due to their location (Furness & Costa, 1975; Marshall, 1982). However, this expectation was verified by ensuring that all units included in the analysis contained cardiac and respiratory rhythmicity, as has been previously described for muscle vasoconstrictor (MVC) fibers in cats and rats (Janig, 1985; Habler *et al.*, 1994), and for MSNA recorded recently from the spinotrapezius muscle (Hudson *et al.*, 2011). In N rats the mean firing rate, and range of firing rates recorded were similar to those found in single fibres discriminated from whole nerve recordings in rats (Habler *et al.*, 1994), and to those units discriminated from MSNA recordings in spinotrapezius (0.33±0.036 vs 0.28±0.07 or 0.2±0.1, see Hudson et al., 2011). Further evidence that the nerves

recorded from are sympathetic is that when recordings were maintained long enough, unloading the baroreceptors by infusing the NO donor SNP, produced a marked increase in nerve activity (see below). The recent study performed on the same experimental preparation of the spinotrapezius found that recordings of presumed sympathetic nerve activity, of a nature similar to that recorded in this study were also sensitive to the ganglionic transmission blocker trimetaphan, producing further evidence that they were indeed sympathetic in nature. The recordings made from CHU rats had similar firing characteristics (cardiac and respiratory rhythmicity and the activity was augmented during SNP infusion). In light of these findings, it seems reasonable to conclude that all discriminated units recorded in both N and CHU rats, that contained cardiac and respiratory rhythmicity were indeed sympathetic neurones.

It should be noted that the sites from which the recordings were made from were generally on larger diameter arteries (estimated ~300μm, see Marshall 1982). One of the advantages of this preparation of the spinotrapezius muscle, is that it is clear where the arterial vessels going. Hence, we assumed that the nerves on the surface of an arterial vessel were predominantly supplying that vessel and its branches. However, the possibility that some of the neurones recorded from were in fact supplying fat or connective tissue around the blood vessels cannot be excluded. .

5.4.4 Comparisons of ongoing MSNA in N and CHU rats

An important new finding of the present study was that ongoing firing frequency in MSNA recorded spinotrapezius muscle vasculature in CHU rats is significantly higher

than that recorded in N rats. Further, when instantaneous frequencies of the ongoing MSNA were analysed it was found that the proportion of the interspike intervals giving rise to firing frequencies of 1-10Hz was significantly higher in CHU than N rats. Given that ongoing sympathetic nerve activity contributes to the ongoing vascular tone it can be concluded that the sympathetic nerve activity directed to the vascular smooth muscle is accentuated as a consequence of chronic hypoxia *in utero.*

Considering the instantaneous frequencies in more detail, spikes in single unit MSNA appear stochastically, and not in a uniform manner. i.e single unit activity contains doublets or triplets of spikes at much higher instantaneous frequencies than the interval for the subsequent spike. Indeed, it is an advantage of the focal recording technique, that it allows analysis of the instantaneous frequencies of individual neurones to be calculated more easily than conventional techniques. Analysis of ongoing activity in both N and CHU rats revealed that the number of spikes that occurred with very short interspike intervals was low, as previously reported (Hudson *et al.*, 2011). However, the present analyses revealed that there were more medium length interspike intervals, corresponding to frequencies of 1-10Hz, in CHU rats. In fact, the proportion of interspike intervals producing instantaneous firing frequencies of 1-5Hz *and* 5-10Hz were higher in CHU than N (~25% vs ~18% with instantaneous frequencies of 1-5Hz in N and CHU rats respectively, see Figure 5.7). This is of course consistent with the higher ongoing mean firing rate, and helps explain the finding that CHU rats had higher ongoing activity in the sympathetic neurones supplying the spinotrapezius muscle vasculature. It also leads to a reasonable

expectation that the neurotransmitters released by sympathetic nerve varicosities to act on the vascular smooth muscle may be different in N and CHU rats.

Considering the potential consequences of higher instantaneous frequencies in ongoing MSNA, there is evidence that ATP is particularly important in vasoconstriction evoked by couplets of activity (Sneddon & Burnstock, 1984; Sneddon & Burnstock, 1985; Kennedy *et al.*, 1986a), and that noradrenaline becomes more important in vasoconstriction evoked by more sustained sympathetic nerve firing. Johnson et al. (2001) questioned this conclusion in their findings made *in vivo*, showing that ATP and NA were both important in the vasoconstriction evoked in the hindlimb muscle of the rat by stimulation of the sympathetic chain with couplets and trains of pulses. Coney et al., (2007) suggested that there is only a role for NPY in sympathetically evoked vasoconstriction during stimulation at higher frequencies (>20Hz).

Thus, whilst ongoing activity in CHU rats is unlikely to induce release of NPY, it is possible that there may be increased release of both noradrenaline and ATP in CHU rats relative to N rats. Other models of the consequences of hypoxia during pregnancy have found evidence of increased basal levels of catecholamine in the plasma (Gagnon *et al.*, 1994; Simonetta *et al.*, 1997), and thus, it will be important that future work considers the possible effects of increased NA and ATP release and its consequences for *in vivo* vascular regulation of skeletal muscle and other vascular beds.

At this stage, it can be stated that even thought he present study provides evidence of raised MSNA and particular increases in the instantaneous frequencies achieved within this MSNA in CHU rats, the tonic level of FVC was comparable between N and CHU rats (see Chapters 3 & 4). Thiu, it seems that the influence of the raised MSNA may be counterbalanced by greater tonic vasodilator influences in CHU rats, for example the influence of H_2O_2, as discussed in Chapter 3.

5.4.5 Mechanisms underling the increased ongoing firing rate in MSNA of CHU rats

As described in the Methods and Results, average phase histograms of phase-aligned phase histograms, triggered by the ABP and tracheal pressure traces in N and CHU rats, were compared to allow assessment of the extent of modulation of MSNA by the cardiac and respiratory cycle. Evidence in the literature shows that modulation of MSNA by these cycles, particularly the respiratory cycles, is altered in states of disease such as hypertension or congestive heart failure. For example, Goso et al., (2001) found that in patients with congestive heart failure there was a loss of lung inflation mediated reflex inhibition of sympathetic nerve activity, whilst Simms et al., (2009) found that the cyclic increase in lumbar sympathetic nerve activity during the respiratory cycle was enhanced in the spontaneously hypertensive rat relative to its normotensive control. Presenting data in this manner allows the assessment of the degree of neural silence during the expiratory phase of the respiratory cycle, and the 'post-systolic' phase of the cardiac cycle, as well as the periods of augmented MSNA. When such analysis were performed on the present

data there was no apparent difference in the patterning of MSNA relative to the respiratory cycle, or to the cardiac cycle, between N and CHU rats.

It might have been preferable to use power spectral analysis as a further assessment of the degrees of cardiac and respiratory modulation. However, because the recorded periods of baseline activity were relatively short (usually around 6-7 mins) the number of spikes occurring over this time was too low to create a reliable power spectrum. Power spectral analysis of some of the multiunit recordings which contained highest number of units was possible, but there were not sufficient numbers of these to allow for reliable conclusions.

5.4.6 Response to baroreceptor unloading

Bolus infusion of the NO donor SNP was given at a sufficient dose to simulate the fall in ABP induced by graded systemic hypoxia (see below), and the fall in ABP induced in N rats of the present study was comparable to that reported by Hudson et al., (2011). The SNP infusion induced a significant rise in MSNA in N rats, comparable to that reported recently (Hudson *et al.*, 2011). There was also an increase in single unit activity recorded from CHU rats, but this did not achieve statistic significance ($p=0.056$); in 3 rats SNP infusion caused average single unit firing rate to more than double, but in 2 rats, firing rate was only increased by ~50%. By comparison, in N rats, in four of seven successful recordings, firing rate was more than doubled, and in three cases tripled, whilst only one rat showed less than a 50% increase in single unit MSNA. The absolute level of firing frequency attained during SNP infusion was not

statistically different between N and CHU rats (p=0.18) although this is likely due to the small number of recordings achieved.

Thus, whilst it is possible that there is a mild impairment in the reflex response to baroreceptor unloading in CHU rats, it is more likely that the reason the increase in MSNA during SNP infusion did not reach statistical significance was due to the small number of rats studied. Further, as baseline MSNA in CHU rats was higher, MSNA would have had to reach a higher level than in N rats in order to achieve statistical significance. Consistent with these conclusions, it was clear that the HR of the response to infusion of SNP was fully comparable between N and CHU suggesting that the activation of the cardiac sympathetic nerves, and inhibition of the cardiac vagal neurones, by baroreceptor unloading was fully comparable in N and CHU rats.

5.4.7 Response evoked by graded systemic hypoxia

During graded systemic hypoxia, a similar graded augmentation of MSNA was observed in both N and CHU rats, that became statistically significant in both groups when breathing 8% O_2. In the present study, CHU rats showed a smaller fall in ABP, and a more pronounced tachycardia than the N rats, but the data reported in the previous chapters showed that in larger groups of animals, the falls in ABP induced by systemic hypoxia were similar in N and CHU rats. Thus, it is likely that is finding represents the natural variability seen in individual animal experiments with such a small group size.

The fall in ABP induced by systemic hypoxia in this particular group of CHU rats would have been expected to lead to a smaller baroreceptor-mediated increase in MSNA in CHU rats. However, the fact that the increase in R_F induced by hypoxia was greater in this particular group of CHU rats than in the N rats, it would have been expected to lead to a greater respiratory-dependent increase in MSNA in CHU rats, irrespective of any increase in MSNA that might be evoked by peripheral chemostimulation independently of the respiratory-dependent effects (Guyenet, 2000). Thus, it is difficult to deduce from the present findings whether systemic hypoxia causes greater or smaller reflex increases in MSNA in CHU rats than in N rats. All that can be stated is that under the conditions of the experiments of the present chapter, the level of MSNA achieved in N and CHU rats whilst breathing 8%O_2 was very similar.

5.4.8 Sympathetic innervation density

There are several limitations of the glyoxylic acid staining technique which must be considered before interpreting the results obtained with the technique. Firstly, shrinking of the artery occurs when drying the artery onto the glass slide. The tibial artery is a relatively small artery, and as such has less smooth muscle and elastic tissue, and is less prone to shrinking than some of the larger caliber arteries used in previous studies (Furness & Costa, 1975; Omar & Marshall, 2010). Further, all arteries were treated equally, and so whilst the innervation density observed may not represent the absolute density *in vivo*, the data does allow comparison of the relative density of innervation the N and CHU rat, unless there is a subtle difference in the

extent of shrinkage in small arteries of N and CHU rats that is not apparent from gross observation of size and shape.

The use of a confocal microscope to image the whole vessel preparations represents an improvement on use of conventional light microscopes used in previous studies (Ruijtenbeek *et al.*, 2000; Omar & Marshall, 2010), for confocal microscopy allows for much improved focus on the three dimensional structure of the whole artery. The ability to z-stack images based on the focal plane improves the accuracy of the fluorescent intensity measurement, because blurring that occurs when viewing with conventional microscopy on a vessel with significant thickness in the Z plane markedly increases the perceived intensity.

A limitation of the method generally used for analysis of innervation density, the grid intersect method, is that when two fibers run very close to each other in a bundle, it can be difficult to differentiate them from a single larger fiber. Because the use of confocal microscopy improved resolution of individual fibers, this less of a problem. Nevertheless, in order to minimize the errors that might be introduced, all counts were made three times on separate occasions, and the mean result was used. The results obtained were very consistent between counts. If significant error was introduced by mistaking two closely apposed fibres for a single fibre, it would have been likely affect the results recorded in CHU more than N rats, simply because there were more fibres present on the surface of the CHU arteries. Thus, it is unlikely that this limitation represents a large source of error, and any error was likely to have resulted in underestimation of the difference between N and CHU.

This study marks the first time that the sympathetic innervation of arterial vessels has been investigated in adult mammals following hypoxia *in utero*. The results clearly show, by two separate methods of analysis, that there is a substantially greater sympathetic innervation density on the surface of the tibial artery, which supplies hind limb skeletal muscle, in CHU rats than N rats. Previous studies have provided evidence for increased innervation density in the femoral artery of the hypoxic chick embryo at hatching (Ruijtenbeek *et al.*, 2000), but now it is clear that whatever hyperinnervation may be present at birth in CHU rats persists into adulthood in mammals. The only other study that can be compared to the present on is a study of the postnatal effect of reduced nutrient delivery on sympathetic nerve density by Sanders et al., (2004). They found that femoral, saphenous and mesenteric arteries from young rat offspring (at 21 days old) from mothers subjected to uterine artery ligation showed no difference in sympathetic innervation density. However, little detail on their method of analysis is provided, nor are there any sample images. Thus, it is very difficult to make comparisons between the present data and the data presented in their study.

In light of the fact that the ongoing firing rate in the individual sympathetic neurone supplying skeletal muscle was enhanced in CHU rats, it seems likely that the vascular smooth muscle of skeletal muscle arteries from CHU rats is exposed to chronically higher levels of sympathetic neurotransmitter. Further, it is reasonable to propose that when MSNA is increased by reflex stimulation, this would result in increased release of sympathetic cotransmitters onto the vascular smooth muscle of

CHU rats. Thus, studies of vascular sensitivity to sympathetic nerve activity in skeletal muscle vascular beds are required to ascertain the exact consequences of this for basal vascular tone. At this point, it is important to note that at the age studied, the CHU rats were not hypertensive relative to N rats, and baseline FVC was similar. This, it would appear that compensatory mechanisms may be present in CHU rats. Thus, vascular responses measured in the femoral artery to stimulation of the lumbar sympathetic chain are investigated in N and CHU rats in chapter 6.

Chapter 6 – Responses evoked by sympathetic nerve stimulation following chronic hypoxia *in utero*

6.1 Introduction

In Chapter 5, evidence was presented that levels of ongoing activity in the sympathetic nerves innervating skeletal muscle vasculature are higher in young adult CHU rats than in N rats, but this does not lead to hypertension at this age. There has been little attempt to examine the manner in which the vascular response to sympathetic nerve activity may be affected by hypoxic insult during fetal life.

In a study comparing newborn lambs born of high altitude sheep who underwent gestation at high altitude (3600m) with those born of normal sheep at sea level, Herrera et al., (2007) found that isolated small femoral arteries of the high-altitude lambs showed augmented vascular reactivity to noradrenaline and phenylephrine, relative to sea level lambs. Further, during systemic hypoxaemia (10% F_iO_2, 60 mins), there was an augmented increase in femoral vascular resistance in the high altitude lambs relative to the sea level lambs, suggesting that the increase in vasoconstrictor tone during systemic hypoxia is higher in the high altitude newborns than in sea level newborns. What is not known is whether these indices of increased vasoconstrictor responsiveness persist into adult life, and hence have long term consequences. Further, it is not clear whether the differences seen were the result of the 50+ generations the high altitude sheep have spent at high altitude, or of the particular conditions the lambs experienced during pregnancy.

Further, in a study of juvenile and adult rats that had been subjected to reduced uterine perfusion for the latter stage of pregnancy, Anderson et al., (2006) found that responses in isolated mesenteric arteries to the α-adrenoreceptor agonist were

augmented in the direct male and female offspring, and the next generation of offspring relative to responses in arteries from control rats. Thus, this study also raises the possibility that low O_2 levels *in utero* may increase arterial responsiveness to adrenoreceptor stimulation.

It is known that in control rats, stimulation of the lumbar sympathetic chain with doublets at 20Hz or with a train of impulses at 20Hz results in vasoconstriction in the hindlimb, in vivo (Johnson *et al.*, 2001). They found that noradrenaline was the major neurotransmitter mediating this vasoconstriction, as the α-adrenoreceptor antagonist phentolamine markedly reduced the magnitude of vasoconstriction evoked by each type of stimulation by ~80%. Suramin, the purinergic P_2 receptor antagonist had a smaller effect in reducing responses by ~40%. Thus, the authors concluded that it is likely that ATP plays a facilitatory role, rather than being the main neurotransmitter as has been suggested from *in vitro* studies of isolated vessels (Kennedy *et al.*, 1986a; Sjoiblom-Widfeldt *et al.*, 1990). In a later study performed on rats, Coney et al., (2007) tested hindlimb vasoconstrictor responses to stimulation of the lumbar sympathetic chain with 120 pulses in three different patterns; a constant train of pulses at 2Hz, 6 trains of 20 pulses at 20Hz, and 6 trains of 20 pulses at 40Hz, each given over 60 seconds. They found that the neuropeptide Y (NPY) Y_1 receptor antagonist BIBP-3226 did not affect the vasoconstriction to constant stimulation at 2Hz or burst stimulation at 20Hz, but significantly reduced the response to stimulation at 40Hz,indicating that in the hind limb of the control (N) rat, the sympathetic cotransmitter NPY only becomes important during high frequency nerve activity, as was previously suggested by Pernow et al., (1989).

The studies of Chapter 5 have already described how there are more short interspike intervals in the MSNA recorded from CHU than N rats under baseline conditions, representing firing frequencies of 1-10Hz, and that MSNA was increased in both N and CHU rats by baroreceptor unloading and by graded systemic hypoxia. Thus, in light of the fact that baseline FVC recorded in anaesthetised CHU rats was similar to that recorded in N rats in the experiments of Chapters 3 and 4, but ongoing MSNA, and the sympathetic innervation density on the surface of an artery supplying skeletal muscle is higher in CHU rats, the present study sought to examine whether there are functional alterations in the response evoked by sympathetic nerve activation in CHU rats.

Hypotheses

1. Stimulation of the lumbar sympathetic chain causes larger hindlimb vasoconstrictor responses in CHU rats relative to N.
2. As there are higher levels of high frequency doublets in the MSNA in CHU rats even under baseline conditions, the NPY mediated component of sympathetically mediated vasoconstriction in the hind limb is greater in CHU rats than N rats.

6.2 Methods

Experiments were performed on 12 N rats (343±9g, 71±2 days old) and 11 CHU rats (351±10g, 4 litters, 70±3 days). The anaesthetic regimen, and the basic surgical preparation used in the present study is that described in Chapter 2. Thus, cannulation of the left brachial artery was carried out for recording ABP, and the caudal ventral tail artery was cannulated for infusion of the NPY Y_1 receptor subtype specific antagonist BIBP-3226. Femoral blood flow (FBF) was recorded from the right femoral artery in the manner described in Chapter 2.

6.2.1 Lumbar sympathetic chain stimulation

The surgical preparation used in the present study has been described previously (Johnson *et al.*, 2001; Coney & Marshall, 2003). With the rat lying supine, a midline incision was made through the skin and abdominal muscle, for approximately two thirds of the length of the abdomen, beginning immediately superior to the penis. The incision was parted using metal retractors, and the majority of the small and large intestine was exteriorised and wrapped in gauze that was soaked in warm physiological saline to prevent drying. Using blunt ended, fine glass rods, the right sympathetic chain, running parallel to the abdominal portion of the vena cava at the level of the right renal vein, was isolated by very gentle blunt dissection. When a 2-3mm portion was freed from connective tissue, two stimulating electrodes, constructed from 0.125mm fine sliver wire (Advent Research Metals, Oxford, UK) passed through PP10 polythene tubing (Scientific Laboratory Supplies, Wilford, Nottingham, UK) were looped under the sympathetic chain. Once passed around the sympathetic chain, the electrodes were carefully looped back, to encircle the

sympathetic chain, and then secured in position using Kwic-Sil silicone elastomer compound (World Precision Instruments, Hitchin, Hertfordshire, UK). Electrodes were connected to a constant current stimulating unit (DS2A, Digitimer, Hertfordshire, UK). That the sympathetic chain could be successfully stimulated in this way was initially confirmed by the presence of testicular retraction upon stimulation with a single electrical pulse (1ms, 1mA). When this had been confirmed, the intestines were carefully placed back within the abdominal cavity, and the incision covered in saran wrap to ensure the area remained moist, but was not closed.

6.2.2 Protocol

The stimulation parameters used in the present study to stimulate the sympathetic chain have previously been published (Coney & Marshall, 2003). Thus, 3 different protocols of stimulation were used; a 60 second constant train of 120 pulses at 2Hz, 6 bursts of 20 pulses at 20Hz at 10 second intervals, and 6 bursts of 20 pulses at 40Hz, at 10 second intervals. Thus, each 60 second period of stimulation contained 120 pulses. All pulses were 1ms in duration and given at 1mA, and were controlled using the 'stimulator' function in LabChart (ADInstruments, Oxford, UK) using the stimulator output on the PowerLab 4/20 (ADInstruments, Oxford, UK) that was also used for recording of cardiovascular variables. Each stimulation protocol was carried out twice, giving 6 stimulations in total, in a randomised order. At least 5 minutes of stable cardiovascular variables were recorded prior to each period of stimulation. Following control stimulations, infusion of the NPY Y_1 subtype specific neuropeptide Y receptor antagonist BIBP-3226 (Tocris Biosciences, Bristol, UK) was commenced, at a dose of 10mg.kg^{-1}.min^{-1} (Bischoff *et al.*, 1997; Malmström *et al.*, 1997). After 30

minutes of infusion, the same three stimulation protocols were repeated twice each, again in a randomised order, during continued infusion of BIBP-3226.

6.2.3 Data analysis and statistics

All data is presented as mean±SEM. HR was computed from ABP as described in Chapter 2, and femoral vascular resistance (FVR) was calculated by dividing MABP by MFBF. FVC was also calculated as described in Chapter 3, but was not used in the quantative analysis. Data was extracted from raw recordings using the Data Pad function of the LabChart software (ADInstruments, Oxford, UK). The femoral vascular response to lumbar sympathetic chain stimulation are presented in two ways; first the change in the integral of FVR during the 60 second stimulation, relative to the 60 seconds prior to stimulation (∆intFVR). Second, as the max∆FVC; For trains of stimulation at 2Hz, max∆FVR indicates the maximum change in FVR achieved during the 60 seconds of constant stimulation, relative to the mean FVR of the 60 seconds immediately preceding stimulation. Often, responses to constant stimulation at 2Hz were biphasic in nature, with an initial increase in FVR, which tended back towards baseline values towards the end of the period of stimulation. For bursts of stimulation at 20Hz and 40Hz, max∆FVR indicates the mean of the peaks in FVR achieved by each burst of pulses, relative to the mean FVR of the 60 seconds immediately preceding the first burst of pulses (see Figures 6.2 & 6.3 for example of these peaks). The maximum fall in mean FBF (MFBF) is calculated and presented in the same manner. The mean maximum increase in MFBF above baseline between bursts of stimulations at 20 or 40Hz is also calculated in a similar fashion, and termed ‘max hyperaemia’. The maximum increase in MFBF relative to baseline during the 60s

period of stimulation at 2Hz is also calculated, and often indicated the biphasic response observed in many responses to stimulation with a constant train of pulses at 2Hz.

Statistical analyses were carried out using Aable 20/20 Data Vision v3.0.5 software (Gigawiz, Tulka, OK, USA). Comparison of mean individual baseline variables was made by using the Students unpaired t-test. Comparison of responses between groups, and before and during administration of BIBP-3226 was made by using a mixed model ANOVA with Scheffés *post hoc* analysis. $P<0.05$ was considered statistically significant. Comparisons of baseline cardiovascular variables recorded in the present experiments with those recorded in the other groups of animals described in this thesis were made using a factorial ANOVA with Sheffés *post hoc* analysis.

6.3 Results

6.3.1 Comparison of cardiovascular baselines in N and CHU rats

Baseline ABP, HR, FBF and FVR were not significantly different between N and CHU rats (Table 6.1). When baseline ABP was compared to the baseline ABP recorded in the groups of rats reported in Chapters 3 and 4, there were no significant differences between any of the groups of N rats used although MABP tended to be lower in the present study than in the N rats reported in Chapters 3 and 4. When making the same comparisons in CHU rats, baseline ABP was found to be significantly lower the rats of the present experiment than in the CHU rats of Chapter 3 ($p<0.01$), but not significantly different from the baseline ABP reported in the CHU rats of Chapter 4.

6.3.2 Comparison of vasoconstrictor responses to lumbar sympathetic chain stimulation in N and CHU rats

In N rats, continuous stimulation at 2Hz tended to cause an increase in intFVR ($p=0.065$, see Figures 6.1 and 6.4A), which caused a significant reduction in MFBF ($p<0.01$). Bursts of pulses at 20Hz and 40Hz caused significant increases in IntFVR ($p<0.001$, $P<0.001$, see Figures 6.2, 6.3 and 6.4A), which caused significant decreases in MFBF ($p<0.001$, $p<0.001$, Figure 6.4D).

The responses evoked by sympathetic chain stimulation in CHU rats were qualitatively similar to those recorded in N rats. Continuous stimulation at 2Hz caused no significant change in IntFVR or MFBF, but pulses at 20Hz and 40Hz caused significant increases in IntFVR ($p<0.001$, $p=0.003$ respectively, see Figure

6.4A), which caused significant reductions in MFBF ($p<0.001$, $p<0.001$, see Figure 6.4D).

Considering the magnitude of the responses evoked by continuous stimulation at 2Hz, or burst stimulation at 20Hz and 40Hz, the maximum rise in FVR from baseline values during stimulation was significantly blunted in CHU rats during stimulation using 2Hz and 20Hz trains of pulses), and tended to be reduced when using 40Hz trains (see Figure 6.4B). There were no significant differences in the falls in MFBF evoked by sympathetic chain stimulation in N or CHU rats (Figure 6.4D).

6.3.3 The effect of BIBP-3226 on vasoconstrictor responses to lumbar sympathetic chain stimulation.

In one N rat win which a test was made, the hypertensive response evoked by the NPY receptor agonist leu-pro-NPY (128μg.kg^{-1} bolus i.a.) was markedly reduced by BIBP-3226 (Pre-BIBP:+28mmHg, during BIBP-3226: 15mmHg). It is therefore reasonable to assume that the NPY Y_1 receptors were effectively antagonized, by ~ 50%, given that the dose of NPY raises plasma concentrations well above those previously recorded in human plasma (Pernow *et al.*, 1987). Further, in a previous study, the regimen used for the dose of BIBP-3226 in the present study was shown to be an effective in inhibiting the NPY Y_1 receptor (Coney & Marshall, 2007).

In N rats, BIBP-3226 significantly blunted the increase in IntFVR to 2Hz and 20Hz trains of stimulation, and tended to do so when using 40Hz trains of stimulation ($p=0.14$, see Figure 6.5). However, maximum increases in FVR were not reduced by

BIBP-3226 during any stimulation protocol. Further, the fall in MFBF was not significantly altered by BIBP-3226 (see Figure 6.5B-D).

By contrast, in CHU rats, there was no blunting effect of BIBP-3226 on the increase in IntFVR by any pattern of stimulation, whichever index is used to describe the response (Figure 6.5 A&B). Further there was also no reduction in the maximum fall in MFBF (Figure 6.5D).

Figure 6.1 – Original recording of cardiovascular variables during sympathetic chain stimulation with constant pulses at 2Hz.

Original recording made in and N rat during stimulation of the sympathetic chain with a constant train of 120 pulses at 2Hz. Arterial blood pressure (ABP), femoral blood flow (FBF), electrical stimulus, mean femoral vascular conductance (FVC), mean femoral vascular resistance (FVR), mean arterial blood pressure (MABP), mean femoral blood flow (MFBF) and heart rate (HR) are shown.

Figure 6.1

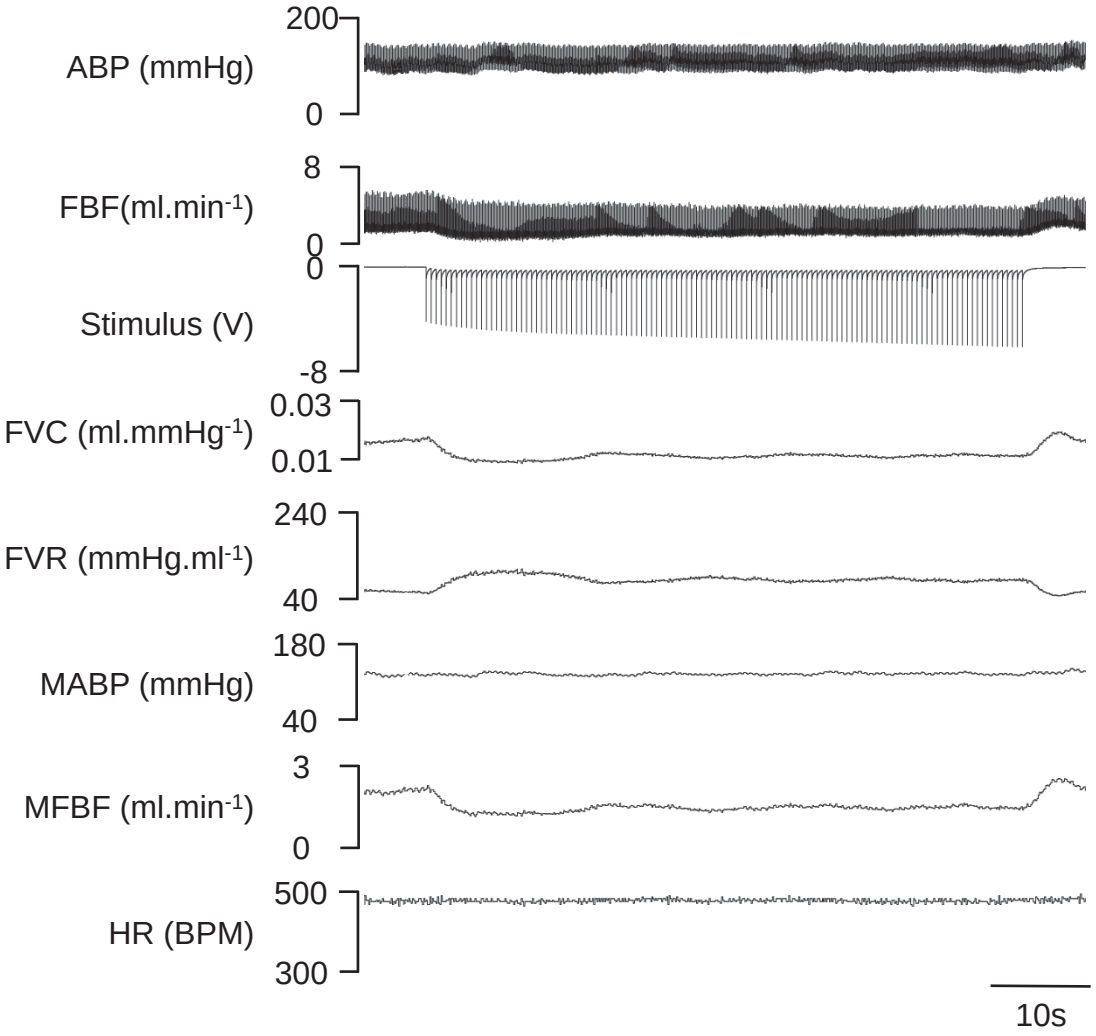
ABP (mmHg)
200
0
FBF(ml.min-1)
8
0
Stimulus (V)
0
-8
FVC (ml.mmHg-1)
0.03
0.01
FVR (mmHg.ml-1)
240
40
MABP (mmHg)
180
40
MFBF (ml.min-1)
3
0
HR (BPM)
500
300
10s

Figure 6.2 - Original recording of cardiovascular variables during sympathetic chain stimulation with bursts of pulses at 20Hz

Original recording made in and N rat during stimulation with bursts of 20 pulses at 20Hz. Abbreviations as per Figure 6.1.

Figure 6.2

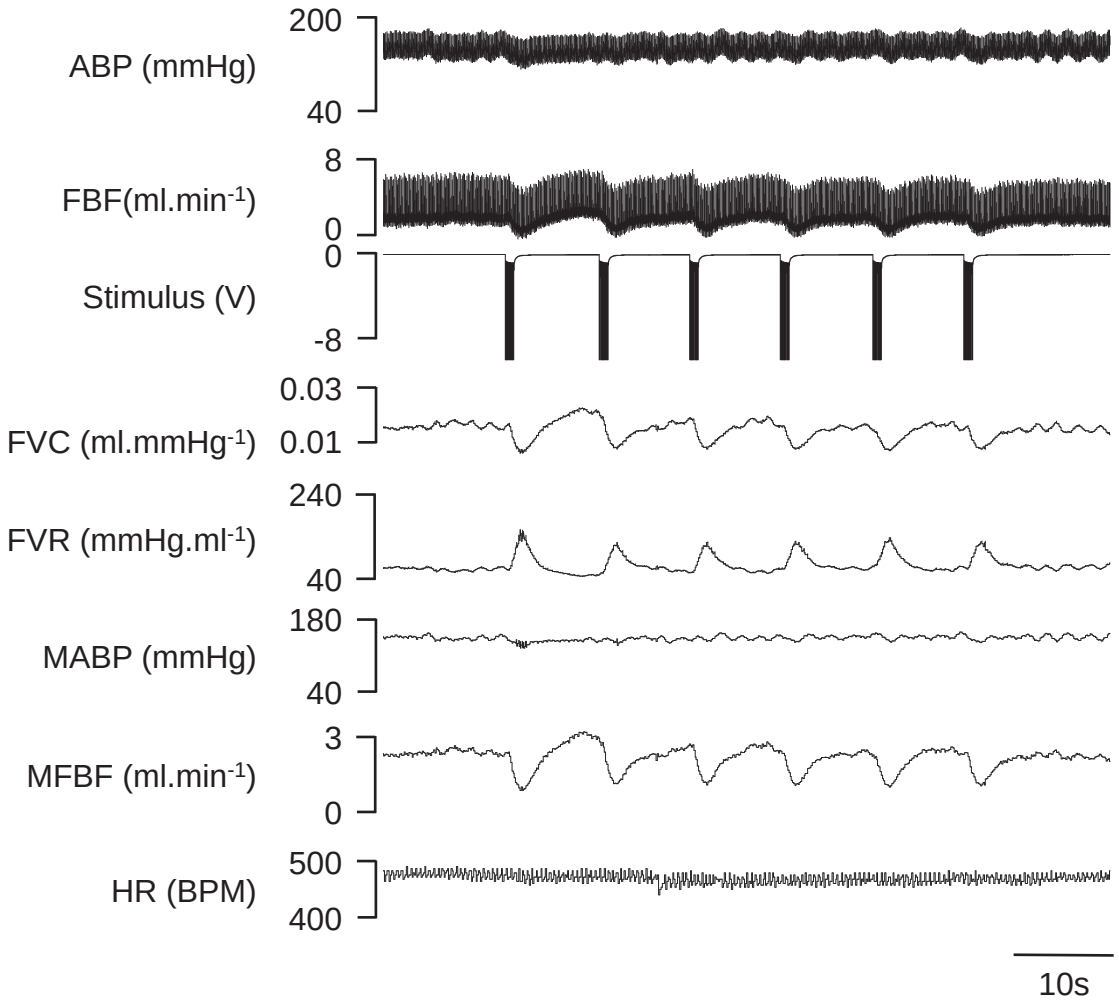
ABP (mmHg)
200
40
FBF(ml.min-1)
8
0
Stimulus (V)
0
-8
FVC (ml.mmHg-1)
0.03
0.01
FVR (mmHg.ml-1)
240
40
MABP (mmHg)
180
40
MFBF (ml.min-1)
3
0
HR (BPM)
500
400
10s

Figure 6.3 - Original recording of cardiovascular variables during sympathetic chain stimulation with bursts of pulses at 40Hz

Original recording made in and N rat during stimulation with bursts of 20 pulses at 40Hz. Abbreviations as per Figure 6.1.

Figure 6.3

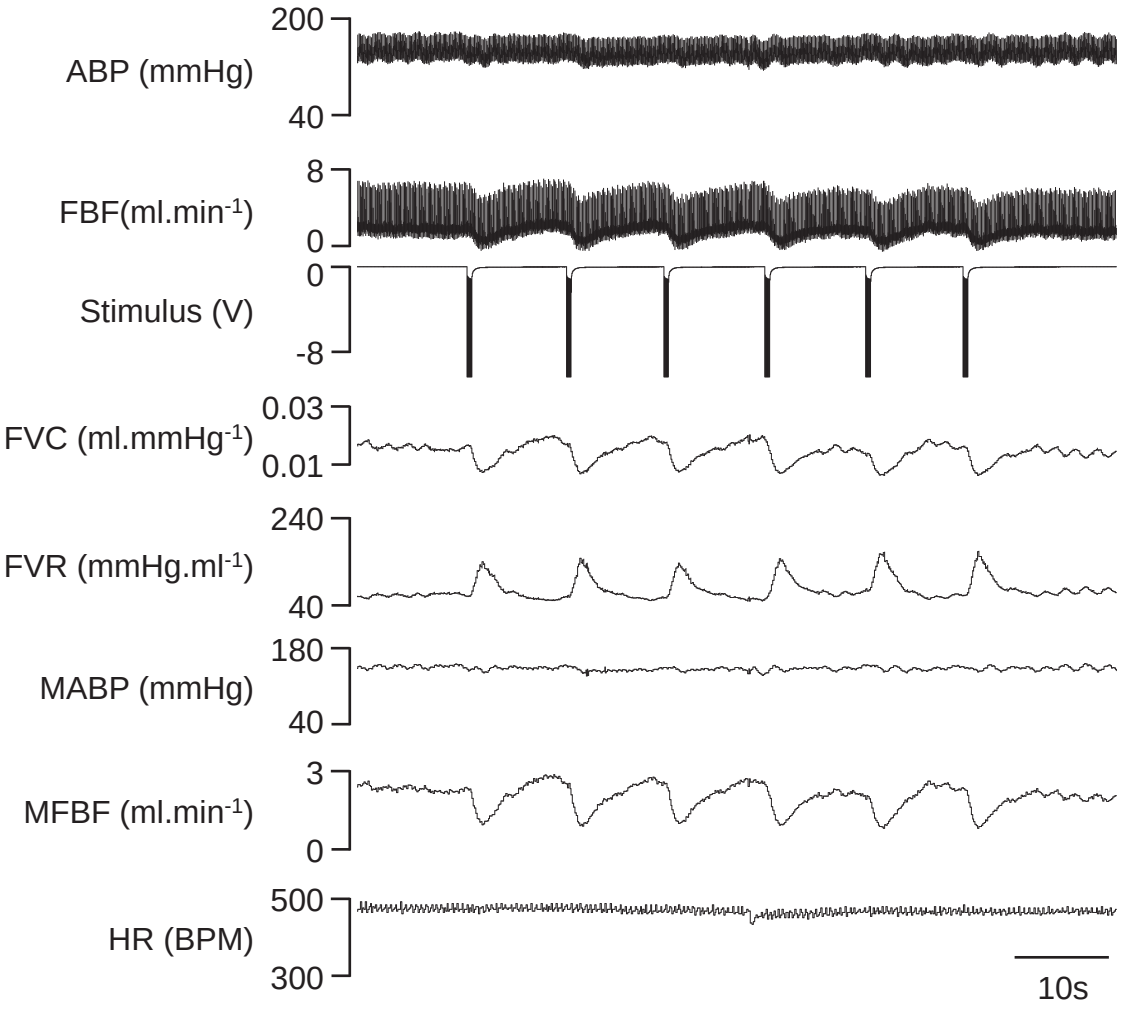
200
ABP (mmHg)
40
8
FBF(ml.min-1)
0
0
Stimulus (V)
-8
0.03
FVC (ml.mmHg-1)
0.01
240
FVR (mmHg.ml-1)
40
180
MABP (mmHg)
40
3
MFBF (ml.min-1)
0
500
HR (BPM)
300
10s

Table 6.1 – Cardiovascular baselines in N and CHU rats used in experiments presented in the present study

Group	MABP (mmHg)	HR (BPM)	MFBF ($ml.min^{-1}$)	FVR ($mmHg.ml^{-1}.min^{-1}$)
N (n=12)	127±3	452±16	2.28±0.13	58±4
CHU (N=4, n=11)	122±3	441±11	2.57±0.18	51±4
N+BIBP	131±3	461±15	2.28±0.13	58±3
CHU+BIBP	127±4	448±10	2.57±0.18	54±5

Mean baseline cardiovascular variables recorded in N and CHU rats under control conditions, and during infusion of BIBP-3226 (+BIBP). MABP; mean arterial blood pressure, HR; heart rat, MFBF; mean femoral blood flow, FVC; femoral vascular resistance

Figure 6.4 – Mean changes in cardiovascular variables evoked by stimulation of the sympathetic chain in N and CHU rats.

All data is presented as mean±SEM. * - P<0.05 vs N, p=0.09 – CHU vs N

A: Change from baseline in integrated femoral vascular resistance (∆intFVR) during the stimulation of the lumbar sympathetic chain with trains of pulses at 2, 20 and 40Hz in N (filled columns) and CHU (open columns) rats.

B: Maximum change from baseline in femoral vascular resistance (∆FVR) during the stimulation of the lumbar sympathetic chain with trains of pulses at 2, 20 and 40Hz in N (filled columns) and CHU (open columns) rats.

C: Maximum rise in MFBF between trains of stimulation of the lumbar sympathetic chain with trains of pulses at 2, 20 and 40Hz in N (filled columns) and CHU (open columns) rats.

D: Maximum fall from baseline in MFBF during stimulation of the lumbar sympathetic chain with trains of pulses at 2, 20 and 40Hz in N (filled columns) and CHU (open columns) rats.

Figure 6.4

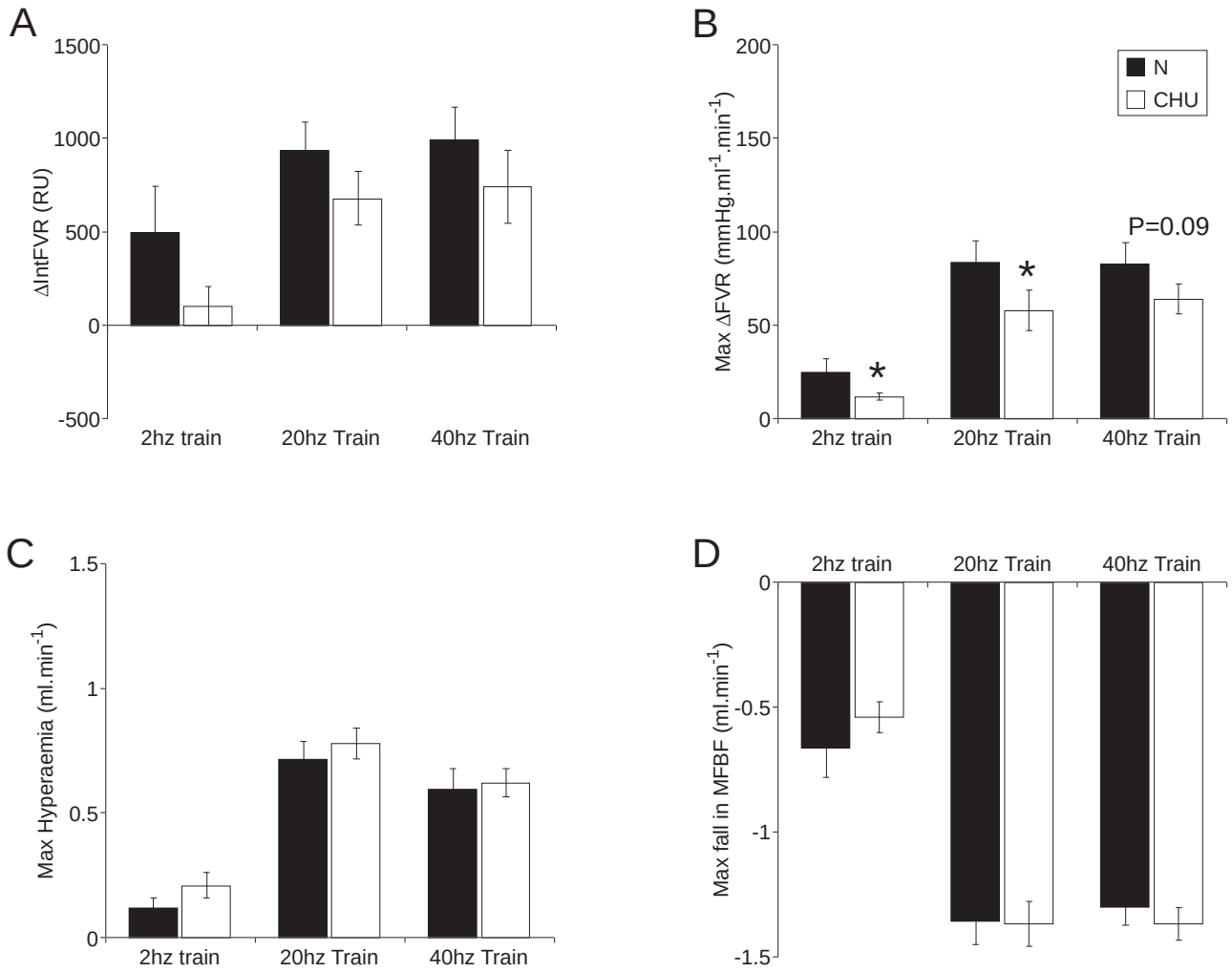
A
1500
1000
500
0
-500
ΔIntFVR (RU)
2hz train
20hz Train
40hz Train
B
200
150
100
50
0
Max ΔFVR (mmHg.ml-1.min-1)
N
CHU
P=0.09
*
*
2hz train
20hz Train
40hz Train
C
1.5
1
0.5
0
Max Hyperaemia (ml.min-1)
2hz train
20hz Train
40hz Train
D
2hz train
20hz Train
40hz Train
0
-0.5
-1
-1.5
Max fall in MFBF (ml.min-1)

Figure 6.5 – effect of an NPY Y_1 receptor antagonist on mean changes in cardiovascular variables evoked by stimulation of the sympathetic chain in N and CHU rats.

All data is presented as mean±SEM. * - P<0.05 vs control conditions, p=0.14 N vs N+BIBP-3226

A: Change from baseline in integrated femoral vascular resistance (∆intFVR) during the stimulation of the lumbar sympathetic chain with trains of pulses at 2, 20 and 40Hz in N (filled columns) and CHU (open columns) rats before (solid) and during (patterned) BIBP-3226 infusion.

B: Maximum change from baseline in femoral vascular resistance (∆FVR) during the stimulation of the lumbar sympathetic chain with trains of pulses at 2, 20 and 40Hz in N (filled columns) and CHU (open columns) rats before (solid) and during (patterned) BIBP-3226 infusion.

C: Maximum rise in MFBF between trains of stimulation of the lumbar sympathetic chain with trains of pulses at 2, 20 and 40Hz in N (filled columns) and CHU (open columns) rats before (solid) and during (patterned) BIBP-3226 infusion.

D: Maximum fall from baseline in MFBF during stimulation of the lumbar sympathetic chain with trains of pulses at 2, 20 and 40Hz in N (filled columns) and CHU (open columns) rats before (solid) and during (patterned) BIBP-3226 infusion.

Figure 6.5

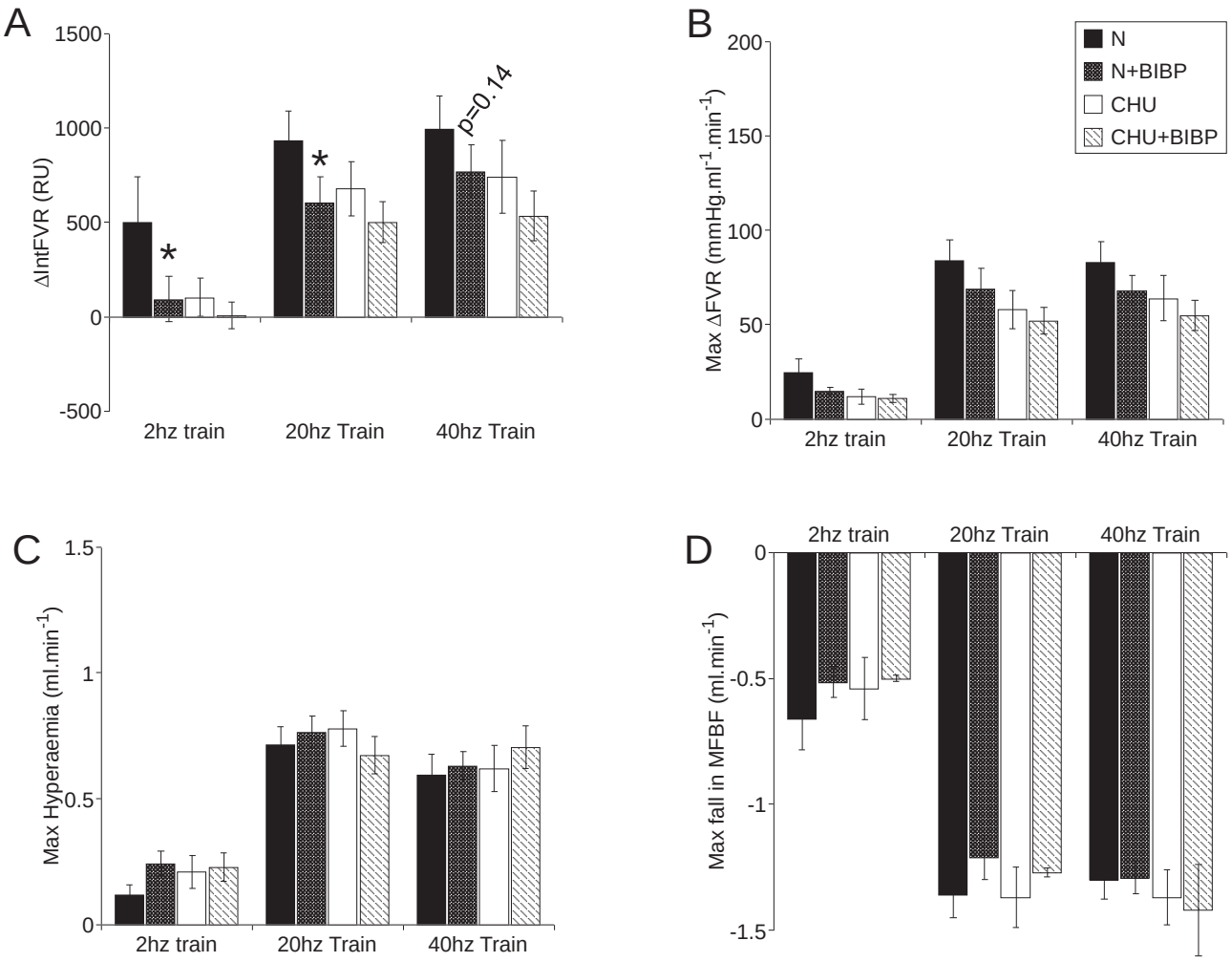
A
1500
1000
500
0
-500
ΔIntFVR (RU)
*
*
p=0.14
2hz train
20hz Train
40hz Train
B
200
150
100
50
0
Max ΔFVR (mmHg.ml-1.min-1)
N
N+BIBP
CHU
CHU+BIBP
2hz train
20hz Train
40hz Train
C
1.5
1
0.5
0
Max Hyperaemia (ml.min-1)
2hz train
20hz Train
40hz Train
D
2hz train
20hz Train
40hz Train
0
-0.5
-1
-1.5
Max fall in MFBF (ml.min-1)

6.4 Discussion

6.4.1 Main Findings

This is the first study to examine the relationship between chronic hypoxia *in utero* and the coupling of sympathetic nerve activity to the vascular smooth muscle of blood vessels supplying the hindlimb vasculature. The results indicated maximum vasoconstriction during stimulation of the lumbar sympathetic chain was reduced in CHU rats relative to N rats during constant stimulation at 2Hz, or burst stimulation at 20Hz, and tended to be reduced during burst stimulation at 40Hz. Further, the NPY Y_1 antagonist BIBP-3226 reduced the increase in intFVR during stimulation with constant stimulation at 2Hz and burst stimulation at 20Hz trains in N rats, and tended to reduce the increase in intFVC during burst stimulation at 40Hz. However, the responses evoked by these patterns of stimulation in CHU rats were not altered by BIBP-3226.

6.4.2 Comparison of the present N rats with those of previous studies

The protocol used in the present study was based on that used by Coney & Marshall (2007) on N rats, thus it is important to compare the baselines in the two studies. Two groups of N rats were used by Coney & Marshall, one for testing the effects of inhibition of α_2-adrenoreceptors, and the second for testing the effects of NPY Y_1 receptor inhibition. In the first group, MABP was markedly lower than that of the present study (106±5 vs 127±3mmHg), whilst FBF and HR was lower (1.26±0.08 vs 2.28±0.13ml.min^{-1} and 419±19 vs 452±16bpm) and FVR was higher (86±6 vs 58±4 mmHg.ml^{-1}.min^{-1}). However, in the second group, MABP was similar to that of the

present study, as was FBF and HR, although FVR was slightly higher (69±10 vs 58±4). Although arterial blood gasses were not recorded in the present study, the blood gasses reported by Coney & Marshall were similar to those reported in other Chapters of this thesis.

It is difficult to make direct comparisons between the control responses to sympathetic chain stimulation presented by Coney & Marshall (2007) and those reported in the present study, as the units used to present intFVR are different. However, consistent with Coney and Marshall (2007), the present study showed that the largest increase in intFVR was obtained during stimulation with bursts of 40Hz, and the smallest increase with constant stimulation at 2Hz. In other words, as described previously (Coney & Marshall, 2003), the same number of pulses delivered in bursts was more effective in producing vasoconstriction that stimulation at constant frequency.

In the study of Coney & Marshall (2007), there was no effect of BIBP-3226 on the baselines of the cardiovascular variables measured, and the same finding was made in the present study. In particular, there was no effect of BIBP-3226 on baseline FVR in either study. Thus there is no reason to suppose that NPY acting on Y1 receptors contributes to basal vascular tone in rats (for further discussion see below). However, while Coney & Marshall (2007) found that BIBP-3226 had no significant effect on the increase in intFVR evoked by constant stimulation at 2Hz or burst stimulation at 20Hz (although there was a tendency for it to be reduced), it was found to significantly reduce the increase in intFVR during burst stimulation at 40Hz. Thus, they concluded

that the cotransmitter NPY becomes important particularly during high frequency bursts of sympathetic nerve activity. In contrast, the present study found that BIBP-3226 significantly reduced the increase in intFVR evoked by constant stimulation at 2Hz and burst stimulation at 20Hz, and tended to reduce it during bursts of stimulation at 40Hz ($p=0.14$). Consistent with this, the study of Pernow et al., (1989) found that NPY was released continuous stimulation at 2Hz, and burst stimulation at 2 and 6.9Hz, into the venous efflux of the dog gracillis muscle. It is not clear why the results of the present study differ from those of Coney & Marshall (2007) but the results of the present study appear to indicate that stimulation with constant low frequencies, as well as with bursts at high frequencies lead to significant release and vasoconstrictor activity of NPY in skeletal muscle vasculature of N rats.

6.4.3 NPY in basal vascular tone

Some degree of controversy exists over the role of NPY in control of basal vascular tone. Studies from the Shoemaker laboratory showed that in pentobarbital anaesthetised Sprague Dawley rats, a bolus of 100μg.kg^{-1} BIBP-3226 caused a significant rise in femoral vascular conductance, indicating a tonic vasoconstrictor influence of NPY Y_1 receptors (Jackson *et al.*, 2004). It is important to note however, that in that study, blood flow is very low compared with studies performed in this laboratory (Coney & Marshall, 2007), and much lower than studies of hindlimb blood flow in conscious animals (Amaral *et al.*, 2000). Hodges et al., (2009) in a later study from the same laboratory put this disparity down to the sympathoactivation associated with pentobarbital anaesthetic (Hodges *et al.*, 2009). Both the present study study, and previous studies (Pernow *et al.*, 1987; Pernow *et al.*, 1989; Coney &

Marshall, 2007) have found that there is no role for NPY in basal vascular tone in rats. However, the results of Jackson et al., (2004), when taken with the assumption that the rats were in a state of sympathetic activation, provide further evidence that in conditions of sympathetic hyperactivity, NPY may become important in the setting of high vascular tone.

6.4.4 Responses evoked by sympathetic chain stimulation in CHU rats

The CHU rats, like the N rats, showed much larger vasoconstrictor responses to simulation of the sympathetic chain with bursts of pulses at 20Hz and 40Hz than with the same number of pulses delivered at a constant frequency of 2Hz. Thus, the muscle vasculature of CHU rats is similarly more sensitive to bursts of sympathetic stimulation. However, the CHU rats showed significantly smaller maximum vasoconstrictor responses to stimulation of the lumbar sympathetic chain with continuous pulses at 2Hz and bursts of pulses at 20Hz, and tended to show reduced maximal responses to burst stimulation at 40Hz. This is particularly interesting, given the data presented in Chapter 5 which shows that there is a higher density of sympathetic noradrenergic nerves and therefore more catecholamine on the surface of arteries supplying skeletal muscle in CHU rats. Given that the increases in MSNA evoked by baroreceptor unloading were as large in CHU rats as in N rats, it seems that these changes may be accompanied by a compensatory reduction in the sensitivity of the skeletal muscle vasculature to sympathetic activity at rest and during activation. This allows for baseline vascular tone in skeletal muscle to remain normal.

This finding is also consistent with the fact that at 10-12 weeks of age, CHU rats have similar blood pressure to N rats.

Considering previous studies, the late-stage hypoxic chick embryo, it was found that there was sympathetic hyperinnervation of the femoral artery, as the present study showed in 10 week old CHU rats (Chapter 5) but there was no alteration in the sensitivity to exogenously applied sympathetic agonists in isolated mesenteric arteries from the hypoxic chick embryo (Ruijtenbeek *et al.*, 2000; Rouwet *et al.*, 2002). Published studies on mammals have not examined sympathetic innervation density in any model of insult during pregnancy but the responsiveness to sympathomimetic agonists was tested in isolated resistance arteries of adult rats subjected to placental insufficiency *in utero* and in lambs of high-altitude ewes. They both found that sensitivity to such sympathetic agonists was augmented (Anderson *et al.*, 2006; Herrera *et al.*, 2007). All of these studies failed to address the physiological role of sympathetic vasoconstriction, as they were carried out on large caliber arteries which are not necessarily representative of the whole vascular bed they supply. Further, they only examined the effects of catecholaminergic agonists, even though it is well known that sympathetic control of the vasculature involves complex interactions and feedback between a compliment of at least 3 neurotransmitters; noradrenaline, ATP and neuropeptide Y (see General Introduction). Further, these *in vitro* experiments were done in the absence of any ongoing vasodilator tone produced by NO generated by shear stress (see General Introduction), and they were performed in conditions relatively hyperoxic compared to the *in vivo* situation. This is important because local oxygen tension is known to be an important

modulator of the actions of sympathetic neurotransmitters (Heistad & Wheeler, 1970; Coney & Marshall, 2007). This is an advance on these studies in being the first examination of the impact of chronic hypoxia *in utero* on responses evoked by sympathetic chain stimulation in skeletal muscle vasculature in offspring *in vivo*.

Turning to effect of the NPY Y_1 receptors antagonist BIBP-3226, in contrast to the effects seen in N rats, this antagonist had no effect on responses evoked by any pattern of sympathetic stimulation in CHU rats. Thus, not only are the vasoconstrictor responses to sympathetic stimulation blunted in CHU rats, but the role of the potent vasoconstrictor NPY is also impaired. This is a novel finding. Clearly, it would be interesting in future studies to test whether NPY is present in sympathetic nerve fibres of CHU rats, and whether it can be released by any mode of sympathetic stimulation, and to test whether the vascular smooth muscle of CHU rats is sensitive to NPY.

6.4.5 The use of lumbar sympathetic chain

Obviously, stimulation of the lumbar sympathetic chain activates sympathetic nerves innervating the tail, sacral regions as well as the hind limbs. Thus, it activates all, or at least a large proportion of the fibres contained in the sympathetic chain in an *en masse* fashion, with no particular specificity for fibers supplying any individual vascular bed or tissue.

By contrast, ongoing sympathetic nerve activity does not activate all fibers at the same time; rather it is a stochastic, although highly organised, pattern of firing.

Further to this, it is uncommon for individual neurones to show bursts of activity at higher firing frequencies, as they tend to fire in doublets or triplets at most, within the cardiac and respiratory patterning that is present (Macefield & Wallin, 1999; Murai *et al.*, 2006; Hudson *et al.*, 2011). However, preliminary experiments performed in the present study, it was found that attempting to model this by using doublets at higher frequencies (20, 40 and 60Hz) as recorded in Chapter 5, was not viable for the purposes of the present protocol because the vasoconstrictor response produced fell within the range of normal fluctuations in FVR. Such fluctuations in FVR are particularly evident in Figures 6.2 and 6.3. Thus, in order to produce responses that were consistent and outside the range of normal fluctuations, 20 pulses given at 20 or 40Hz, 6 times over 60 seconds were used, as was described in previous studies (Johnson *et al.*, 2001; Coney & Marshall, 2007).

Stimulation of the lumbar sympathetic chain using constant pulses at 2Hz, and with bursts of pulses at 20Hz and 40Hz was chosen as they represented average frequencies, and instantaneous frequencies in the range recorded in single units in the present study and others (Macefield & Wallin, 1999; Hudson *et al.*, 2011). Stimulation with the same total number of impulses over a 60 seconds period for all stimulation patterns meant that the mean responses over these time period were comparable, and allowed demonstration of the importance of patterning and not just of mean firing rate in MSNA. It should be noted that the majority of studies on the vascular responses evoked by sympathetic stimulation, impulses are generally delivered at constant frequencies ranging from 1-20Hz, thus ignoring the irregular, rhythmic activity that is present in MSNA under physiological conditions.

Thus, on balance, whilst stimulation of the lumbar sympathetic chain in the manner presented in this study is unphysiological in stimulating many fibres simultaneously, and the number of pulses delivered per unit time, it is an appropriate method for examining *in vivo* vascular responsiveness to sympathetic nerve activity. Further, given that an important part of the hypotheses tested involves the different sympathetic co-transmitters, and notably the role of NPY, other methods discussed earlier such as field stimulation applied to larger arterial vessel in vitro, or application of agonists to isolated vessels were not appropriate.

6.4.6 BIBP-3226 as an NPY Y1 receptor antagonist

As mentioned in the Results, BIBP-3226, used as an infusion at 10μg.min^{-1}.kg^{-1} has been demonstrated to cause potent selective inhibition of the neuropeptide Y Y_1 receptor (Bischoff *et al.*, 1997), and has been shown to significantly attenuate the hypertensive response to exogenous infusion of the NPY receptor agonist leu-pro-NPY (Coney & Marshall, 2007). This was checked, and confirmed, in a control rat in this study. Thus, it is reasonable to assume that it was effective as an NPY Y_1 receptor antagonist in the present experiments on N rats, and given that the regimen was similar, there is no reason to suggest this was not also true of the experiments in CHU rats.

It is important to note that, whilst BIBP-3226 has classically been understood to be a specific NPY Y_1 receptor antagonist, recent work has shown that it also inhibits the neuropeptide FF (NPFF) receptors (Mollereau *et al.*, 2002; Fang *et al.*, 2006).

Indeed, it has been used as a putative NPFF receptor antagonist in preparations of mouse colon (Fang *et al.*, 2005). Given that the role for NPFF in the vasculature, particularly in the skeletal muscle vasculature, is not well characterised, it is not possible to rule out inhibition of this receptor as a confounder for these results. Future studies describing the role of NPFF in vascular regulation will see this concern addressed, but as such, at present, little further comment can be made.

In conclusion, by using lumbar sympathetic chain stimulation the experiments of the present study examined the functional consequences of chronic hypoxia *in utero* for sympathetic vasoconstriction in the hind limb. The findings indicate a reduction in vasoconstrictor responses to sympathetic stimulation with impulses at constant low frequency and with bursts of high frequency in CHU rats relative to N rats. Further, BIBP-3226 has no effect on the magnitude of vasoconstriction in CHU rats, whereas it reduced it in N rats, suggesting a blunted role for NPY in mediating vasoconstriction evoked by sympathetic stimulation in CHU rats.

As suggested above, future experiments should seek to examine whether the loss of the NPY component of vasoconstriction is due to failure of release of NPY, a change in receptor density, or a failure of synthesis of NPY. The results of the studies described so far in this thesis suggest that in the face of increased ongoing MSNA, increased innervation density, and a reduced sensitivity to increases in MSNA, ongoing femoral vascular resistance (and therefore also conductance) is maintained at a basal level similar to that of N rats. Further, studies so far were performed on 10-12 week old N and CHU rats. The question arises as to whether basal levels of FVR,

vascular responses to sympathetic stimulation, or the role of NPY change during aging. Thus, in Chapter 7 the responses evoked by sympathetic chain stimulation were tested in 36 week old CHU and N rats.

Chapter 7 – Cardiovascular aging following chronic hypoxia *in utero*

7.1 Introduction

The offspring born of women who were pregnant during the Dutch famine of 1944 suffer from angina pectoris on average 3 years earlier than those born in the same area of Holland, but of pregnancies during times of plenty (Painter *et al.*, 2006). Further, preeclampsia is associated with higher childhood blood pressure (Geelhoed *et al.*, 2010). Indeed, preeclampsia, and the consequences of this for the offspring as they age, leave them with permanent systemic and pulmonary vascular dysfunction (Jayet *et al.*, 2010). The exact mechanisms leading to this are unclear.

It is also known that in humans, with age, the role of the sympathetic nervous system in controlling basal vascular tone and in responses to cardiovascular stressors can become perturbed, and the risk of cardiovascular disease increases (Lakatta, 2002; Seals & Dinenno, 2004). Seals & Dinenno (2004) reported that in aging humans, there is chronic sympathetic overactivity, which leads to reduced baroreflex buffering capability, conduit artery hypertrophy, and reduced systemic α-adrenergic sensitivity This study has shown that such overactivity exists in the MSNA of young CHU offspring (Chapter 5).

Furthermore, Wilson et al., (2004) found that following inhibition of presynaptic release of noradrenaline with bretylium, sensitivity of cutaneous blood flow to intradermal microdialysis of exogenous noradrenaline was reduced in aged subjects. Moreover, Dinenno et al., (2002) found that the decrease in forearm vascular conductance elicited by intravascular tyramine, to release endogenous stores of

noradrenaline, was blunted in aged subjects, and that is was due to reduced sensitivity of the α_1, not α_2 adrenoreceptor subtype. There are many other studies of aged human subjects confirming that vascular sensitivity to noradrenaline, exogenous and endogenously released, is blunted in aged subjects (Richardson *et al.*, 1992; Davy *et al.*, 1998; Frank *et al.*, 2000; Jones *et al.*, 2001).

The rate-limiting step in catecholamine synthesis is tyrosine hydroxylation by the enzyme tyrosine hydroxylase (TH), which requires tetrahydrobiopterin (BH_4) as an essential cofactor (Zigmond *et al.*, 1989; Kumer & Vrana, 1996). Thus, in aged individuals loss of BH_4, by its interaction with superoxide may be a mechanism by which sympathetic vasoconstriction becomes impaired (Moens & Kass, 2007). Indeed, administration of BH4 in older subjects can ameliorate the difference in sympathetic vasoconstriction between young and old subjects in the cutaneous circulation (Eskurza *et al.*, 2005; Lang *et al.*, 2009).

In Chapters 3 and 4, evidence is presented supporting the hypothesis that there is a chronically high level of oxidative stress in CHU rats. One possible source of oxidative stress in those studies is superoxide anions produced by uncoupled eNOS, the uncoupling of which is known to be caused by reductions in the bioavailability of its cofactor BH_4. Further, its uncoupling may impact upon BH_4 availability through generation of superoxide anions, which oxidize BH_4. It is therefore possible this same oxidative stress may also have consequences for the synthesis and hence release of catacholamines from the sympathetic nerve varicosities in CHU rats.

Chapter 6 detailed how maximum vasoconstrictor responses to lumbar sympathetic chain stimulation were blunted in CHU rats. It seems reasonable to anticipate that this may be further exacerbated in aged CHU rats.

As in skeletal muscle, along with ATP and NA, NPY, has been demonstrated to be important in control of cutaneous vasculature (Stephens *et al.*, 2004), and it has been demonstrated that in aging subjects, the role of NPY in cutaneous vasoconstriction can be lost (Thompson & Kenney, 2004). The evidence presented in Chapter 6 of the present study suggested that NPY is released during stimulation of the sympathetic chain with pulses at 2, 20 and 40Hz in young N rats, but that there is a reduced role for NPY in CHU rats.

This raises the question as to whether the role of NPY in sympathetic vasoconstriction is increased in rat skeletal muscle vasculature in older CHU rats, given the possibility that the role for noradrenaline may be blunted, and the expectation that hypertension develops with age in CHU rats.

It was therefore hypothesised that:

1. As a consequence of the ongoing high levels of sympathetic nerve activity found in young CHU rats, older CHU rats will be hypertensive relative to older N rats at the same age.
2. Sensitivity to sympathetic nerve activity is reduced in aged CHU rats, either due to decreased vascular sensitivity, or because of reduced catecholamine release due to oxidative stress

3. On the basis that the role of NA in sympathetic vasoconstriction in older CHU rats may be decreased, NPY may make a larger contribution as a sympathetic cotransmitters in aged CHU rats than aged N rats.
4. Given the evidence of oxidative stress presented in Chapters 3 and 4, this study sought to assess vascular oxidative stress in skeletal muscle small arteries to determine if there is direct evidence of formation of peroxynitirite.

Further to the above, a recent study, Hauton and Ousley (2009) found that there was a higher proportion of adipose tissue in the 10-12 week old CHU rat relative to the N rat, but that many of the other organ masses were similar to N rats. The exception was that the adrenal glands were significantly smaller in N rats than in CHU rats. It is known that growth restricted newborn rats develop metabolic syndrome and obesity (Mcmillen & Robinson, 2005), which is known to be a risk factor for cardiovascular disease (Franks *et al.*, 2010). Therefore body mass and the proportional contribution of major tissues to total body mass, including adipose tissue, was measured in older N and CHU rats.

7.2 Methods

7.2.1 Generation of aged N and CHU Rats

These experiments were carried out on 12 older CHU rats (age 264±7 days, 320±30g, 6 litters) and 13 older N rats (age 252±2 days, 666±24g). The older N rats were born and raised under standard laboratory conditions at Charles River Laboratories, Margate, UK), fed the VRF1 pelleted diet (4.75% crude oil, 19.11% crude protein, 3.85% crude fibre, SDS Diets, Lillico Biotechnology, Horley, UK) with water *ad libitum.* They were transported to The Biomedical Services Unit (BMSU), University of Birmingham 4 weeks prior to the acute experiment. During these four weeks, the 12 N rats were fed the slightly different RM1 pelleted diet (2.71% crude oil, 14.38% crude protein, 4.65% crude fibre, SDS Diets, Lillico Biotechnology, Horley, UK). One N rat died during the aging period whilst at Charles River laboratories.

12 male CHU offspring, bred as described in Chapter 2, from 6 litters (2 from each) that were housed in the BMSU, University of Birmingham, under standard laboratory conditions and fed the RM1 diet (SDS Diets, Lillico Biotechnology, Horley, UK) and water *ad libitum.* These animals were housed as littermate pairs from weaning onwards. None of the CHU rats died during the aging period.

7.2.2 Animal preparation

The animals were anaesthetised as described in Chapter 2, and the surgical preparation was the same as that presented in Chapter 6, for electrical stimulation of

the lumbar sympathetic chain. Interestingly, the infusion rate of Alfaxan that was required to maintain surgical anaesthesia in older N and CHU rats was approximately half that of their young counterparts, rates of 0.5-0.8ml.hr^{-1} being required. In addition to the cardiovascular variables measured in Chapter 6, arterial blood was sampled from the left brachial artery under baseline conditions for blood gas analysis, in the same way described for analysis of normoxic blood gasses described in Chapter 3. Unfortunately, due to technical problems with the blood gas analyser, arterial blood gas analysis was only possible in 5 of the 12 older CHU rats described in this Chapter.

ABP and FBF were recorded in the same way decribed in Chapter 6, and the calculations of HR and FVR were also the same. Similarly to Chapter 6, the sympathetic chain was stimulated with 3 patterns of impulses, each containing 120 pulses in total; continuous stimulation at 2Hz for 60 seconds, and 6 bursts of 20 pulses at 20 or 40Hz, separated over 60 seconds. Each protocol was repeated twice, in a randomized order, before and during infusion of the NPY Y1 receptor antagonist BIBP-3226, as described in Chapter 6.

Comparison between responses in young N and CHU and older N and CHU rats were made using a factorial ANOVA, with Scheffés *post hoc* analysis with $p<0.05$ considered statistically significant. Comparisons of responses recorded before and during infusion of BIBP-3226 were made using a repeated-measures ANOVA with Scheffés *post hoc* analysis.

7.2.3 In vitro analysis of oxidative stress in skeletal muscle vasculature

The method used for assessing the degree of oxidative stress in the small arteries supplying skeletal muscle in N-A and CHU-A rats were the same as that described in Chapter 3. Briefly, the proximal portion of the tibialis anterior muscle was removed from the older N and CHU rats at the end of the *in vivo* experiment (see above), mounted and frozen in liquid N_2. 10µm cross sectional sections were stained with antibodies to show 3NT and αSMA and viewed under fluorescent microscopy. The method of analysis is the same as that described in Chapter 3. Staining was carried out simultaneously in all sections from all four groups analysed (young adult and older adult N and CHU rats), and as such are directly comparable

7.2.4 Body composition

At the end of each in vivo experiment, major body tissues were weighed. In the dead rat the mass of one TA muscle, the liver, one kidney, the spleen, bilateral adrenal gland, bilateral epididymal fat and perirenal fat were removed and weighed.

7.3 Results

7.3 1 General characteristics of the rats used

Total body weight was similar between the older N and CHU rats. The weight of the tissues detailed in Table 7.3 were not significantly different between groups, whether analysed as absolute weight (Table 7.3), or as proportion of total body mass (data not shown).

7.3.2 Baseline cardiovascular characteristics

Under baseline conditions, ABP was significantly higher in older CHU rats than older N rats ($p<0.01$, Table 7.1). However, baseline HR, FBF and FVR were similar between the two groups (Table 7.1). The baseline values of P_aO_2, P_aCO_2 and pH_a, which were sampled after the series of control stimulations of the sympathetic chain, but before administration of BIBP-3226, were also not different between groups (Table 7.2).

7.3.3 The effect of lumbar sympathetic chain stimulation in older N and CHU rats

Stimulation of the lumbar sympathetic chain had no significant effect on ABP or HR in older N or CHU rats when using 2Hz, 20Hz or 40Hz trains of pulses (data not shown). In neither group did stimulation of the sympathetic chain at a constant frequency of 2Hz have a significant effect on intFVR over the duration of the stimulation (figure 7.1A), and there was no change in MFBF. However, FVR did transiently rise by a similar amount before falling back to baseline levels in both older N and CHU rats (Figure 7.1B).

Stimulation of the lumbar sympathetic chain using bursts of impulses at 20Hz tended to cause a rise in intFVR in older N ($p=0.08$) and older CHU rats ($p=0.11$, figure 7.1A), whilst stimulation of the sympathetic chain with bursts of impulses at 40Hz caused a significant rise in intFVR in older N ($p<0.01$) and older CHU rats ($p<0.05$). There were no significant differences between the responses evoked by sympathetic chain stimulation in older N and CHU rats by any pattern of stimulation.

7.3.4 Effect of BIBP-3226 on cardiovascular baselines

The effect of BIBP-3226 on the baseline ABP, HR, FBF and FVR is displayed in Table 7.1. There was no significant change in any of the baselines compared to control baselines.

7.3.5 Effect of BIBP-3226 on responses to lumbar sympathetic chain stimulation

Following administration of BIBP-3226 there was still no significant increase in intFVR during constant stimulation at 2Hz in older N or CHU rats (Figure 7.2A). There was a small transient increase in FVR (fig 7.2B), but this was not different to that of control conditions in either group, and the same was true of the mean maximum fall in MFBF (Figure 7.3D).

BIBP-3226 had no significant effect on the responses evoked by stimulation of the sympathetic chain in older N or CHU rats, except that the maximum increase in FVC evoked by stimulation of the sympathetic chain with bursts of impulses at 20Hz in older CHU rats was significantly higher during infusion of BIBP-3226.

7.3.6 Comparison of responses to lumbar sympathetic chain stimulation in young and middle aged N and CHU rats

Comparisons were made between the older N and CHU rats presented in this chapter and the results from young adult N and CHU rats presented in Chapter 6. Baseline ABP was similar between N and N-A rats, but baseline ABP was significantly higher in CHU-A rats than CHU rats ($p<0.01$). Baseline FVR was similar between N and N-A rats, and between CHU and CHU-A rats, as was baseline FBF and baseline HR. There was no effect of age the increase in intFVR evoked by stimulation of the sympathetic chain with impulses at a constant 2Hz or with bursts of impulses at 20 or 40Hz in. Similarly, the mean maximum increase in FVR evoked by sympathetic chain stimulation with any of the described patterns of stimulation was not changed with increasing age. However, comparison of the data obtained in young adult and older N and CHU rats (cf Figures 6.4 and 7.1) indicates that the responses evoked in the older N and CHU rats had much greater variance than in young adult N and CHU rats. Thus, larger group sizes would have been required to discriminate any difference.

7.3.7 Vascular oxidative stress in the skeletal muscle small arteries of middle aged N and CHU rats

Representative photomicrographs of arterial vessels within the TA muscle of older N and CHU rats are found in Figure 7.3. Thus, Figure 7.3 A-D shows staining in a section from an older N rat with DAPI, SMA and 3-NT staining, whilst Figure 7.3D

shows a merged image, where yellow staining represents colocalisation of SMA and 3NT staining. Figure 7.3 E-H represent the equivalent photomicrographs in an older CHU rat.

The level of 3-nitrotyrosine immunoreactivity in identified areas of αSMA immunoreactivity was similar between older N and older CHU rats (Fig. 7.4B), and was similar to the levels observed in young N and CHU rats (7.4A, same graph as Figure 3.8).

Table 7.1 – Baseline cardiovascular variables in 36 week old N and CHU rats before and during infusion of the NPY Y_1 receptor antagonist BIBP-3226.

Group		ABP (mmHg)	HR (bpm)	FBF ($ml.min^{-1}$)	FVR ($mmHg.ml^{-1}.min^{-1}$)
Older N	Control	126±3	430±5	2.3±0.2	65±7
	+BIBP	123±3	397±10	1.9±0.1	61±4
Older CHU	Control	139±3**	432±12	2.5±0.2	59±4
	+BIBP	126±3	396±13	2.0±0.2	60±5

Baseline cardiovascular variables in older N and older CHU rats before (control) and during infusion of the NPY Y_1 receptor antagonist BIBP-3226 (+BIBP). Mean±SEM data under control conditions, and during infusion of BIBP-3226.

** - $p<0.01$ – difference between group baselines

Table 7.2 – Arterial blood gasses measured in older N and CHU rats under baseline conditions.

Group	P_aO_2	P_aCO_2	pH_a
Older N (n=12)	85.6±1.8	37.1±0.7	7.48±0.006
Older CHU (n=5)	84.8±1.9	34.8±1.9	7.46±0.008

PaO_2, $PaCO_2$ and pH in older N and CHU rats sampled after control stimulations of the sympathetic chain, but before infusion of BIBP-3226, whilst breathing room air. There are no significant differences in P_aO_2, P_aCO_2 or pH_a between groups.

Table 7.3 – Body mass characteristics in older N and CHU rats

	Older N	Older CHU
Age (days)	257±2	264±7
Total Body mass (g)	666±24	651±30
Tibialis Anterior (mg)	1014±32	983±30
Liver (g)	19±0.6	18±0.9
Kidney (g)	1.85±0.08	1.67±0.06
Spleen (g)	1.36±0.07	1.44±0.09
Adrenal gland (mg)	65.0±3.8	66.7±6.7
Epididymal Fat (g)	17.5±1.1	17.7±1.3
Perirenal Fat (g)	21.6±3.0	23.4±3.5

Mean±SEM data for body composition characteristics in 36 week old N and CHU rats Total Body mass, mass of one tibialis anterior skeletal muscle, liver, one kidney, spleen, bilateral adrenal glands, bilateral epididymal adipose tissue, bilateral perirenal adipose tissue. There were no significant differences in the weight of any tissue measured between groups.

Figure 7.1 – Mean changes in cardiovascular variables evoked by stimulation of the sympathetic chain in older N and CHU rats.

Mean±SEM data for the cardiovascular responses evoked by lumbar sympathetic chain stimulation in older N (Closed bars) and oler CHU rats (open bars), using patterns of stimulation at 2Hz, 20Hz and 40Hz frequencies.

A: ∆intFVR during lumbar sympathetic chain stimulation in N and CHU rats

B: Mean Maximum ∆FVR during lumbar sympathetic chain stimulation in N and CHU rats. Each ∆FVR represents a significant increase from baseline.

C: Maximum rise in FBF from baseline during the lumbar sympathetic chain stimulation protocols in N and CHU rats

D: Maximum fall in MFBF during the lumbar sympathetic chain stimulation protocols in N and CHU rats

There were no significant differences between the responses seen in N-A and CHU-A rats.

Figure 7.1

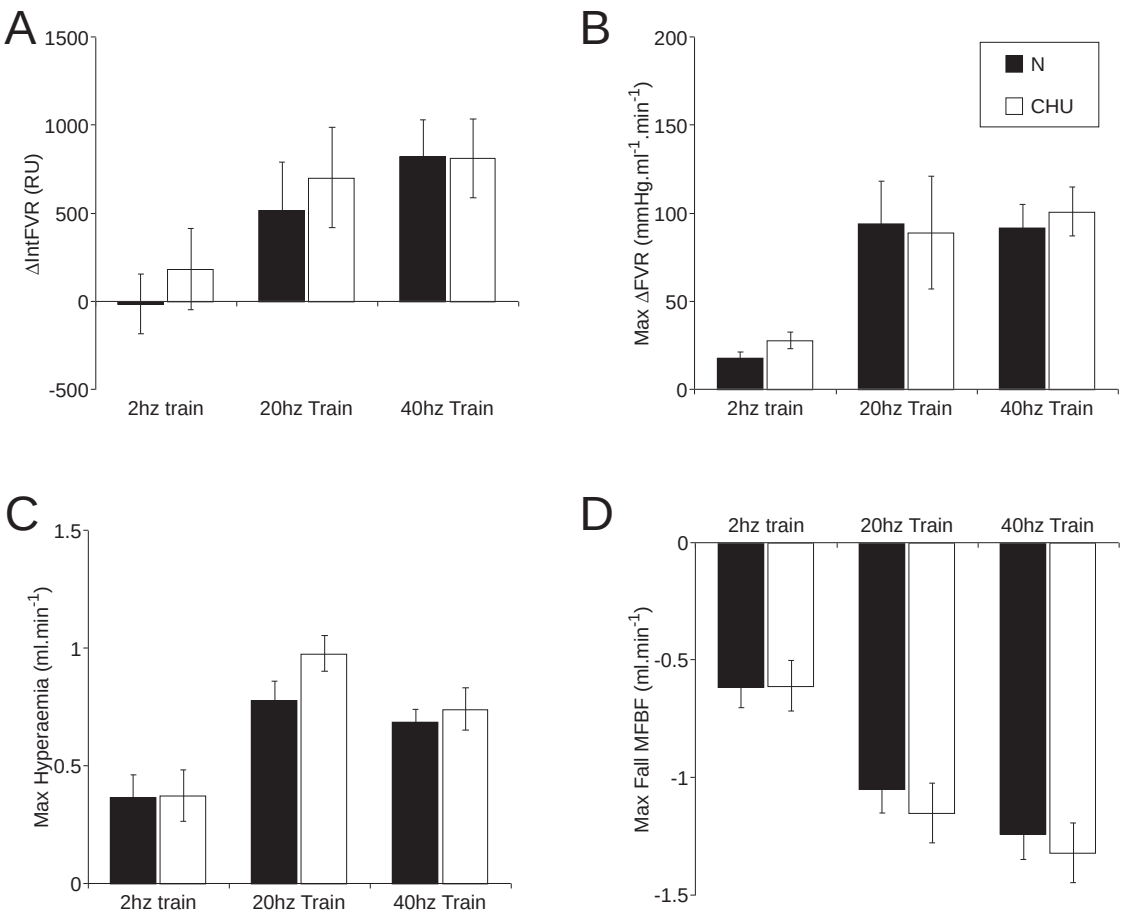
A
1500
1000
500
0
-500
ΔIntFVR (RU)
2hz train
20hz Train
40hz Train
B
200
150
100
50
0
Max ΔFVR (mmHg.ml-1.min-1)
N
CHU
2hz train
20hz Train
40hz Train
C
1.5
1
0.5
0
Max Hyperaemia (ml.min-1)
2hz train
20hz Train
40hz Train
D
2hz train
20hz Train
40hz Train
0
-0.5
-1
-1.5
Max Fall MFBF (ml.min-1)

Figure 7.2 – Effect of an NPY Y_1 receptor antagonist on mean changes in cardiovascular variables evoked by stimulation of the sympathetic chain in N and CHU rats.

Mean±SEM data for the cardiovascular responses evoked by lumbar sympathetic chain stimulation in older N (Closed bars) and older CHU rats (open bars), using patterns of stimulation at 2Hz, 20Hz and 40Hz frequencies, before and during (patterned bars) infusion of the NPY Y_1 receptor antagonist BIBP-3226

A: ∆intFVR during lumbar sympathetic chain stimulation in N and CHU rats before and after infusion of BIBP-3226.
B: Maximum ∆FVR during lumbar sympathetic chain stimulation in N and CHU rats before and after infusion of BIBP-3226.
C: Maximum rise in FBF from baseline during the lumbar sympathetic chain stimulation protocols in N and CHU rats before and after infusion of BIBP-3226.
D: Maximum fall in MFBF during the lumbar sympathetic chain stimulation protocols in N and CHU rats before and after infusion of BIBP-3226.

† - $p<0.05$ vs control stimulation

Figure 7.2

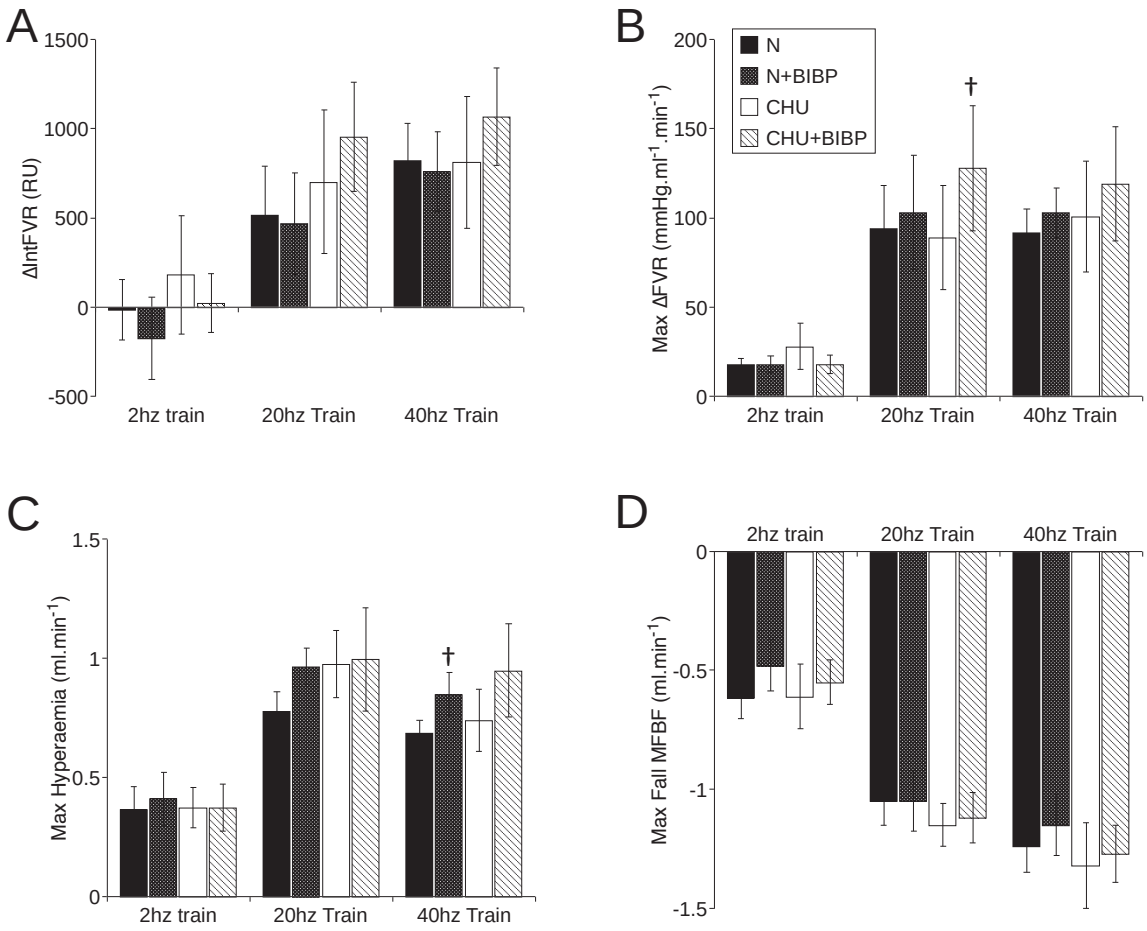
A
1500
1000
500
0
-500
ΔIntFVR (RU)
2hz train
20hz Train
40hz Train
B
200
150
100
50
0
Max ΔFVR (mmHg.ml-1.min-1)
N
N+BIBP
CHU
CHU+BIBP
†
2hz train
20hz Train
40hz Train
C
1.5
1
0.5
0
Max Hyperaemia (ml.min-1)
†
2hz train
20hz Train
40hz Train
D
2hz train
20hz Train
40hz Train
0
-0.5
-1
-1.5
Max Fall MFBF (ml.min-1)

Figure 7.3 – Examples of 3-Nitrotyrosine staining in the vascular smooth muscle of small arteries of the tibialis anterior muscle in older N and CHU rats.

Representative dual α-SMA and 3-NT staining of arterial vessels within transverse sections of the TA from 36 week old N and CHU rats

A & E: DAPI staining in N and CHU rats respectively

B & F: α-SMA staining in N and CHU rats respectively

C & G: 3-NT staining in N and CHU rats respectively

D & H: Merge of all three staining images. Yellow denotes combined α-SMA and 3-NT staining, indicating vascular interaction with peroxynitrite.

Figure 7.3

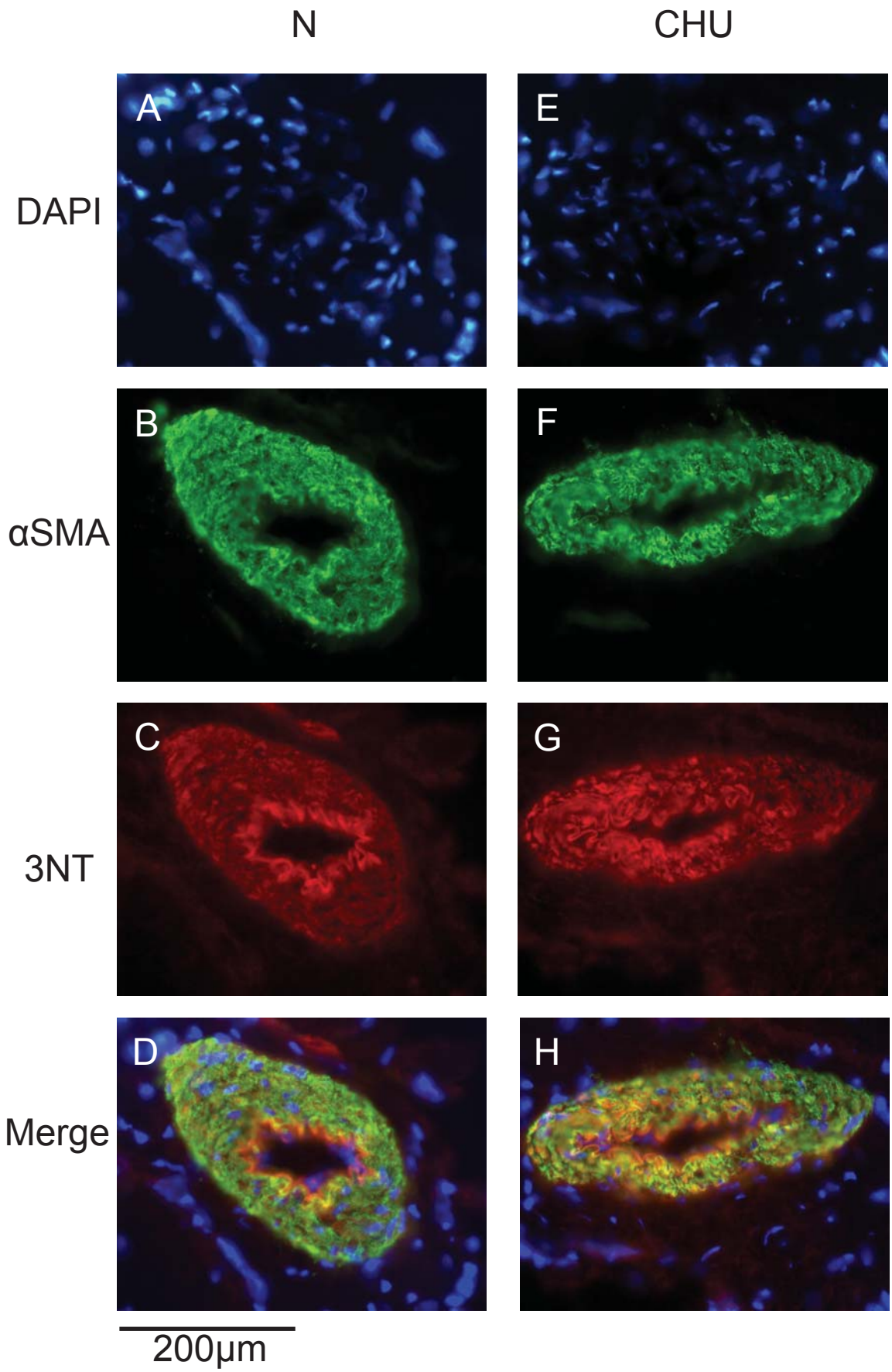

Figure 7.4 – Mean 3-Nitrotyrosine staining the small arteries of young and older N and CHU rats

Fluorescent intensity in selected 'regions of interest' (See section 3.3, arbitrary units, mean±SEM) of 3-NT staining in young adult and older N and CHU rats, indicative of the level of peroxynitrite present in the vessels wall of arterial vessels of TA muscle. Fluorescent intensity is similar in N and CHU rats. There was no significant difference in fluorescent intensity measured in older N and CHU rats, or between young and older rats in either group.

A: Fluorescent intensity (arbitrary units, mean±SEM) of 3-NT staining in young adult, 10-12 week old N and CHU rats, indicating the level of peroxynitrite present in the skeletal muscle vasculature. Fluorescent intensity is similar in N and CHU rats

B: Fluorescent intensity (arbitrary units, mean±SEM) of 3-NT staining in older 36 week old N and CHU rats, indicating the level of peroxynitrite present in the skeletal muscle vasculature. Fluorescent intensity is similar in N and CHU rats.

Figure 7.4

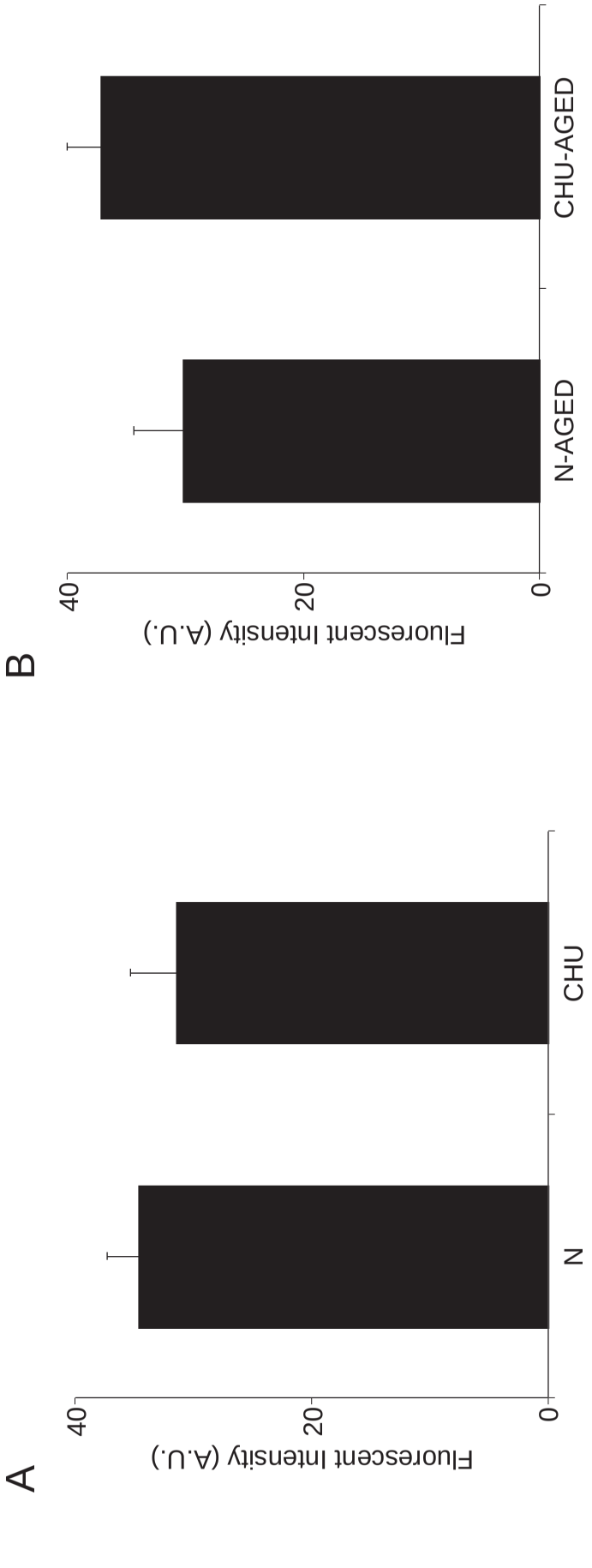
A
Fluorescent Intensity (A.U.)
0
20
40
N
CHU
B
Fluorescent Intensity (A.U.)
0
20
40
N-AGED
CHU-AGED

7.4 Discussion

7.4.1 Main Findings

The main findings of the present study are that older CHU rats were hypertensive relative to aging N rats. However, while responses measured in the hindlimb evoked by stimulation of the sympathetic chain were blunted in young CHU rats relative to young N rats, they are similar between aged CHU and N rats, and there was no significant effect of BIBP-3226 on responses evoked by lumbar sympathetic chain stimulation in ageing N or CHU rats.

7.4.2 Aging, CHU and Hypertension

Evidence in Chapters 3 and 4, and from other authors (Williams *et al.*, 2005b; Franco *et al.*, 2007) suggests that in the hindlimb vasculature there is ongoing oxidative stress in CHU rats relative to N, but that this does not have obvious effects on ongoing vascular tone at 10-12 weeks of age. It was reported in Chapter 6 that generally, in the surgical preparation used for stimulation of the sympathetic chain resulted in lower baseline ABP than the preparations used in the experiments in Chapters 3 and 4. Thus, comparisons of ABP are only made between groups of N and CHU rats presented in Chapter 6 and in this chapter, when the same surgical preparation.

One of the important findings of the present study is that older CHU rats were hypertensive relative to older N rats (Table 7.1), and relative to young CHU rats. Evidence is presented in Chapter 4 demonstrating that in young CHU rats ongoing

MSNA is higher in CHU rats than N rats, and also that sympathetic innervation density in the tibial artery, supplying skeletal muscle, was markedly higher in CHU rats than N rats. However, the evidence of Chapter 6 suggested that the sensitivity to experimental stimulation of the lumbar sympathetic chain, measured by responses in the hindlimb muscle vasculature, were reduced in young adult CHU rats, and thus normal vascular conductance remained. The findings of the present study suggest the possibility that raised MSNA at the younger age in CHU may be instrumental in contributing to raised ABP in middle-aged CHU rats, and therefore it will be important that future studies examine levels of ongoing MSNA in older CHU rats.

However, in contrast with the results of Chapter 6, the present study found that in 36-week old CHU rats, the vasoconstrictor responses evoked by stimulation of the lumbar sympathetic chain were similar to those evoked in older N rats of the same age. At the same time, there is a trend for vasoconstrictor responses in the middle aged N rats to be blunted relative to young adult N rats. Previous evidence has shown that in aging humans, cutaneous vascular sensitivity of adrenergic neurotransmitters reduces with age (Richardson *et al.*, 1992; Davy *et al.*, 1998; Frank *et al.*, 2000; Jones *et al.*, 2001). Indeed the same is true of leg vasculature, which predominantly supplies skeletal muscle (Smith *et al.*, 2007). In this study, there were no significant effects of age on the response to lumbar sympathetic chain stimulation at any of the frequencies used, in N rats. There were non significant effects in CHU rats, the result of which was that whilst at 10-12 weeks of age CHU rats have significantly lower responses to stimulation than N rats, at 36 weeks of age, the magnitude of effect is the same. However, it is difficult to comment confidently on the

statistical significant of the data presented in this chapter. The variance experienced in the results of sympathetic chain stimulation were far greater than expected. Retrospective statistic power analysis suggests that, for example, to reliably reject the null hypothesis, that the response to stimulation at 20Hz is not different between middle aged N and CHU rats, measured as ΔintFVC, given the increased variation in the results, a sample size of 75 would be required. Thus, future experiments must consider increasing the sample size appropriately in order to be statistically sure of the findings.

In Chapter 6, the idea that in young CHU rats, the reduced sensitivity to sympathetic nerve stimulation may be a mechanism that compensates for the ongoing increase in MSNA and increased sympathetic innervation density, was discussed. If this 'compensated state' was present in young adult CHU rats, the evidence in the present Chapter suggests it is no longer present in older, 36 week old CHU rats. This of course assumes that ongoing MSNA is still increased relative to N rats, as it was in CHU rats at 12 weeks of age, but evidence shows that MSNA tends to increase with age, at least in humans (Dinenno *et al.*, 2000; Seals & Dinenno, 2004). This is of course only representative of the vasculature supplying skeletal muscle, but this may explain why at 12 weeks of age, CHU rats had similar ABP to N rats, whereas at 36 weeks of age, CHU rats are relatively hypertensive.

Measuring MSNA by the method described in Chapter 5 was not attempted in older, 36 week old rats. There are significant practical difficulties that would be associated with attempting to do so as their size and increased adiposity would make it very

difficult to maintain a physiologically viable anaesthetised preparation whilst placed on the side without mechanical ventilatory support. It is likely that 'bulk' recordings from the lumbar sympathetic chain would be more appropriately suited to examining levels of sympathetic nerve activity in older rats given these limitations. Analysis of sympathetic innervation density was also not carried out on aged N or CHU rats in the present study. However, previous work showed that sympathetic innervation density markedly increases in the femoral artery with age in normal rats (Omar & Marshall, 2010). Further work characterising the time course of changes in sympathetic innervation density following chronic hypoxia *in utero* would be particularly useful, as they may provide insight into how hypertension develops in this model.

7.4.3 The role of NPY

Previous work has shown that in humans, aging is associated with loss of NPY-mediated vasoconstriction in the cutaneous circulation during sympathetic nerve activation (Thompson & Kenney, 2004). In Chapter 6, evidence is presented showing that in young adult N, there is a role for NPY in mediating vasoconstriction evoked by stimulation of the lumbar sympathetic chain at constant low frequency or with higher frequency bursts of impulses. The evidence presented in this Chapter suggests that this contribution is no longer evident in older N rats and is also not evident in older CHU rats, in agreement with the aforementioned study, that the role of NPY in sympathetic vasoconstriction is reduced by aging. Clearly, NPY does not become more important during ageing in CHU rats than in N rats for maintenance of vascular tone, as it was hypothesised. Indeed, if NPY makes no contribution to the regulation

of hindlimb vascular tone in middle-aged CHU rats, it would appear that in CHU as in N rats, NA makes a major contribution. The role of ATP as a sympathetic cotransmitter was not examined, and further experiments could test its relative contribution in young and older N and CHU rats.

7.4.4 Oxidative stress

Colocalisation of 3-NT and α-SMA immunoreactivity was carried out in older N and CHU rats in the same manner described in chapter 3. The limitations of this approach were discussed in Chapter 3. There was no difference in the levels of 3-NT staining in the vascular wall of small arteries in the TA muscle in older N and CHU rats, and indeed no difference between young and older N or CHU rats (Figure 7.3 and 7.4). Thus, there is no reason to suggest that the level of oxidative stress in the vascular smooth muscle is changed with aging in N or CHU rats. A different approach, using opened vessels, or using homogenized conduit vessels and other markers of oxidative stress, such as levels of glutathione peroxidase, may be more appropriate to provide information about changes in the level of oxidative stress with age.

In summary, evidence presented in this Chapter show that older CHU rats are hypertensive relative to older N rats, at 36 weeks of age. There is no evidence that oxidative stress in the vascular smooth muscle of the skeletal muscle vasculature is increased. The reasons that older CHU rats are hypertensive relative to older N rats are not clear. However, evidence in young adult CHU rats, presented in Chapters 3-6, has shown that there is increased ongoing MSNA, higher sympathetic innervation density in skeletal muscle vasculature, and increase oxidative stress in young adult

CHU rats, and any number of these factors may persist during aging, and could represent an underlying mechanism contributing to increased blood pressure. Evidence in this chapter has shown that responses evoked by lumbar sympathetic chain stimulation are similar in 36-week old N and CHU rats, but CHU-A rats are hypertensive relative to N-A rats. The NPY Y_1 receptor antagonist had no significant effect on the vasoconstrictor responses.

7.4.5. Effect of CHU on body mass

In an extension of the findings of Hauton & Ousley (2009) the total body mass, and relative contributions of a number of major organs to total body composition were examined. However, whilst Hauton & Ousley found that total body mass, and relative contribution of white adipose tissue was substantially higher in those rats exposed to CHU as measured at 12 weeks of age, this study has found that by 36 weeks of age, these differences have become normalised. Further, the adrenal glands, and all other major organs, appeared to be of similar size in 36-week old CHU rats as in age-matched normal rats. Thus, any gross differences appear to have become normalised by this stage. However, this does not rule out the possibility that the microstructure or function are not substantially altered in the CHU rats relative to N, and this may well warrant further investigation in the future.

Chapter 8 – General discussion

8.1 Summary of findings

The studies that are presented in this thesis were designed to explore various components of cardiovascular and respiratory regulation in rat offspring, following exposure to chronic hypoxia *in utero*, with particular focus on the regulation of vascular tone in skeletal muscle vasculature, oxidative stress, and the role of the sympathetic nerves that innervate the blood vessels supplying skeletal muscle. Evidence has been presented that there are tonically increased levels of ROS in the hind limb vasculature of young adult male CHU rats, as indicated by the vasoconstrictor effect of a SOD inibitor in CHU rats, and the effect of NOS inhibition followed by infusion of an NO donor on hypoxia-induced muscle vasodilatation. The role of adenosine, and its action upon the A_1 and A_{2A} receptor subtypes was found to be broadly similar to that found in N rats.

It was also found that ongoing levels of MSNA were increased in CHU rats relative to N rats, as was the innervation density on the surface of blood vessels supplying skeletal muscle, although reflexly-evoked increases in MSNA by baroreceptor unloading or by graded systemic hypoxia were unchanged in young CHU rats relative to N rats. On the other hand, maximum vasoconstrictor responses evoked in the hindlimb muscle by stimulation of the lumbar sympathetic chain with different patterns of impulses were blunted in CHU rats, and in contrast to the N rat, inhibition of NPY Y_1 receptors had no blunting effect on these responses. Finally, it was found that by early middle age, CHU rats are hypertensive relative to age-matched N rats, but showed similar responses to lumbar sympathetic chain stimulation. Ie. responses

are no longer blunted in CHU rats relative to N rats. Further, by this age, inhibition of NPY Y_1 receptors did not blunt the responses in either N or CHU rats.

8.2 Modeling the consequences of fetal programming

As discussed in Chapter 1, a number of different animal models have been developed with the aims of simulating the adverse conditions to which a human fetus may be subject, and modelling the consequences of these, both at birth and in the developing offspring. The direct consequences of the model used in the present study, pregnant dam breathing 12%O_2, are not clear. To the author's knowledge, no attempt has yet been made to elucidate whether the developing fetuses in the hypoxic dam actually become hypoxic, or whether the consequences observed in the offspring are a result of the adaptations made by the mother and fetus to maintain oxygen delivery. A study by Postigo et al., (Postigo *et al.*, 2009) found that there were adaptations in pregnant Europeans undergoing pregnancy at high altitude that served to maintain O_2 delivery. Whilst absolute O_2 delivery was reduced in the group of pregnancies at altitude, the fetuses were smaller than those at sea level, and as a result, O_2 delivery per unit body mass was normalised. It is not practical to make such measurements in rats, due to their size, and no attempt at measuring such variables has been made in larger animals such as sheep. It is known that in rodents, chronic hypoxia *in utero* does lead to IUGR (Williams *et al.*, 2005a; Morton *et al.*, 2011), which in humans, is a common consequence of obstetric complications. What is important to consider is that this study, and others, are attempting to simulate pathological conditions in humans, particularly pre-eclampsia. Pregnancy at altitude represents a small number of cases compared to the number of women who suffer

pre-eclampsia during pregnancy. Thus, whether the fetus becomes hypoxic or not may not be of such importance, as regardless, there are a range of reflex and hormonal adaptations which may well have distinct effects. What is key is that the IUGR phenotype is produced, and thus, there is relevance to human disease processes. Experiments examining whether or not the rodent fetus becomes hypoxic would be relatively simple, assaying levels of hypoxia inducible factor (HIF) in fetal tissues for example, and would represent a useful advance in the future.

Turning to the particular use of rodents to model hypoxia-induced fetal programming, the rat is a particularly useful model for several reasons. Firstly, there is extensive knowledge of the normal functioning of rat cardiovascular physiology, and its similarities with that of the human. Secondly, there are a large number of successful rodent models of cardiovascular disease which induce similar mechanisms of disease in rats and humans (Hasenfuss, 1998). Thirdly, in modeling fetal programming, rodent models are a relatively inexpensive way to model fetal programming in the offspring, as they have a relatively short gestation period. From a cost and scientific point of view, it is also an advantage that they have a relatively short life span, for this opens the possibility for investigation effects of fetal programming on the ageing process. Further, there are many well-developed surgical preparations, a number of which have been demonstrated in experiments in this study, which allow for invasive measurements of cardiovascular parameters that are not otherwise possible in humans, or large mammalian models for reasons of cost and ethics! However, that is not to say that rodent models are without limitation. Human pregnancies predominantly result in singletons, whereas rat pregnancies

result in a much larger numbers of offspring, often 10-15 pups. Thus, the placental adaptations to maternal hypoxia seen in the rat may be different from the manner in which the human placenta adapts to similar conditions. From a cardiovascular point of view, it is worth noting that rats are quadrupeds, and therefore not subject to the gravitational, and subsequent orthostatic responses that effect cardiovascular regulation. Also, the central nervous system is less highly developed in rats, and so any attempt to study influences of higher brain function on the cardiovascular system, such as that of emotional stress, are limited in the rat. However, as indicated above adverse conditions in either humans or rats do produce the IUGR phenotype. In this particular respect, the sheep models of reduced fetal oxygen supply are useful, but are less extensively used for various reasons, not least cost.

On balance, the rat model of chronic hypoxia *in utero* represents a very useful, cost-effective, repeatable and widely available model of fetal programming of cardiovascular disease. As the body of evidence indicating dysfunctional vascular regulation in the offspring of hypoxic pregnancies grows, attempts must be made to translate these findings to humans. This represents a significant challenge, as there are serious ethical considerations to be made when studying already babies that are already compromised or unhealthy. Studies performed in later stages in development and in adulthood are more likely to be acceptable. However, the aim of the animal-based experiments is to elucidate the mechanisms of cardiovascular disease resulting from chronic hypoxia *in utero*. Thus, developing treatments for the consequences must be the ultimate aim.

8.3 Fetal programming of oxidative stress

Turning to discuss the experimental observations made in the present study, at least two key pieces of evidence presented in this study, which adds to a mounting body of evidence that vascular oxidative stress is a major consequence of chronic hypoxia *in utero*. First, the SOD inhibitor DETC reduced baseline hind limb vascular tone in young adult male CHU rats, suggesting that there is ongoing dismutation of O_2^- by SOD which, when blocked by DETC, leads to increasing O_2^- levels and thus, to vasoconstriction, probably by decreasing NO bioavailability. Second, following NOS inhibition infusion of the NO donor SNAP significantly increased the magnitude of hind limb vasodilatation during acute systemic hypoxia, indicating that under control conditions in CHU rats, NO bioavailability may be impaired, and limiting the release mechanism for adenosine and or its own dilator activity. In the absence of ROS generated by uncoupled eNOS, due to NOS inhibition, and in the presence of SNAP-derived NO, the mechanisms of hypoxia-induced adenosine release, and thus, vasodilatation are restored. This adds to evidence presented by Williams et al., (2005b) and Morton et al., (2011) indicating oxidative stress impairs endothelial dilator function in isolated mesenteric arterial vessels of CHU rats by suggesting that oxidative stress disrupts normal functioning in the wholehind limb vasculature *in vivo*.

Oxidative stress is a risk factor for cardiovascular disease (Heitzer *et al.*, 2001) and is well implicated in development of atherosclerosis (Miller *et al.*, 1998; Harrison *et al.*, 2003). Chronic intrauterine hypoxia has recently been shown to lead to classic indications of developing atherosclerosis in the rat offspring (Wang *et al.*, 2009). This is particularly significant because rodent models do not normally develop significant

atherosclerosis as humans do (Folkow & Svanborg, 1993). Indeed, the oxidative stress demonstrated by the present study study and others, if translated to humans, may well go some way to explain the increased incidence of coronary heart disease in those offspring of mothers who were pregnant during the Dutch famine (Barker, 1995). The exact source of the vascular oxidative stress suggested by the present study is not completely clear, although the present study has provided evidence that, at least in larger vessels in skeletal muscle, it is not the vascular smooth muscle. Studies in opened isolated vessels in which the endothelium as a source of ROS can may be more easily investigated, or of markers of oxidative stress in venous efflux may provide further insight into the source of ROS, and give independent verification of the presence of enhanced levels of ROS.

8.4 The role of Adenosine

There is much evidence that the muscle vasodilatation that occurs in systemic hypoxia in N rats is largely due to adenosine being released from endothelial cells as a consequence of a change in the balance between O_2 and NO at the common binding site on mitochondrial cytochrome oxidase, and acting on endothelial A_1 receptors to release NO. This whole process is blocked when NOS is inhibited but release can be restored when a tonic level of NO is provided and then, again adenosine induces vasodilatation in hypoxia by acting on A_1 receptors that are presumed to be on the vascular smooth muscle. The results of the present study confirmed these findings in N rats and also indicated fully comparable process underlies hypoxia-induced muscle vasodilatation in CHU rats. This finding is particularly significant because in a recent study in this laboratory, adenosine was

found to play no role in the hypoxia-induced vasodilatation in CHU rats. There is no obvious reason for this disparity, but it does raise the possibility that the levels of oxidative stress may have been greater in the CHU rats of the study by Coney & Marshall (2007), if it is assumed that O_2^- limits the NO available to compete with O_2 at cytochrome oxidase and so limits or prevents the release of adenosine. This possibility requires investigation in future studies.

8.5 Fetal programming of the sympathetic nervous system

A major new important finding in the present study is that ongoing MSNA recorded from individual post-ganglionic sympathetic neurones on the surface of blood vessels supplying skeletal muscle is significantly increased in young male CHU rats relative to N rats. Further, the density of sympathetic neurones on the surface of the tibial artery, supplying skeletal muscle, is increased. This is interesting particularly because baseline vascular tone in skeletal muscle, albeit in the presence of the vasodilator effects of H_2O_2 (see above), is similar to N rats. Thus, an obvious question arises about the vascular sensitivity to sympathetic nerve activation in CHU rats. In fact, the present study showed for the first time that muscle vasoconstrictor responsiveness to sympathetic stimulation with a train of constant impulses at 2Hz, and with bursts of pulses at 20 and 40Hz, was substantially blunted in CHU rats relative to N. Thus, one can argue that a degree of compensation occurs, such that the effects of increased MSNA and sympathetic nerve density is counterbalanced by a reduction in the effectiveness of the sympathetic neurotransmitters. Indeed it seems that part of that compensatory mechanism is a reduction in the role of the sympathetic cotransmitter NPY.

That said, the results of Chapter 5 indicate that the change in MSNA induced by unloading of the baroreceptors, and by graded systemic hypoxia are similar between N and CHU rats, whilst the results of Chapters 3 and 4 indicate that that the increases in FVC evoked by systemic hypoxia are comparable between N and CHU rats. Thus, whilst Chapter 6 suggests that responses to sympathetic nerve stimulation are reduced in CHU rats, functional increases in FVC during systemic hypoxia, which activates the sympathetic nervous system are comparable. It is possible that effect of the increase in MSNA induced by hypoxia is blunted, and the fact that the increase in FVC is similar in N and CHU rats indicates that the vasodilator influences of hypoxia are smaller in CHU rats, and this has been hidden by the fact that the effectiveness of increase vasoconstrictor activity is also reduced.

The mechanisms that lead to increased MSNA and increased sympathetic innervation density are not clear. This study tested the possibility that it may be due to a failure of cyclic inhibition by the cardiac or respiratory cycles, or indeed an enhanced cyclic augmentation, but showed that the degree of cardiac and respiratory rhythmicity occurring in the MSNA of N and CHU rats was similar. This leaves the possibility that the increased MSNA in CHU rats is of central origin, but it appears not to involved in the interactions of the baro- and chemo-reflex with the central generation of autonomic outflow.

A further possibility is that MSNA is increased as a result of increased peripheral firing probability due to changes in ion-channel expression on pre- or post-ganglionic

neurones. The maintenance and control of sympathetic innervation density is controlled by a number of factors, discussed in Chapter 5, but importantly it is controlled by NGF signalling (Storkebaum & Carmeliet, 2011). Alterations in NGF signaling have been shown to change the expression of ion channels in sympathetic neurones *in vitro* (Luther & Birren, 2009). Thus, expression of NGF receptors and production of NGF by skeletal muscle vasculature at various time points during development may be useful in elucidating possible mechanisms that lead to increase MSNA and innervation density in CHU rats.

The consequences of increased MSNA and sympathetic innervation density for the vascular wall of skeletal muscle arteries are, as yet, unknown. Wang et al., (2009) showed thickening of the aortic wall in 16 month old CHU rat offspring.Thus, it would be interesting to establish whether this finding extends to the feed arteries and resistance vessels. It is also known that arterial stiffness increases with age, partly as a consequence of enhanced tonic sympathetic activation (Dinenno *et al.*, 2000; Seals & Dinenno, 2004). It is possible that the increase in sympathetic innervation density in CHU rats simply reflects the fact that more vascular smooth muscle is present in the arterial wall, and thus, greater levels of sympathetic neurotransmitter must be present to exert the same level of control. On the other hand, it may be that vessel walls are thickened in response to increased sympathetic nerve activity, and that the thickening reflects increased connective tissue. .

Work prior to this study, published in abstract form (Rook *et al.*, 2008b) showed that there is a marked increase in the capillary:fibre (C:F) ratio in the extensor digitorum

longus muscle, a muscle of mixed fibre type like the TA, of the rat hindlimb in CHU rats. Thus, either the number of capillaries supplied by each arteriole, or the number of arterioles must be increased in CHU relative to N rats. If the latter is true, then it is possible that the increase in sympathetic innervation density measured in the tibial artery reflects the fact that the same sympathetic nerves must go on to innervate a large number of arterioles. Analysis of the morphology of the whole vascular bed supplying the rat hindlimb, as well as analysis of arteriolar sympathetic innervation density may go some way to addressing the likelihood of these possibilities.

8.6 Wider implications of the present study

The vast majority of studies of the cardiovascular effects of chronic hypoxia *in utero* thus far, have been carried in out preparations of isolated blood vessels (Rouwet *et al.*, 2002; Williams *et al.*, 2005b; Herrera *et al.*, 2007; Morton *et al.*, 2010, 2011). The evidence presented in this study, that in skeletal muscle of CHU rats, ongoing sympathetic control of the vasculature is altered, demonstrates the need for more studies to be carried out in conscious, or anaesthetised *whole animals*, as in isolated preparations the complex interplay of the sympathetic nervous system, local endothelial control and local O_2 tension is lost. Thus, the impact of these studies is limited. For mechanistic insight, studies of isolated vessels are useful. However, in future work, careful consideration must be given to the consequences of the lack of ongoing sympathetic tone in the isolated preparation; the results should be presented with this as a significant limitation.

8.7 Summary and conclusion

The present study presents evidence that in intact, anaesthetised CHU rats there is tonic oxidative stress in the blood vessels supplying the skeletal muscle of the hind limb, and the ongoing sympathetic nerve activity in the neurones innervating these vessels is increased. Further, the sympathetic innervation density of arteries supplying hind limb skeletal muscle is increased. However, vasoconstrictor responses to sympathetic stimulation via the lumbar sympathetic chain stimulation are reduced. This is the first study examining the role of the sympathetic nervous system in cardiovascular regulation in the whole animal following *in utero* hypoxic insult, and is the first study to demonstrate that the aging CHU rat is hypertensive. Further, it adds important information to the body of evidence indicating that chronic hypoxia *in utero* leads to oxidative stress. The consequences of this oxidative stress, autonomic dysfunction and hypertension must now be examined both in animal models, and in humans.

Bibliography

Albert V & Campbell GR. (1990). Relationship between the sympathetic nervous system and vascular smooth muscle: a morphometric study of adult and juvenile spontaneously hypertensive rat/Wistar-Kyoto rat caudal artery. *Heart Vessels* **5,** 129-139.

Alexander BT. (2003). Placental Insufficiency Leads to Development of Hypertension in Growth-Restricted Offspring. *Hypertension* **41,** 457-462.

Alexander BT. (2007). Prenatal Influences and Endothelial Dysfunction: A Link Between Reduced Placental Perfusion and Preeclampsia. *Hypertension* **49,** 775-776.

Amaral SL, Zorn TM & Michelini LC. (2000). Exercise training normalizes wall-to-lumen ratio of the gracilis muscle arterioles and reduces pressure in spontaneously hypertensive rats. *J Hypertens* **18,** 1563-1572.

Anderson CM, Lopez F, Zimmer A & Benoit JN. (2006). Placental Insufficiency Leads to Developmental Hypertension and Mesenteric Artery Dysfunction in Two Generations of Sprague-Dawley Rat Offspring. *Biology of Reproduction* **74,** 538-544.

Anderson K & Faber J. (1991). Differential sensitivity of arteriolar alpha 1- and alpha 2- adrenoceptor constriction to metabolic inhibition during rat skeletal muscle contraction. *Circ Res* **69,** 174-184.

Andrew PJ & Mayer B. (1999). Enzymatic function of nitric oxide synthases. *Cardiovasc Res* **43,** 521-531.

Bae S, Xiao Y, Li G, Casiano CA & Zhang L. (2003). Effect of maternal chronic hypoxic exposure during gestation on apoptosis in fetal rat heart. *American Journal of Physiology - Heart and Circulatory Physiology* **285,** H983-H990.

Barker D. (1991). The intrauterine origins of cardiovacular and obstructive lung disease in adult life. The Marc Daniels Lecture 1990. *J R Coll Physicians Lond* **25,** 129-133.

Barker DJP. (1995). Fetal origins of coronary heart disease. *BMJ* **311,** 171-174.

Barker DJP. (1997). Maternal nutrition, fetal nutrition, and disease in later life. *Nutrition* **13,** 807-813.

Barker DJP. (1998). *Mothers, babies, and health in later life*. Churchill Livingstone, Edinburgh.

Belardinelli L, Giles WR & West A. (1988). Ionic mechanisms of adenosine actuons in pacemaker cells from rabbit heart. *Journal of Physiology* **405,** 615-633.

Berne RM, Knabb RM, Ely SW & Rubio R. (1983). Adenosine in the local regulation of blood flow: a brief overview. *Fed Proc* **42,** 3136-3142.

Berne RM, Levey M, Koeppen B & Stanton B. (2003). *Physiology*. Mosby.

Berne RM, Winn HR & Rubio R. (1981). The local regulation of cerebral blood flow. *Progress in Cardiovascular Disease* **24,** 243-260.

Bischoff A, Freund A & Michel MC. (1997). The Y1 antagonist BIBP 3226 inhibits potentiation of methoxamine-induced vasoconstriction by neuropeptide Y. *Naunyn-Schmiedeberg's Archives of Pharmacology* **356,** 635-640.

Blanco CE, Dawes GS, Hanson MA & McCooke HB. (1984). The response to hypoxia of arterial chemoreceptors in fetal sheep and new-born lambs. *The Journal of Physiology* **351,** 25-37.

Boehm S. (1999). ATP Stimulates Sympathetic Transmitter Release via Presynaptic P2X Purinoceptors. *The Journal of Neuroscience* **19,** 737-746.

Boehm S. (2003). Signalling via nucleotide receptors in the sympathetic nervous system. *Drug News and perspectives* **16,** 141.

Brawley L, Itoh S, Torrens C, Barker A, Bertram C, Poston L & Hanson M. (2003). Dietary protein restriction in pregnancy induces hypertension and vascular defects in rat male offspring. *Pediatr Res* **54,** 83-90.

Brion M-JA, Leary SD, Smith GD, McArdle HJ & Ness AR. (2008). Maternal anemia, iron intake in pregnancy, and offspring blood pressure in the Avon Longitudinal Study of Parents and Children. *The American Journal of Clinical Nutrition* **88,** 1126-1133.

Brown GC & Cooper CE. (1994). Nanomolar concentrations of nitric oxide reversibly inhibit synaptosomal respiration by competing with oxygen at cytochrome oxidase. *FEBS Letters* **356,** 295-298.

Brunelle JK, Bell EL, Quesada NM, Vercauteren K, Tiranti V, Zeviani M, Scarpulla RC & Chandel NS. (2005). Oxygen sensing requires mitochondrial ROS but not oxidative phosphorylation. *Cell Metab* **1,** 409-414.

Bryan PT & Marshall JM. (1999a). Adenosine receptor subtypes and vasodilatation in rat skeletal muscle during systemic hypoxia: a role for A1 receptors. *J Physiol* **514,** 151-162.

Bryan PT & Marshall JM. (1999b). Cellular mechanisms by which adenosine induces vasodilatation in rat skeletal muscle: significance for systemic hypoxia. *J Physiol* **514,** 163-175.

Buckley NM, Gootman PM, Gootman N, Reddy GD, Weaver LC & Crane LA. (1976). Age-Dependent Cardiovascular Effects of Afferent Stimulation in Neonatal Pigs. *Neonatology* **30,** 268-279.

Burnstock G. (1976). Purinergic receptors. *Journal of Theoretical Biology* **62,** 491-503.

Burnstock G. (1990a). Changes in expression of autonomic nerves in aging and disease. *Journal of the Autonomic Nervous System* **30,** S25-S34.

Burnstock G. (1990b). Noradrenaline and ATP as cotransmitters in sympathetic nerves. *Neurochem Int* **17,** 357-368.

Burnstock G. (2009a). Purinergic cotransmission. *Experimental Physiology* **94,** 20-24.

Burnstock G. (2009b). Purinergic signalling: past, present and future. *Brazilian Journal of Medical and Biological Research* **42,** 3-8.

Burnstock G, Douarin ML, Gershon M, Teitleman G, Rothman T, Gootman P, Gootman N, Turlapaty A, Bevan JA, Bevan R, Johnson M, Iacovitte L, Higgins D, Bunge R, Burton H, Potter D, Black I, Bohn M, Jonakait G & Kessler J. (1981). Development of the Autonomic Nervous System. In *Ciba Foundatation Symposium*, ed. Elliott K & Lawrenson G. Pitman Books Ltd., London.

Burnstock G & Holman ME. (1960). Autonomic Nerve-Smooth Muscle Transmission. *Nature* **187,** 951-952.

Burnstock G & Robinson P. (1967). Localization of catecholamines and acetylcholinesterase in autonomic nerves. *Circ Res* **21,** 43-55.

Byrne CD & Phillips DI. (2000). Fetal origins of adult disease: epidemiology and mechanisms. *Journal of Clinical Pathology* **53,** 822-828.

Cai H & Harrison DG. (2000). Endothelial Dysfunction in Cardiovascular Diseases: The Role of Oxidant Stress. *Circ Res* **87,** 840-844.

Cajal S. (1905). Las células del gran simpático del hombre adulto. *Trab del Lab de Invest biol* **4,** 2.

Camm EJ & Giussani DA. (2010). Maternal vitamin C administration prevents memory impairment in adulthood following prenatal hypoxia. In *The Developmental Origins of Health and Disease*, pp. P-2A027.

Carvajal JA, Germain AM, Huidobro-Toro JP & Weiner CP. (2000). Molecular mechanism of cGMP-mediated smooth muscle relaxation. *Journal of Cellular Physiology* **184,** 409-420.

Chamley JH, Mark GE, Campbell GR & Burnstock G. (1972). Sympathetic ganglia in culture. *I Neurons Z Zellforsch* **135,** 287-314.

Chen C-A, Druhan LJ, Varadharaj S, Chen Y-R & Zweier JL. (2008). Phosphorylation of Endothelial Nitric-oxide Synthase Regulates Superoxide Generation from the Enzyme. *J Biol Chem* **283,** 27038-27047.

Chun LLY & Patterson PH. (1977). Role of nerve growth factor in development of rat sympathetic neurones in vitro. *J Cell Biol* **75,** 712-718.

Chung TKH, Lau TK, Yip ASK, Chiu HFK & Lee DTS. (2001). Antepartum Depressive Symptomatology Is Associated With Adverse Obstetric and Neonatal Outcomes. *Psychosomatic Medicine* **63,** 830-834.

Cleeter MWJ, Cooper JM, Darley-Usmar VM, Moncada S & Schapira AHV. (1994). Reversible inhibition of cytochrome c oxidase, the terminal enzyme of the mitochondrial respiratory chain, by nitric oxide: Implications for neurodegenerative diseases. *FEBS Letters* **345,** 50-54.

Clementi E, Brown GC, Foxwell N & Moncada S. (1999). On the mechanism by which vascular endothelial cells regulate their oxygen consumption. *Proceedings of the National Academy of Sciences of the United States of America* **96,** 1559-1562.

Cochard P, Goldstein M & Black IB. (1978). Ontogenetic appearance and disappearance of tyrosine hydroxylase and catecholamines in the rat embryo. *Proceedings of the National Academy of Sciences* **75,** 2986-2990.

Cochard P, Goldstein M & Black IB. (1979). Initial development of the noradrenergic phenotype in autonomic neuroblasts of the rat embryo in vivo. *Developmental Biology* **71,** 100-114.

Coney AM & Marshall JM. (1998). Role of adenosine and its receptors in the vasodilatation induced in the cerebral cortex of the rat by systemic hypoxia. *The Journal of Physiology* **509,** 507-518.

Coney AM & Marshall JM. (2003). Contribution of adenosine to the depression of sympathetically evoked vasoconstriction induced by systemic hypoxia in the rat. *J Physiol* **549,** 613-623.

Coney AM & Marshall JM. (2007). Contribution of alpha2-adrenoceptors and Y1 neuropeptide Y receptors to the blunting of sympathetic vasoconstriction induced by systemic hypoxia in the rat. *J Physiol* **582,** 1349-1359.

Coney AM & Marshall JM. (2010). Effects of maternal hypoxia on muscle vasodilatation evoked by acute systemic hypoxia in adult rat offspring: changed roles of adenosine and A1 receptors. *The Journal of Physiology* **588,** 5115-5125.

Cowen T, Haven AJ, Wen-Qin C, Gallen DD, Franc F & Burnstock G. (1982). Development and ageing of perivascular adrenergic nerves in the rabbit. A quantitative fluorescence histochemical study using image analysis. *Journal of the Autonomic Nervous System* **5,** 317-336.

Cunnane TC & Stjärne L. (1984). Transmitter secretion from individual varicosities of guinea-pig and mouse vas deferens: Highly intermittent and monoquantal. *Neuroscience* **13,** 1-20.

Daly MD. (1997). *Peripheral arterial chemorecetpors and respiratory-cardiovascular integration*. Clarendon Press, Oxford.

Dampney RA. (1994). Functional organization of central pathways regulating the cardiovascular system. *Physiological Reviews* **74,** 323-364.

Dampney RAL, Goodchild AK, Robertson LG & Montgomery W. (1982). Role of ventrolateral medulla in vasomotor regulation: a correlative anatomical and physiological study. *Brain Research* **249,** 223-235.

Dart C & Standen NB. (1993). Adenosine-activated potassium current in smooth muscle cells isolated from the pig coronary artery. *The Journal of Physiology* **471,** 767-786.

Davy KP, Seals DR & Tanaka H. (1998). Augmented Cardiopulmonary and Integrative Sympathetic Baroreflexes but Attenuated Peripheral Vasoconstriction With Age. *Hypertension* **32,** 298-304.

Dawson TL, Gores GJ, Nieminen AL, Herman B & Lemasters JJ. (1993). Mitochondria as a source of reactive oxygen species during reductive stress in rat hepatocytes. *AJP - Cell Physiology* **264,** C961-967.

de Wit C, von Bismarck P & Pohl U. (1994). Synergistic action of vasodilators that increase cGMP and cAMP in the hamster cremaster microcirculation. *Cardiovasc Res* **28,** 1513-1518.

Dermietzel R. (1971). Electronenmikroskopische untersuchung uber die innervation der pars pylorica de mausemagens. *Z Mikrosk anat Forsch* **84,** 225-256.

DhÌtal KK, Gerli R, Lincoln J, Milner P, Tanganelli P, Weber G, Fruschelli C & Burnstock G. (1988). Increased density of perivascular nerves to the major cerebral vessels of the spontaneously hypertensive rat: differential changes in noradrenaline and neuropeptide Y during development. *Brain Research* **444,** 33-45.

Dinenno FA, Dietz NM & Joyner MJ. (2002). Aging and Forearm Postjunctional Œ±-Adrenergic Vasoconstriction in Healthy Men. *Circulation* **106,** 1349-1354.

Dinenno FA, Jones PP, Seals DR & Tanaka H. (2000). Age-associated arterial wall thickening is related to elevations in sympathetic activity in healthy humans. *American Journal of Physiology - Heart and Circulatory Physiology* **278,** H1205-H1210.

Ding Y, Li Y-L, Zimmerman MC, Davisson RL & Schultz HD. (2009a). Role of CuZn superoxide dismutase on carotid body function in heart failure rabbits. *Cardiovascular Research* **81,** 678-685.

Ding Y, Li Y-L, Zimmerman MC & Schultz HD. (2009b). Elevated Mitochondrial Superoxide Contributes to Enhanced Chemoreflex in Heart Failure Rabbits. *Am J Physiol Regul Integr Comp Physiol*.

Docherty JR & McGrath JC. (1980). A comparison of pre- and post-junctional potencies of several alpha-adrenoceptor agonists in the cardiovascular system and anococcygeus muscle of the rat. *Naunyn-Schmiedeberg's Archives of Pharmacology* **312,** 107-116.

Donoghue S, Felder RB, Jordan D & Spyer KM. (1984). The central projections of carotid baroreceptors and chemoreceptors in the cat: a neurophysiological study. *The Journal of Physiology* **347,** 397-409.

Donoso MV, Brown N, Carrasco C, Cortes V, Fournier A & Huidobro-Toro JP. (1997). Stimulation of the Sympathetic Perimesenteric Arterial Nerves Releases Neuropeptide Y Potentiating the Vasomotor Activity of Noradrenaline: Involvement of Neuropeptide Y-Y1 Receptors. *Journal of Neurochemistry* **69,** 1048-1059.

Drew G & Whiting S. (1979). Evidence for two distinct types of postsynaptic Alpha-adrenoreceptor in vascular smooth muscle in vivo. *British Journal of Pharmacology* **67,** 207-215.

Eden GJ & Hanson MA. (1987a). Effects of chronic hypoxia from birth on the ventilatory response to acute hypoxia in the newborn rat. *The Journal of Physiology* **392,** 11-19.

Eden GJ & Hanson MA. (1987b). Maturation of the respiratory response to acute hypoxia in the newborn rat. *The Journal of Physiology* **392,** 1-9.

Edmunds NJ & Marshall JM. (2001). Oxygen delivery and oxygen consumption in rat hindlimb during systemic hypoxia: role of adenosine. *The Journal of Physiology* **536,** 927-935.

Edmunds NJ, Moncada S & Marshall JM. (2003). Does nitric oxide allow endothelial cells to sense hypoxia and mediate hypoxic vasodilatation? in vivo and in vitro studies. *J Physiol* **546,** 521-527.

Edvinsson L, Owman C & Sjorberg N-O. (1976). Autonomic nerves, mast cells, and amine receptors in human brain vessels. A histochemical and pharmacological study. *Brain Research* **115,** 377-393.

Edwards LJ, Simonetta G, Owens JA, Robinson JS & McMillen IC. (1999). Restriction of placental and fetal growth in sheep alters fetal blood pressure responses to angiotensin II and captopril. *The Journal of Physiology* **515,** 897-904.

Ekelund U & Erlinge D. (1997). In vivo receptor characterization of neuropeptide Y-induced effects in consecutive vascular sections of cat skeletal muscle. *British Journal of Pharmacology* **120,** 387-392.

Eldridge FL, Millhorn DE & Kiley JP. (1984). Respiratory effects of a long-acting analog of adenosine. *Brain Research* **301,** 273-280.

Eskurza I, Myerburgh LA, Kahn ZD & Seals DR. (2005). Tetrahydrobiopterin augments endothelium-dependent dilatation in sedentary but not in habitually exercising older adults. *The Journal of Physiology* **568,** 1057-1065.

Euler USv. (1946). A Specific Sympathomimetic Ergone in Adrenergic Nerve Fibres (Sympathin) and its Relations to Adrenaline and Nor-Adrenaline. *Acta Physiologica Scandinavica* **12,** 73-97.

Fang Q, Guo J, Chang M, Chen L-x, Chen Q & Wang R. (2005). Neuropeptide FF receptors exert contractile activity via inhibition of nitric oxide release in the mouse distal colon. *Peptides* **26,** 791-797.

Fang Q, Guo J, He F, Peng Y-l, Chang M & Wang R. (2006). In vivo inhibition of neuropeptide FF agonism by BIBP3226, an NPY Y1 receptor antagonist. *Peptides* **27,** 2207-2213.

Folkow B & Svanborg A. (1993). Physiology of cardiovascular aging. *Physiological Reviews* **73,** 725-764.

Ford CP, Wong KV, Lu VB, de Chaves EP & Smith PA. (2008). Differential neurotrophic regulation of sodium and calcium channels in an adult sympathetic neuron. *Journal of Neurophysiology* **99,** 1319-1332.

Francis N, Farinas I, Brennan C, Rivas-Plata K, Backus C, Reichardt L & Landis S. (1999). NT-3, like NGF, is required for survival of sympathetic neurons, but not their precursors. *Developmental Biology* **210,** 411-427.

Franco MCP, Akamine EH, Reboucas N, Carvalho MHC, Tostes RCA, Nigro D & Fortes ZB. (2007). Long-term effects of intrauterine malnutrition on vascular function in female offspring: Implications of oxidative stress. *Life Sci* **80,** 709-715.

Franco MdCP, Akamine EH, Di Marco GS, Casarini DE, Fortes ZB, Tostes RCA, Carvalho MHC & Nigro D. (2003a). NADPH oxidase and enhanced superoxide generation in intrauterine undernourished rats: involvement of the renin-angiotensin system. *Cardiovasc Res* **59,** 767-775.

Franco MdCP, Nigro D, Fortes ZB, Tostes RCA, Carvalho MHC, Lucas SRR, Gomes GN, Coimbra TM & Gil FZ. (2003b). Intrauterine undernutrition; renal and vascular origin of hypertension. *Cardiovascular Research* **60,** 228-234.

Frank L, Wood DL & Roberts RJ. (1978). Effect of diethyldithiocarbamate on oxygen toxicity and lung enzyme activity in immature and adult rats. *Biochemical Pharmacology* **27,** 251-254.

Frank SM, Raja SN, Bulcao C & Goldstein DS. (2000). Age-related thermoregulatory differences during core cooling in humans. *American Journal of Physiology - Regulatory, Integrative and Comparative Physiology* **279,** R349-R354.

Franks PW, Hanson RL, Knowler WC, Sievers ML, Bennett PH & Looker HC. (2010). Childhood Obesity, Other Cardiovascular Risk Factors, and Premature Death. *New England Journal of Medicine* **362,** 485-493.

Fredholm BB, Irenius E, Kull B & Schulte G. (2001). Comparison of the potency of adenosine as an agonist at human adenosine receptors expressed in Chinese hamster ovary cells. *Biochemical Pharmacology* **61,** 443-448.

Fried G. (1980). Small noradrenergic storage vesicles isolated from the rat vas deferens - biochemical and morphological characterisation. *Acta Physiologica Scandinavica* **Suppl 493,** 1-28.

Fried G, Terenius L, Hokfelt T & Goldstein M. (1985). Evidence for differential localization of noradrenaline and neuropeptide Y in neuronal storage vesicles isolated from rat vas deferens. *The Journal of Neuroscience* **5,** 450-458.

Fukai T, Siegfried MR, Ushio-Fukai M, Cheng Y, Kojda G & Harrison DG. (2000). Regulation of the vascular extracellular superoxide dismutase by nitric oxide and exercise training. *J Clin Invest* **105,** 1631-1639.

Furness JB & Costa M. (1975). The use of glyoxylic acid for the fluorescence histochemical demonstration of peripheral stores of noradrenaline and 5-hydroxytryptamine in whole mounts. *Histochemistry* **41,** 335-352.

Gagnon R. (2003). Placental insufficiency and its consequences. *European Journal of Obstetrics & Gynecology and Reproductive Biology* **110,** S99-S107.

Gagnon R, Challis J, Johnston L & Fraher L. (1994). Fetal endocrine responses to chronic placental embolization in the late-gestation ovine fetus. *American Journal of Obstetrics and Gynecology* **170,** 929-938.

Gebber GL. (1980). Central oscillators responsible for sympathetic nerve discharge. *American Journal of Physiology - Heart and Circulatory Physiology* **239,** H143-H155.

Geelhoed JJM, Fraser A, Tilling K, Benfield L, Davey Smith G, Sattar N, Nelson SM & Lawlor DA. (2010). Preeclampsia and gestational hypertension are associated with childhood blood pressure independently of family adiposity measures / clinical perspective. *Circulation* **122,** 1192-1199.

Giussani DA, Salinas CE, Villena M & Blanco CE. (2007). The role of oxygen in prenatal growth: studies in the chick embryo. *The Journal of Physiology* **585,** 911-917.

Giussani DA, Spencer JA & Hanson MA. (1994). Fetal cardiovascular reflex responses to hypoxaemia. *Fetal and Maternal Medicine Review* **6,** 17-39.

Gootman N, Gootman P, Buckley N, Cohen M, Levine M & Spielberg R. (1972). Central vasomotor regulation in the newborn piglet Sus scrofa. *American Journal of Physiology* **222,** 994-999.

Gootman PM, Buckley NM, Gootman N, Crane LA & Buckley BJ. (1978). Integrated cardiovascular responses to combined somatic afferent stimulation in newborn piglets. *Neonatology* **34,** 187-198.

Goso Y, Asanoi H, Ishise H, Kameyama T, Hirai T, Nozawa T, Takashima S, Umeno K & Inoue H. (2001). Respiratory modulation of muscle sympathetic nerve activity in patients with chronic heart failure. *Circulation* **104,** 418-423.

Gray SD. (1973). Rat spinotrapezius muscle preparation for microscopic observation of the terminal vascular bed. *Microvascular Research* **5,** 395-400.

Guyenet PG. (2000). Neural structures that mediate sympathoexcitation during hypoxia. *Respir Physiol* **121,** 147-162.

Guyenet PG, Koshiya N, Huangfu D, Verberne AJ & Riley TA. (1993). Central respiratory control of A5 and A6 pontine noradrenergic neurons. *American Journal of Physiology - Regulatory, Integrative and Comparative Physiology* **264,** R1035-R1044.

Habler HJ, Janig W, Krummel M & Peters OA. (1993). Respiratory modulation of the activity in postganglionic neurons supplying skeletal muscle and skin of the rat hindlimb. *Journal of Neurophysiology* **70,** 920-930.

Habler HJ, Janig W, Krummel M & Peters OA. (1994). Reflex patterns in postganglionic neurons supplying skin and skeletal muscle of the rat hindlimb. *Journal of Neurophysiology* **72,** 2222-2236.

Hamza I & Gitlin J. (2002). Copper chaperones for Cytochrome c Oxidase and human disease. *Journal of bbioenergetics and biomembranes* **34,** 381-388.

Hansen J, Sander M & Thomas GD. (2000). Metabolic modulation of sympathetic vasoconstriction in exercising skeletal muscle. *Acta Physiologica Scandinavica* **168,** 489-503.

Hansen J, Thomas GD, Jacobsen TN & Victor RG. (1994). Muscle metaboreflex triggers parallel sympathetic activation in exercising and resting human skeletal muscle. *American Journal of Physiology - Heart and Circulatory Physiology* **266,** H2508-H2514.

Hanson MA, Kumar P & Williams BA. (1989). The effect of chronic hypoxia upon the development of respiratory chemoreflexes in the newborn kitten. *J Physiol* **411,** 563-574.

Harrison D, Griendling KK, Landmesser U, Hornig B & Drexler H. (2003). Role of oxidative stress in atherosclerosis. *The American Journal of Cardiology* **91,** 7-11.

Hasenfuss G. (1998). Animal models of human cardiovascular disease, heart failure and hypertrophy. *Cardiovascular Research* **39,** 60-76.

Hauton D & Ousley V. (2009). Prenatal hypoxia induces increased cardiac contractility on a background of decreased capillary density. *BMC Cardiovascular Disorders* **9,** 1.

Hébert MT & Marshall JM. (1988). Direct observations of the effects of baroreceptor stimulation on skeletal muscle circulation of the rat. *The Journal of Physiology* **400,** 45-59.

Heistad DD & Wheeler RC. (1970). Effect of acute hypoxia on vascular responsiveness in man: I. Responsiveness to lower body negative pressure and ice on the forehead. II. Responses to norepinephrine and angiotensin. III. Effect of hypoxia and hypocapnia. *The Journal of Clinical Investigation* **49,** 1252-1265.

Heitzer T, Schlinzig T, Krohn K, Meinertz T & Menzel T. (2001). Endothelial Dysfunction, Oxidative Stress, and Risk of Cardiovascular Events in Patients With Coronary Artery Disease. *Circulation* **104,** 2673-2678.

Herrera EA, Pulgar VM, Riquelme RA, Sanhueza EM, Reyes RV, Ebensperger G, Parer JT, Valdez EA, Giussani DA, Blanco CE, Hanson MA & Llanos AJ. (2007). High-altitude chronic hypoxia during gestation and after birth modifies cardiovascular responses in newborn sheep. *AJP - Regulatory, Integrative and Comparative Physiology* **292,** R2234-2240.

Hodges GJ, Jackson DN, Mattar L, Johnson JM & Shoemaker JK. (2009). Neuropeptide Y and neurovascular control in skeletal muscle and skin. *Am J Physiol Regul Integr Comp Physiol* **297,** R546-555.

Hofmann F, Ammendola A & Schlossmann J. (2000). Rising behind NO: cGMP-dependent protein kinases. *Journal of Cell Science* **113,** 1671-1676.

Holland J, Kirkwood A. Pritchard, Miguel A. Pappolla, Michael S. Wolin, Nancy J. Rogers & Michael B. Stemerman. (1990). Bradykinin induces superoxide anion release from human endothelial cells. *Journal of Cellular Physiology* **143,** 21-25.

Horeyseck G & Jänig W. (1974). Reflexes in postganglionic fibres within skin and muscle nerves after mechanical non-noxious stimulation of skin. *Experimental Brain Research* **20,** 115-123.

Hudson S, Johnson CD & Marshall JM. (2011). Changes in muscle sympathetic nerve activity and vascular responses evoked in the spinotrapezius muscle of the rat by systemic hypoxia. *The Journal of Physiology* **589,** 2401-2414.

Huxley RR, Shiell AW & Law CM. (2000). The role of size at birth and postnatal catch-up growth in determining systolic blood pressure: a systematic review of the literature. *Journal of Hypertension* **18,** 815-831.

IJzerman RG, Stehouwer CDA, de Geus EJ, van Weissenbruch MM, Delemarre-van de Waal HA & Boomsma DI. (2003). Low Birth Weight Is Associated With Increased Sympathetic Activity: Dependence on Genetic Factors. *Circulation* **108,** 566-571.

Jackson DN, Ellis CG & Shoemaker JK. (2010). Estrogen modulates the contribution of neuropeptide Y to baseline hindlimb blood flow control in female Sprague-Dawley rats. *American Journal of Physiology - Regulatory, Integrative and Comparative Physiology* **298,** R1351-R1357.

Jackson DN, Noble EG & Shoemaker JK. (2004). Y1- and Alpha-1-receptor control of basal hindlimb vascular tone. *Am J Physiol Regul Integr Comp Physiol* **287,** R228-233.

Jackson MJ, Pye D & Palomero J. (2007). The production of reactive oxygen and nitrogen species by skeletal muscle. *Journal of Applied Physiology* **102,** 1664-1670.

Janig W. (1985). Organisation of the lumbar sympathetic outflow to skeletal muscle and skin of the cat hindlimb and tail. *Reviews of Physiology, Biochemistry and Pharmacology* **102,** 119-213.

Jayet P-Y, Rimoldi SF, Stuber T, Salmon CS, Hutter D, Rexhaj E, Thalmann S, Schwab M, Turini P, Sartori-Cucchia C, Nicod P, Villena M, Allemann Y,

Scherrer U & Sartori C. (2010). Pulmonary and Systemic Vascular Dysfunction in Young Offspring of Mothers With Preeclampsia. *Circulation* **122,** 488-494.

Johnson CD, Coney AM & Marshall JM. (2001). Roles of norepinephrine and ATP in sympathetically evoked vasoconstriction in rat tail and hindlimb in vivo. *Am J Physiol Heart Circ Physiol* **281,** H2432-2440.

Johnson CD & Gilbey MP. (1994). Sympathetic activity recorded from the rat caudal ventral artery in vivo. *J Physiol* **476,** 437-442.

Johnson CD & Gilbey MP. (1996). On the dominant rhythm in the discharges of single postganglionic sympathetic neurones innervating the rat tail artery. *J Physiol* **497,** 241-259.

Jonakait GM, Wolf J, Cochard P, Goldstein M & Black IB. (1979). Selective loss of noradrenergic phenotypic characters in neuroblasts of the rat embryo. *Proceedings of the National Academy of Sciences* **76,** 4683-4686.

Jones PP, Shapiro LF, Keisling GA, Jordan J, Shannon JR, Quaife RA & Seals DR. (2001). Altered autonomic support of arterial blood pressure with age in healthy men. *Circulation* **104,** 2424-2429.

Jung O, Marklund SL, Geiger H, Pedrazzini T, Busse R & Brandes RP. (2003). Extracellular Superoxide Dismutase Is a Major Determinant of Nitric Oxide Bioavailability: In Vivo and Ex Vivo Evidence From ecSOD-Deficient Mice. *Circulation Research* **93,** 622-629.

Kanbar R, Depuy SD, West GH, Stornetta RL & Guyenet PG. (2011). Regulation of visceral sympathetic tone by A5 noradrenergic neurons in rodents. *The Journal of Physiology* **589,** 903-917.

Kass DA, Takimoto E, Nagayama T & Champion HC. (2007). Phosphodiesterase regulation of nitric oxide signaling. *Cardiovascular Research* **75,** 303-314.

Kayyali US, Donaldson C, Huang H, Abdelnour R & Hassoun PM. (2001). Phosphorylation of Xanthine Dehydrogenase/Oxidase in Hypoxia. *J Biol Chem* **276,** 14359-14365.

Kennedy C, Saville VL & Burnstock G. (1986a). The contributions of noradrenaline and ATP to the responses of the rabbit central ear artery to sympathetic nerve stimulation depend on the parameters of stimulation. *European Journal of Pharmacology* **122,** 291-300.

Kennedy C, Saville VL & Burnstock G. (1986b). The contributions of noradrenaline and ATP to the responses of the rabbit central ear artery to sympathetic nerve stimulation depend on the parameters of stimulation. *Eur J Pharmacol* **122,** 291-300.

Khan IM, Gilbert SJ, Caterson B, Sandell LJ & Archer CW. (2008). Oxidative stress induces expression of osteoarthritis markers procollagen IIA and 3B3(-) in adult bovine articular cartilage. *Osteoarthritis and Cartilage* **16,** 698-707.

Klinger M, Freissmuth M & Nanoff C. (2002). Adenosine receptors: G protein-mediated signalling and the role of accessory proteins. *Cellular Signalling* **14,** 99-108.

Kobinger W & Pichler L. (1981). [alpha]2-adrenoceptor agonistic effect of B-HT 920 in isolated perfused hindquarters of rats. *European Journal of Pharmacology* **76,** 101-105.

Kondo M, Miyazaki T, Fujiwara T, Yano A & Tabei R. (1992). Increased density of fluorescent adrenergic fibers around the middle cerebral arteries of stroke-prone spontaneously hypertensive rats. *Virchows Archiv B Cell Pathology Zell-pathologie* **61,** 117-122.

Kontos HA, Wei EP, Raper AJ, Rosenblum WI, Navari RM & Patterson JL, Jr. (1978). Role of tissue hypoxia in local regulation of cerebral microcirculation. *Am J Physiol Heart Circ Physiol* **234,** H582-591.

Koshiya N & Guyenet PG. (1994). Role of the pons in the carotid sympathetic chemoreflex. *American Journal of Physiology - Regulatory, Integrative and Comparative Physiology* **267,** R508-R518.

Koshiya N, Huangfu D & Guyenet PG. (1993). Ventrolateral medulla and sympathetic chemoreflex in the rat. *Brain Research* **609,** 174-184.

Kukreja RC, Kontos HA, Hess ML & Ellis EF. (1986). PGH synthase and lipoxygenase generate superoxide in the presence of NADH or NADPH. *Circulation Research* **59,** 612-619.

Kumar P & Bin-Jaliah I. (2007). Adequate stimuli of the carotid body: More than an oxygen sensor? *Respiratory Physiology & Neurobiology* **157,** 12-21.

Kumer SC & Vrana KE. (1996). Intricate Regulation of Tyrosine Hydroxylase Activity and Gene Expression. *Journal of Neurochemistry* **67,** 443-462.

Kuntz A. (1953). *The Autonomic Nervous System*. Lea & Febiger, Philidelphia.

Kuo LE & Zukowska Z. (2007). Stress, NPY and vascular remodeling: Implications for stress-related diseases. *Peptides* **28,** 435-440.

Lagercrantz H & Stjarne L. (1974). Evidence that most noradrenaline is stored without ATP in sympathetic large dense core nerve vesicles. *Nature* **249,** 843-845.

Lakatta EG. (2002). Age-associated Cardiovascular Changes in Health: Impact on Cardiovascular Disease in Older Persons. *Heart Failure Reviews* **7,** 29-49.

Landauer RC, Pepper DR & Kumar P. (1995). Effect of chronic hypoxaemia from birth upon chemosensitivity in the adult rat carotid body in vitro. *The Journal of Physiology* **485,** 543-550.

Landmesser U, Dikalov S, Price SR, McCann L, Fukai T, Holland SM, Mitch WE & Harrison DG. (2003). Oxidation of tetrahydrobiopterin leads to uncoupling of endothelial cell nitric oxide synthase in hypertension. *J Clin Invest* **111,** 1201-1209.

Lang JA, Holowatz LA & Kenney WL. (2009). Local tetrahydrobiopterin administration augments cutaneous vasoconstriction in aged humans. *The Journal of Physiology* **587,** 3967-3974.

Langley SC & Jackson AA. (1994). Increased systolic blood pressure in adult rats induced by fetal exposure to maternal low protein diets. *Clin Sci* **86,** 217.

Larsen BT, Bubolz AH, Mendoza SA, Pritchard KA, Jr. & Gutterman DD. (2009). Bradykinin-Induced Dilation of Human Coronary Arterioles Requires NADPH Oxidase-Derived Reactive Oxygen Species. *Arteriosclerosis, Thrombosis, and Vascular Biology* **29,** 739-745.

Law CM, Barker DJ, Bull AR & Osmond C. (1991). Maternal and fetal influences on blood pressure. *Archives of Disease in Childhood* **66,** 1291-1295.

Lei SB, Dryden WF & Smith PA. (2001). Nerve growth factor regulates sodium but not potassium channel currents in sympathetic B neurons of adult bullfrogs. *Journal of Neurophysiology* **86,** 641-650.

Linder L, Lautenschlager BM & Haefeli WE. (1996). Subconstrictor Doses of Neuropeptide Y Potentiate {alpha}1-Adrenergic Venoconstriction In Vivo. *Hypertension* **28,** 483-487.

Liu J, Shigenaga MK, Liang-Junyan Y, Mori A & Ames BN. (1996). Antioxidant Activity of Diethyldithiocarbamate. *Free Radical Research* **24,** 461-472.

Llanos AbJ, Riquelme RA, Sanhueza EM, Hanson MA, Blanco CE, Parer JT, Herrera EA, Pulgar VM, Reyes RV, Cabello G & Giussani DA. (2003). The Fetal Llama versus the Fetal Sheep: Different Strategies to Withstand Hypoxia. *High Altitude Medicine & Biology* **4,** 193-202.

Loewy AD. (1990). Central Autonomic Pathways. In *Central Regulation of Autonomic Functions*, ed. Loewy AD & Spyer KM, pp. 88-103. Oxford University Press, New York.

Louey S & Thornburg KL. (2005). The prenatal environment and later cardiovascular disease. *Early Human Development* **81,** 745-751.

Lundberg JM. (1996). Pharmacology of cotransmission in the autonomic nervous system: integrative aspects on amines, neuropeptides, adenosine triphosphate, amino acids and nitric oxide. *Pharmacological Reviews* **48,** 113-178.

Lundberg JM, Rudehill A, Sollevi A, Fried G & Wallin G. (1989). Co-release of neuropeptide Y and noradrenaline from pig spleen in vivo: Importance of subcellular storage, nerve impulse frequency and pattern, feedback regulation and resupply by axonal transport. *Neuroscience* **28,** 475-486.

Lundberg JM, Terenius L, Hokfelt T, Martling CR, Tatemoto K, Mutt V, Polak J, Bloom S & Goldstein M. (1982). Neuropeptide Y (NPY)-like immunoreactivity in peripheral noradrenergic neurons and effects of NPY on sympathetic function. *Acta Physiologica Scandinavica* **116,** 477-480.

Luther JA & Birren SJ. (2009). p75 and TrkA Signaling Regulates Sympathetic Neuronal Firing Patterns via Differential Modulation of Voltage-Gated Currents. *J Neurosci* **29,** 5411-5424.

Lynge & Hellsten. (2000). Distribution of adenosine A1, A2A and A2B receptors in human skeletal muscle. *Acta Physiologica Scandinavica* **169,** 283-290.

Macefield VG & Wallin BG. (1999). Firing properties of single vasoconstrictor neurones in human subjects with high levels of muscle sympathetic activity. *The Journal of Physiology* **516,** 293-301.

MacLean DA, Sinoway LI & Leuenberger U. (1998). Systemic Hypoxia Elevates Skeletal Muscle Interstitial Adenosine Levels in Humans. *Circulation* **98,** 1990-1992.

Malmström RE, Balmér KC & Lundberg JM. (1997). The neuropeptide Y (NPY) Y1 receptor antagonist BIBP 3226: effects on vascular responses to exogenous and endogenous NPY in the pig in vivo. *British Journal of Pharmacology* **121,** 595-603.

Malpas SC. (1998). The rhythmicity of sympathetic nerve activity. *Progress in Neurobiology* **56,** 65-96.

Marko SB & Damon DH. (2008). VEGF promotes vascular sympathetic innervation. *Am J Physiol Heart Circ Physiol* **294,** H2646-2652.

Markwald RR, Kirby BS, Crecelius AR, Carlson RE, Voyles WF & Dinenno FA. (2011). Combined inhibition of nitric oxide and vasodilating prostaglandins abolishes forearm vasodilatation to systemic hypoxia in healthy humans. *The Journal of Physiology* **589,** 1979-1990.

Marshall JM. (1982). The influence of the sympathetic nervous system on individual vessels of the microcirculation of skeletal muscle of the rat. *The Journal of Physiology* **332,** 169-186.

Marshall JM. (1987). Analysis of cardiovascular responses evoked following changes in peripheral chemoreceptor activity in the rat. *The Journal of Physiology* **394,** 393-414.

Marshall JM. (1994). Peripheral chemoreceptors and cardiovascular regulation. *Physiological Reviews* **74,** 543-594.

Marshall JM & Metcalfe JD. (1988a). Analysis of the cardiovascular changes induced in the rat by graded levels of systemic hypoxia. *The Journal of Physiology* **407,** 385-403.

Marshall JM & Metcalfe JD. (1988b). Cardiovascular changes associated with augmented breaths in normoxia and hypoxia in the rat. *The Journal of Physiology* **400,** 15-27.

Matoba T & Hiroaki S. (2003). Hydrogen Peroxide Is an Endothelium-Derived Hyperpolarizing Factor in Animals and Humans. *Journal of Pharmacological Sciences* **92,** 1-6.

Matoba T, Shimokawa H, Nakashima M, Hirakawa Y, Mukai Y, Hirano K, Kanaide H & Takeshita A. (2000). Hydrogen peroxide is an endothelium-derived hyperpolarizing factor in mice. *J Clin Invest* **106,** 1521-1530.

McGillivray-Anderson K & Faber J. (1991). Effect of reduced blood flow on alpha 1- and alpha 2-adrenoceptor constriction of rat skeletal muscle microvessels. *Circ Res* **69,** 165-173.

Mcmillen IC & Robinson JS. (2005). Developmental Origins of the Metabolic Syndrome: Prediction, Plasticity, and Programming. *Physiological Reviews* **85,** 571-633.

Merkel LA, Lappe RW, Rivera LM, Cox BF & Perrone MH. (1992). Demonstration of vasorelaxant activity with an A1-selective adenosine agonist in porcine coronary artery: involvement of potassium channels. *Journal of Pharmacology and Experimental Therapeutics* **260,** 437-443.

Messina EJ, Sun D, Koller A, Wolin MS & Kaley G. (1992). Role of endothelium-derived prostaglandins in hypoxia-elicited arteriolar dilation in rat skeletal muscle. *Circulation Research* **71,** 790-796.

Mian R & Marshall JM. (1991). The role of adenosine in dilator responses induced in arterioles and venules of rat skeletal muscle by systemic hypoxia. *J Physiol* **443,** 499-511.

Miller FJ, Gutterman DD, Rios CD, Heistad DD & Davidson BL. (1998). Superoxide Production in Vascular Smooth Muscle Contributes to Oxidative Stress and Impaired Relaxation in Atherosclerosis. *Circulation Research* **82,** 1298-1305.

Mione MC, Dhital KK, Amenta F & Burnstock G. (1988). An increase in the expression of neuropeptidergic vasodilator, but not vasoconstrictor, cerebrovascular nerves in aging rats. *Brain Research* **460,** 103-108.

Miura H, Bosnjak JJ, Ning G, Saito T, Miura M & Gutterman DD. (2003). Role for Hydrogen Peroxide in Flow-Induced Dilation of Human Coronary Arterioles. *Circulation Research* **92,** e31-e40.

Miyahara H & Suzuki H. (1987). Pre- and post-junctional effects of adenosine triphosphate on noradrenergic transmission in the rabbit ear artery. *The Journal of Physiology* **389,** 423-440.

Moens AL & Kass DA. (2007). Therapeutic Potential of Tetrahydrobiopterin for Treating Vascular and Cardiac Disease. *Journal of Cardiovascular Pharmacology* **50,** 238-246.

Mollereau C, Mazarguil H, Marcus D, Quelven I, Kotani M, Lannoy V, Dumont Y, Quirion Rm, Detheux M, Parmentier M & Zajac J-M. (2002). Pharmacological characterization of human NPFF1 and NPFF2 receptors expressed in CHO cells by using NPY Y1 receptor antagonists. *European Journal of Pharmacology* **451,** 245-256.

Moore K, Dalley A & Agur A. (2009). Clinically Oriented Anatomy. In *Clinically oriented Anatomy*. Lippincott Williams & Wilkins.

Morii S, Ngai AC, Ko KR & Winn HR. (1987). Role of adenosine in regulation of cerebral blood flow: effects of theophylline during normoxia and hypoxia. *AJP - Heart and Circulatory Physiology* **253,** H165-175.

Morris JL. (1994). Roles of noradrenaline and ATP in sympathetic vasoconstriction of the guinea-pig main ear artery. *J Auton Nerv Syst* **49,** 217-225.

Morris JL. (1999). Cotransmission from sympathetic vasoconstrictor neurons to small cutaneous arteries in vivo. *American Journal of Physiology - Heart and Circulatory Physiology* **277,** H58-H64.

Morris MJ, Cox HS, Lambert GW, Kaye DM, Jennings GL, Meredith IT & Esler MD. (1997). Region-Specific Neuropeptide Y Overflows at Rest and During Sympathetic Activation in Humans. *Hypertension* **29,** 137-143.

Morrison JL. (2008). Sheep models of intrauterine growth restriction: Fetal adaptations and consequences. *Clinical and Experimental Pharmacology and Physiology* **35,** 730-743.

Morrison S, Milner T & Reis D. (1988). Reticulospinal vasomotor neurons of the rat rostral ventrolateral medulla: relationship to sympathetic nerve activity and the C1 adrenergic cell group. *The Journal of Neuroscience* **8,** 1286-1301.

Mortensen SP, Gonz√° lez-Alonso J, Damsgaard R, Saltin B & Hellsten Y. (2007). Inhibition of nitric oxide and prostaglandins, but not endothelial-derived hyperpolarizing factors, reduces blood flow and aerobic energy turnover in the exercising human leg. *The Journal of Physiology* **581,** 853-861.

Mortensen SP, Gonzalez-Alonso J, Bune LT, Saltin B, Pilegaard H & Hellsten Y. (2009a). ATP-induced vasodilation and purinergic receptors in the human leg: roles of nitric oxide, prostaglandins, and adenosine. *American Journal of Physiology - Regulatory, Integrative and Comparative Physiology* **296,** R1140-R1148.

Mortensen SP, Nyberg M, Thaning P, Saltin B & Hellsten Y. (2009b). Adenosine Contributes to Blood Flow Regulation in the Exercising Human Leg by Increasing Prostaglandin and Nitric Oxide Formation. *Hypertension* **53,** 993-999.

Morton JS, Rueda-Clausen CF & Davidge ST. (2010). Mechanisms of endothelium-dependent vasodilation in male and female, young and aged offspring born growth restricted. *AJP - Regulatory, Integrative and Comparative Physiology* **298,** R930-938.

Morton JS, Rueda-Clausen CF & Davidge ST. (2011). Flow-mediated vasodilation is impaired in adult rat offspring exposed to prenatal hypoxia. *Journal of Applied Physiology* **110,** 1073-1082.

Moudgil R, Michelakis ED & Archer SL. (2005). Hypoxic pulmonary vasoconstriction. *Journal of Applied Physiology* **98,** 390-403.

Mugge A, Elwell J, Peterson T, Hofmeyer T, Heistad D & Harrison D. (1991). Chronic treatment with polyethylene-glycolated superoxide dismutase partially restores endothelium-dependent vascular relaxations in cholesterol-fed rabbits. *Circ Res* **69,** 1293-1300.

Muldowney S & Faber J. (1991). Preservation of venular but not arteriolar smooth muscle alpha- adrenoceptor sensitivity during reduced blood flow. *Circ Res* **69,** 1215-1225.

Murai H, Takata S, Maruyama M, Nakano M, Kobayashi D, Otowa K-i, Takamura M, Yuasa T, Sakagami S & Kaneko S. (2006). The activity of a single muscle sympathetic vasoconstrictor nerve unit is affected by physiological stress in humans. *American Journal of Physiology - Heart and Circulatory Physiology* **290,** H853-H860.

Murotsuki J, Gagnon R, Matthews SG & Challis JRG. (1996). Effects of long-term hypoxemia on pituitary-adrenal function in fetal sheep. *Am J Physiol-Endocrinol Metab* **271,** E678-E685.

Nakazono K, Watanabe N, Matsuno K, Sasaki J, Sato T & Inoue M. (1991). Does superoxide underlie the pathogenesis of hypertension? *Proceedings of the National Academy of Sciences of the United States of America* **88,** 10045-10048.

Neylon M & Marshall JM. (1991). The role of adenosine in the respiratory and cardiovascular response to systemic hypoxia in the rat. *The Journal of Physiology* **440,** 529-545.

Nohl H & Hegner D. (1978). Do Mitochondria Produce Oxygen Radicals in vivo. *European Journal of Biochemistry* **82,** 563-567.

Norberg K & Hamberger B. (1964). The Sympathetic Adrenergic neuron. *Acta Physiologica Scandinavica* **63,** 1-42.

Notarius CF, Ando S, Rongen GA & Floras JS. (1999). Resting muscle sympathetic nerve activity and peak oxygen uptake in heart failure and normal subjects. *European Heart Journal* **20,** 880-887.

Nozik-Grayck E, Suliman HB & Piantadosi CA. (2005). Extracelluar superoxide dismutase. *The International Journal of Biochemistry and Cell Biology* **37,** 2466-2471.

Nuwayhid B, CR B, Su C, Bevan J & Assali N. (1975). Development of autonomic control of fetal circulation. *American Journal of Physiology* **228,** 337-344.

Nyberg M, Mortensen SP, Thaning P, Saltin B & Hellsten Y. (2010). Interstitial and Plasma Adenosine Stimulate Nitric Oxide and Prostacyclin Formation in Human Skeletal Muscle. *Hypertension* **56,** 1102-1108.

Ojeda N, Gridore D, Hennington B & Alexander B. (2008). Pre-natal programming of blood pressure and hypertension. *Rev Bras Hipertens* **15,** 3-8.

Olsson RA & Pearson JD. (1990). Cardiovascular purinoceptors. *Physiological Reviews* **70,** 761-845.

Omar NM & Marshall JM. (2010). Age-related changes in the sympathetic innervation of cerebral vessels and in carotid vascular responses to norepinephrine in the rat: in vitro and in vivo studies. *Journal of Applied Physiology* **109,** 314-322.

Orike N, Thrasivoulou C, Wrigley A & Cowen T. (2001). Differential regulation of survival and growth in adult sympathetic neurons: An invitro study of neurotrophin responsiveness. *Journal of Neurobiology* **47,** 295-305.

Owen D, Andrews MH & Matthews SG. (2005). Maternal adversity, glucocorticoids and programming of neuroendocrine function and behaviour. *Neuroscience & Biobehavioral Reviews* **29,** 209-226.

Page E. (1939). The relation between hydatid moles, relative ischemia of the gravid uterus, and the placental origin of eclampsia. *Am J Obstet Gynecol* **37,** 291-293.

Painter R. (2006). The pathophysiology of cardiovascular disease after prenatal exposure to maternal undernutrition during the Dutch famine. The Dtuch famine birth cohort study; Hunderwinter Study.

Painter RC, de Rooij SR, Bossuyt PM, Simmers TA, Osmond C, Barker DJ, Bleker OP & Roseboom TJ. (2006). Early onset of coronary artery disease after prenatal exposure to the Dutch famine. *American Journal of Clinical Nutrition* **84,** 322-327.

Paravicini TM & Touyz RM. (2006). Redox signaling in hypertension. *Cardiovascular Research* **71,** 247-258.

Paravicini TM & Touyz RM. (2008). NADPH Oxidases, Reactive Oxygen Species, and Hypertension. *Diabetes Care* **31,** S170-S180.

Paton JFR, Deuchars J, Li YW & Kasparov S. (2001). Properties of solitary tract neurones responding to peripheral arterial chemoreceptors. *Neuroscience* **105,** 231-248.

Pearson J, Brandeis L & Goldstein M. (1980). Appearance of Tyrosine Hydroxylase Immunoreactivity in the Human Embryo. *Developmental Neuroscience* **3,** 140-150.

Pernow J, Lundberg JM & Kaijser L. (1987). Vasoconstrictor effects in vivo and plasma disappearance rate of neuropeptide Y in man. *Life Sci* **40,** 47-54.

Pernow J, Schwieler J, Kahan T, Hjemdahl P, Oberle J, Wallin BG & Lundberg JM. (1989). Influence of sympathetic discharge pattern on norepinephrine and neuropeptide Y release. *American Journal of Physiology - Heart and Circulatory Physiology* **257,** H866-H872.

Peyronnet J, Roux JC, Tang LQ, Pequignot JM, Lagercrantz H & Dalmaz Y. (2000). Prenatal hypoxia impairs the postnatal development of neural and functional chemoafferent pathway in rat. *The Journal of Physiology* **524,** 525-537.

Porter JE, Balasubramaniam A, Abel PW & Conlon JM. (1994). Differential actions of lamprey peptide methionine-tyrosine at Y1 and Y2 neuropeptide Y receptors. *Regulatory Peptides* **54,** 489-493.

Postigo L, Heredia G, Illsley NP, Torricos T, Dolan C, Echalar L, Tellez W, Maldonado I, Brimacombe M, Balanza E, Vargas E & Zamudio S. (2009). Where the O2 goes to: preservation of human fetal oxygen delivery and consumption at high altitude. *The Journal of Physiology* **587,** 693-708.

Prabhakar NR. (2006). Oxygen sensing at the mammalian carotid body: why multiple O2 sensors and multiple transmitters? *Experimental Physiology* **91,** 17-23.

Pyner S, Coney A & Marshall J. (2003). The role of free radicals in the muscle vasodilatation of systemic hypoxia in the rat. *Exp Physiol* **88,** 733-740.

Queiroz G, Talaia C & Gonaalves J. (2003). ATP Modulates Noradrenaline Release by Activation of Inhibitory P2Y Receptors and Facilitatory P2X Receptors in the Rat Vas Deferens. *Journal of Pharmacology and Experimental Therapeutics* **307,** 809-815.

Qureshi N, Dayao E, Shirali S, Zukowska-Grojec Z & Hauser G. (1998). Endogenous neuropeptide Y mediates vasoconstriction during endotoxic and hemorrhagic shock. *Regulatory Peptides* **75-76,** 215-220.

Rajagopalan S, Kurz S, Munzel T, Tarpey M, Freeman BA, Griendling KK & Harrison DG. (1996). Angiotensin II-mediated hypertension in the rat increases vascular superoxide production via membrane NADH/NADPH oxidase activation - Contribution to alterations of vasomotor tone. *J Clin Invest* **97,** 1916-1923.

Ralevic V. (2002). Hypoxic vasodilatation: is an adenosine, prostaglandins, NO signalling cascade involved? *The Journal of Physiology* **544,** 2.

Rang H, Dale M, Ritter J & Moore P. (2003). Chemical mediators. In *Pharmacology*, 5 edn. Elsevier Churchill Livingston, London.

Raucher S & Dryer SE. (1995). Target-derived factors regulate the expresion of calcium activated pottasium currents in developing chick sympathetic neurones. *Journal of Physiology* **486,** 605-614.

Ray CJ, Abbas MR, Coney AM & Marshall JM. (2002). Interactions of adenosine, prostaglandins and nitric oxide in hypoxia-induced vasodilatation: in vivo and in vitro studies. *J Physiol* **544,** 195-209.

Ray CJ & Marshall JM. (2005). Measurement of nitric oxide release evoked by systemic hypoxia and adenosine from rat skeletal muscle in vivo. *J Physiol* **568,** 967-978.

Ray CJ & Marshall JM. (2006). The cellular mechanisms by which adenosine evokes release of nitric oxide from rat aortic endothelium. *The Journal of Physiology* **570,** 85-96.

Remensnyder JP, Mitchell JH & Sarnoff SJ. (1962). Functional sympatholysis during muscle activity: Observations on influence of the carotid sinus on oxygen uptake. *Circ Res* **11,** 370-380.

Richardson D, Tyra J & McCray A. (1992). Attenuation of the Cutaneous Vasoconstrictor Response to Cold in Elderly Men. *Journal of Gerontology* **47,** M211-M214.

Roberts JM & Gammill HS. (2005). Preeclampsia: Recent Insights. *Hypertension* **46,** 1243-1249.

Roche B, Lhote F, Chasseray J-E, Godefroy Y, Meyer O, Leon A, Kahn M-F & Guillevin L. (1992). Fetal congenital heart block and maternal systemic lupus erythematosus: Can plasma exchanges play a useful role? *Transfusion Science* **13,** 463-466.

Rodford JL, Torrens C, Siow RCM, Mann GE, Hanson MA & Clough GF. (2008). Endothelial dysfunction and reduced antioxidant protection in an animal model of the developmental origins of cardiovascular disease. *The Journal of Physiology* **586,** 4709-4720.

RodrÌguez-MaÒas L, Mariam El-Assar, Susana Vallejo, Pedro LÛpez-DÛriga, Joaquin SolÌs, Roberto Petidier, Manuel Montes, Juli·n Nevado, Marta Castro, Carmen GÛmez-Guerrero, ConcepciÛn PeirÛ & Carlos F. S·nchez-Ferrer. (2009). Endothelial dysfunction in aged humans is related with oxidative stress and vascular inflammation. *Aging Cell* **8,** 226-238.

Rook WHR, Glen KE, Marshall JM & Coney AM. (2008a). Changes in the regulation of vascular tone in adult male rats exposed to chronic hypoxia in utero. In *Proc Physiol Soc*, pp. C85.

Rook WHR, Marshall JM, Coney AM & Glen KE. (2008b). Chronic hypoxia in utero (CHU) in the rat changes capillarity and oxidative function in skeletal muscle of the offspring. In *Proc Physiol Soc*, pp. PC28.

Rothstein JD, Bristol LA, Hosler B, Brown RH & Kuncl RW. (1994). Chronic inhibition of superoxide dismutase produces apoptotic death of spinal neurons. *Proceedings of the National Academy of Sciences* **91,** 4155-4159.

Rouwet EV, Tintu AN, Schellings MWM, van Bilsen M, Lutgens E, Hofstra L, Slaaf DW, Ramsay G & le Noble FAC. (2002). Hypoxia Induces Aortic Hypertrophic Growth, Left Ventricular Dysfunction, and Sympathetic Hyperinnervation of Peripheral Arteries in the Chick Embryo. *Circulation* **105,** 2791-2796.

Rubanyi GM & Vanhoutte PM. (1986). Oxygen-derived free radicals, endothelium, and responsiveness of vascular smooth muscle. *AJP - Heart and Circulatory Physiology* **250,** H815-821.

Rudolph AM. (1984). The fetal circulation and its response to stress. *J Dev Physiol* **6,** 11-19.

Ruijtenbeek K, KESSELS LCGA, DE MEY JGR & BLANCO CE. (2003). Chronic Moderate Hypoxia and Protein Malnutrition Both Induce Growth Retardation, But Have Distinct Effects on Arterial Endothelium-Dependent Reactivity in the Chicken Embryo. *Pediatr Res* **53,** 573-579.

Ruijtenbeek K, le Noble FAC, Janssen GMJ, Kessels CGA, Fazzi GE, Blanco CE & De Mey JGR. (2000). Chronic Hypoxia Stimulates Periarterial Sympathetic Nerve Development in Chicken Embryo. *Circulation* **102,** 2892-2897.

Ruit KG, Osborne PA, Schmidt RE, Johnson EM & Snider WD. (1990). Nerve growth-factor regulated sympathetic ganglion cell morphology and survival in the adult mouse. *J Neurosci* **10,** 2412-2419.

Rump TJ, Muneer PMA, Szlachetka AM, Lamb A, Haorei C, Alikunju S, Xiong H, Keblesh J, Liu J, Zimmerman MC, Jones J, Donohue Jr TM, Persidsky Y & Haorah J. (2010). Acetyl-l-carnitine protects neuronal function from alcohol-induced oxidative damage in the brain. *Free Radical Biology and Medicine* **49,** 1494-1504.

Rybalkin SD, Yan C, Bornfeldt KE & Beavo JA. (2003). Cyclic GMP Phosphodiesterases and Regulation of Smooth Muscle Function. *Circ Res* **93,** 280-291.

Sanders M, Fazzi G, Janssen G, Blanco C & De Mey J. (2004). Prenatal stress changes rat arterial adrenergic reactivity in a regionally selective manner. *European Journal of Pharmacology* **488,** 147-155.

Sapru HN & Krieger AJ. (1977). Carotid and aortic chemoreceptor function in the rat. *Journal of Applied Physiology* **42,** 344-348.

Sathishkumar K, Elkins R, Yallampalli U & Yallampalli C. (2009). Protein Restriction during Pregnancy Induces Hypertension and Impairs Endothelium-Dependent Vascular Function in Adult Female Offspring. *Journal of Vascular Research* **46,** 229-239.

Sausbier M, Schubert R, Voigt V, Hirneiss C, Pfeifer A, Korth M, Kleppisch T, Ruth P & Hofmann F. (2000). Mechanisms of NO/cGMP-Dependent Vasorelaxation. *Circ Res* **87,** 825-830.

Schreihofer AM & Sved AF. (1992). Nucleus tractus solitarius and control of blood pressure in chronic sinoaortic denervated rats. *American Journal of Physiology - Regulatory, Integrative and Comparative Physiology* **263,** R258-R266.

Schweizer M & Richter C. (1994). Nitric Oxide Potently and Reversibly Deenergizes Mitochondria at Low Oxygen Tension. *Biochemical and Biophysical Research Communications* **204,** 169-175.

Seals D, Suwarno N & Dempsey J. (1990). Influence of lung volume on sympathetic nerve discharge in normal humans. *Circ Res* **67,** 130-141.

Seals D, Suwarno N, Joyner M, Iber C, Copeland J & Dempsey J. (1993). Respiratory modulation of muscle sympathetic nerve activity in intact and lung denervated humans. *Circ Res* **72,** 440-454.

Seals DR & Dinenno FA. (2004). Collateral damage: cardiovascular consequences of chronic sympathetic activation with human aging. *American Journal of Physiology - Heart and Circulatory Physiology* **287,** H1895-H1905.

Shimokawa H & Matoba T. (2004). Hydrogen peroxide as an endothelium-derived hyperpolarizing factor. *Pharmacological Research* **49,** 543-549.

Simms AE, Paton JFR, Pickering AE & Allen AM. (2009). Amplified respiratory–sympathetic coupling in the spontaneously hypertensive rat: does it contribute to hypertension? *The Journal of Physiology* **587,** 597-610.

Simonetta G, Rourke A, Ownesm JA, Ribbinson J & McMillen I. (1997). Impact of Placental Restriction on the Development of the Sympathoadrenal System. *Pediatr Res* **42,** 805-811.

Sjoiblom-Widfeldt N, Gustafsson H & Nilsson H. (1990). Transmitter characteristics of small mesenteric arteries from the rat. *Acta Physiologica Scandinavica* **138,** 203-212.

Skinner MR & Marshall JM. (1996). Studies on the roles of ATP, adenosine and nitric oxide in mediating muscle vasodilatation induced in the rat by acute systemic hypoxia. *J Physiol* **495,** 553-560.

Smeda JS. (1990). Analysis of cerebrovascular sympathetic nerve density in relation to stroke development in spontaneously hypertensive rats. *Stroke* **21,** 785-789.

Smith AD & Wrinkler H. (1972). *Fundamental Mechanisms in the release of vatecholamines*. Springer-Verlag, Berlin, Heidelberg, New York.

Smith EG, Voyles WF, Kirby BS, Markwald RR & Dinenno FA. (2007). Ageing and leg postjunctional Œ±-adrenergic vasoconstrictor responsiveness in healthy men. *The Journal of Physiology* **582,** 63-71.

Sneddon P & Burnstock G. (1984). Inhibition of excitatory junction potentials in guinea-pig vas deferens by [alpha], [beta]-methylene-ATP: Further evidence

for ATP and noradrenaline as cotransmitters. *European Journal of Pharmacology* **100,** 85-90.

Sneddon P & Burnstock G. (1985). ATP as a co-transmitter in rat tail artery. *Eur J Pharmacol* **106,** 149-152.

Sprague RS, Bowles EA, Achilleus D & Ellsworth ML. (2010). Erythrocytes as controllers of perfusion distribution in the microvasculature of skeletal muscle. *Acta Physiologica***,** no-no.

Spyer KM. (1996). Central nervous integration of cardiorespiratory control. In *Comprehensive Human Physiology*, ed. Greger R & Windhorst U. Springer-Verlag, Berlin.

Stephens DP, Saad AR, Bennett LAT, Kosiba WA & Johnson JM. (2004). Neuropeptide Y antagonism reduces reflex cutaneous vasoconstriction in humans. *American Journal of Physiology - Heart and Circulatory Physiology* **287,** H1404-H1409.

Stewart AL, Anderson RB, Kobayashi K & Young HM. (2008). Effects of NGF, NT-3 and GDNF family members on neurite outgrowth and migration from pelvic ganglia from embryonic and newborn mice. *BMC Dev Biol* **8**.

Storkebaum E & Carmeliet P. (2011). Paracrine control of vascular innervation in health and disease. *Acta Physiologica* **203,** 61-86.

Storkebaum E, de Almodovar CR, Meens M, Zacchigna S, Mazzone M, Vanhoutte G, Vinckier S, Miskiewicz K, Poesen K, Lambrechts D, Janssen GMJ, Fazzi GE, Verstreken P, Haigh J, Schiffers PM, Rohrer H, Van der Linden A, De Mey JGR & Carmeliet P. (2010). Impaired Autonomic Regulation of Resistance Arteries in Mice With Low Vascular Endothelial Growth Factor or Upon Vascular Endothelial Growth Factor Trap Delivery. *Circulation* **122,** 273-U107.

Su C, Bevan J, Assali N & Brinkman C, 3d. (1977a). Regional variation of lamb blood vessel responsiveness to vasoactive agents during fetal development. *Circ Res* **41,** 844-848.

Su C, Bevan JA, Assali NS & Brinkman ICR. (1977b). Development of Neuroeffector Mechanisms in the Carotid Artery of the Fetal Lamb. *Journal of Vascular Research* **14,** 12-24.

Su C, Bevan JA & Burnstock G. (1971). [3H]Adenosine Triphosphate: Release during Stimulation of Enteric Nerves. *Science* **173,** 336-338.

Supramaniam VG, Jenkin G, Loose J, Wallace EM & Miller SL. (2006). Chronic fetal hypoxia increases activin A concentrations in the late-pregnant sheep. *Bjog* **113,** 102-109.

Taddei S, Virdis A, Ghiadoni L, Salvetti G, Bernini G, Magagna A & Salvetti A. (2001). Age-Related Reduction of NO Availability and Oxidative Stress in Humans. *Hypertension* **38,** 274-279.

Tapanainen P, Bang P, Wilson K, Unterman T, Vremen H & Rosenfeld R. (1994). Maternal hypoxia as a model for intrauterine growth retardation: effects on insulin-like growth factors and their binding proteins. *Pediatr Res* **36,** 152-158.

Tateishi J & Faber JE. (1995). ATP-Sensitive K+ Channels Mediate {alpha}2D-Adrenergic Receptor Contraction of Arteriolar Smooth Muscle and Reversal of Contraction by Hypoxia. *Circ Res* **76,** 53-63.

Tatemoto K, Carlquist M & Mutt V. (1982). Neuropeptide Y: a novel brain peptide with structural similarities to peptide YY and pancreatic polypeptide. *Nature* **296,** 659-660.

Taylor EW, Jordan D & Coote JH. (1999). Central Control of the Cardiovascular and Respiratory Systems and Their Interactions in Vertebrates. *Physiol Rev* **79,** 855-916.

Teppema LJ & Dahan A. (2010). The Ventilatory Response to Hypoxia in Mammals: Mechanisms, Measurement, and Analysis. *Physiological Reviews* **90,** 675-754.

Thomas GD, Hansen J & Victor RG. (1994a). Inhibition of alpha 2-adrenergic vasoconstriction during contraction of glycolytic, not oxidative, rat hindlimb muscle. *American Journal of Physiology - Heart and Circulatory Physiology* **266,** H920-H929.

Thomas GD & Victor RG. (1998). Nitric oxide mediates contraction-induced attenuation of sympathetic vasoconstriction in rat skeletal muscle. *The Journal of Physiology* **506,** 817-826.

Thomas T, Elnazir BK & Marshall JM. (1994b). Differentiation of the peripherally mediated from the centrally mediated influences of adenosine in the rat during systemic hypoxia. *Experimental Physiology* **79,** 809-822.

Thomas T & Marshall JM. (1994). Interdependence of respiratory and cardiovascular changes induced by systemic hypoxia in the rat: the roles of adenosine. *J Physiol* **480,** 627-636.

Thomas T & Marshall JM. (1995). A study on rats of the effects of chronic hypoxia from birth on respiratory and cardiovascular responses evoked by acute hypoxia. *J Physiol* **487,** 513-525.

Thompson CS & Kenney WL. (2004). Altered neurotransmitter control of reflex vasoconstriction in aged human skin. *The Journal of Physiology* **558,** 697-704.

Thompson LP & Weiner CP. (1999). Effects of acute and chronic hypoxia on nitric oxide-mediated relaxation of fetal guinea pig arteries. *American Journal of Obstetrics and Gynecology* **181,** 105-111.

Thrasher TN. (2002). Unloading arterial baroreceptors causes neurogenic hypertension. *American Journal of Physiology - Regulatory, Integrative and Comparative Physiology* **282,** R1044-R1053.

Thrasher TN. (2005). Baroreceptors, baroreceptor unloading, and the long-term control of blood pressure. *American Journal of Physiology - Regulatory, Integrative and Comparative Physiology* **288,** R819-R827.

Timmermans PBMWM & Van Zwieten PA. (1980). Postsynaptic [alpha]1- and [alpha]2-adrenoceptors in the circulatory system of the pithed rat: Selective stimulation of the [alpha]2-type by B-HT 933. *European Journal of Pharmacology* **63,** 199-202.

Timmermans PBMWM & Van Zwieten PA. (1981). Mini-review of the postsynaptic Alpha-2 adrenoreceptor. *Journal of Autonomic Pharmacology* **1,** 171-183.

Torrens C, Brawley L, Barker AC, Itoh S, Poston L & Hanson MA. (2003). Maternal protein restriction in the rat impairs resistance artery but not conduit artery function in pregnant offspring. *The Journal of Physiology* **547,** 77-84.

Tucker BJ, Peterson OW, Ziegler MG & Blantz RC. (1982). Analysis of adrenergic effects of the anesthetics Inactin and alpha-chloralose. *American Journal of Physiology - Renal Physiology* **243,** F253-F259.

VanTeeffelen JWGE & Segal SS. (2003). Interaction between sympathetic nerve activation and muscle fibre contraction in resistance vessels of hamster retractor muscle. *The Journal of Physiology* **550,** 563-574.

Vardhan A, Kachroo A & Sapru HN. (1993). Excitatory amino acid receptors in commissural nucleus of the NTS mediate carotid chemoreceptor responses. *American Journal of Physiology - Regulatory, Integrative and Comparative Physiology* **264,** R41-R50.

Voll R, Mikulowska A, Kalden J & Holmdahl R. (1999). Amelioration of type II collagen induced arthritis in rats by treatment with sodium diethyldithiocarbamate. *Journal of Rheumatology* **26,** 1352-1358.

Wahlestedt C, Yanaihara N & Hakanson R. (1986). Evidence for different pre- and post-junctional receptors for neuropeptide Y and related peptides. *Regulatory Peptides* **13,** 307-318.

Wang Z, Huang Z, Lu G, Lin L & Ferrari M. (2009). Hypoxia during pregnancy in rats leads to early morphological changes of atherosclerosis in adult offspring. *AJP - Heart and Circulatory Physiology* **296,** H1321-1328.

Waypa GB, Chandel NS & Schumacker PT. (2001). Model for Hypoxic Pulmonary Vasoconstriction Involving Mitochondrial Oxygen Sensing. *Circ Res* **88,** 1259-1266.

Waypa GB, Guzy R, Mungai PT, Mack MM, Marks JD, Roe MW & Schumacker PT. (2006). Increases in Mitochondrial Reactive Oxygen Species Trigger Hypoxia-Induced Calcium Responses in Pulmonary Artery Smooth Muscle Cells. *Circ Res* **99,** 970-978.

Willette RN, Barcas PP, Krieger AJ & Sapru HN. (1983). Vasopressor and depressor areas in the rat medulla: Identification by microinjection of l-glutamate. *Neuropharmacology* **22,** 1071-1079.

Willette RN, Barcas PP, Krieger AJ & Sapru HN. (1984). Endogenous GABAergic mechanisms in the medulla and the regulation of blood pressure. *J Pharmacol Exp Ther* **230,** 34-39.

Williams SJ, Campbell ME, McMillen IC & Davidge ST. (2005a). Differential effects of maternal hypoxia or nutrient restriction on carotid and femoral vascular function in neonatal rats. *Am J Physiol Regul Integr Comp Physiol* **288,** R360-367.

Williams SJ, Hemmings DG, Mitchell JM, McMillen IC & Davidge ST. (2005b). Effects of maternal hypoxia or nutrient restriction during pregnancy on endothelial function in adult male rat offspring. *J Physiol* **565,** 125-135.

Wilson TE, Monahan KD, Short DS & Ray CA. (2004). Effect of age on cutaneous vasoconstrictor responses to norepinephrine in humans. *American Journal of Physiology - Regulatory, Integrative and Comparative Physiology* **287,** R1230-R1234.

Yada T, Shimokawa H, Hiramatsu O, Kajita T, Shigeto F, Goto M, Ogasawara Y & Kajiya F. (2003). Hydrogen Peroxide, an Endogenous Endothelium-Derived Hyperpolarizing Factor, Plays an Important Role in Coronary Autoregulation In Vivo. *Circulation* **107,** 1040-1045.

Yamada Y, Miyajima E, Tochikubo O, Matsukawa T & Ishii M. (1989). Age-related changes in muscle sympathetic nerve activity in essential hypertension. *Hypertension* **13,** 870-877.

Yamamoto R, Kawasaki H & Takasaki K. (1984). Postsynaptic alpha-adrenoreceptor populations in several vascular systems of the anaesethised rat. *Journal of Autonomic Pharmacology* **4,** 231-240.

Yang Y-M, Huang A, Kaley G & Sun D. (2009). eNOS uncoupling and endothelial dysfunction in aged vessels. *American Journal of Physiology - Heart and Circulatory Physiology* **297,** H1829-H1836.

Yusof APM & Coote JH. (1988). Patterns of activity in sympathetic postganglionic nerves to skeletal muscle, skin and kidney during stimulation of the medullary raphe area of the rat. *Journal of the Autonomic Nervous System* **24,** 71-79.

Zhao X-H, Sun X-Y, Edvinsson L & Hedner T. (1997). Does the neuropeptide Y Y1 receptor contribute to blood pressure control in the spontaneously hypertensive rat? *Journal of Hypertension* **15,** 19-27.

Zigmond RE, Schwarzschild MA & Rittenhouse AR. (1989). Acute Regulation of Tyrosine Hydroxylase by Nerve Activity and by Neurotransmitters Via Phosphorylation. *Annual Review of Neuroscience* **12,** 415-461.

Zou A-P, Li N & Cowley AW, Jr. (2001). Production and Actions of Superoxide in the Renal Medulla. *Hypertension* **37,** 547-553.

Zukowska-Grojec Z & Vaz AC. (1988). Role of neuropeptide Y (NPY) in cardiovascular responses to stress. *Synapse* **2,** 293-298.

Zweifach BW & Metz DB. (1955). Regional Differences in Response of Terminal Vascular Bed to Vasoactive Agents. *American Journal of Physiology* **182,** 155-165.

Figure 2.1

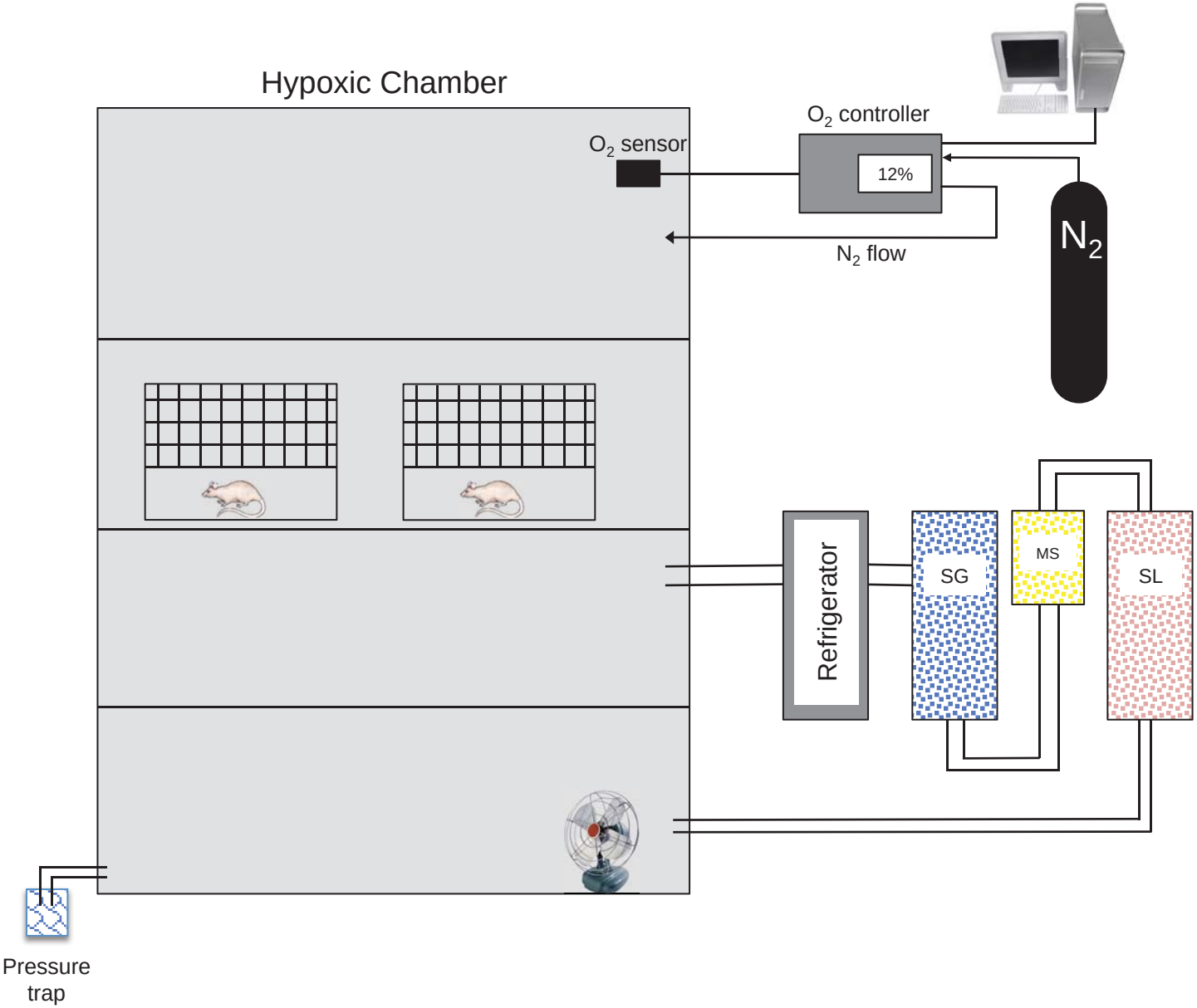
Hypoxic Chamber
O_2 sensor
O_2 controller
12%
N_2 flow
N_2
Refrigerator
SG
MS
SL
Pressure trap

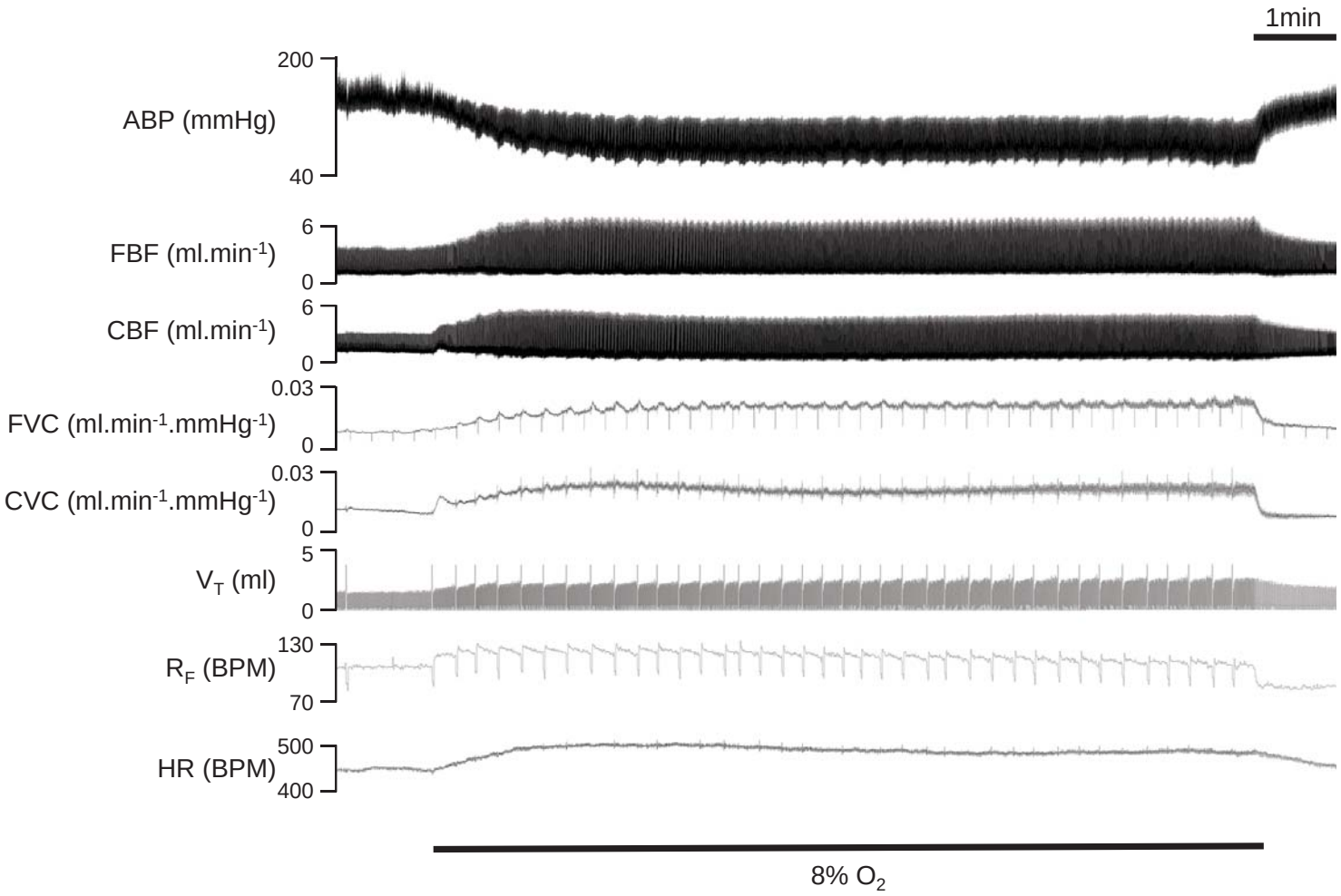
1min
200
ABP (mmHg)
40
6
FBF (ml.min-1)
0
6
CBF (ml.min-1)
0
0.03
FVC (ml.min-1.mmHg-1)
0
0.03
CVC (ml.min-1.mmHg-1)
0
5
VT (ml)
0
130
RF (BPM)
70
500
HR (BPM)
400
8% O2

Figure 3.1

Figure 3.2

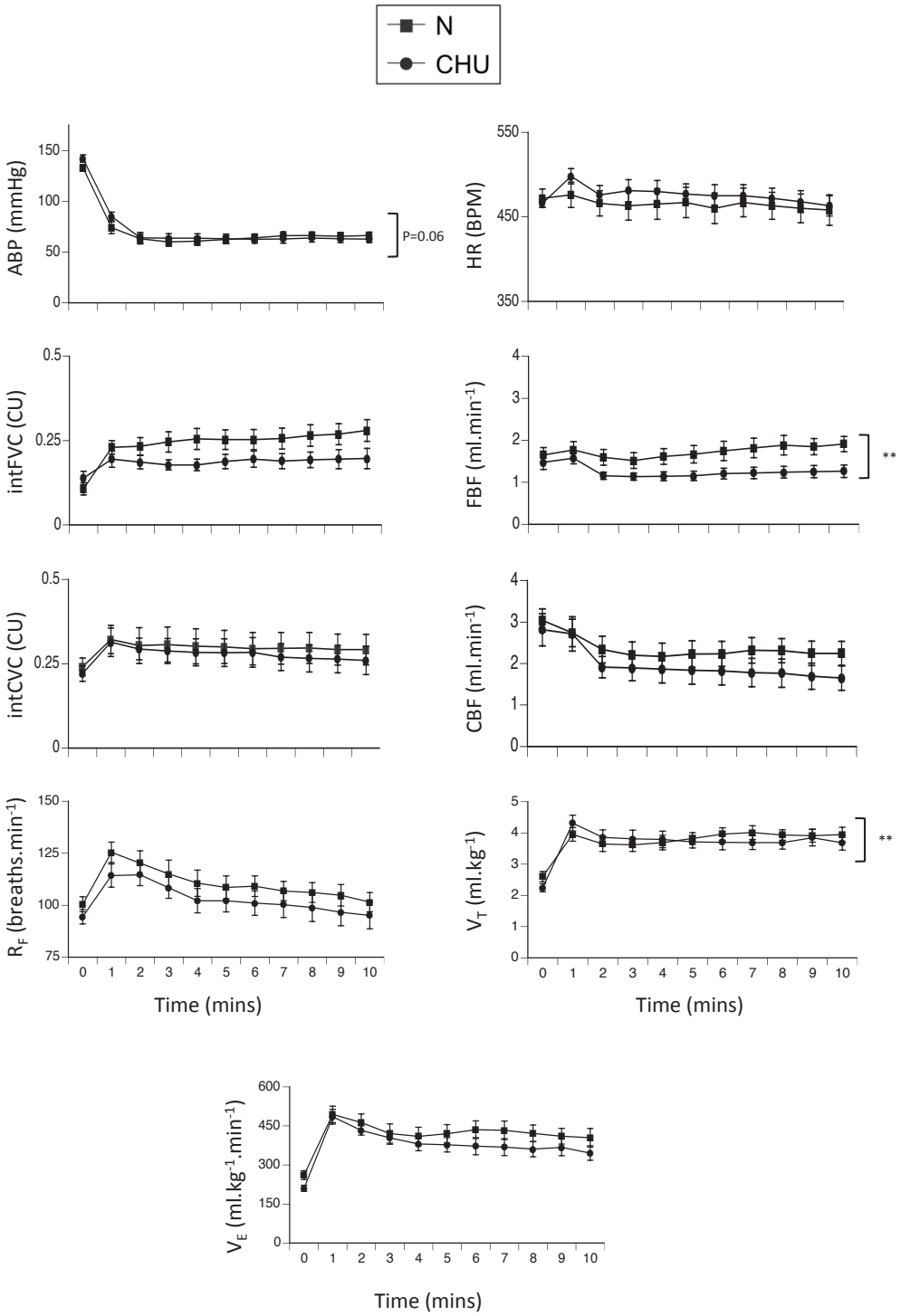
N
CHU
ABP (mmHg)
150
100
50
0
P=0.06
HR (BPM)
550
450
350
intFVC (CU)
0.5
0.25
0
FBF (ml.min-1)
4
3
2
1
0
**
intCVC (CU)
0.5
0.25
0
CBF (ml.min-1)
4
3
2
1
0
RF (breaths.min-1)
150
125
100
75
VT (ml.kg-1)
5
4
3
2
1
0
**
0 1 2 3 4 5 6 7 8 9 10
Time (mins)
VE (ml.kg-1.min-1)
600
450
300
150
0
0 1 2 3 4 5 6 7 8 9 10
Time (mins)

Figure 3.3

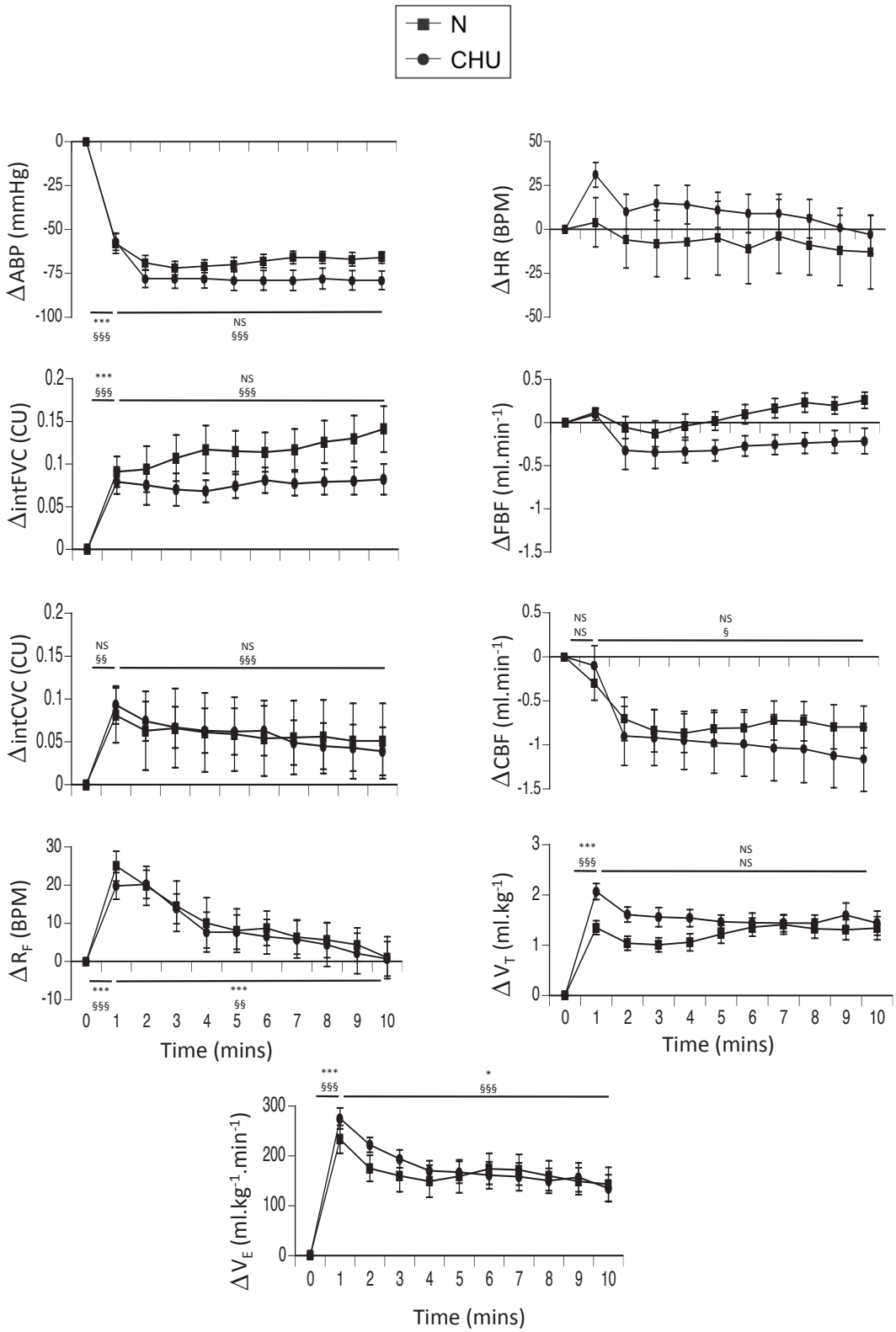
N
CHU
ΔABP (mmHg)
ΔHR (BPM)
ΔintFVC (CU)
ΔFBF (ml.min-1)
ΔintCVC (CU)
ΔCBF (ml.min-1)
ΔRF (BPM)
ΔVT (ml.kg-1)
ΔVE (ml.kg-1.min-1)
Time (mins)
Time (mins)
Time (mins)

Figure 3.4

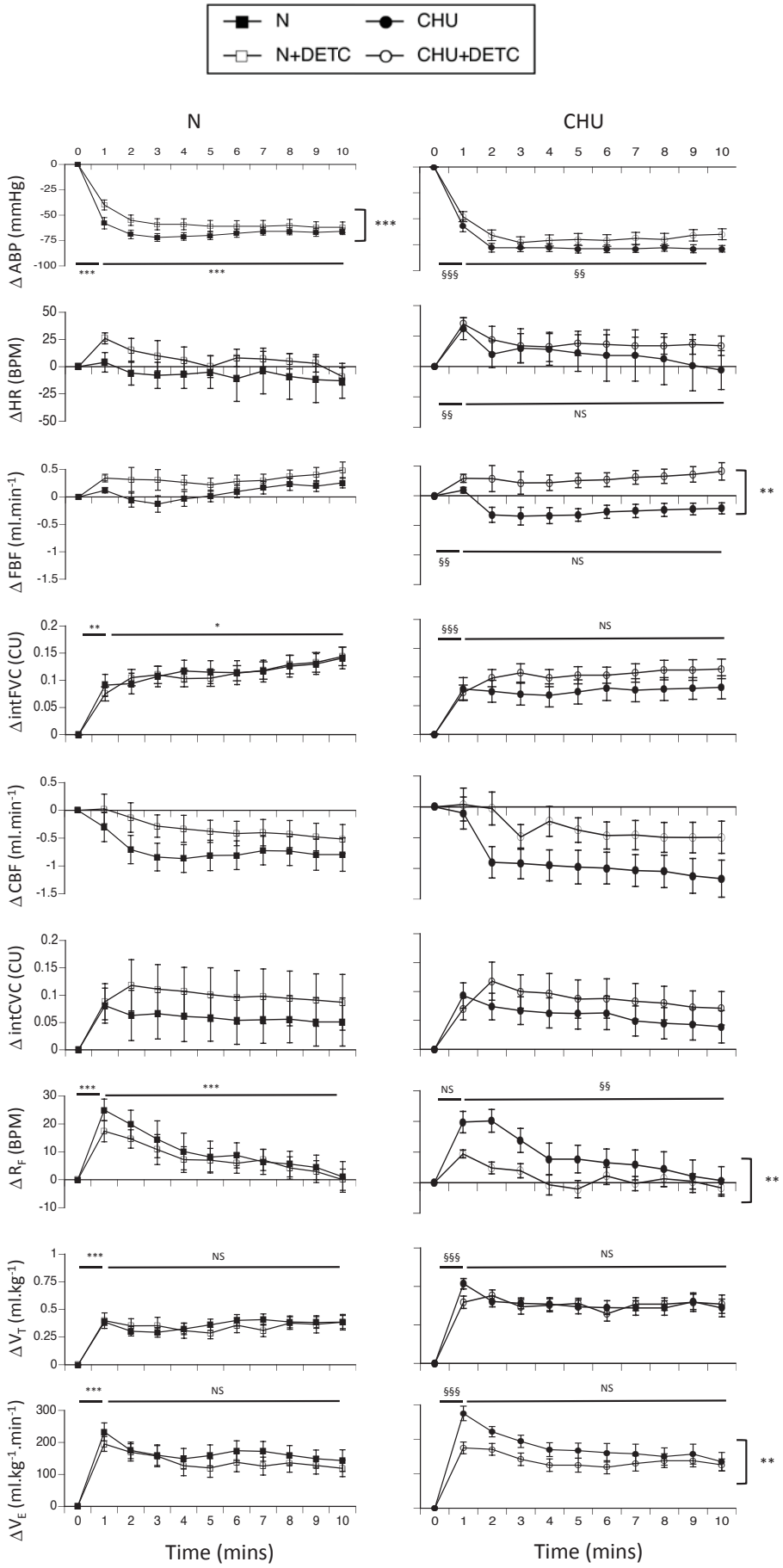
N
CHU
N+DETC
CHU+DETC
N
CHU
Δ ABP (mmHg)
ΔHR (BPM)
Δ FBF (ml.min-1)
Δ intFVC (CU)
Δ CBF (ml.min-1)
Δ intCVC (CU)
Δ RF (BPM)
Δ VT (ml.kg-1)
Δ VE (ml.kg-1.min-1)
Time (mins)
Time (mins)

Figure 4.5

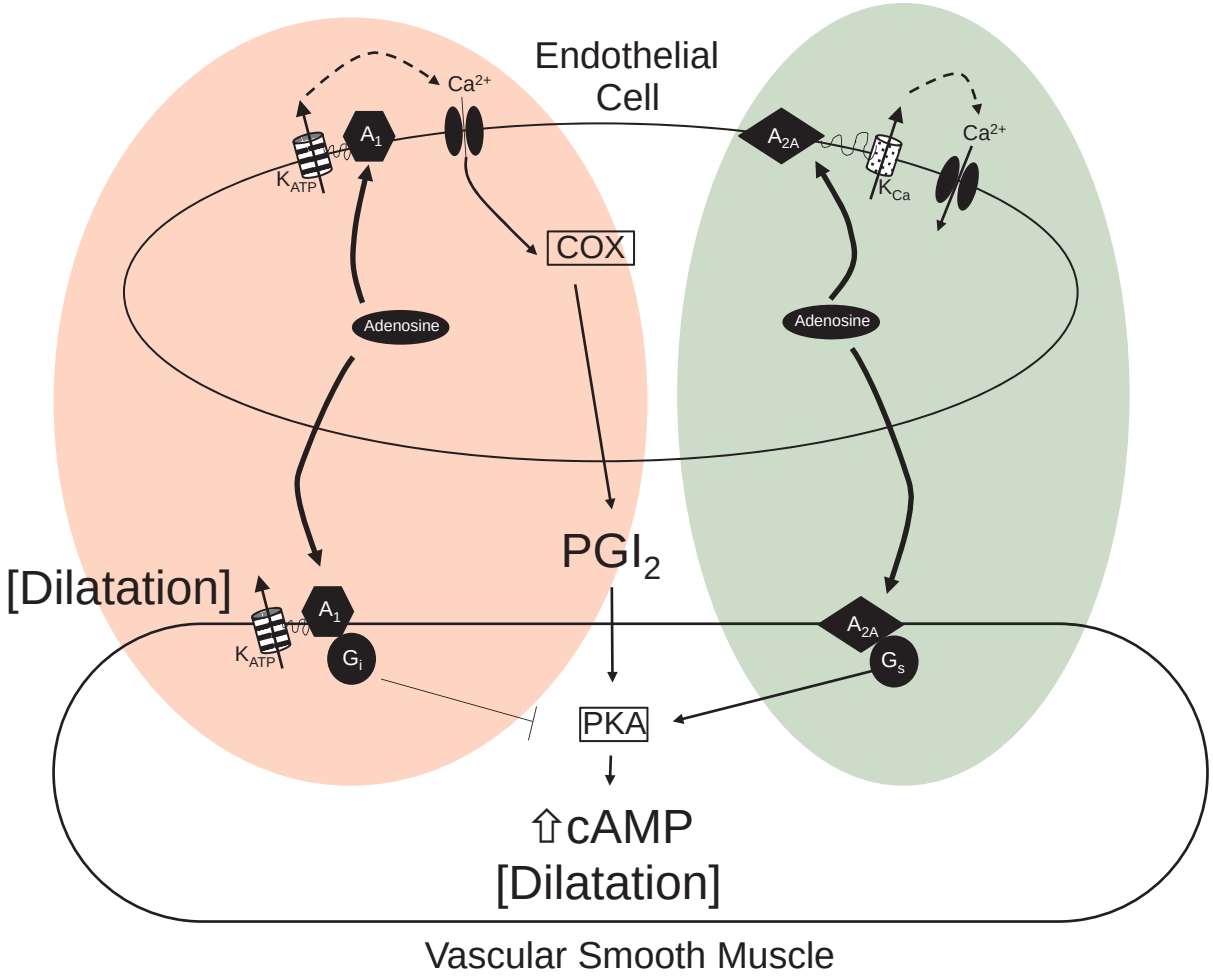
Endothelial Cell
Ca2+
A1
KATP
A2A
Ca2+
KCa
COX
Adenosine
Adenosine
PGI2
[Dilatation]
A1
KATP
Gi
A2A
Gs
PKA
⇧cAMP
[Dilatation]
Vascular Smooth Muscle

Figure 5.2

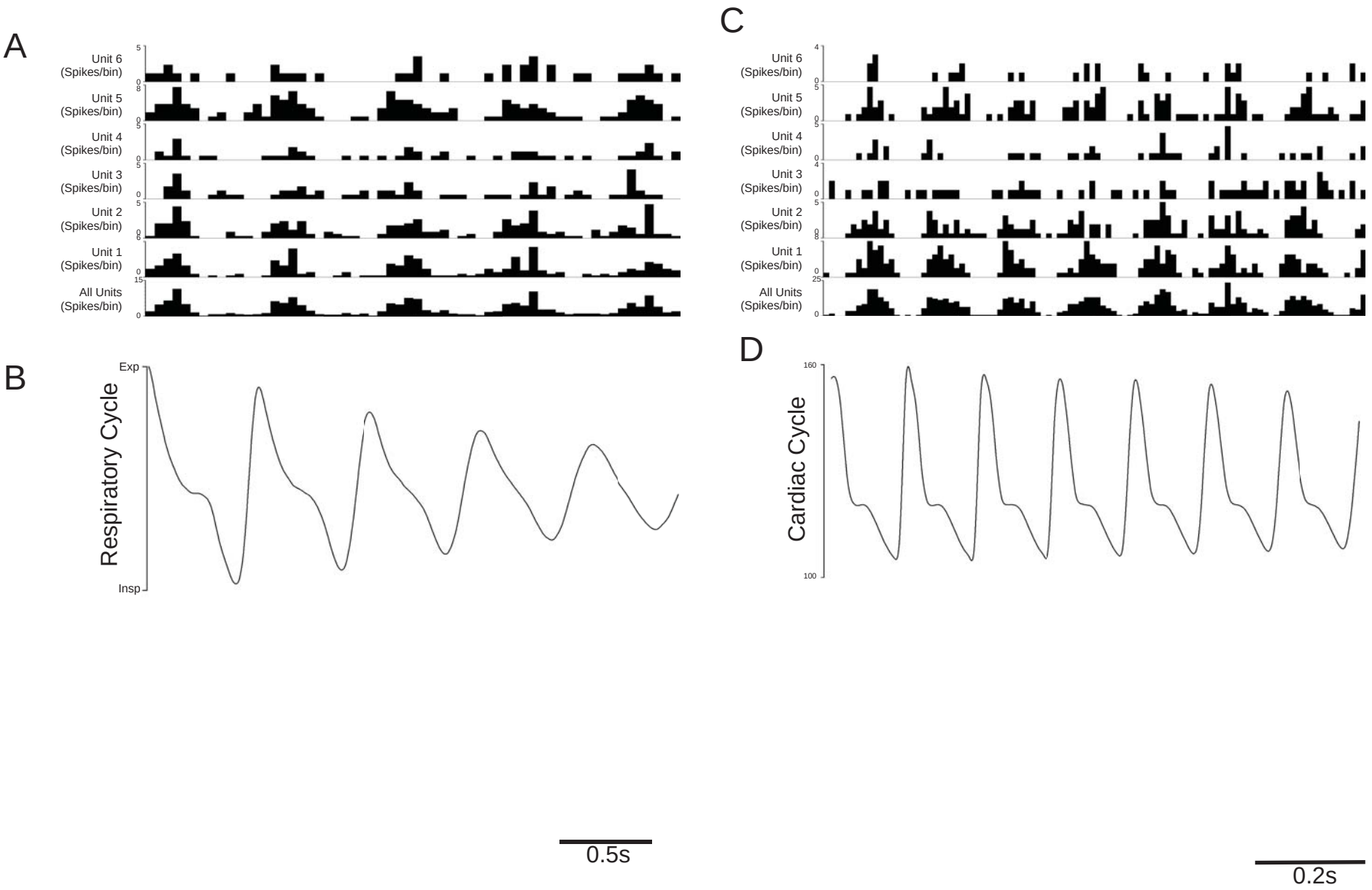
A
Unit 6 (Spikes/bin)
Unit 5 (Spikes/bin)
Unit 4 (Spikes/bin)
Unit 3 (Spikes/bin)
Unit 2 (Spikes/bin)
Unit 1 (Spikes/bin)
All Units (Spikes/bin)
B
Exp
Respiratory Cycle
Insp
0.5s
C
Unit 6 (Spikes/bin)
Unit 5 (Spikes/bin)
Unit 4 (Spikes/bin)
Unit 3 (Spikes/bin)
Unit 2 (Spikes/bin)
Unit 1 (Spikes/bin)
All Units (Spikes/bin)
D
Cardiac Cycle
0.2s

Figure 5.4

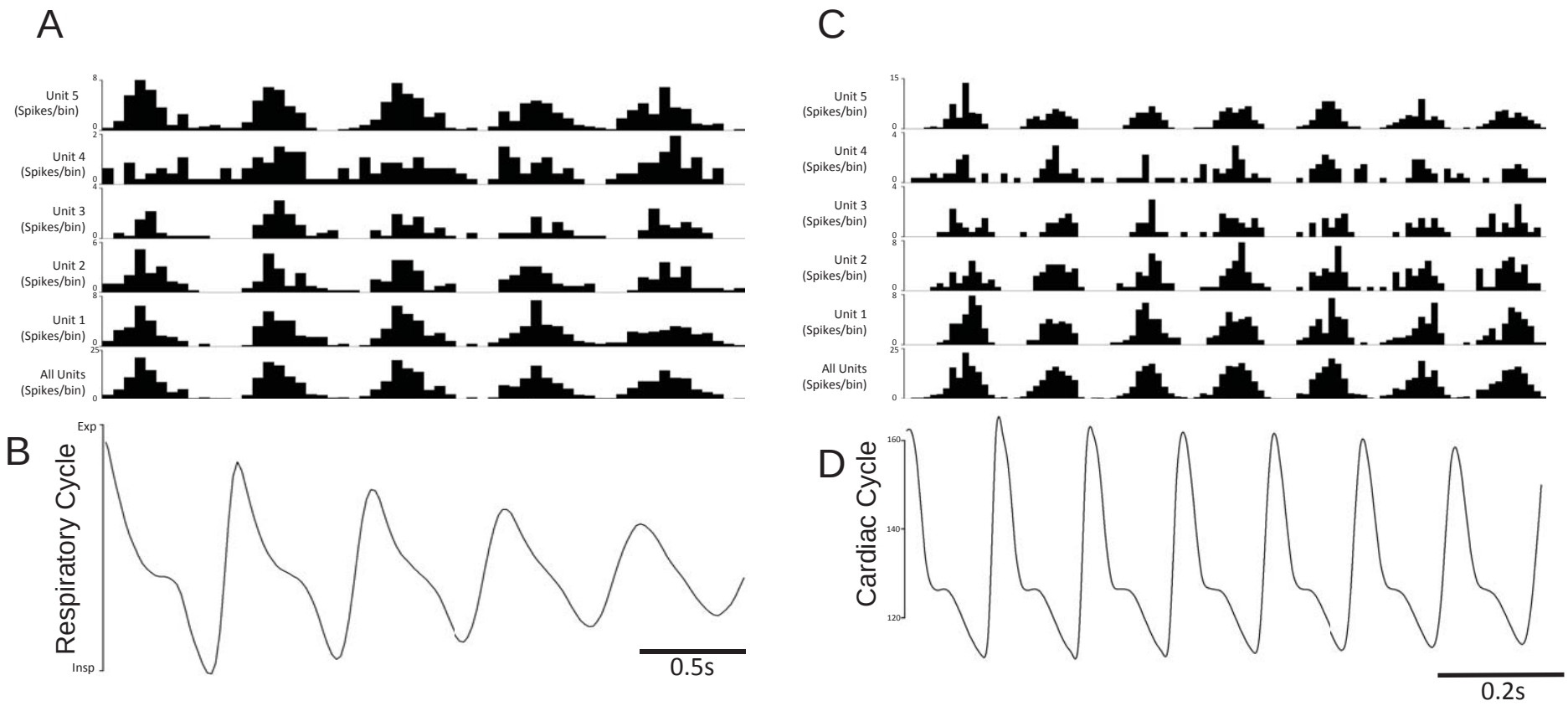
A
Unit 5 (Spikes/bin)
Unit 4 (Spikes/bin)
Unit 3 (Spikes/bin)
Unit 2 (Spikes/bin)
Unit 1 (Spikes/bin)
All Units (Spikes/bin)
B
Exp
Respiratory Cycle
Insp
0.5s
C
Unit 5 (Spikes/bin)
Unit 4 (Spikes/bin)
Unit 3 (Spikes/bin)
Unit 2 (Spikes/bin)
Unit 1 (Spikes/bin)
All Units (Spikes/bin)
D
Cardiac Cycle
0.2s

Figure 5.5

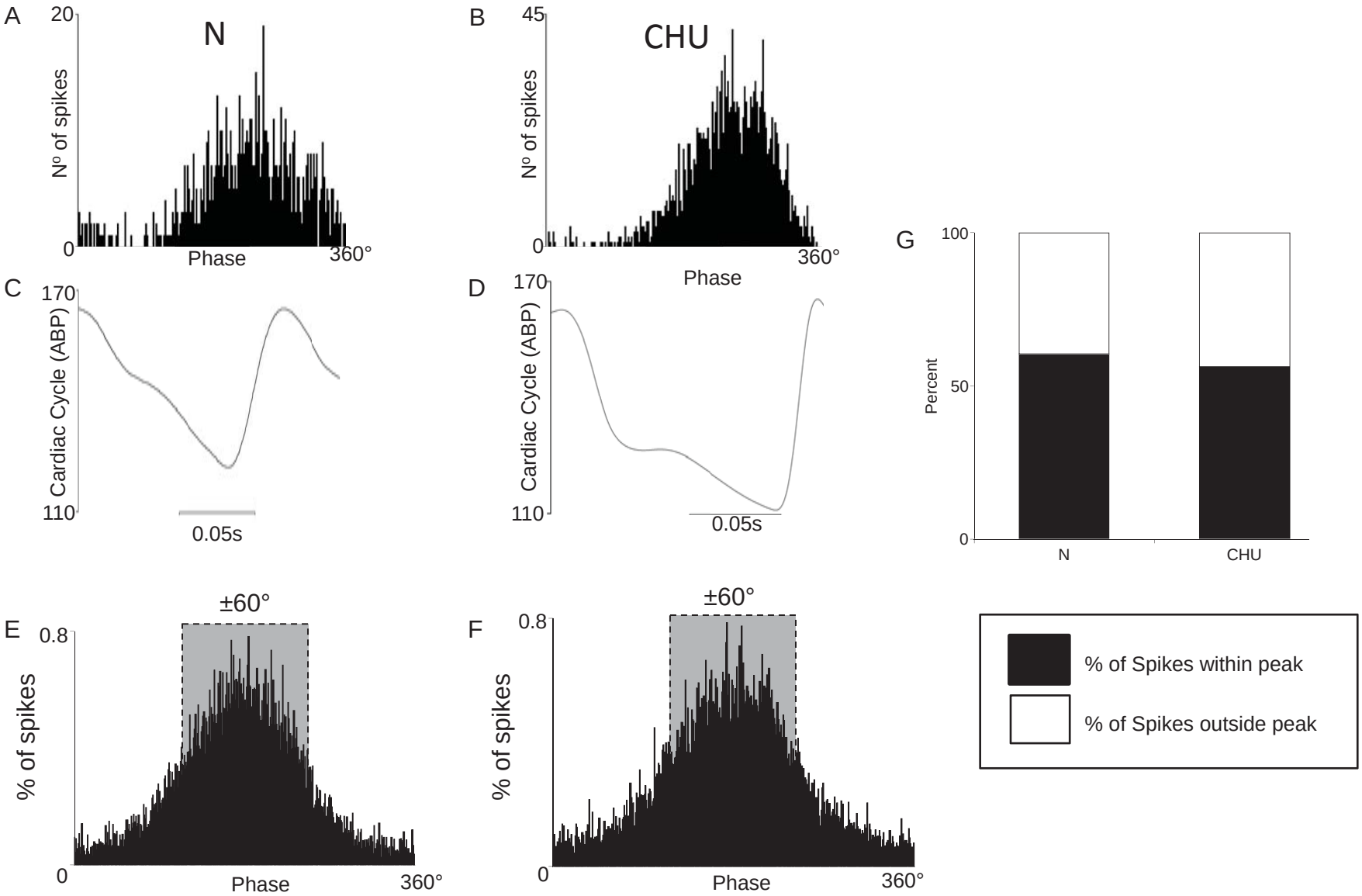
A
N
20
0
Nº of spikes
Phase
360°
B
CHU
45
0
Nº of spikes
Phase
360°
C
170
110
Cardiac Cycle (ABP)
0.05s
D
170
110
Cardiac Cycle (ABP)
0.05s
G
100
50
0
Percent
N
CHU
E
±60°
0.8
0
% of spikes
Phase
360°
F
±60°
0.8
0
% of spikes
Phase
360°
% of Spikes within peak
% of Spikes outside peak

Figure 5.6

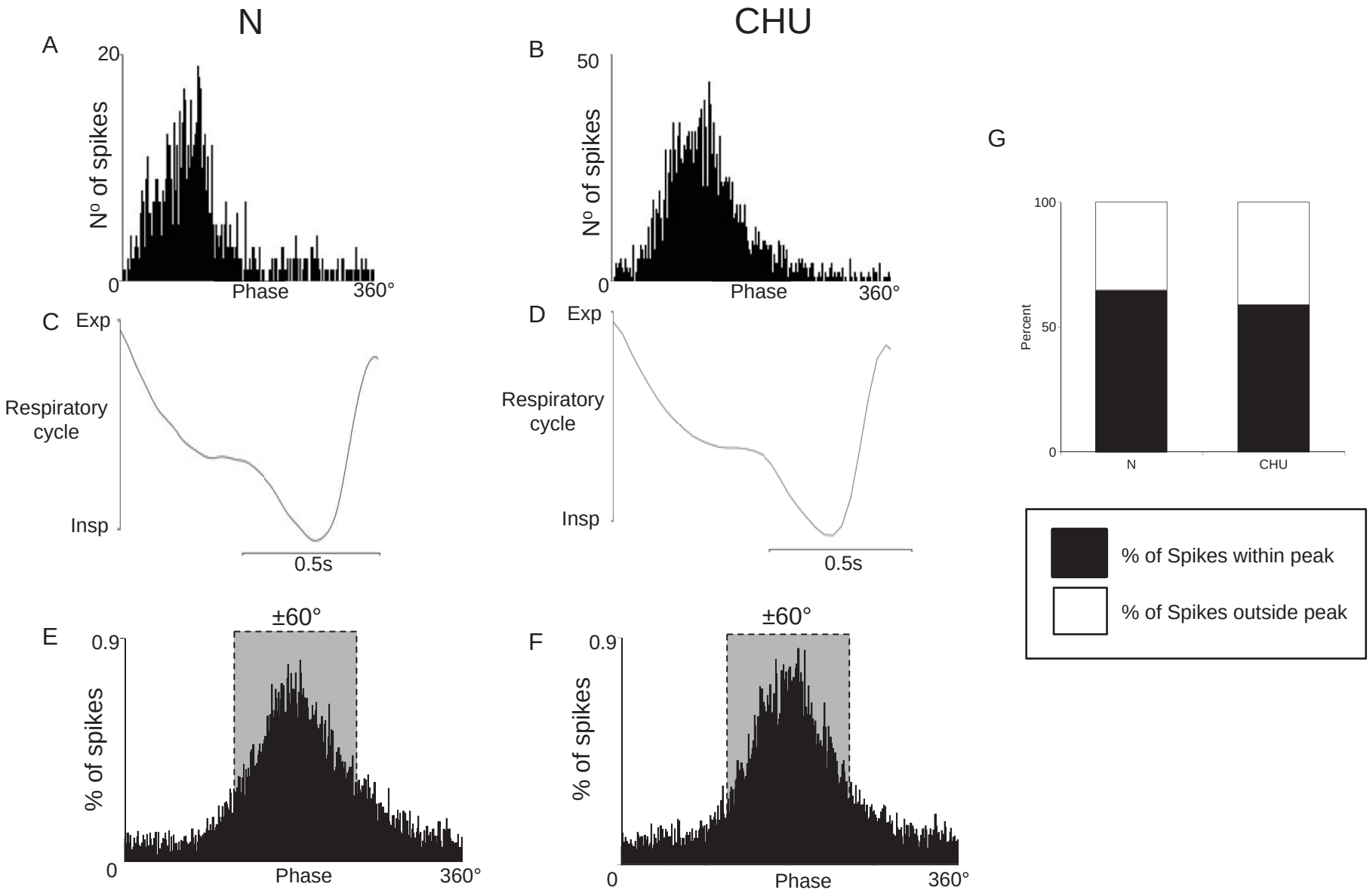
N
CHU
A
B
20
0
Nº of spikes
Phase
360°
50
C
D
Exp
Respiratory cycle
Insp
0.5s
G
100
50
Percent
N
CHU
% of Spikes within peak
% of Spikes outside peak
E
F
±60°
0.9
% of spikes

Figure 5.8

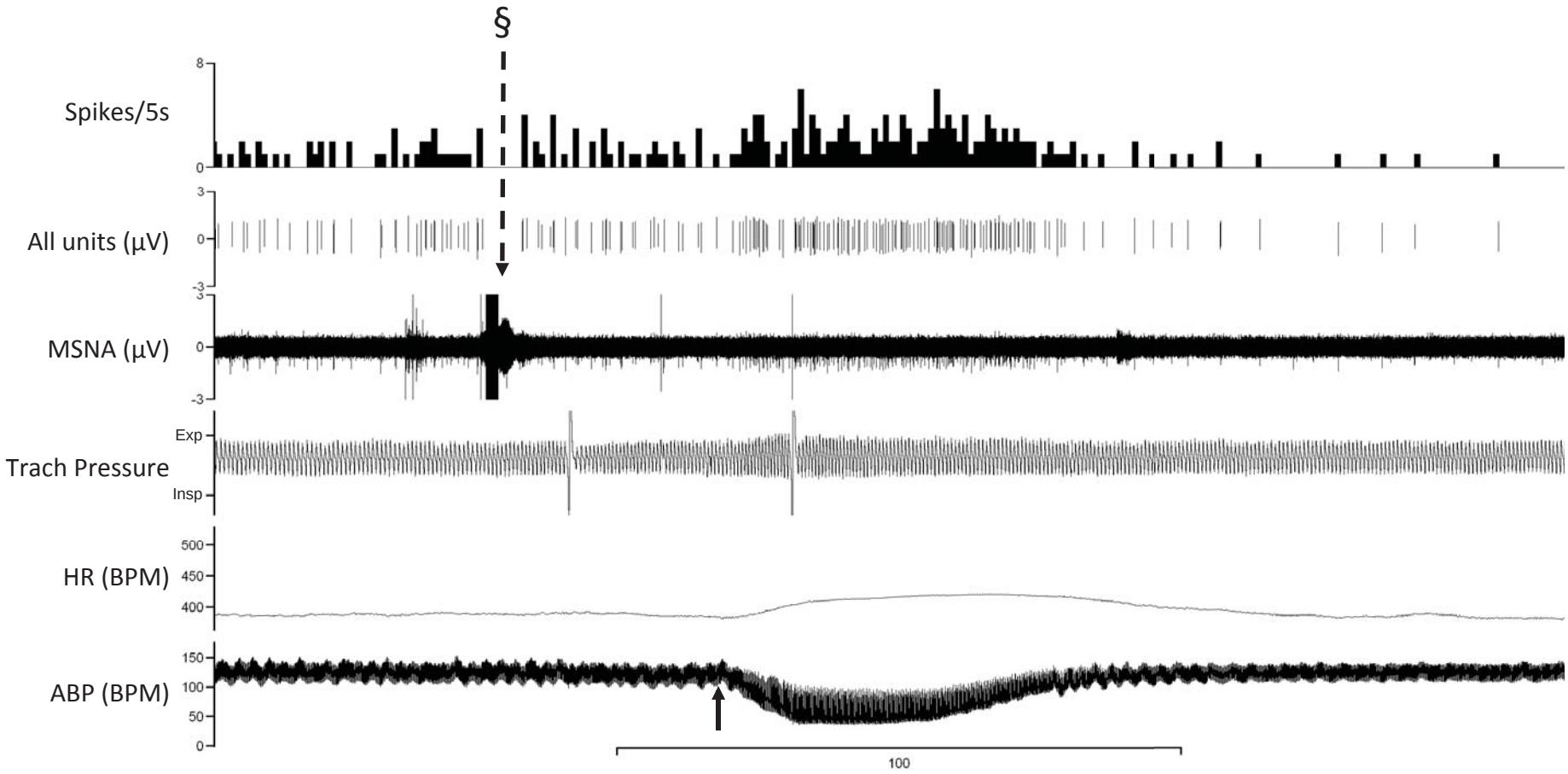
§
Spikes/5s
8
0
All units (µV)
3
0
-3
MSNA (µV)
3
0
-3
Trach Pressure
Exp
Insp
HR (BPM)
500
450
400
ABP (BPM)
150
100
50
0
100

Figure 5.10

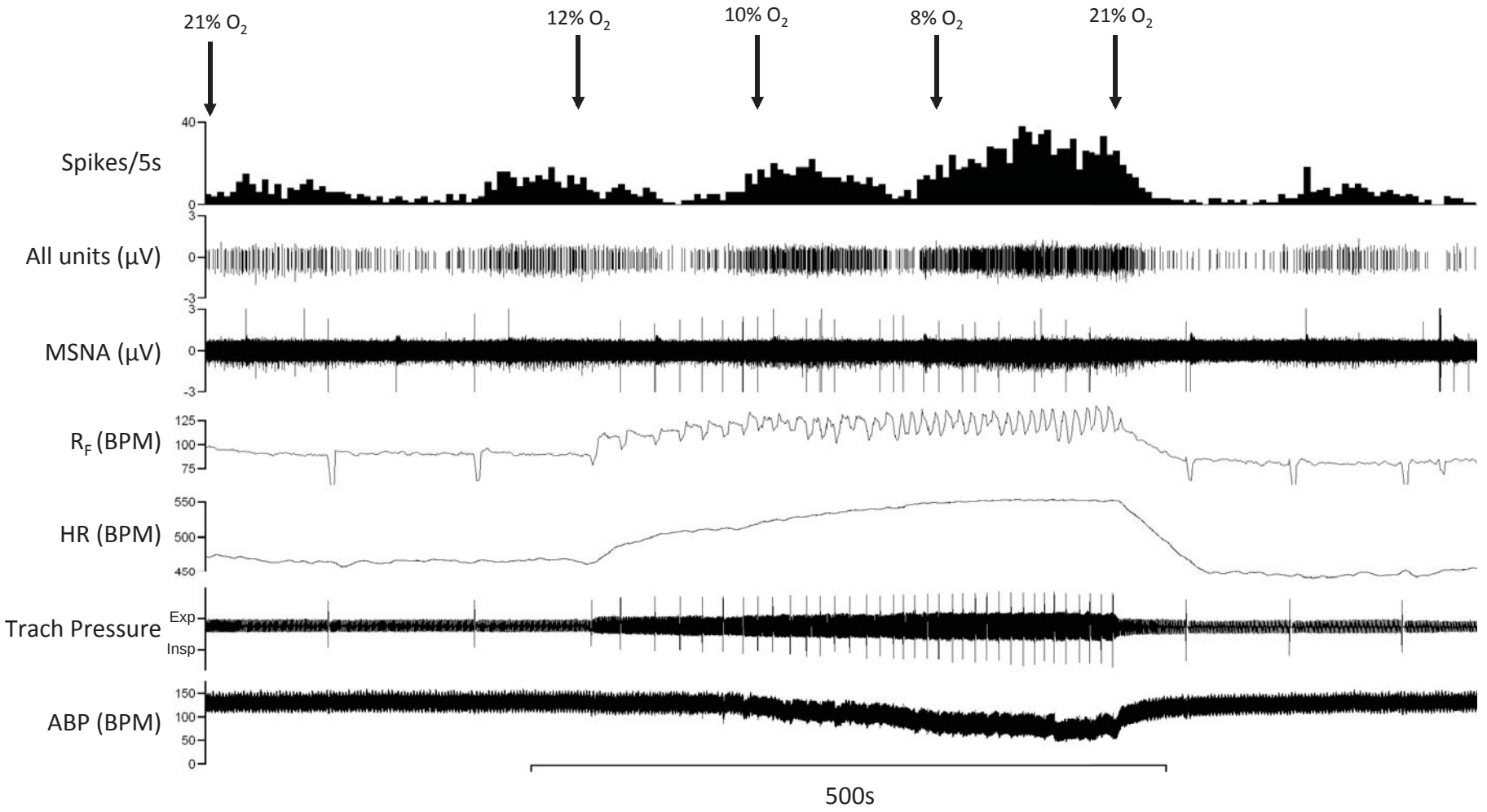
21% O2
12% O2
10% O2
8% O2
21% O2
Spikes/5s
40
0
All units (μV)
3
0
-3
MSNA (μV)
3
0
-3
RF (BPM)
125
100
75
HR (BPM)
550
500
450
Trach Pressure
Exp
Insp
ABP (BPM)
150
100
50
0
500s

Figure 5.12

A

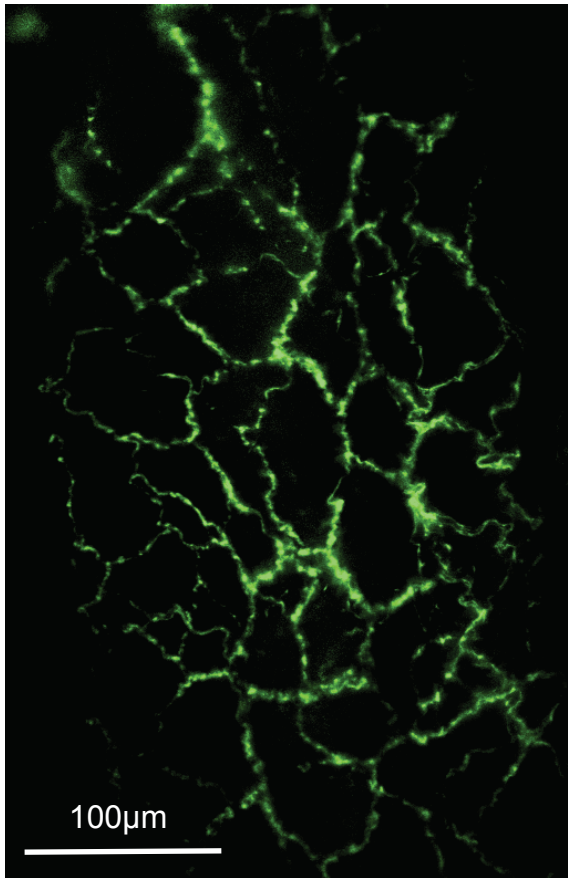

N

B

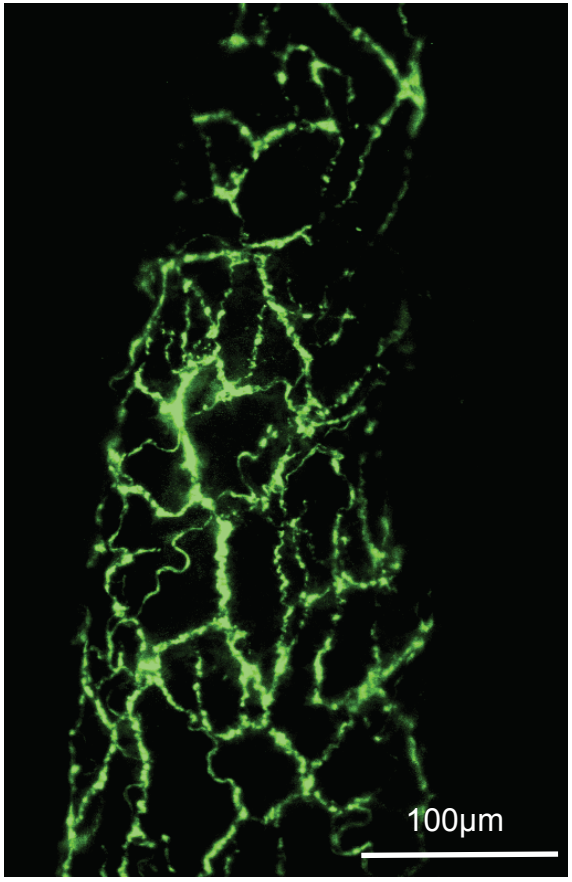

CHU

Figure 6.1

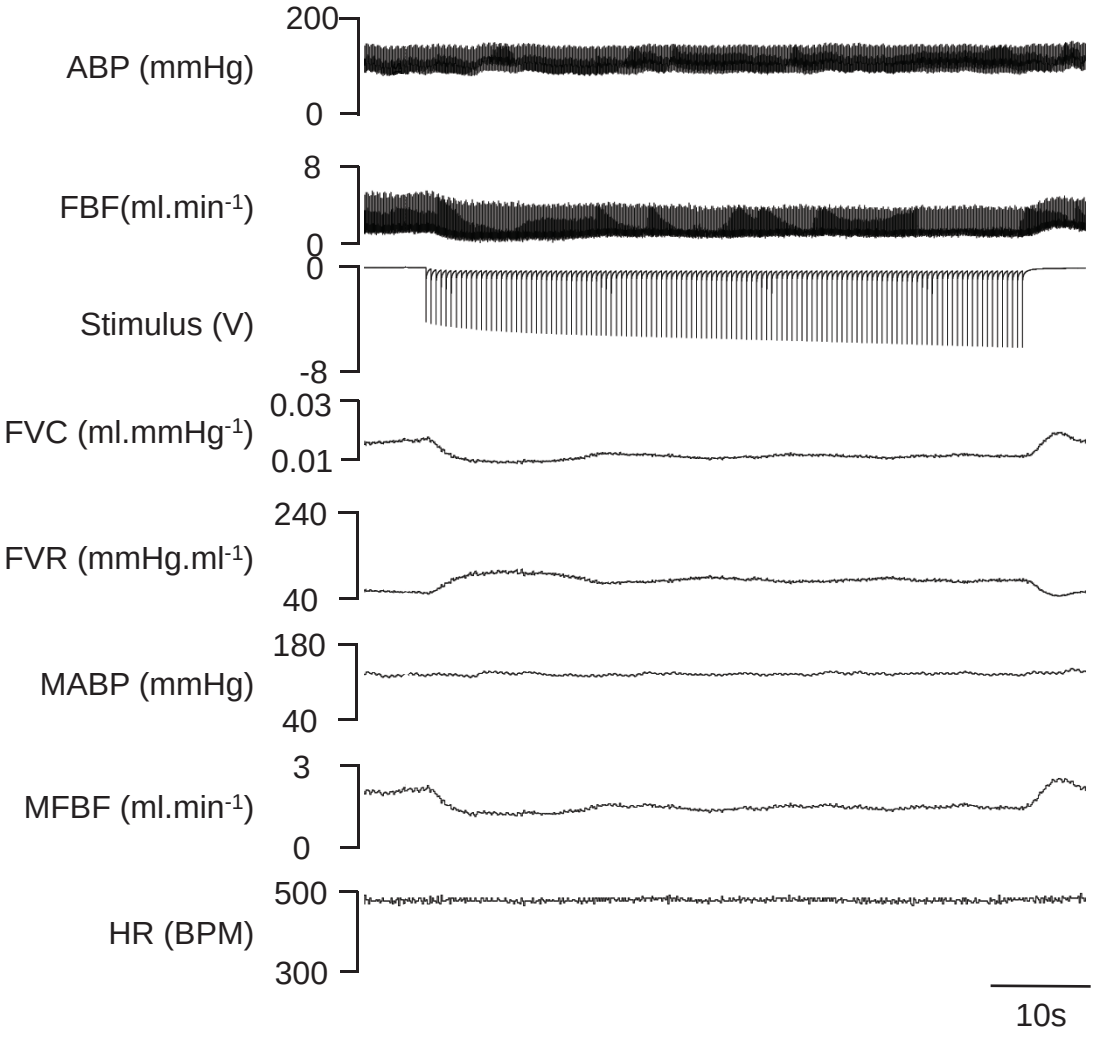
200
ABP (mmHg)
0
8
FBF(ml.min-1)
0
0
Stimulus (V)
-8
0.03
FVC (ml.mmHg-1)
0.01
240
FVR (mmHg.ml-1)
40
180
MABP (mmHg)
40
3
MFBF (ml.min-1)
0
500
HR (BPM)
300
10s